

**IMPROVING RAINFALL EROSIVITY ESTIMATES FOR THE
DESIGN OF SOIL CONSERVATION STRUCTURES
IN SOUTH AFRICA**

RA Johnson

Submitted in fulfilment of the requirements
for the degree of MSc Engineering

Bioresources Engineering
School of Engineering
University of KwaZulu-Natal
Pietermaritzburg
South Africa

February 2018

Supervisor: Prof. JC Smithers

Co-supervisor: Dr. A Senzanje

EXAMINER'S COPY

The financial assistance of the National Research Foundation (NRF) towards this research is hereby acknowledged. Opinions expressed and conclusions arrived at are those of the author and are not necessarily attributed to the NRF

DECLARATION

I, Robyn Anne Johnson, declare that:

- (i) The research reported in this dissertation, except where otherwise indicated, is my original work.
- (ii) This dissertation has not been submitted for any degree or examination at any other university.
- (iii) This dissertation does not contain other persons' data, pictures, graphs or other information, unless specifically acknowledged as being sourced from other persons.
- (iv) This dissertation does not contain other persons' writing, unless specifically acknowledged as being sourced from other researchers. Where other written sources have been quoted, then: their words have been rewritten, but the general information attributed to them has been referenced; where their exact words have been used, their writing has been placed inside quotation marks and referenced.
- (v) Where I have reproduced a publication of which I am an author, co-author or editor, I have indicated, in detail, which part of the publication was actually written by myself alone and have fully referenced such publications.
- (vi) This dissertation does not contain text, graphics or tables copied and pasted from the Internet, unless specifically acknowledged and the source being detailed in the thesis and in the References section.

Signed:.....|.....

Date:.....

As the candidate's supervisor, I have approved this dissertation for submission.

Signed:.....

J.C. Smithers

As the candidate's co-supervisor, I have approved this dissertation for submission.

Signed:.....

A. Senzanje

ACKNOWLEDGEMENTS

Acknowledgement is given to the following people and organisations, without whose support this study would not have been possible:

- Prof. Jeffrey Smithers and Dr. Aidan Senzanje, for their invaluable input and guidance throughout this study. Their continued support, encouragement and patience will always be appreciated.
- Numerous members of staff in the Departments of Bioresources Engineering and Hydrology departments at UKZN, for their valued input, assistance and advice at various stages of this study.
- The National Research Foundation, for providing the funding required to enable this study.
- The South African Weather Services, for providing rainfall data.
- Dr. Seth Dabney from the United States Department of Agriculture (USDA) Agricultural Research Services, as well as Dr. Giulio Ferruzi and Dr. Linda Scheffe from the USDA Natural Resources Conservation Services, for providing assistance and clarification regarding the RUSLE2 software.
- My special family and friends, for their constant support and motivation throughout my studies, and for making my years at UKZN both happy and memorable.

ABSTRACT

Soil erosion is a major problem, both in South Africa and globally. Soil erosion reduces the productivity of land and has major environmental, as well as economic, impacts. South Africa, in particular, experiences considerable challenges in combatting soil erosion owing to a combination of factors. Examples of these factors include low vegetal cover as a result of arid climatic conditions, as well as intense thunderstorm activity. As more data and computing power become available, it is important that approaches to the design of soil conservation structures and design tools be updated, in order to reduce soil erosion.

In this study, literature has been reviewed in order to obtain an overview of mechanical soil conservation measures in South Africa, soil loss estimation models currently used and design approaches to the determination of contour bank intervals. Literature showed that site-specific evaluation, using soil loss prediction tools, is the preferable approach to determining contour bank intervals, rather than the use of empirical equations. It was also found that the Revised Universal Soil Loss Equation (RUSLE) held the most potential as a model, in terms of creating a design tool for the design of soil conservation systems in South Africa. This was due to manageable input requirements as well as reliability – a result of widespread and extensive application of the model.

This study applied the erosivity density approach in order to calculate rainfall erosivity (*i.e.* the ability of rainfall to cause erosion) across South Africa. Owing to the paucity of suitable short duration rainfall data, a second approach was attempted in which rainfall erosivity calculated from short duration data was related to daily rainfall data characteristics. It was found that the both approaches resulted in erosivity density patterns similar to what had been determined in previous studies. The erosivity density method produced results with a very fine level of detail, while the daily data method resulted in a more general overview of erosivity patterns and did not pick up localised variations as effectively. The erosivity density method showed lower rainfall erosivity values than the daily data method, in general. It also produced a much lower maximum annual rainfall erosivity than the daily data method (5 866 MJ.mm.ha⁻¹.h⁻¹ vs. 16 399 MJ.mm.ha⁻¹.h⁻¹).

The verification of the interpolation of the erosivity density values gave poor results (an overall error of 75 %), indicating that the spatial density of the data was too low. This was improved in the daily data approach through the use of a greater number of daily rainfall stations,

achieving an overall interpolation error of 43%. However, when verifying the results against observed erosivity at test stations, the erosivity density method performed better, achieving an error of 55 %, compared with 91 % for the daily data method. Both methods showed potential, but require a larger network of short duration stations, in order to improve accuracy.

A tool was developed to assist in contour interval determination. This took the form of a Microsoft Excel spreadsheet. The tool utilised the updated rainfall erosivity values determined in the study and focussed on determining recommended contour intervals in sugarcane plantations. The tool took into account the timing of erosive rainfall relative to crop development and tillage operations. Various scenarios were modelled and the results of the spreadsheet were compared to current methods used in the sugarcane industry. The spreadsheet was found to be highly sensitive to slope and the results suggested that soil erosion in sugarcane plantations has previously been underestimated, particularly on steep slopes.

The study highlighted the need for ongoing research in the field of soil conservation.

TABLE OF CONTENTS

	Page
1. INTRODUCTION	1
2. MECHANICAL SOIL CONSERVATION MEASURES	5
2.1 Vegetated Waterways	6
2.2 Contour Banks	7
2.2.1 Purpose of contour banks	7
2.2.2 Methods of contour bank spacing.....	8
3. MODELLING SOIL LOSS	11
3.1 Types of Soil Loss Models	11
3.1.1 Empirical models.....	11
3.1.2 Physically-based models	12
3.1.3 Conceptual models	12
3.2 Empirical Soil Loss Estimation Models Used in South Africa	13
3.2.1 Soil Loss Estimation Model for Southern Africa (SLEMSA)	13
3.2.2 Universal Soil Loss Equation (USLE)	14
3.2.3 Revised Universal Soil Loss Equation (RUSLE).....	17
4. METHODS TO DETERMINE RAINFALL EROSIVITY WITH LIMITED, CONTINUOUSLY RECORDED RAINFALL DATA.....	33
4.1 Regression Analysis Method	33
4.1.1 Linear regression with various daily rainfall parameters	34
4.1.2 Power regression with daily rainfall amount.....	35
4.1.3 Sinusoidal function to account for seasonality of erosivity	37
4.2 Erosivity Density Method.....	39
5. ESTIMATING RAINFALL EROSIVITY IN SOUTH AFRICA USING THE EROSIVITY DENSITY METHOD	41
5.1 Methodology.....	41
5.1.1 Data acquisition.....	41
5.1.2 Calculation of erosivity density.....	45
5.1.3 Use of thresholds	47
5.1.4 Spatial interpolation of erosivity density data.....	48
5.1.5 Selection of independent test stations.....	49
5.1.6 Use of Quinary Catchment rainfall data.....	51

5.2	Results and Discussion of Erosivity Density Method	53
5.2.1	Effect of different energy equations	54
5.2.2	Effect of thresholds	57
5.2.3	Cross-validation results	60
5.2.4	Verification results	61
5.2.5	Maps	70
5.3	Conclusion on the Erosivity Density Method.....	74
6.	USING DAILY DATA TO IMPROVE ESTIMATES OF RAINFALL EROSIVITY ..	78
6.1	Methodology.....	78
6.1.1	Identification of homogeneous regions	78
6.1.2	Development of rainfall erosivity relationships	80
6.1.3	Selection of daily stations.....	83
6.1.4	Spatial interpolation of rainfall erosivity data	85
6.1.5	Selection of independent test stations.....	85
6.2	Results of Daily Data Method	86
6.2.1	Cross-validation results	86
6.2.2	Verification results	88
6.2.3	Maps	92
6.3	Comparison of Calculation Methods	95
6.4	Comparison with Previous Studies	99
6.5	Conclusion on the Daily Data Method	101
7.	DEVELOPMENT OF A TOOL TO ESTIMATE CONTOUR INTERVALS.....	103
7.1	Structure of the Contour Interval Calculation Tool	103
7.1.1	Tolerable soil loss.....	104
7.1.2	Rainfall data	104
7.1.3	Soil erodibility	105
7.1.4	Slope	105
7.1.5	Support practice factor	105
7.1.6	Cover factor	105
7.1.7	Calculation of slope length.....	110
7.2	Comparison of Spreadsheet and Nomograph Results.....	110
7.3	A Synthesis of the Comparison and Suggestions for the Way Forward.....	118
8.	DISCUSSION AND CONCLUSIONS	120
9.	REFERENCES	124

10. APPENDIX A: EROSIVITY DENSITY MAPS.....	131
11. APPENDIX B: RAINFALL EROSIVITY MAPS OBTAINED USING THE EROSIVITY DENSITY METHOD	138
12. APPENDIX C: RELATIONSHIPS BETWEEN DAILY RAINFALL AMOUNTS AND RAINFALL EROSIVITY.....	145
13. APPENDIX D: RAINFALL EROSIVITY MAPS OBTAINED USING THE DAILY DATA METHOD	160

LIST OF FIGURES

		Page
Figure 2.1	Soil conservation measures for agricultural land (Morgan, 2005; after El-Swaify <i>et al.</i> , 1982).....	5
Figure 2.2	Components of a contour bank system (Russell, 1998b).....	6
Figure 2.3	Graph for the determination of contour bank intervals in low rainfall areas (after Russell, 1998c).....	9
Figure 3.1	Contour spacing nomograph (Smithen, 1989).....	15
Figure 3.2	Nomograph to determine contour bank spacing for sugarcane cultivation (Platford, 1987).....	16
Figure 3.3	Example simulation of the RUSLE2 Profile Module.....	17
Figure 3.4	The soil erodibility nomograph to estimate K (Renard <i>et al.</i> , 1997).....	20
Figure 3.5	Soil erodibility map of South Africa (Le Roux <i>et al.</i> , 2006).....	23
Figure 3.6	Iso-erodent map of the USA (Wischmeier and Smith, 1978).....	29
Figure 4.1	Rainfall erosivity map of South Africa produced by Smithen and Schulze (1982).....	35
Figure 4.2	General relationship between precipitation amount and rainfall erosivity for individual storms, using the power function (Richardson <i>et al.</i> , 1983).....	36
Figure 4.3	Annual rainfall erosivity map of South Africa (Le Roux <i>et al.</i> , 2006)...	38
Figure 5.1	Original continuously recording stations available to the study, with records exceeding 10 complete years.....	42
Figure 5.2	Selection of representative stations in research catchments.....	43
Figure 5.3	Short duration stations used in the estimation of erosivity density.....	44
Figure 5.4	Record length distribution of final selection of continuously recording stations.....	45
Figure 5.5	Graphical representation of the five selected energy equations for use in RAINX.....	46
Figure 5.6	Location of verification stations within the homogeneous clusters defined by Smithers and Schulze (2000).....	50
Figure 5.7	Quinary Catchments determined by Schulze and Horan (2011).....	52
Figure 5.8	Annual rainfall distribution across the Quinary Catchments derived by summing the monthly median rainfall amounts (Schulze <i>et al.</i> , 2011)..	53

Figure 5.9	The effect of different energy equations on mean monthly erosivity density values for all short duration stations	54
Figure 5.10	The effect of different energy equations on the mean annual rainfall erosivity for all short duration stations	55
Figure 5.11	Location of the Cedara station (0239482) in KwaZulu-Natal	56
Figure 5.12	The effect of different energy equations on erosivity density values at Cedara, KwaZulu-Natal	57
Figure 5.13	The effect of applying thresholds to data on erosivity density values	58
Figure 5.14	The effect of thresholds on erosivity density values at Cedara, KwaZulu-Natal.....	59
Figure 5.15	Cross validation results for the interpolation of mean annual erosivity density values.....	61
Figure 5.16	Erosivity density for September in the region of the Levubu station	63
Figure 5.17	The effect of data scarcity on errors in verification at Graaff-Reinet	64
Figure 5.18	Reduction in monthly erosivity density due to application of 12.7 mm threshold at Graaff-Reinet	64
Figure 5.19	Comparison of absolute error and relative error at Graaff-Reinet	65
Figure 5.20	Erosivity density for January in the region of the Vredendal station.....	66
Figure 5.21	Comparison of predicted and observed erosivity density for all months and verification stations.....	67
Figure 5.22	Cumulative frequency of relative errors obtained in verification	68
Figure 5.23	Difference between predicted and observed annual rainfall erosivity at the verification test stations, for the erosivity density method	70
Figure 5.24	Mean annual erosivity density in South Africa.....	71
Figure 5.25	Comparison of erosivity density for January and July.....	72
Figure 5.26	Mean annual rainfall erosivity for South Africa calculated using the erosivity density method.....	73
Figure 5.27	Comparison of rainfall erosivity in January and July, calculated using the erosivity density method.....	74
Figure 6.1	Homogeneous clusters identified by Smithers and Schulze (2000).....	79
Figure 6.2	Example of monthly regression analysis of rainfall erosivity against various rainfall parameters (January, Short Duration Cluster 3).....	80
Figure 6.3	Example of monthly regression analysis of erosivity density against various rainfall parameters (January, Short Duration Cluster 3).....	81

Figure 6.4	Example of power regression analysis of daily rainfall erosivity against daily rainfall (January, Short Duration Cluster 3)	83
Figure 6.5	Locations of daily rainfall stations used in calculating rainfall erosivity	84
Figure 6.6	Location of daily test stations within the homogeneous clusters	86
Figure 6.7	Cross-validation results of the interpolation of rainfall erosivity at daily data stations.....	87
Figure 6.8	Differences between predicted and observed annual rainfall erosivity at the verification test stations, for the ‘daily data’ method	91
Figure 6.9	Location of short duration stations within short duration clusters	92
Figure 6.10	Mean annual rainfall erosivity calculated using daily data.....	93
Figure 6.11	Example of 'bull's-eyes' caused by different regression equations on each side of a cluster border	94
Figure 6.12	Comparison of rainfall erosivity for January and July using the ‘daily data’ method	94
Figure 6.13	Comparison of annual rainfall erosivity using two different calculation methods.....	95
Figure 6.14	Error map to show the difference in magnitude of annual rainfall erosivity using the daily data method compared to the erosivity density method.	96
Figure 6.15	Comparison of January rainfall erosivity results using two different calculation methods	97
Figure 6.16	Comparison of July rainfall erosivity results using two different calculation methods	98
Figure 6.17	Comparison of calculation methods at validation stations.....	99
Figure 6.18	Annual rainfall erosivity maps for South Africa as derived by Smithen and Schulze (1981), left, and Le Roux <i>et al.</i> (2006), right.....	100
Figure 6.19	Annual rainfall erosivity maps for South Africa as derived using the erosivity density method (left) and the daily data method (right)	100
Figure 7.1	An example of how RUSLE2 disaggregates monthly precipitation values to obtain daily values (USDA-ARS, 2013)	104
Figure 7.2	Relationship between the canopy cover sub-factor and the <i>C</i> factor for sugarcane adopted in this study	107
Figure 7.3	Canopy cover characteristics for sugarcane, from planting until 1 st harvest	109
Figure 7.4	Location of test Quinary W11B3	111

Figure 7.5	The effect of slope on the spreadsheet calculations of recommended contour interval for various levels of soil erodibility	113
Figure 7.6	Comparison of the nomograph and spreadsheet results for a moderately erodible soil and burnt cane harvesting	114
Figure 7.7	Comparison of the effect of slope on <i>S</i> factor values for the spreadsheet (McCool <i>et al.</i> , 1987) and the nomograph (Wischmeier and Smith, 1978)	115
Figure 7.8	The effect of the <i>C</i> factor on the results of the spreadsheet	116
Figure 7.9	Comparison of the average annual <i>CR</i> product and the actual <i>CR</i> product throughout the crop cycle	117
Figure 7.10	The effect of the application of a 'minimum tillage' support practice factor to the spreadsheet.....	118
Figure 10.1	Erosivity density map of South Africa for January.....	131
Figure 10.2	Erosivity density map of South Africa for February.....	132
Figure 10.3	Erosivity density map of South Africa for March.....	132
Figure 10.4	Erosivity density map of South Africa for April.....	133
Figure 10.5	Erosivity density map of South Africa for May.....	133
Figure 10.6	Erosivity density map of South Africa for June.....	134
Figure 10.7	Erosivity density map of South Africa for July	134
Figure 10.8	Erosivity density map of South Africa for August.....	135
Figure 10.9	Erosivity density map of South Africa for September	135
Figure 10.10	Erosivity density map of South Africa for October	136
Figure 10.11	Erosivity density map of South Africa for November	136
Figure 10.12	Erosivity density map of South Africa for December.....	137
Figure 10.13	Mean annual erosivity density map of South Africa.....	137
Figure 11.1	Rainfall erosivity map of South Africa for January, calculated using the erosivity density method.....	138
Figure 11.2	Rainfall erosivity map of South Africa for February, calculated using the erosivity density method.....	139
Figure 11.3	Rainfall erosivity map of South Africa for March, calculated using the erosivity density method.....	139
Figure 11.4	Rainfall erosivity map of South Africa for April, calculated using the erosivity density method.....	140

Figure 11.5	Rainfall erosivity map of South Africa for May, calculated using the erosivity density method.....	140
Figure 11.6	Rainfall erosivity map of South Africa for June, calculated using the erosivity density method.....	141
Figure 11.7	Rainfall erosivity map of South Africa for July, calculated using the erosivity density method.....	141
Figure 11.8	Rainfall erosivity map of South Africa for August, calculated using the erosivity density method.....	142
Figure 11.9	Rainfall erosivity map of South Africa for September, calculated using the erosivity density method.....	142
Figure 11.10	Rainfall erosivity map of South Africa for October, calculated using the erosivity density method.....	143
Figure 11.11	Rainfall erosivity map of South Africa for November, calculated using the erosivity density method.....	143
Figure 11.12	Rainfall erosivity map of South Africa for December, calculated using the erosivity density method.....	144
Figure 11.13	Annual rainfall erosivity map of South Africa, calculated using the erosivity density method.....	144
Figure 12.1	Regression analysis of daily rainfall amount and rainfall erosivity for Cluster 1.....	146
Figure 12.2	Regression analysis of daily rainfall amount and rainfall erosivity for Cluster 2.....	147
Figure 12.3	Regression analysis of daily rainfall amount and rainfall erosivity for Cluster 3.....	148
Figure 12.4	Regression analysis of daily rainfall amount and rainfall erosivity for Cluster 5.....	149
Figure 12.5	Regression analysis of daily rainfall amount and rainfall erosivity for Cluster 6.....	150
Figure 12.6	Regression analysis of daily rainfall amount and rainfall erosivity for Cluster 7.....	151
Figure 12.7	Regression analysis of daily rainfall amount and rainfall erosivity for Cluster 8.....	152
Figure 12.8	Regression analysis of daily rainfall amount and rainfall erosivity for Cluster 9.....	153

Figure 12.9	Regression analysis of daily rainfall amount and rainfall erosivity for Cluster 10.....	154
Figure 12.10	Regression analysis of daily rainfall amount and rainfall erosivity for Cluster 11.....	155
Figure 12.11	Regression analysis of daily rainfall amount and rainfall erosivity for Cluster 12.....	156
Figure 12.12	Regression analysis of daily rainfall amount and rainfall erosivity for Cluster 13.....	157
Figure 12.13	Regression analysis of daily rainfall amount and rainfall erosivity for Cluster 14.....	158
Figure 12.14	Regression analysis of daily rainfall amount and rainfall erosivity for Cluster 15.....	159
Figure 13.1	Rainfall erosivity map of South Africa for January, calculated using the daily data method.....	160
Figure 13.2	Rainfall erosivity map of South Africa for February, calculated using the daily data method.....	161
Figure 13.3	Rainfall erosivity map of South Africa for March, calculated using the daily data method.....	161
Figure 13.4	Rainfall erosivity map of South Africa for April, calculated using the daily data method.....	162
Figure 13.5	Rainfall erosivity map of South Africa for May, calculated using the daily data method.....	162
Figure 13.6	Rainfall erosivity map of South Africa for June, calculated using the daily data method.....	163
Figure 13.7	Rainfall erosivity map of South Africa for July, calculated using the daily data method.....	163
Figure 13.8	Rainfall erosivity map of South Africa for August, calculated using the daily data method.....	164
Figure 13.9	Rainfall erosivity map of South Africa for September, calculated using the daily data method.....	164
Figure 13.10	Rainfall erosivity map of South Africa for October, calculated using the daily data method.....	165
Figure 13.11	Rainfall erosivity map of South Africa for November, calculated using the daily data method.....	165

Figure 13.12	Rainfall erosivity map of South Africa for December, calculated using the daily data method.....	166
Figure 13.13	Annual rainfall erosivity map of South Africa, calculated using the daily data method.....	166

LIST OF TABLES

		Page
Table 2.1	Suggested soil loss tolerances in $t.ha^{-1}.a^{-1}$ (after Smithen, 1989).....	10
Table 3.1	Erodibility factors for various soil erodibility classes (Lorentz and Schulze, 1995)	19
Table 3.2	Permeability classes for different soil texture classes (after Renard <i>et al.</i> , 1997)	22
Table 3.3	<i>P</i> factor when only slope is known (after Wischmeier and Smith, 1978)	27
Table 5.1	Relative errors between predicted and observed erosivity density values at the verification test stations (%)	62
Table 5.2	Prediction errors of mean annual erosivity density ($MJ.ha^{-1}.h^{-1}$).....	67
Table 5.3	Relative errors between predicted and observed rainfall erosivity values at the verification test stations, for the erosivity density method (%)	69
Table 6.1	Validation results for the interpolation of rainfall erosivity values (%) .	89
Table 6.2	Relative errors between predicted and observed rainfall erosivity values at the verification test stations, for the ‘daily data’ method (%)	90
Table 7.1	Ratios used to apply effects of tillage on sugarcane canopy cover and fall height	110
Table 7.2	Soil erodibility factors used in the development of the nomograph (after Platford, 1987)	112
Table 7.3	Soil properties used in the testing of the spreadsheet	112

1. INTRODUCTION

Soil erosion is a process which involves the detachment of soil particles by erosive agents, such as water and wind, and their subsequent transport from their original location (Morgan, 2005). A number of soil erosion categories have been defined, including rill, interrill, gully, streambed and streambank erosion (Aksoy and Kavvas, 2005). Rill erosion and interrill erosion typically contribute a large portion of a catchment's gross erosion and these are the types of soil erosion most commonly encountered in agricultural applications (Wischmeier and Smith, 1978). The Agricultural Research Services of the United States Department of Agriculture (USDA-ARS) provide the following descriptions of rill and interrill erosion. Interrill erosion is predominantly caused by raindrop impact and thin layers of overland flow. This type of erosion generally causes uniform erosion over an area. Rill erosion takes place when surface runoff is concentrated into small channels (rills), causing localised erosion of these channels. Rill erosion increases with distance along the flow path, as runoff volumes and velocities increase (USDA-ARS, 2013).

Soil erosion is a significant environmental issue internationally, and particularly in South Africa (Le Roux *et al.*, 2008). In fact, according to Garland *et al.* (2000), previous studies have indicated that more than 70% of South Africa's surface area is affected by water erosion to some degree, with the predominant cause being poor agricultural practices. Soil erosion has both on-site and off-site effects, which result in significant economic losses. On-site effects include loss and redistribution of soil in the field, breakdown of the structure of the soil and a decline in both nutrients and organic matter in the soil (Morgan, 2005). Another effect of soil erosion is a reduction in available soil moisture. This is the result of two main factors. Firstly, the runoff rate on eroded soils is generally higher than that of non-eroded soils, leading to less water entering the soil profile (Pimentel *et al.*, 1995). Secondly, according to Hudson (1994), the available water holding capacity of the soil is strongly influenced by the organic matter content. Therefore, as the organic matter is eroded, the soil water holding capacity decreases. These effects result in reduced soil fertility and arable soil depth, as well as increased susceptibility to drought. Ultimately, soil erosion results in decreased productivity, with an associated increase in fertiliser use to maintain yields (Morgan, 2005).

Off-site effects of soil erosion include sedimentation, with a resultant reduction in life span, of water storage infrastructure. For example, the Welbedacht Dam, on the Caledon River in South

Africa, lost 32 % of its capacity to sedimentation in the three years following its construction (Russell, 1998a). As most of the favourable dam sites in South Africa have already been used, the cost of building new dams is increasing because the new sites are less economically viable. In 1990, the annual cost of creating new water storage, to compensate for that lost due to sedimentation, was estimated as being between R71 500 000 and R104 000 000 (Scotney and McPhee, 1990; cited by Russell, 1998a). The reduced capacity or blockage of rivers and drainage structures also leads to increased flooding risk (Morgan, 2005).

In many parts of South Africa, certain conditions exacerbate the problem of erosion and make the undertaking of soil conservation particularly challenging. These factors include “arid climatic conditions, intense thundershower activity with inherent high rainfall erosivity, shallow erodible soils, limited vegetation cover, and/or poor conservation management techniques” (Morgan, 2005). It is therefore critical that erosion control be improved, particularly in agricultural areas. In South Africa, responsibility is placed on land owners to reduce soil erosion on their land (*e.g.* Conservation of Agricultural Resources Act, 1983). Although standards are in place to conserve agricultural land, the methods must be continually updated as more information and computing power becomes available.

Most factors influencing soil erosion, such as the effect of tillage practices, land cover or soil texture, are universal and applicable in different locations with similar conditions. This enables the application of the extensive research undertaken by institutions, such as the United States Department of Agriculture (USDA), in other locations. The one factor which is highly dependent on location is precipitation. Climate data is location-specific and estimation of erosion must utilise local precipitation data and precipitation characteristics. Although rainfall erosivity, a measure of the ability of rainfall to cause soil erosion, has been estimated for South Africa (*e.g.* Smithen and Schulze, 1982; Le Roux *et al.*, 2006), previous studies have utilised limited amounts of continuously recorded rainfall data, from which rainfall intensity can be determined. These studies generally relied on models and relationships with daily precipitation data. Given the increasing number of continuously recording rainfall stations, coupled with increasing record lengths, it is expected that estimates of rainfall erosivity could be improved. Hence, the main aim of this study was to improve the estimates of rainfall erosivity in South Africa by using available continuously recorded data, from which rainfall intensity can be calculated.

A study performed by the USDA Agricultural Research Service (USDA-ARS) found that in the absence of sufficient data, determining rainfall erosivity directly from short duration data caused inconsistent trends and the method was not recommended (USDA-ARS, 2013). The method adopted by the USDA-ARS was an erosivity density method. This method is, as yet, untested in South Africa and so the aim of this study was to test the application of the erosivity density method in South Africa. In addition to this, a second approach was adopted, which involved developing relationships with more readily available daily rainfall data.

Many soil loss estimation models have been developed to estimate how much soil is being lost from agricultural lands, for example the Universal Soil Loss Equation (Wischmeier and Smith, 1965), the Soil Loss Estimation Model for Southern Africa (Elwell, 1978) and the Agricultural Catchments Research Unit model (Schulze, 1995). Each of these models has its own applications, advantages and limitations. As computing power has improved, so these models have come to play an increasing role in soil and water conservation. Significant advances have been made in modelling soil erosion, and soil conservation design tools now range from relatively simplistic empirical models to incredibly complex physically-based models. Although complex, physically-based models should be able to provide more accurate estimates of soil loss than simpler empirical models, they often require vast amounts of information, not all of which is readily available to the average farmer or design engineer (Smith, 1999). Therefore, a secondary aim of this project was to develop a relatively simple soil conservation design tool, which incorporated updated and readily available data, yet was easy to use.

The objectives of this study were to:

- (a) provide an overview of mechanical soil conservation methods in South Africa,
- (b) investigate the design approaches used to determine contour bank intervals,
- (c) review the main soil loss estimation models used currently in South Africa and internationally,
- (d) update estimates of rainfall erosivity across South Africa using the erosivity density method,
- (e) assess the impact of various rainfall energy equations on estimates of rainfall erosivity,
- (f) assess the impact of applying thresholds to rainfall events on the estimates of rainfall erosivity,
- (g) estimate and interpolate rainfall erosivity across South Africa using daily rainfall data,
- (h) assess the performance of the approaches to estimate rainfall erosivity, and

- (i) develop and assess a user-friendly software tool to determine contour bank spacing for the design of soil conservation structures.

Chapter 2 contains a brief overview of the mechanical soil conservation methods used in South Africa, as well as various design approaches for determining contour bank intervals. A review of soil loss estimation models follows in Chapter 3, while methods for estimating rainfall erosivity are discussed in Chapter 4. Chapter 5 describes the process of estimating rainfall erosivity using the erosivity density method in South Africa, and includes results of the application of this approach in South Africa. Similarly, Chapter 6 describes the ‘daily data’ method and contains the results obtained from the application of this approach in South Africa. The development of a design tool to determine contour bank intervals is presented in Chapter 7. Finally, Chapter 8 contains a discussion on the literature reviewed and the results emanating from this research, as well as conclusions drawn from the study.

2. MECHANICAL SOIL CONSERVATION MEASURES

One of the main objectives of studying soil loss is to prevent or minimise soil loss in various applications. By understanding the factors contributing to soil loss, these factors can, to a certain extent, be controlled to protect the soil and achieve a desired outcome. In soil and water conservation, the various measures used to protect the soil are divided into three main categories: soil management measures, agronomic measures and mechanical measures (Morgan, 2005). Soil management measures include activities which conserve or improve the soil structure (*e.g.* minimum tillage), while agronomic measures are those which use the vegetation to protect the soil, such as cover cropping. Mechanical measures are those activities which change the topography and alter the pattern of runoff (Morgan, 2005). Examples of the various measures are summarised in Figure 2.1.

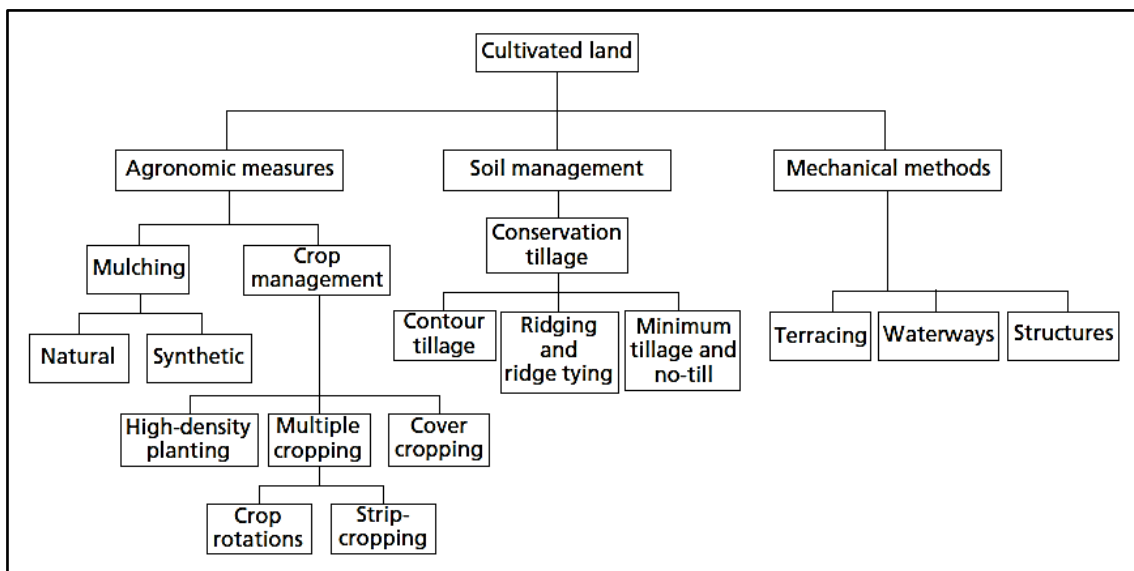


Figure 2.1 Soil conservation measures for agricultural land (Morgan, 2005; after El-Swaify *et al.*, 1982)

Mechanical measures are not always necessary in certain instances. However, in most cases it is beneficial to install some form of engineering works, in order to provide a foundation on which agronomic or soil management measures can be based (Matthee, 1984). According to Morgan (2005), contouring has moderate control over the detachment of soil particles and strong control over the transport of these particles, in the process of runoff erosion.

Contour banks and vegetated waterways are the mechanical conservation measures commonly used in South Africa to control runoff erosion. In a typical runoff control plan, the contour banks intercept water flowing downslope, and lead it into either a natural waterway or an artificial grassed waterway (Matthee, 1984), as shown in Figure 2.2. The artificial grassed waterway then conveys the runoff to an established natural channel.

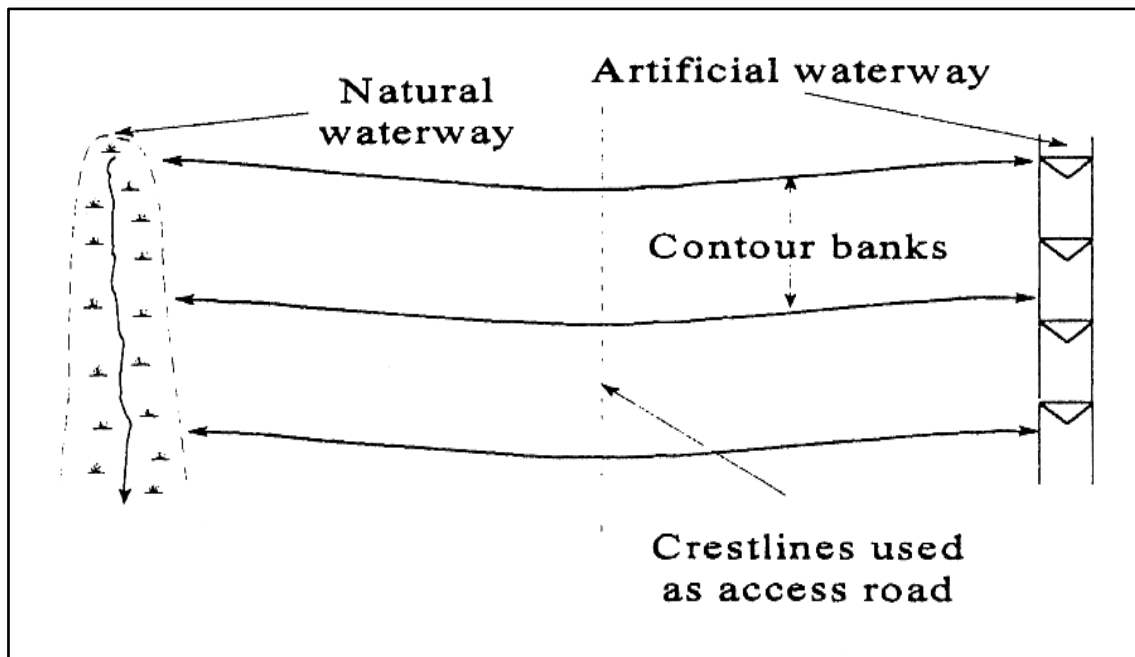


Figure 2.2 Components of a contour bank system (Russell, 1998b)

In this chapter, these two mechanical structures, namely vegetated waterways and contour banks, are defined and their roles in runoff management are explained.

2.1 Vegetated Waterways

A vegetated waterway is “a shaped or graded channel that is established with suitable vegetation to carry surface water at a non-erosive velocity to a stable outlet” (USDA-NRCS, 2012). Vegetated waterways are used where the duration of flow is less than the maximum inundation period that can be withstood by the grass, and the frequency of operation is low enough to maintain an adequate grass cover (USDA-NRCS, 2007a). According to the USDA-NRCS (2012), vegetated waterways have three main purposes. These are to:

- (a) carry surface water from contour banks or other concentrations of water without causing scouring or flooding,
- (b) reduce gully formation, and

- (c) conserve or improve water quality.

Grassed waterways are usually wide and shallow, in order to limit the velocity of the water in the channel and thus to minimise soil erosion.

2.2 Contour Banks

Contour banks, also known as terraces, are typically earth embankments that are built across the main slope of a field. Their main purpose is to intercept runoff water (Matthee, 1984). According to ASABE Standard S268.5 (2012), contour banks have three major functions. These are to decrease soil erosion, retain moisture for utilisation by crops and to improve the quality of the water, as explained below.

2.2.1 Purpose of contour banks

There are numerous ways in which contour banks reduce soil loss from a given area. Firstly, the contour banks shorten the distance over which surface runoff travels by dividing the slope into shorter sections. This reduces runoff velocity and volume and, hence, decreases rill erosion. Secondly, the contour banks force tillage operations to be performed on the contour, rather than up and down the slope. Lastly, contour banks transport water to suitable outlet points at low velocities (Matthee, 1984). According to Huffman *et al.* (2011), contour banks “serve to retain runoff and increase the amount of water available for crop production.” Contour banks intercept runoff flowing downslope, thereby allowing a greater proportion of the water to infiltrate the soil and become available for use by crops. Contour banks improve water quality by reducing the runoff velocity, resulting in less energy with which to transport sediment, leading to cleaner runoff.

There are many components in the design of a contour bank system. These include the determination of the correct contour bank spacing and layout of contour banks, the design of a suitable channel which has sufficient capacity, as well as the design of a cross-section which is stable and can be farmed if required (Huffman *et al.*, 2011). Except in the case of level contours, the channels should have continuous positive drainage along their entire length, and must convey the maximum flow at non-scouring velocities (ASABE Standard S268.5, 2012). According to Huffman *et al.* (2011), the most important factors in the design are “soil characteristics, cropping and soil management practices, and climatic conditions”.

2.2.2 Methods of contour bank spacing

The spacing of contour banks is calculated in order to effectively reduce sheet and rill erosion. Two main approaches are used to calculate suitable contour bank spacing. These are the vertical interval equation and soil erosion prediction tools.

2.2.2.1 Vertical interval equation

The present version of the Vertical Interval Equation, as shown in Equation 2.1, is provided in ASABE Standard S268.5 (2012). Ranges of parameter values have been determined for a number of countries, including the USA (ASABE Standard S268.5, 2012) and South Africa (Matthee, 1984; Matthee, 1989).

$$VI = XS + Y \quad (2.1)$$

where

VI = maximum vertical interval [m],

X = a variable which takes into account climate characteristics (Matthee, 1984),

S = land slope [%], and

Y = a variable which takes into account on soil erodibility, the crop and the cropping system (Matthee, 1984).

In South Africa, the form shown in Equation 2.2 is commonly used (Matthee, 1989). It can be seen that Equation 2.2 assigns one set of parameter values to the equation and thereby ignores location-specific factors, such as climate and soil types.

$$VI = \frac{S}{10} + 0.61 \quad (2.2)$$

Russell (1998c) presents graphs to assist with the determination of contour spacing. An example of these graphs can be found in Figure 2.3. Three graphs were developed for low rainfall (MAP < 750 mm), medium rainfall (MAP between 750 and 900 mm) and high rainfall (MAP > 900 mm) areas respectively. The vertical interval of the contour banks is determined based on the slope of the land and the soil erodibility, *i.e.* the resistance of the soil type to erosion.

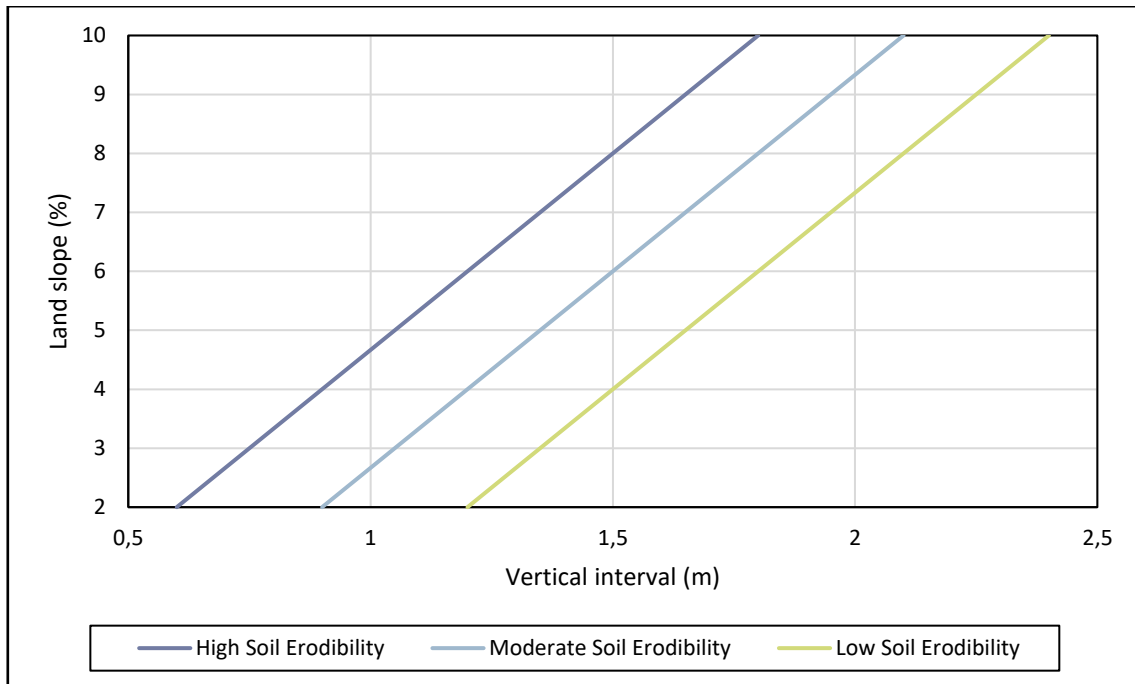


Figure 2.3 Graph for the determination of contour bank intervals in low rainfall areas (after Russell, 1998c)

Although the graphs take into account some factors affecting soil erosion, *i.e.* rainfall and soil type, many factors are still ignored, such as crop type and management practices. In order to determine the necessary contour bank spacing at a specific site, a soil erosion prediction tool can be used to model the contour bank scenario and estimate the resultant soil erosion.

2.2.2.2 Soil erosion prediction tools

The preferred method of contour bank spacing is to use site-specific evaluation of the potential rill and sheet erosion of the fields with the proposed contour banks. In the USA, this is commonly done using the Natural Resources Conservation Service (NRCS) erosion prediction software/technology (ASABE Standard S268.5, 2012). Examples of commonly used soil erosion models are provided in the following chapter. Site-specific evaluation aims to calculate the slope length (*i.e.* contour bank interval), under given conditions, which will lead to a “tolerable soil loss”. The predicted soil loss of the field with the planned contour bank interval must not exceed the tolerable soil loss.

The definition of “soil loss tolerance”, alternatively termed “permissible soil loss”, is “the maximum rate of soil erosion that can occur and still permit soil productivity to be sustained economically” (Renard *et al.*, 1997). Soil loss tolerance does not only take into account the loss

of productivity due to erosion, but also the rate of soil formation from parent material. Although the above definition is relevant for agricultural applications, it is becoming increasingly evident that offsite effects should also be taken into account in determining soil loss tolerance. For example, soil loss tolerance determination should also factor in the pollution and sedimentation effects downstream of the eroded area, due to the attachment of fertilisers and pesticides to the eroded soil particles (Morgan, 2005). If the soil loss is less than the value of the soil loss tolerance, erosion control measures are considered to be adequate, and the activities causing soil loss are deemed sustainable. A related concept is that of Soil Life Expectancy. This is defined as “how long a soil can be subjected to a specific crop or practice before its sustained productivity is seriously affected by losses” (Matthee, 1984). The equation used to determine soil life takes into account the effective depth of the soil, the required soil depth for crop production and the rates of soil loss and formation. Table 2.1 lists recommended soil loss tolerances for use in South Africa.

Table 2.1 Suggested soil loss tolerances in $t \cdot ha^{-1} \cdot a^{-1}$ (after Smithen, 1989)

Material underlying topsoil or E horizon	Clay in B Horizon (%)				
	Undifferentiated	0-6	6-15	15-35	Above 35
Organic O Vertic A	9	-	-	-	-
Yellow Brown Apedal Red Apedal Red structured B	-	6	7	8	9
E Horizon O Horizon Pedocutanic B Soft Plinthic B Neocutanic B Prismacutanic B Lithocutanic B	-	4	5	6	7
Hard Plinthite Rock	-	3	4	5	6

Following the above explanation of soil conservation methods, it is evident that mechanical methods play a large role in the preservation of soil in agricultural applications. The use of detailed soil erosion prediction tools is the preferred method in determining contour bank spacing, rather than generic equations. The following chapter discusses available soil erosion models to estimate soil loss.

3. MODELLING SOIL LOSS

The estimation of soil loss is often required for planning and design purposes. In order to improve the accuracy of soil loss estimations, it is necessary to represent the processes governing soil loss as accurately as possible. Many different models have been developed to estimate soil loss under different conditions. As stated by Merritt *et al.* (2003), “these models differ greatly in terms of their complexity, their inputs and requirements, the processes they represent and the manner in which these processes are represented, the scale of their intended use and the types of output information they provide.”

This chapter gives an overview of the main types of soil erosion models available and describes some of the most widely used empirical models.

3.1 Types of Soil Loss Models

While the spectrum of soil erosion models is vast, it can be separated into three broad categories, namely empirical, physically-based and conceptual models. These categories are described below. It must be noted that a model may fit into more than one category, and that the categorisation of models can be subjective (Merritt *et al.*, 2003).

3.1.1 Empirical models

In general terms, empirical models can be considered the simplest of the three classes of models. They are also known as statistical or metric models (Merritt *et al.*, 2003). Empirical models relate sediment loss to a number of variables through regression equations (Morgan, 2005). Although empirical models tend to over-simplify erosion processes, they are highly useful in circumstances where limited data are available. In this regard, they may be preferable to more complex models in a number of cases (Merritt *et al.*, 2003). Well-known examples of empirical models for estimating soil loss are the Universal Soil Loss Equation (USLE) developed by Wischmeier and Smith (1965), as well as the more recent Revised Universal Soil Loss Equation (RUSLE) developed by Renard *et al.* (1991). Both the USLE and RUSLE were developed by the United States Department of Agriculture (USDA). Smith (1999) states that “empirical relationships should normally be considered valid only within the range of experimental conditions under which they were derived.” The inability to extrapolate empirical equations beyond their data range means that they cannot normally be applied to extreme events or other geographical locations (Morgan, 2005). However, in the case of the USLE, Wischmeier and

Smith (1965) state that if the values of the factors can be determined, it is possible to apply the equation at any site.

3.1.2 Physically-based models

According to Merritt *et al.* (2003), “physics-based models are based on the solution of fundamental physics equations describing streamflow and sediment...in a catchment”. These models typically utilise a differential continuity equation, applying the laws of conservation of mass and momentum, to quantify erosion and deposition (Morgan, 2005). Theoretically, all of the parameters used in these models should be measurable, however, this is not always possible and in many cases parameter values must be obtained by calibrating against observed data (Merritt *et al.*, 2003). This means that some of the erosion processes are actually represented by empirical relationships (Morgan, 2005).

The structures of physically-based models are generally much more complex than those of empirical or conceptual models. In addition to this, physically-based models often allow predictions on an event basis, rather than the average annual values commonly produced by empirical models (Le Roux *et al.*, 2006). The USDA-Water Erosion Prediction Project (WEPP) is a process-based model which takes into account detachment, transport and deposition of sediment (Nearing *et al.*, 1989).

3.1.3 Conceptual models

Conceptual models bridge the gap between empirical and physically-based models (Le Roux *et al.*, 2006). According to Sorooshian (1991), conceptual models are based on general physical processes. However within these, the sub-processes are modelled empirically and linked according to a conceptual order. Conceptual soil erosion models typically use the concept of internal storages to model catchment responses. Sediment flow paths are modelled as a series of storages, with the behaviour of each process typically calibrated against observed data (Merritt *et al.*, 2003).

Conceptual models are typically used to model sediment yield, rather than long-term average soil loss (Le Roux *et al.*, 2006). Soil loss is defined as the amount of soil which is relocated from its original position through the process of erosion (detachment, transport and deposition). In contrast, sediment yield is the amount of soil that is eroded minus the amount which is deposited before it reaches the point of interest (Renard *et al.*, 1997). The sediment yield is

typically the amount of sediment leaving a catchment via the catchment's river (Morgan, 2005). The Modified Universal Soil Loss Equation (MUSLE), developed by Williams (1975) is an example of a conceptual model used to calculate sediment yield.

3.2 Empirical Soil Loss Estimation Models Used in South Africa

Complex models that simulate the erosion processes can provide accurate estimates of soil loss. However, this detailed approach is often not practical or possible due to the limited availability of numerous input parameters, which are not practical for the average farmer or engineer to measure or obtain. These models also often require calibration and therefore cannot be easily or quickly transferred and applied to a number of different sites (Lorentz and Schulze, 1995). A large number of measured parameters may not be available in many locations in South Africa (Smith, 1999). For these reasons, simple empirical methods have been found to be more effective in providing adequate estimates of soil loss for initial planning and design purposes. A number of these empirical models are discussed below.

The soil loss models most commonly used in southern Africa include the Soil Loss Estimation Model for Southern Africa (SLEMSA), the USLE and the RUSLE (Smith, 1999). This section provides an overview of each of these models.

3.2.1 Soil Loss Estimation Model for Southern Africa (SLEMSA)

The Soil Loss Estimation Model for Southern Africa (SLEMSA) was developed specifically for the Zimbabwean Highveld by Elwell (1978). Smith (1999) warns that the estimations should only be used as a guide, or rating, when used outside of this area. According to the former Natal Department of Agricultural Technical Services, SLEMSA was designed to give "an estimate of soil loss for a range of possible crop rotations under a given set of rainfall, slope and soil conditions, and specified contour spacings" (Department of Agricultural Technical Services, 1976). The SLEMSA algorithm is given in Equation 3.1. The standard field plot used in the calculations is a weed-free, bare, fallow field with dimensions of 30 m by 10 m. The slope of the standard field plot is taken to be 4.5 % and the soil is of a known erodibility. The soil erodibility and rainfall energy are incorporated into the variable K, below.

$$Z = KCX \tag{3.1}$$

where

Z = predicted mean annual soil loss [$\text{t}\cdot\text{ha}^{-1}\cdot\text{a}^{-1}$] or Erosion Hazard Units [EHU],

K = mean annual soil loss from a standard field plot [$\text{t}\cdot\text{ha}^{-1}\cdot\text{a}^{-1}$],

C = the ratio of soil lost from a cropped plot to that lost from bare fallow plot, and

X = the ratio of soil lost from a plot of length L and slope per cent S , to that lost from the standard plot.

Experiments were conducted by Smithen and Schulze (1979) to compare results of SLEMSA and the USLE. The investigation showed that SLEMSA is highly sensitive to rainfall energy. SLEMSA has a very simple method of determining the C factor, based simply on total canopy coverage. In comparison the USLE has various sub-factors which take into account canopy cover, mulch cover and the residual effect of land use. The investigation concluded that, in the catchment in question, SLEMSA gave estimates of soil loss which were approximately half of the USLE values. However, no assessment was provided as to which of these values were closer to the actual value of soil loss. It was stated that either model could be used to obtain an estimate of soil loss, and that the choice of model was a subjective one (Smithen and Schulze, 1979). A further limitation of SLEMSA is that it only calculates sheet erosion, and hence neglects rill erosion.

3.2.2 Universal Soil Loss Equation (USLE)

The Universal Soil Loss Equation (USLE) was first presented by Wischmeier and Smith (1965) in the USDA Agriculture Handbook No. 282. It was further developed by Wischmeier and Smith (1978) in the USDA Agriculture Handbook No. 537, and has become one of the most widely recognised and frequently applied empirical soil loss estimation methods, forming the basis for a number of other methods and equations (Lorentz and Schulze, 1995). The USLE is given in Equation 3.2.

$$A = R \cdot K \cdot LS \cdot C \cdot P \quad (3.2)$$

where

A = long term annual average soil loss per unit area [$\text{t}\cdot\text{ha}^{-1}\cdot\text{a}^{-1}$],

R = an index of annual rainfall erosivity [$\text{MJ}\cdot\text{mm}\cdot\text{ha}^{-1}\cdot\text{h}^{-1}\cdot\text{a}^{-1}$],

K = soil erodibility factor [$\text{t}\cdot\text{h}\cdot\text{MJ}^{-1}\cdot\text{mm}^{-1}$],

LS = slope length and gradient factor [dimensionless],

C = cover and management factor [dimensionless], and

P = conservation support practice factor [dimensionless].

Although the USLE was a great advancement in erosion science at the time of its release, many weaknesses have been revealed with time and use. According to Smith (1999), one of the major disadvantages was that the database was restricted to the USA east of the Rocky Mountains. It was also limited to slopes with a gradient of 7 % or less and soils with a low smectite content. Smith (1999) also stated that the USLE was never widely adopted in South Africa, due in part to the fact that it is assumed that empirical models do not perform well in conditions different to those in which the model is derived. However, this is not entirely true as the USLE was adapted to South African applications in a number of cases, as described below.

A nomograph has been developed by Smithen (1989) in order to assist in the determination of contour bank spacing. The nomograph is shown in Figure 3.1 and makes use of the Universal Soil Loss Equation (USLE). The use of this nomograph requires details such as climate, cropping practices and soil type. The soil loss tolerances can be estimated using the soil types and properties described in Table 2.1.

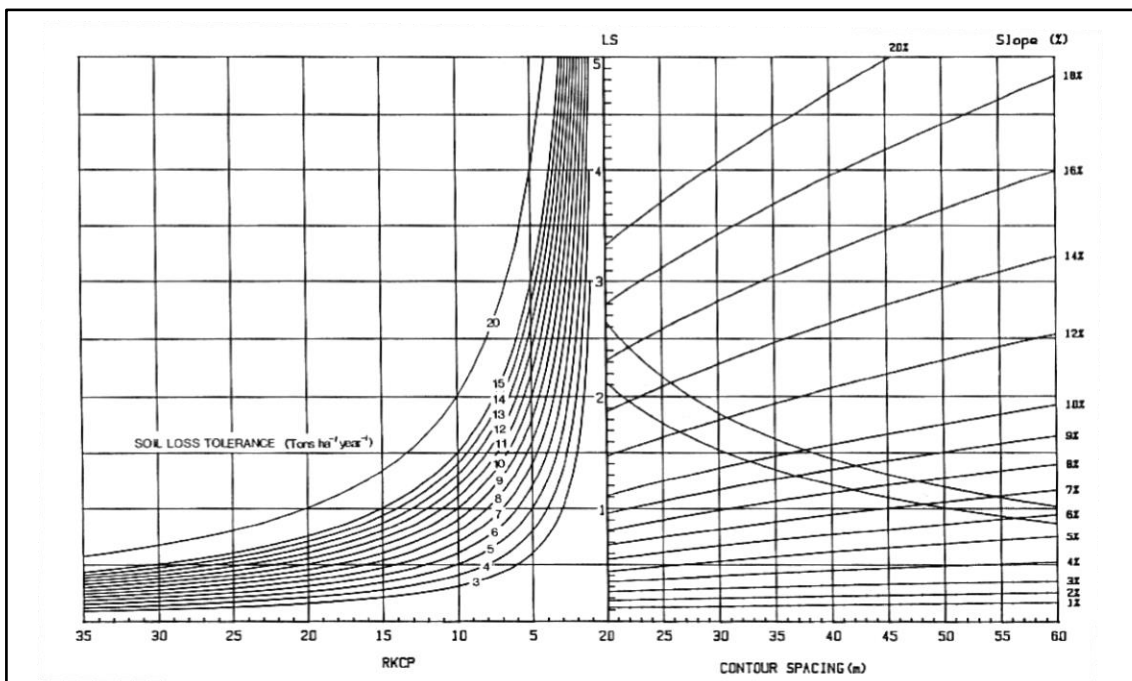


Figure 3.1 Contour spacing nomograph (Smithen, 1989)

A nomograph presented by Platford (1987), to calculate contour bank spacing, was designed specifically for the sugarcane industry. As such, it takes into account the relevant factors pertaining to sugarcane cultivation, such as tillage and harvesting methods. The USLE equation was also used in the derivation of the nomograph, shown in Figure 3.2.

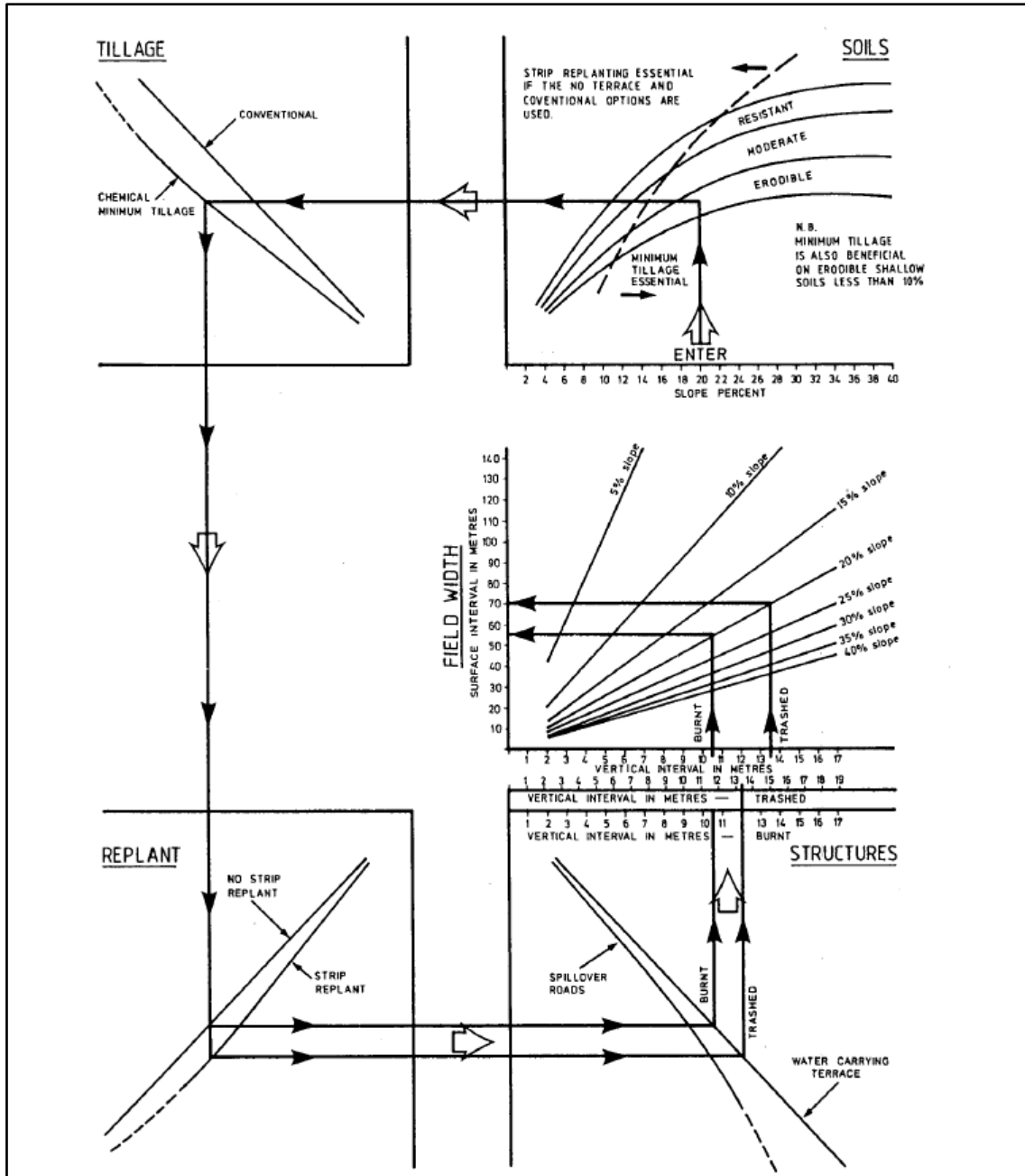


Figure 3.2 Nomograph to determine contour bank spacing for sugarcane cultivation (Platford, 1987)

3.2.3 Revised Universal Soil Loss Equation (RUSLE)

The USLE was later refined and was presented as the Revised Universal Soil Loss Equation, RUSLE, by Renard *et al.* (1991). The RUSLE is explained in detail in Agriculture Handbook No. 703 (Renard *et al.*, 1997) and it has the same form as the USLE. Both the USLE and RUSLE calculate erosion from sheet and rill erosion only, excluding erosion from gullies or concentrated flow. As with the USLE, the RUSLE gives an estimate of the long term average annual soil loss and is not event-based, although modifications have been developed to predict event-based sediment yield (Lorentz and Schulze, 1995).

The latest software developed to utilise this equation is the Revised Universal Soil Loss Equation, Version 2 (RUSLE2). This software was developed co-operatively by the USDA-NRCS, the USDA-ARS and the University of Tennessee, and models the various conditions of a contour bank system, including factors such as slope, cropping system and climate (USDA-ARS, 2013). Figure 3.3 shows the input screen of the RUSLE2 Profile Module. Data requirements include the profile of the terraced land, climatic information, which is preloaded and based on location within the USA, and soils information, as well as the proposed crop and tillage system.

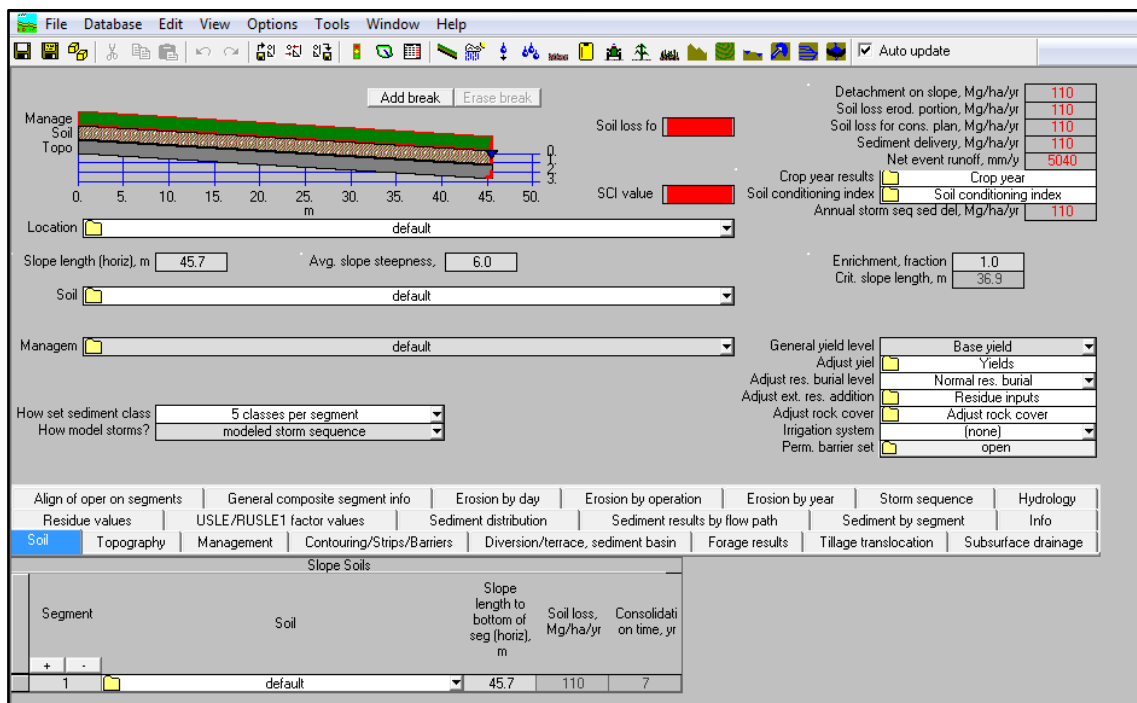


Figure 3.3 Example simulation of the RUSLE2 Profile Module

It has been noted by Kinnell (2010) that although the USLE and RUSLE are generally shown in the form of Equation 3.2, the model theoretically contains two steps. This is because the model is created with a standard runoff plot concept. The standard runoff plot is defined to have a slope of 9 % and a length of 22.1 m. The plot is a tilled, bare, fallow area and tillage occurs up and down the slope. The first step in the USLE is to predict the erosion for the unit plot using Equation 3.3.

$$A_1 = RK \quad (3.3)$$

where

A_1 = long term average soil loss per unit area of the unit plot [$\text{t}\cdot\text{ha}^{-1}\cdot\text{a}^{-1}$].

It must be noted that R and K are the only factors that have associated units. The remaining factors are then multiplied to the result from Equation 3.3 in order to estimate erosion for the conditions at the plot of interest, as shown in Equation 3.4.

$$A = A_1 LSCP \quad (3.4)$$

where

A = long term average soil loss per unit area [$\text{t}\cdot\text{ha}^{-1}\cdot\text{a}^{-1}$].

It must be reiterated that the USLE is an empirical model. While the factors of the equation are physical factors in soil loss, they do not represent strictly physical interrelationships, but rather statistical interrelationships developed from a large database (Lorentz and Schulze, 1995). Although the RUSLE uses the same factors as the USLE, major updates were performed in revising the equation, including improved input data and time-dependent variables. Each one of the five RUSLE factors is discussed below.

3.2.3.1 Annual soil loss (A)

A represents the long term average annual soil loss for a given slope. It must be emphasised that soil loss is not the same as sediment yield. The A factor also averages the erosion along the slope, so erosion at specific points along the slope may differ from the computed average erosion.

3.2.3.2 Soil erodibility factor (*K*)

Formally, soil erodibility is the “change in the soil per unit of applied external force or energy” (Renard *et al.*, 1997) and it has the metric units of t.h.MJ⁻¹.mm⁻¹. This gives the amount of soil removed by one “erosivity unit”. In practical terms, it can be thought of as how easily soil is detached by erosive forces such as rain splash and runoff. It takes into account soil properties and accounts for the influence that they have on soil loss. These properties include detachment, transport, deposition, infiltration into the soil and roughness due to tillage (Renard *et al.*, 1997). A number of different methods can be used to determine the *K* factor, depending on the amount of information available.

The *K* factor can be determined from a simple knowledge of the type of soil. Both the Binomial Soil Classification (MacVicar *et al.*, 1977) and the Taxonomic Soil Classification (Soil Classification Working Group, 1991) systems may be used. An erosion potential class (*e.g.* high, low, moderate) has been assigned to each soil type (Department of Agricultural Technical Services, 1976). The erodibility factor, *K*, can then be determined from Table 3.1. An experienced user may refine the estimate of *K* by making field observations and studying the local conditions.

Table 3.1 Erodibility factors for various soil erodibility classes (Lorentz and Schulze, 1995)

Soil Erodibility Class	Soil <i>K</i> -Factor
Very High	> 0.70
High	0.50 – 0.70
Moderate	0.25 – 0.50
Low	0.13 – 0.25
Very Low	< 0.13

The *K* factor can also be determined using a particle size distribution analysis (Renard *et al.*, 1997). Equation 3.5 is used to find the geometric mean of the particle sizes.

$$D_g = EXP[0.01 \sum(f_i \cdot \ln(m_i))] \quad (3.5)$$

where

$$D_g = \text{geometric mean particle size [mm]},$$

f_i = primary particle size fraction [%], and

m_i = arithmetic mean of the particle size limits of that size [mm].

The geometric mean is then used to estimate K using Equation 3.6 (Renard *et al.*, 1997).

$$K = 7.954 \left\{ 0.034 + 0.0405 \exp \left[-\frac{1}{2} \left(\log(D_g) + \frac{1.659}{0.7101} \right)^2 \right] \right\} \quad (3.6)$$

Wischmeier *et al.* (1971), cited by Wischmeier and Smith (1978), developed a nomograph to estimate K , which takes into account many physical properties of the soil, as shown in Figure 3.4. These include the particle size distribution, the amount of organic matter in the soil, as well as the structure and permeability of the soil. It must be noted that Figure 3.4 provides K values in United States customary units (ton.acre.h.(hundreds of acre.ft-tonf.in)⁻¹). In order to convert the K factor to SI units (t.ha.h.ha⁻¹.MJ⁻¹.mm⁻¹), it must be divided by 7.59 (Renard *et al.*, 1997).

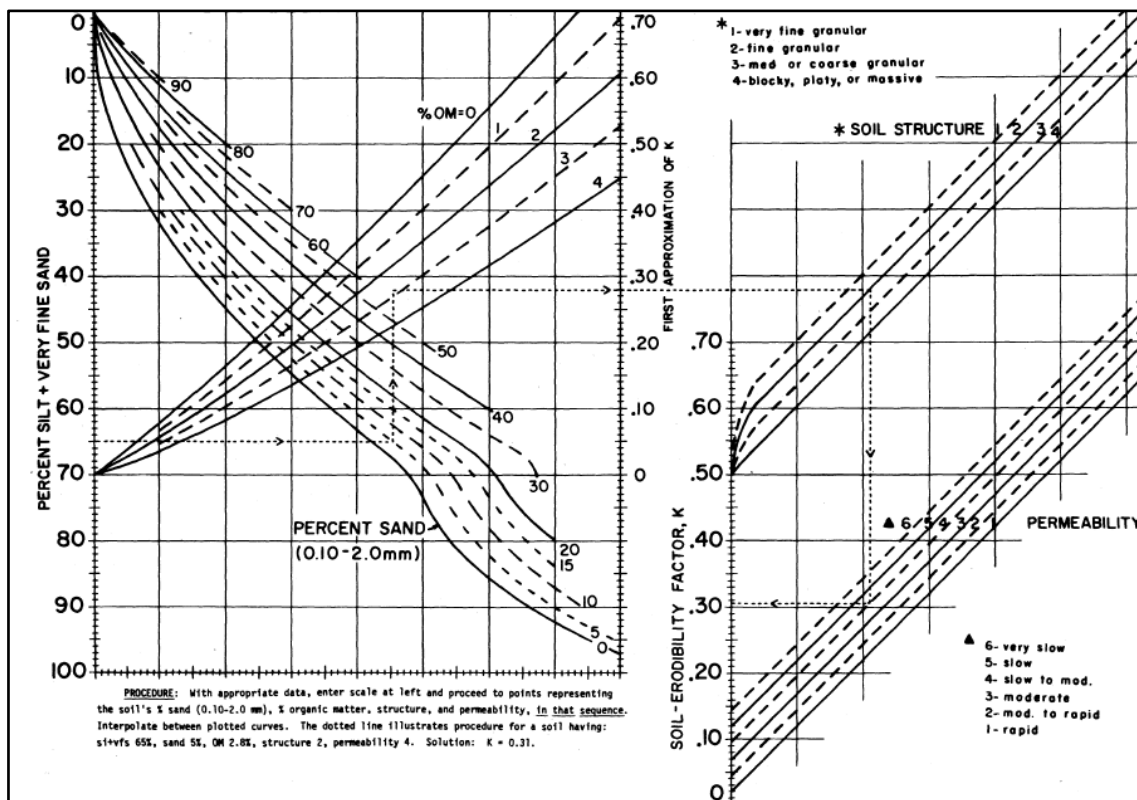


Figure 3.4 The soil erodibility nomograph to estimate K (Renard *et al.*, 1997)

This nomograph is known as the standard nomograph. It was found that the standard nomograph fitted medium textured soils best, but did not perform well with soils of a high clay or sand content. This was remedied by introducing a slight alteration to the soil structure sub-factor,

resulting in the modified nomograph. The modified nomograph differs from the standard nomograph only in how the soil structure sub-factor is calculated. All other sub-factors in the modified nomograph remained unchanged. The modified nomograph is represented by Equation 3.7.

$$K = k_t k_o + k_s + k_p / 100 \quad (3.7)$$

where

K = soil erodibility factor,

k_t = texture sub-factor,

k_o = organic matter sub-factor,

k_s = soil structure sub-factor, and

k_p = soil profile permeability sub-factor.

The soil texture sub-factor takes into account the textural class of the soil, and is based on the particle size distribution of the soil. The organic matter sub-factor relies only on the percentage of organic matter in the soil. The soil structure sub-factor relies on the soil structure class. There are 4 classes used, namely:

- 1 : very fine granular
- 2: fine granular
- 3: medium to coarse granular
- 4: blocky, platy or massive

The soil profile permeability sub-factor is related to the permeability class of the soil, determined by the saturated hydraulic conductivity. Soils are classified as follows:

- 1: rapid
- 2: moderate to rapid
- 3: moderate
- 4: slow to moderate
- 5: slow
- 6: very slow

The properties of each class are shown in Table 3.2. The hydrologic soil group refers to a classification system developed by the USDA, which classifies soil types according to their water transmission properties, in order to determine their runoff potential (USDA-NRCS, 1986).

Table 3.2 Permeability classes for different soil texture classes (after Renard *et al.*, 1997)

Texture	Permeability class	Saturated hydraulic conductivity (mm/h)	Hydrologic soil group
Silty clay, clay	6	< 1	D
Silty clay loam, sand clay	5	1 - 2	C-D
Sandy clay loam, clay loam	4	2 - 5	C
Loam, silt loam	3	5 - 20	B
Loamy sand, sandy loam	2	20 - 60	A
Sand	1	> 60	A+

While other empirical soil loss models, such as SLEMSA and the USLE, tend to use an average K factor for the entire year, RUSLE software developed by the USDA incorporates temporal variation in the K factor (USDA-ARS, 2013). This is due to the fact that erodibility is higher when soils are thawing, as well as when high antecedent moisture conditions are present, producing greater runoff per unit of rainfall, and therefore, per unit of erosivity (USDA-ARS, 2013).

Although not applicable at a field scale, a number of studies have assigned soil erodibility values to soils on a national scale in South Africa (*e.g.* Le Roux *et al.*, 2006; Schulze and Horan, 2007). The soil erodibility map of South Africa, presented by Le Roux *et al.* (2006), is shown in Figure 3.5.

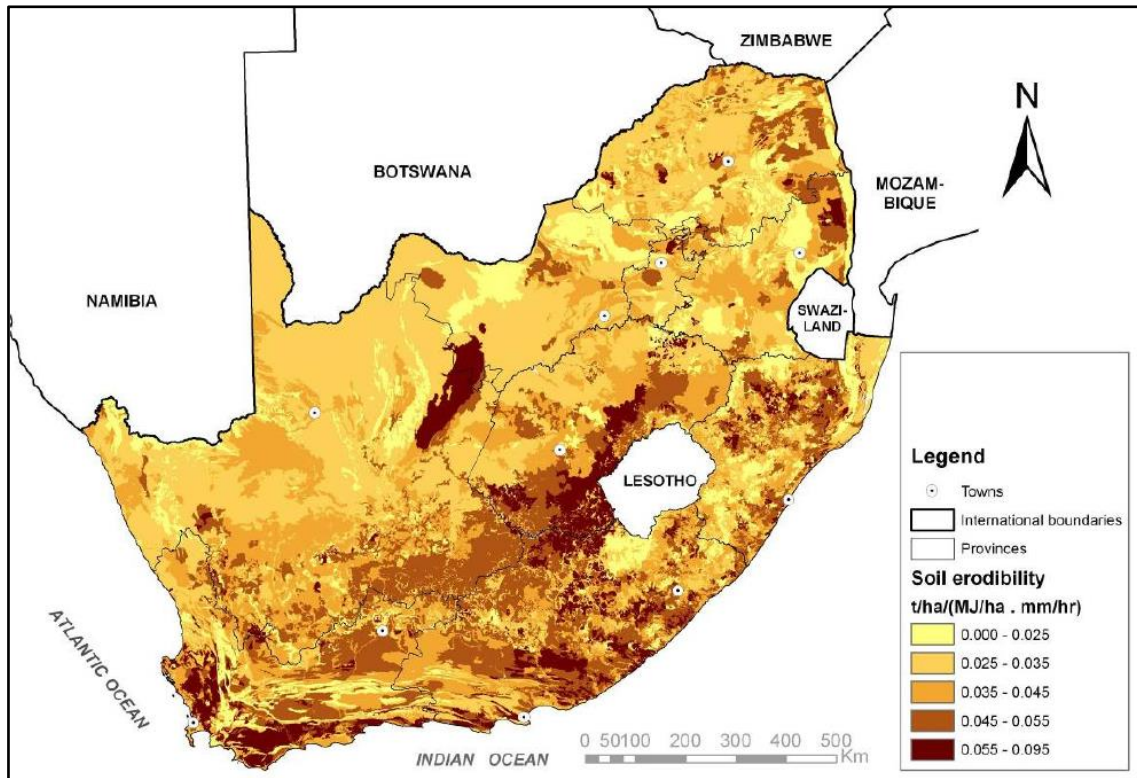


Figure 3.5 Soil erodibility map of South Africa (Le Roux *et al.*, 2006)

3.2.3.3 Slope length and steepness factor (*LS*)

The *LS* factor accounts for the topography in the area of interest. Two properties make up the *LS* factor. These are the length of the slope and the gradient of the slope. Slope length is defined as the distance from the source of the overland flow to either where the gradient decreases adequately for deposition to occur or where the flow enters a distinct natural or artificial channel (Lorentz and Schulze, 1995).

Erosion increases as the length of the slope increases (Renard *et al.*, 1997). It is best to measure the slope length in the field. Slope lengths determined using contour maps are often too long as the maps do not show the areas of water concentration where the slopes end. The slope length factor, *L*, is calculated using Equation 3.8.

$$L = \left(\frac{\lambda_1}{22.1} \right)^{m_{sl}} \quad (3.8)$$

where

L = slope length factor [dimensionless],

λ_1 = slope length [m], and

m_{sl} = a variable which is dependent on the ratio, β_r , of rill (caused by flow) to interrill (caused mainly by rainfall impact) erosion.

The variable m_{sl} is computed using Equation 3.9.

$$m_{sl} = \frac{\beta_r}{1 + \beta_r} \quad (3.9)$$

The value of β_r is dependent on whether a slope is more susceptible to rill or interrill erosion. If the slope is moderately subject to both forms of erosion, then β_r can be calculated using Equation 3.10.

$$\beta_r = \frac{\sin S_{deg}}{0.0896 \left[3.0(\sin S_{deg})^{0.8} + 0.56 \right]} \quad (3.10)$$

where

$$S_{deg} = \text{slope angle } [^\circ].$$

If the conditions indicate that a slope is very susceptible to rill erosion (*e.g.* a steep slope that has just been tilled), the value of β_r must be doubled. In the same way, if the rill erosion appears to have a much lower effect than interrill erosion (*e.g.* on gently sloping grasslands), the value of β_r must be halved (Lorentz and Schulze, 1995).

An increase in slope steepness has a greater effect on soil loss than an increase in slope length (Lorentz and Schulze, 1995). The recommended equation for the slope steepness factor (S) has changed over time. Wischmeier and Smith (1978) presented Equation 3.11 for determining the slope steepness factor.

$$S = 65.41 \sin^2 S_{deg} + 4.56 \sin S_{deg} + 0.065 \quad (3.11)$$

Subsequent to this, McCool *et al.* (1987) presented Equations 3.12 and 3.13 for determining the slope steepness factor. These are the steepness equations used in the RUSLE2 technology (USDA-ARS, 2013).

$$S = 10.8 \sin S_{deg} + 0.03 \quad \text{for } S_{\%} < 9\% \quad (3.12)$$

$$S = 16.8 \sin S_{deg} - 0.50 \quad \text{for } S_{\%} \geq 9\% \quad (3.13)$$

Liu *et al.* (1994) found that limited data were available to assess the effect of steep slopes on soil loss. While most of the previous slope steepness factor equations were developed from plots with gradients up to 25%, Liu *et al.* (1994) studied plots with gradients ranging from 9% to 55%. Equation 3.14 was proposed for slopes greater than 9% (Liu *et al.*, 1994).

$$S = 21.91 \sin S_{deg} - 0.96 \quad \text{for } S_{\%} \geq 9\% \quad (3.14)$$

If the slope of interest is less than 5 m in length, Equation 3.15 should be used to determine the slope steepness factor (McCool *et al.*, 1987).

$$S = 3.0(\sin S_{deg})^{0.8} + 0.56 \quad (3.15)$$

In order to obtain the final *LS* factor, the *L* and *S* factors must be multiplied together. If the slope is not uniform (*i.e.* concave or convex), the *LS* factor can be adjusted using tables available in the RUSLE guide developed by Renard *et al.* (1997).

3.2.3.4 Cover and management factor (*C*)

Lorentz and Schulze (1995) argue that the cover and management factor, *C*, may be the most sensitive factor in calculating soil loss using the RUSLE. This is due to the large range of possible values that *C* may assume, its variation throughout the year and the difficulties often experienced in estimating it. Many methods exist for the calculation of *C*, and the choice of method depends on what information is available.

The *C* factor can be obtained using the SCS Runoff Curve Number, *CNII* (Øverland, 1990; cited by Lorentz and Schulze, 1995). However, this relationship was created using experiments in South America and may not provide accurate results elsewhere. Its use requires caution and sound judgement (Lorentz and Schulze, 1995). A major shortfall of this method is that the Curve Number is based on a single crop or natural vegetation condition, and therefore does not reflect the variation in cover throughout the year. The relationship is shown in Equation 3.16.

$$C = EXP\left(\frac{CNII - 97.5}{10.9}\right) \quad (3.16)$$

where

CNII = initial SCS Runoff Curve Number.

The most complex methods of determining C require comprehensive information regarding the crop and its management. The method presented by Renard *et al.* (1997) involves the use of five sub-factors, as shown in Equation 3.17. These sub-factors make up a soil loss ratio, which is the ratio between soil loss on the standard plot, and soil loss under specific crop conditions.

$$SLR = PLU \cdot CC \cdot SC \cdot SR \cdot SM \quad (3.17)$$

where

SLR = soil loss ratio,

PLU = prior land use sub-factor,

CC = canopy cover sub-factor,

SC = surface vegetation or mulch cover sub-factor,

SR = surface roughness sub-factor, and

SM = soil moisture sub-factor.

Each of these sub-factors must be calculated individually and each requires detailed information. An SLR is calculated for each time step over which the sub-factors are assumed to remain constant. The various SLRs are then weighted according the percentage of erosivity expected to occur for each time step (Renard *et al.*, 1997). This results in a weighted average, annual C factor representing the conditions as the crop develops through its various growth stages. It is especially important to accurately determine the magnitude of C when the majority of erosive rainfall occurs, as the crop can have a large erosion-reducing effect.

The equation used in RUSLE2 to calculate the C factor is shown in Equation 3.18 (USDA-ARS, 2013). In RUSLE2, the cover factor is calculated daily and is comprised of a number of sub-factors – each requiring extensive data to calculate.

$$c = c_c g_c s_r r_h s_b s_c s_m \quad (3.18)$$

where

c = daily cover-management factor,

c_c = daily canopy sub-factor,

g_c = daily ground surface cover sub-factor,

s_r = soil surface roughness sub-factor,

r_h = daily ridge height sub-factor,

s_b = daily soil biomass sub-factor,

s_c = daily soil consolidation sub-factor, and

s_m = daily antecedent soil moisture sub-factor used in R_{eq} zones.

3.2.3.5 Conservation support practice factor (P)

According to Renard *et al.* (1997), the support practice factor is “the ratio of soil loss with a specific support practice to the corresponding loss with upslope and downslope tillage”. On cultivated lands, support practices include contouring, strip cropping, contour banks and subsurface drainage. These practices reduce the volume of runoff, as well as the rate of runoff by altering the pattern of flow, the slope of the land and the direction in which the runoff flows.

Contouring causes the runoff to flow across the slope, decreasing the gradient of the flow path. This reduces both the detachment and transport capacity of the flow. If contour tillage is practised, the P factor can be determined by the slope of the land, as summarised in Table 3.3 (Wischmeier and Smith, 1978). P assumes a value of one for uncultivated lands, unless specific conservation practices are detailed. Table 3.3 also shows the recommended maximum slope length for fields, depending on the slope of the land. Contouring is not considered to be effective at reducing soil erosion on slopes longer than the limits specified (Wischmeier and Smith, 1978).

Table 3.3 P factor when only slope is known (after Wischmeier and Smith, 1978)

Land slope (%)	P factor	Maximum slope length (m)
1-2	0.60	122.0
3-5	0.50	91.5
6-8	0.50	61.0
9-12	0.60	36.6
13-16	0.70	24.4
17-20	0.80	18.3
21-25	0.90	15.3

In RUSLE2, the equations for determining the support practice factor for contouring take into account land steepness, ridge height of contours, contour row grade and runoff conditions (USDA-ARS, 2013).

Renard *et al.* (1997) suggested using Equation 3.19 to determine the P factor for contour banks for a contour bank slope of less than 0.9 %. The benefit factor can be obtained from tables, according to the spacing of the contour banks (Renard *et al.*, 1997). For contour bank slopes equal to, or greater than, 0.9 %, the P factor for contour banks is 1.0 (*i.e.* no benefit).

$$P = 1 - B_d \cdot (1 - 0.1 \cdot EXP(2.4g_t)) \quad (3.19)$$

where

g_t = slope of the contour bank (%), and

B_d = benefit factor for deposition.

The equation used in RUSLE2 to calculate the support practice factor of contour bank systems is comprised of many sub-factors and takes into account properties such as incoming sediment load, deposition rates of particle size classes and discharge rates (USDA-ARS, 2013). Equations have also been developed to account for the effects of porous barriers (*e.g.* strip cropping), impoundments and subsurface drainage (USDA-ARS, 2013).

In cases where multiple support practices are implemented (*e.g.* contour tillage and contour banks), the P factors for each of the practices must be multiplied together to form an overall P factor.

3.2.3.6 Rainfall erosivity factor (R)

According to Smithen and Schulze (1982), values for the soil, topography, vegetation and management factors can be determined universally with the aid of available tables and nomographs. However, the rainfall erosivity factor depends on the local climate and must be determined from location-specific data.

The R factor was developed from the analysis of large rainfall and soil loss datasets (Wischmeier and Smith, 1965). It was found that with all other factors held constant, the soil loss was directly proportional to the product of the total rainfall event kinetic energy (E) and the maximum 30-minute intensity of the rainfall event (I_{30}). If this product (EI_{30}) for all of the storms in a year, is summed, the result is the total rainfall erosivity for that year. Using many

years of record, an average annual erosion index for a station may be computed. The station values can then be interpolated in order to obtain a map of rainfall erosivity for a country. Figure 3.6 shows one of the early iso-erodent maps developed for the USA.

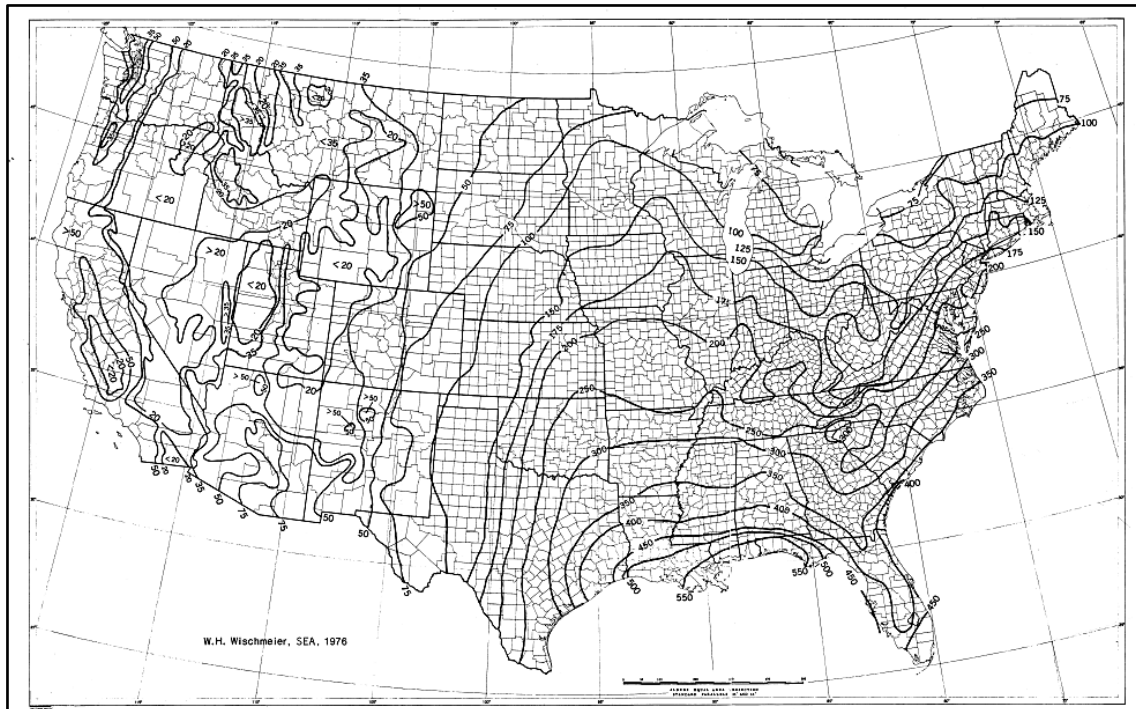


Figure 3.6 Iso-erodent map of the USA (Wischmeier and Smith, 1978)

There is debate regarding whether EI_{30} is, in fact, an accurate representative of rainfall erosivity. Morgan (2005) argues that there is no clear evidence that the I_{30} factor is the best parameter to relate to rainfall erosivity, instead of the maximum 5- or 15-minute intensities. In addition, the EI_{30} rainfall erosivity index assumes that even low intensity rainfall causes erosion. However, it has been shown that erosion occurs almost solely when rainfall intensities are above $25 \text{ mm}\cdot\text{h}^{-1}$ (Hudson, 1965; cited by Morgan, 2005).

Hudson (1965) proposed a different rainfall erosivity index, $KE > 25$, which is simply the sum of the kinetic energy of the storm in the time increments when the rainfall intensity is greater than $25 \text{ mm}\cdot\text{h}^{-1}$. Although this index is better suited for tropical climates, it would be possible to alter the threshold for more temperate climates, *e.g.* $KE > 10$. Hudson's index is also relatively simple and does not have very stringent data requirements (Morgan, 2005). However, the EI_{30} index is the index chosen for use in the RUSLE model, and the two indices cannot be interchanged (Morgan, 2005). The EI_{30} index is substituted directly for the factor R in the

RUSLE model – however, care must be taken to ensure that the units are consistent with those used in other the other factors, otherwise a conversion factor must be applied.

In order to calculate EI_{30} values, an estimation of the storm energy needs to be undertaken. Unit energy is defined by USDA-ARS (2013) as “energy content per unit area per unit rainfall depth”. According to Renard *et al.* (1997), storm energy (E) is calculated using Equation 3.20.

$$E = \sum_{k=1}^m e_k \Delta V_k \quad (3.20)$$

where

E = energy of rainfall event [$\text{MJ}\cdot\text{ha}^{-1}$],

m = number of periods in rainfall event with rainfall intensity considered to be uniform,

k = index for periods where rainfall intensity is considered to be uniform,

e_k = unit energy in the k^{th} period [$\text{MJ}\cdot\text{ha}^{-1}\cdot\text{mm}^{-1}$], and

ΔV_k = the amount of rainfall in the k^{th} period [mm].

A number of equations have been developed in order to calculate the unit energy of storms. The equation recommended by Wischmeier and Smith (1965) for use in the USLE was that developed by Wischmeier and Smith (1958), as shown in Equation 3.21.

$$e_k = 0.0119 + 0.0873 \log_{10} i_k \quad (3.21)$$

where

i_k = rainfall intensity for the k^{th} period [$\text{mm}\cdot\text{h}^{-1}$].

Equation 3.21 required an upper limit to be set as it was found that median drop size did not increase with rainfall intensity greater than $76 \text{ mm}\cdot\text{h}^{-1}$ (Carter *et al.*, 1974). The corresponding energy limit was $0.283 \text{ MJ}\cdot\text{mm}^{-1}\cdot\text{ha}^{-1}$.

McGregor and Mutchler (1976) developed an equation for unit energy using raindrop-size and intensity data from Holly Springs in the USA, as seen in Equation 3.22.

$$e_k = 0.273 + 0.2168 \exp(-0.048i_k) - 0.4126 \exp(-0.072i_k) \quad (3.22)$$

Brown and Foster (1987) recommended Equation 3.23 for the calculation of unit energy. The first term of this equation represents the upper limit of unit energy.

$$e_k = 0.29[1 - 0.72\exp(-0.05i_k)] \quad (3.23)$$

A study performed by McGregor *et al.* (1995) suggested changing the intensity coefficient of Equation 3.23 from -0.05 to -0.082, resulting in Equation 3.24. This is the equation that is used in the RUSLE2 software to calculate unit energy (USDA-ARS, 2013).

$$e_k = 0.29[1 - 0.72\exp(-0.082i_k)] \quad (3.24)$$

Van Dijk *et al.* (2002) reviewed previous research and proposed Equation 3.25 as a universal unit energy equation. The parameters of this equation were obtained by averaging the parameters of a number of different energy equations.

$$e_k = 0.283(1 - 0.52e^{-0.042i_k}) \quad (3.25)$$

According to Morgan (2005), this equation is fairly accurate in that it generally provides estimates within 10 % of measured values. However, it still has problems when applied to climates with a strong coastal effects, or areas which are semi-arid or sub-humid, where it over-predicts and under-predicts, respectively (van Dijk *et al.*, 2002).

In previous studies (Wischmeier & Smith, 1978; Smithen and Schulze, 1982), rainfall events under 12.5 mm were excluded from the calculations, unless 6.3 mm or more fell in 15 minutes. The main reason for this was to reduce the cost of abstracting and analysing the rainfall-intensity data. Wischmeier and Smith (1978) found that “the erosion from these light rains is usually too small for practical significance and that, collectively, they have little effect on the distribution of the annual *EI* or erosion”. In a study conducted by McGregor *et al.* (1995), it was found that the omission of storms of less than 13 mm from the calculations resulted in an average decrease of the annual *R* value by approximately 3.5 %.

In addition to this lower threshold, the developers of RUSLE2 found a need to implement an upper threshold on rainfall events (USDA-ARS, 2013). When calculating rainfall erosivity for the USA, it was found that one particular location had recently experienced what was estimated to be a 1 in 600 year storm, which resulted in an *EI*₃₀ value double that of a nearby location. It was decided that the records used to compute rainfall erosivity values should have an upper limit placed on the storm return periods. Extreme storms with large return periods, such as a 1 in 600 year storm, that have occurred in the last 30 years are not necessarily good indicators of what will happen in the next 30 years (USDA-ARS, 2013). The developers concluded that “an

average annual record that excludes extreme events is the best predictor of the immediate future for conservation planning where the objective is to protect the on-site soil resource from excessive degradation by erosion” (USDA-ARS, 2013). For this reason, any storms with a return period greater than 50 years were excluded by the developers of RUSLE2 in the calculation of the *R* factor.

It can be seen that the major factors affecting soil erosion are taken into account by the RUSLE. A variety of options exist by which to obtain input information, depending on the level of data available. In addition to this, research conducted elsewhere can readily be used in the calculation of soil erosion in South Africa. For example, the effects of tillage on crop residues will be similar regardless of the location in which the tillage takes place. However, the effect of rainfall can only be determined from local data. The next chapter focusses specifically on rainfall erosivity, and the different ways in which rainfall erosivity can be calculated when continuously recorded, short duration rainfall data is scarce.

4. METHODS TO DETERMINE RAINFALL EROSION WITH LIMITED, CONTINUOUSLY RECORDED RAINFALL DATA

The major limiting factor when calculating rainfall erosivity for a large area, such as a country, is the lack of adequate data. In order to measure the intensity of rainfall, short duration, continuously recorded data are required. When RUSLE2 was developed, the initial approach was to find the average annual rainfall erosivity at as many short duration stations as possible and to spatially interpolate these values to produce an average annual rainfall erosivity map (USDA-ARS, 2013). However, it was found that the resulting map did not produce smooth, regular trends, but rather many “bull’s-eyes” and inconsistent trends. This was not acceptable for use within the model and the inconsistencies were attributed to short and differing record lengths at the various stations. In addition to this, stations that measure short duration rainfall data are relatively few compared with those that measure daily rainfall data. Data from daily rainfall stations are also usually more reliable than short duration rainfall stations, having longer record lengths and less missing data (USDA-ARS, 2013).

For these reasons, various methods have been developed in order to utilise daily data for rainfall erosivity estimation. This chapter describes these methods, as well as how some of them have been applied in South Africa.

4.1 Regression Analysis Method

One method used to calculate rainfall erosivity is the use of regression analysis to determine relationships between daily precipitation data and rainfall erosivity. The low spatial resolution of short duration stations, coupled with the relatively short records, is problematic in terms of obtaining accurate estimates of rainfall erosivity over large areas. In order to overcome this problem, many studies have found relationships between daily rainfall parameters and rainfall erosivity at continuously recording rainfall sites and applied these relationships to daily stations. This gives a much denser network of points over which rainfall erosivity can be spatially interpolated. Commonly used regression models for rainfall erosivity estimation include the linear function, as demonstrated by Smithen and Schulze (1982), the power function proposed by Richardson *et al.* (1983) and the sinusoidal function proposed by Yu and Rosewell (1996).

4.1.1 Linear regression with various daily rainfall parameters

Smithen and Schulze (1982) made use of regression analysis to estimate annual EI_{30} values for South Africa. The approach did not simply use the direct precipitation amount, but developed parameters from daily rainfall data with which were used as predictor variables to estimate EI_{30} . These parameters included total rainfall, effective rainfall, Modified Fournier's Index and the so-called Burst Factor.

The 'total rainfall' is the simplest parameter. EI_{30} was simply related to total rainfall for a period of time. The 'effective rainfall' parameter excludes any events which are deemed non-erosive, *i.e.* events of less than 12.5 mm of total rainfall separated by more than 6 hours.

The Modified Fournier's Index (MFI) is given in Equation 4.1.

$$MFI = \sum_{i=1}^{12} \frac{Pe_i^2}{P} \quad (4.1)$$

where

Pe_i = effective rainfall amount for month i [mm], and

P = annual rainfall [mm].

It was assumed that a parameter which included rainfall intensity in some way would correlate well with EI_{30} . Maximum daily rainfall in a time period indicates intensity to a certain degree, and is readily available. Equation 4.2 gives the Burst Factor (BF) as presented by Smithen (1981).

$$BF = \sum_{i=1}^{12} \frac{M_i Pe_i}{P} \quad (4.2)$$

where

M_i = maximum daily rainfall for month i [mm].

Owing to the limited number of stations for which EI_{30} could be computed, the homogeneous regions into which van Rooy (1972) had divided the country were used. A key station was selected to represent each of the fourteen regions, and a regression analysis of EI_{30} against other rainfall parameters was performed at each key station. Simple linear regression with untransformed data was used to determine the correlation between annual EI_{30} values and each of the parameters listed above. The parameters which gave the best prediction were determined

for each station. It was assumed that the relationships between rainfall and EI_{30} at the key stations represented the other daily rainfall stations in the respective homogeneous regions. The equations were then applied to daily rainfall records from 403 other stations across the country. An iso-erodent map was generated, allowing the determination of EI_{30} for any location in the country, as shown in Figure 4.1.

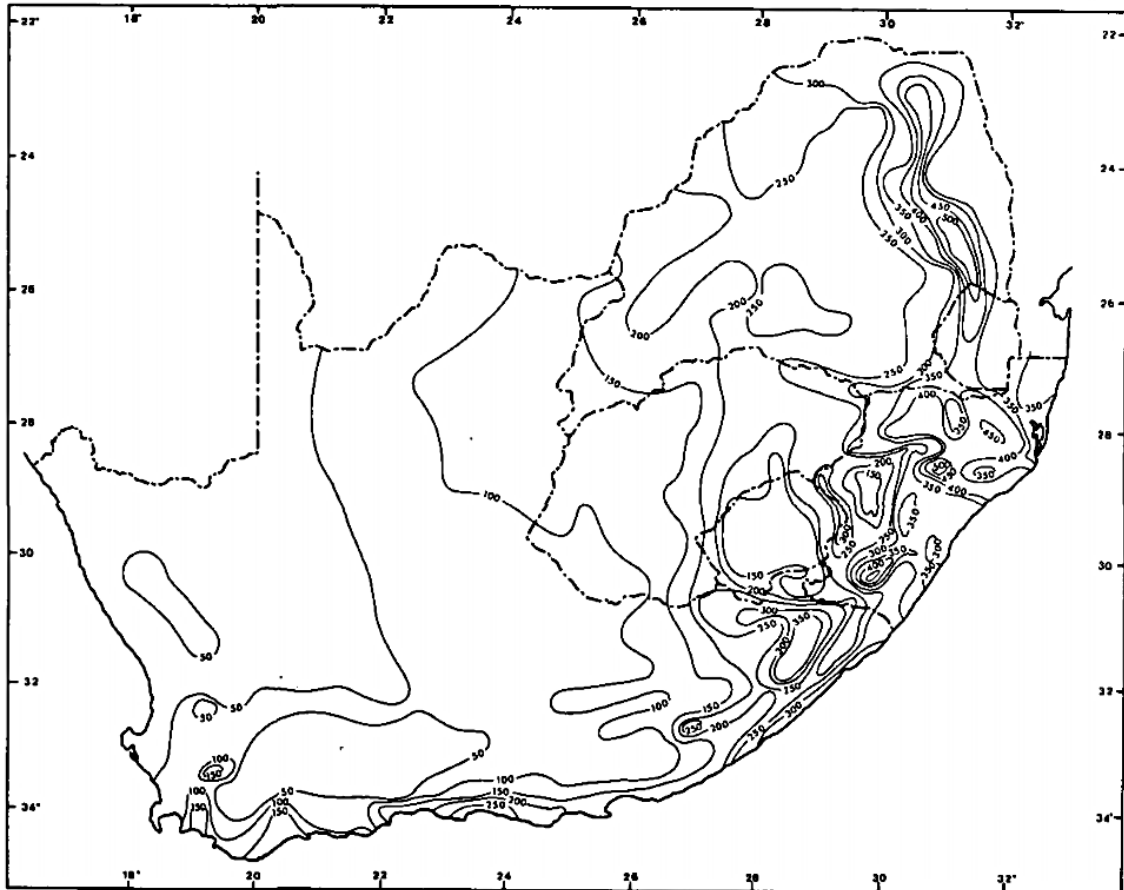


Figure 4.1 Rainfall erosivity map of South Africa produced by Smithen and Schulze (1982)

4.1.2 Power regression with daily rainfall amount

Richardson *et al.* (1983) suggested Equation 4.3 as a representation of the relationship between daily precipitation and EI_{30} .

$$EI_{30} = aP^b + \varepsilon \quad (4.3)$$

where

a, b = parameters determined by regression analysis, and

P = daily precipitation [mm].

The first term is the deterministic component of the relationship, while the second represents the random aspect, which is introduced due to the fact that a rainfall event of a given depth can comprise of rainfall of varying intensities. Figure 4.2 shows the relationship found by Richardson *et al.* (1983) between precipitation and rainfall erosivity. It can be seen that the points are bounded by an envelope representing the minimum and maximum rainfall erosivity possible. For an event of precipitation amount, P , the minimum rainfall erosivity would occur if the precipitation fell at a constant intensity for the entire event. Conversely, the maximum would occur if all of the rainfall fell in 30 minutes or less (Richardson *et al.*, 1983). Therefore, if the daily precipitation amounts are taken as individual events, the minimum 30-minute intensity is represented by $P/24$, while the maximum 30-minute intensity is represented by $P/0.5$. These values can be substituted into an energy equation and used to calculate the maximum and minimum EI_{30} values for a given precipitation amount.

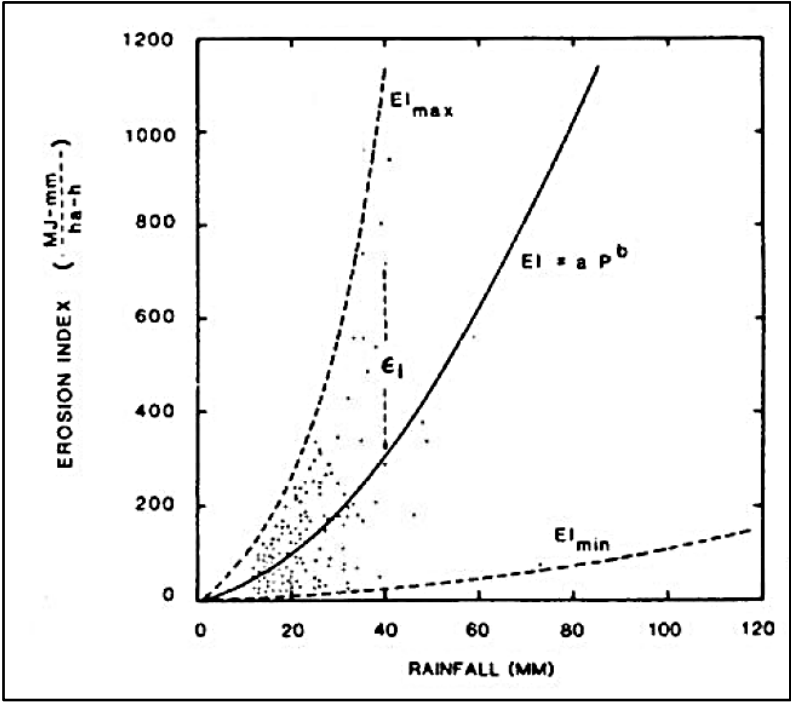


Figure 4.2 General relationship between precipitation amount and rainfall erosivity for individual storms, using the power function (Richardson *et al.*, 1983)

The parameters a and b are determined by linear regression of the logarithmic transforms of P and EI_{30} . In the study performed by Richardson *et al.* (1983), a was found to vary seasonally, while b showed no trend and was averaged over all of the months to give a constant parameter. Thus Richardson *et al.* (1983) showed how the relationship between precipitation and rainfall erosivity varies with both location and season.

4.1.3 Sinusoidal function to account for seasonality of erosivity

The sinusoidal function was proposed by Yu and Rosewell (1996), using Australian rainfall data, in order to account for seasonal variation in the a coefficient of the power function. The function is shown in Equation 4.4.

$$\hat{E}_j = \alpha[1 + \eta \cos(2\pi f j - \omega)] \sum_{k=1}^N R_k^\beta, \text{ when } R_k > R_0 \quad (4.4)$$

where

\hat{E}_j = rainfall erosivity for the j^{th} month [GJ.mm.ha⁻¹.h⁻¹],

$\alpha, \beta, \eta, \omega$ = parameters,

f = the fundamental frequency (1/12),

N = number of raindays with rainfall amount in excess of R_0 in the month,

R_k = the daily rainfall amount [mm], and

R_0 = the threshold rainfall amount [mm] (usually set to 12.7 mm).

The parameters $\alpha, \beta, \eta, \omega$ and R_0 are optimised by minimising the sum of squared errors between the estimated erosivity and the actual erosivity calculated using pluviograph data.

According to Yu and Rosewell (1996), this function is preferable to the power function for two reasons. Firstly, when using the power function method, due to the logarithmic transformations required to estimate parameters, when data is re-transformed, the error term is omitted. This is due to the fact that the error term is assumed to have a mean value of zero. Although this is true when the parameters are determined in logarithmic units, the mean is not zero in the original arithmetic units. Because of this omission, bias is introduced and underestimation of rainfall erosivity occurs. Secondly, when using a power function, different parameters may have to be calculated for each month. By using a sinusoidal function, the parameters can be determined once for the entire year, reducing the total number of parameters required.

Le Roux *et al.* (2006) updated the South African rainfall erosivity estimates using the model developed by Yu and Rosewell (1996) in Australia. This model was deemed applicable due to the similarities in climate between Australia and South Africa. Both countries are comprised of

winter rainfall areas in the south west, and summer rainfall areas towards the north and east of the country. In addition to this, the interior of both countries is classified as semi-arid.

Daily rainfall data from 1984-2000 was used by Le Roux *et al.* (2006) in the model and no regional parameterisation was performed, with the exception of the α value (*i.e.* the β , η , ω parameters were assigned the same values as those used in the Australian study). The α parameter takes rainfall seasonality into account and must therefore be specific to each station. Once the model had been applied, the results were interpolated using the Inverse Distance Weighting technique, accounting for the influence of topography.

Most importantly, the study by Le Roux *et al.* (2006) produced monthly estimates of South African rainfall erosivity, rather than an annual average. The temporal resolution of the rainfall erosivity index is particularly important when the potential exists for the most erosive rains to fall on areas at a time when the crop cover may be low (Le Roux *et al.*, 2008). The map of the annual rainfall erosivity values produced by Le Roux *et al.* (2006) is shown in Figure 4.3.

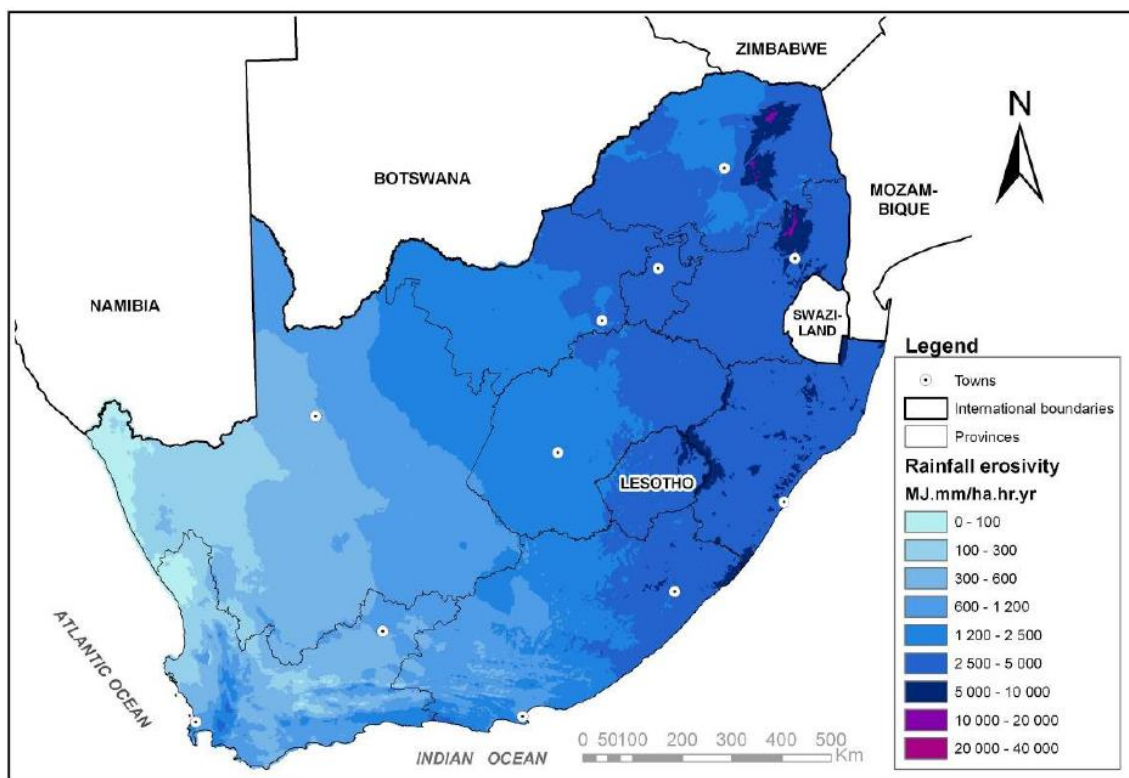


Figure 4.3 Annual rainfall erosivity map of South Africa (Le Roux *et al.*, 2006)

4.2 Erosivity Density Method

The erosivity density method of calculating rainfall erosivity is another method that was developed in order to provide estimates of rainfall erosivity, using daily data to supplement short duration precipitation data. The following section summarises the erosivity density method presented by the USDA-ARS (2013). Erosivity density is defined as “the erosivity content per unit precipitation” (USDA-ARS, 2013). Using this method, rainfall erosivity is calculated by multiplying the erosivity density at a point by the average monthly precipitation, which is determined from daily rainfall data. This relationship is shown in Equation 4.5 for the j^{th} month.

$$R_{m(j)} = \alpha_{(j)} P_{md(j)} \quad (4.5)$$

where

R_m = average monthly rainfall erosivity [MJ.mm.ha⁻¹.h⁻¹],

α_j = average monthly erosivity density [MJ.ha⁻¹.h⁻¹], and

P_{md} = average monthly precipitation determined from daily precipitation data [mm].

Erosivity density is calculated from short duration precipitation data as shown in Equation 4.6.

$$\alpha = \frac{\sum_{i=1}^n E_{(i)} I_{30(i)}}{\sum P_{sd}} \quad (4.6)$$

where

i = the index for storm in a month greater than 12 mm but smaller than a 50-year return period event,

n = total number of storms greater than 12 mm but smaller than a 50-year return period event, in a given month

$E_{(i)}$ = energy computed for the i^{th} storm [MJ.ha⁻¹.mm⁻¹],

$I_{30(i)}$ = maximum 30 minute rainfall intensity for the i^{th} storm [mm.h⁻¹], and

P_{sd} = short duration precipitation amount from all storms in a month [mm].

According to Wischmeier and Smith (1978), a storm event is defined by an event in which more than half an inch (12.7 mm) of rain falls, separated from other periods of rain by more than 6 hours. A storm of less than half an inch is included if one quarter of an inch (6.4 mm), or more,

falls in 15 minutes. It must be noted that minor discrepancies exist regarding the threshold amount of rain, due to inconsistencies in unit conversion. While the USDA-ARS (2013) states the value as 12 mm, and Smithen and Schulze (1982) define the threshold as 12.5 mm, the correct conversion results in a threshold value of 12.7 mm.

Once the erosivity density has been determined at a number of stations, it can then be interpolated between the stations to estimate the monthly erosivity density at any point. When calculated in the USA for RUSLE2, erosivity density was found to vary smoothly and consistently, as opposed to the “bull’s-eyes” and inconsistencies experienced when interpolating rainfall erosivity directly (USDA-ARS, 2013).

There are a number of advantages to using the erosivity density approach. Firstly, this approach produces much smoother, more consistent trends than those obtained from interpolating rainfall erosivity directly. Secondly, this method makes use of a much larger network of daily precipitation gauges to supplement the relatively small network of continuously recording rainfall stations. Thirdly, by computing rainfall erosivity using a ratio, rather than an absolute value, missing data at the short duration stations does not influence the results, unless the missing data is biased. Lastly, the RUSLE2 Science Document (USDA-ARS, 2013) sums up the benefit of the erosivity density approach in that “a shorter record length and a record length with more missing data can be used to compute erosivity density values than can be used to directly compute erosivity values with the standard method.” While the minimum record length considered acceptable for calculating rainfall erosivity directly is twenty years, a record length of ten years was shown to be adequate for erosivity density calculations by the USDA-ARS (2013).

In summary, a number of methods exist in which rainfall erosivity can be estimated in the absence of adequate short duration rainfall data. Regression with daily rainfall data appears to be the most common method, as evidenced by the large number of studies discussed above, which utilised linear, power or sinusoidal regression techniques. However, the erosivity density method has not yet been applied and evaluated in South Africa, despite the numerous benefits associated with this approach, as detailed above. The following chapter describes the steps taken to apply this method in South Africa in order to update the rainfall erosivity estimations countrywide.

5. ESTIMATING RAINFALL EROSION IN SOUTH AFRICA USING THE EROSION DENSITY METHOD

This chapter explains the steps taken in order to apply the erosion density method for calculating rainfall erosion in South Africa.

5.1 Methodology

One of the objectives of the study was to update estimates of rainfall erosion using short duration rainfall data and the erosion density method. This section details the steps taken in order to calculate erosion density using short duration data, and thereafter estimate rainfall erosion countrywide.

5.1.1 Data acquisition

Data from a number of sources, including data from the former South African Weather Bureau (SAWB), the former South African Sugar Association Experiment Station (SASEX) and FORESTEK, as well as data from a number of research catchments, as compiled by Smithers and Schulze (2000), were used in the study. The majority of the data came from the SAWB. As stated in the previous section, a record length of 10 years has been shown to be sufficient for erosion density calculations (USDA-ARS, 2013). The minimum record length for the continuously recording rainfall stations used was therefore selected as 10 complete years. 106 stations from the original data set of 609 fulfilled this requirement and the distribution of these stations is shown in Figure 5.1.

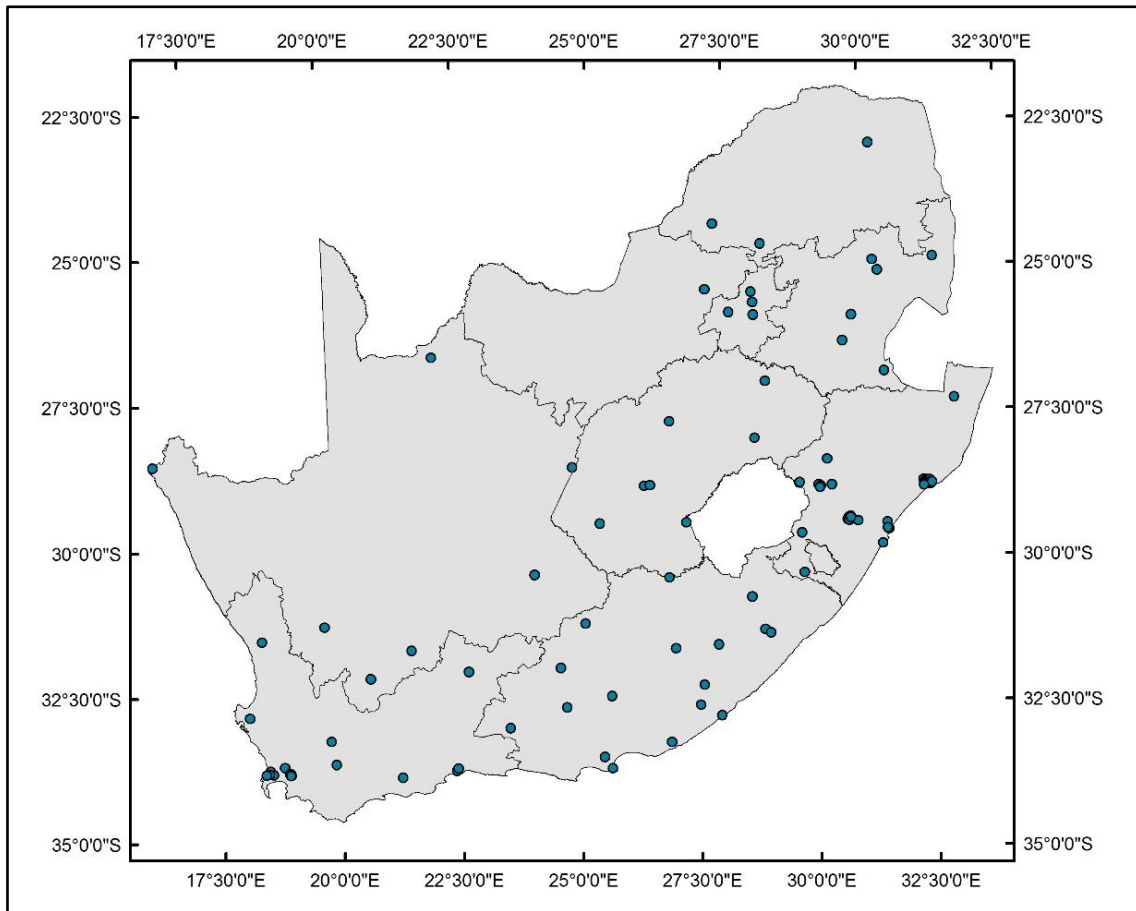


Figure 5.1 Original continuously recording stations available to the study, with records exceeding 10 complete years

In some areas, many stations were located in close proximity to one another, for example in research catchments, as shown in Figure 5.2. In order to prevent localised variations in erosivity density values and provide smooth trends, one station from each group of stations was selected to represent the location. In each case, the station with the longest record was chosen to represent the group, as it was assumed that a longer record provides a more accurate representation of the climate for that area. In cases where multiple stations had the same record length, the station closest to the centroid of the group of stations was selected to represent the group. This process removed 31 stations from the data set, leaving 75 stations.

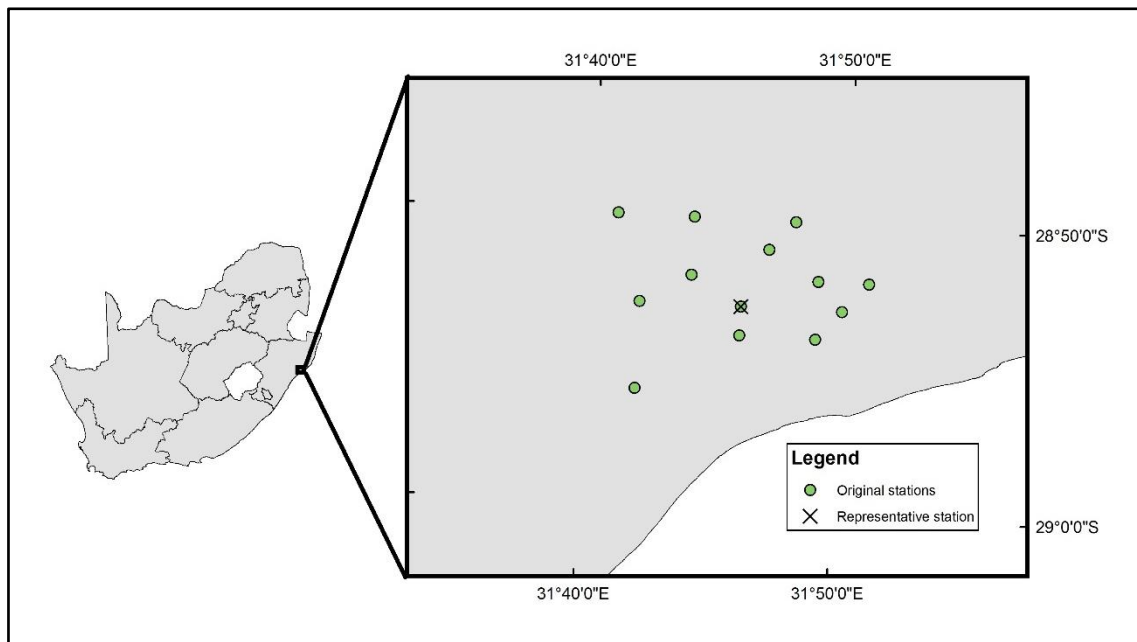


Figure 5.2 Selection of representative stations in research catchments

The remaining stations were plotted and the spatial distribution was analysed in order to locate any areas with a low station density. Where areas were lacking data, an attempt was made to obtain more recent data from the South African Weather Services (SAWS). These data were recorded in 5 minute intervals, as opposed to the breakpoint digitised data from the other stations. The data had to be converted into the correct format for processing and this was performed using a script written in the Python programming language.

The SAWS provided data for 8 new stations and additional records for 3 existing stations, namely Cedara, Kimberley and Van Zylsrus. After the addition of these new stations, the final number of continuously recording rainfall stations was 83. The distribution of these stations is shown in Figure 5.3. It can be seen that the stations are fairly sparsely distributed, with very few in the north west of the country. However, across the remainder of the country, the stations are reasonably evenly distributed.

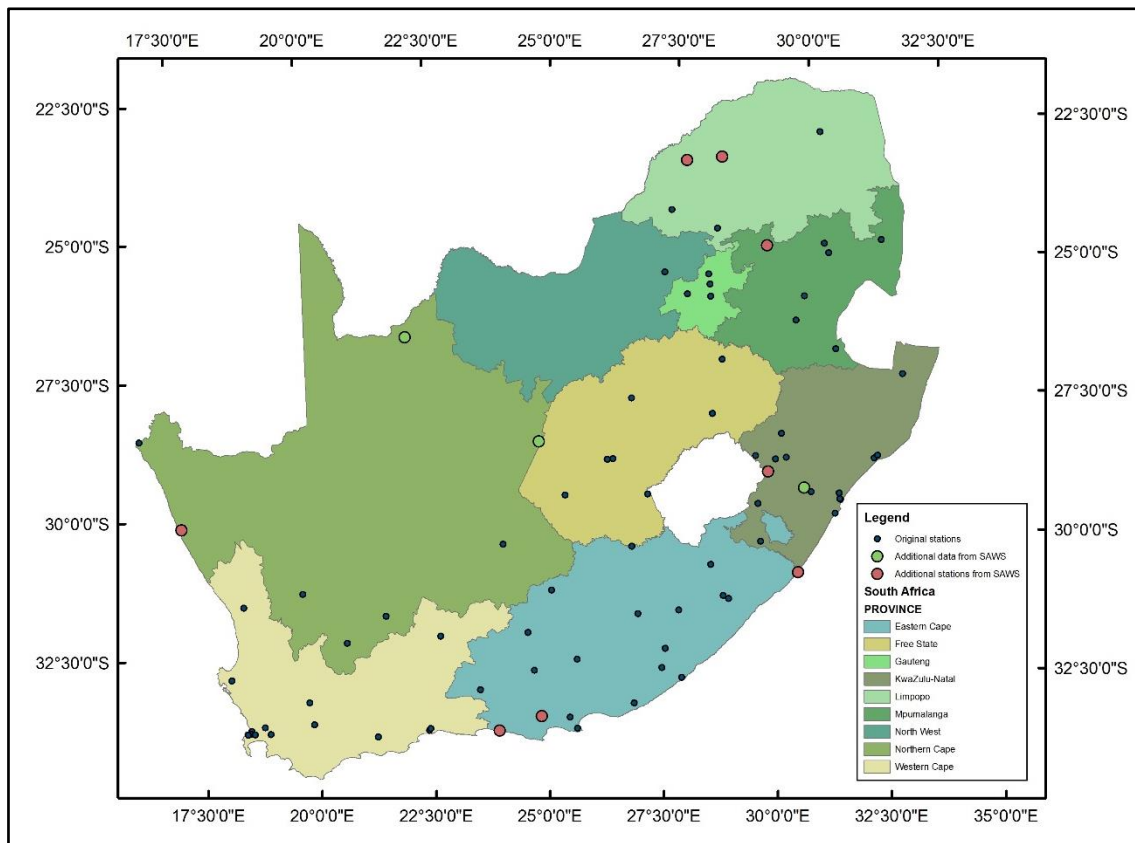


Figure 5.3 Short duration stations used in the estimation of erosivity density

The record length distribution of the stations is shown in Figure 5.4. It can be seen that the majority of the stations have a record length shorter than 25 years. However, there are a number of stations with record lengths in excess of 40 years. This figure illustrates the benefit of shorter required record lengths for the erosivity density approach. Calculating rainfall erosivity directly from this data set, rather than using the erosivity density approach, would mean discarding almost half of the stations (with a record length shorter than 20 years). However, the erosivity density method allows for shorter record lengths, increasing the amount of usable data.

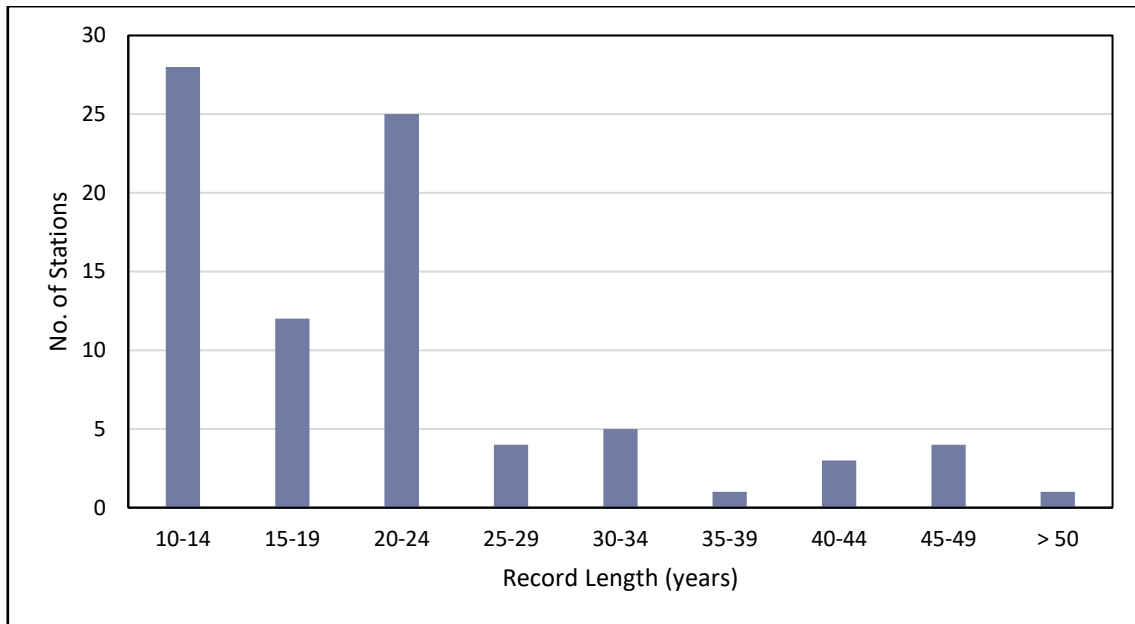


Figure 5.4 Record length distribution of final selection of continuously recording stations

5.1.2 Calculation of erosivity density

RAINX is a computer programme that was developed by the Department of Agricultural Engineering at the University of Natal in Pietermaritzburg. The programme uses rainfall data digitised from autographic rainfall charts and runs hydrological analyses on these digitised data (Schulze and Arnold, 1980). RAINX is written in the FORTRAN programming language. The programme is comprised of a number of subroutines, two of which were of most relevance to this study. The subroutine SUMRY determines rainfall amounts for a range of time steps, calculates the kinetic energy of the rainfall and checks for missing data. The subroutine MAXI calculates each day's maximum 30 minute rainfall intensity. The subroutines were edited slightly in order to produce outputs necessary for the study.

The first change that was made to the programme code was to add further energy equations to the programme. Originally, RAINX only calculated kinetic energy of rainfall using two, relatively old, equations. The first was the energy equation used in the SLEMSA model, Equation 5.1 (Elwell and Stocking, 1973).

$$E_k = (29.82 - 127.51/I) \quad (5.1)$$

where

E_k = kinetic energy of rainfall [$\text{J}\cdot\text{m}^{-2}\cdot\text{mm}^{-1}$], and

I = rainfall intensity [$\text{mm}\cdot\text{h}^{-1}$].

The second was that developed by Wischmeier and Smith (1958), Equation 3.21. Since RAINX was developed, a number of alternative energy equations have been developed, as explained in Chapter 3. It was decided to include a further 3 equations to the programme both to update the programme and to enable comparisons between the various equations.

The first additional equation was that of Brown and Foster (1987), shown in Equation 3.23. This equation was recommended by Renard *et al.* (1997) for other countries in which RUSLE was being developed. The second equation was that of McGregor *et al.* (1995), shown in Equation 3.24. This equation was chosen as it was used in calculating rainfall erosivity for the RUSLE2 software. This allows a standard to be maintained in calculating EI_{30} values. The third additional equation was the “universal” equation developed by van Dijk *et al.* (2002) shown in Equation 3.25. This was included as the authors promoted this as a “universal” equation that could be applied in a number of locations successfully. It was therefore included for comparative purposes. The graphical representation of these energy equations is shown in Figure 5.5. Although it can be seen in Figure 5.5 that all of the equations eventually tend towards similar values (between $0.283 \text{ MJ}\cdot\text{ha}^{-1}\cdot\text{h}^{-1}$ and $0.298 \text{ MJ}\cdot\text{ha}^{-1}\cdot\text{h}^{-1}$), the differences in the lower intensity ranges are substantial.

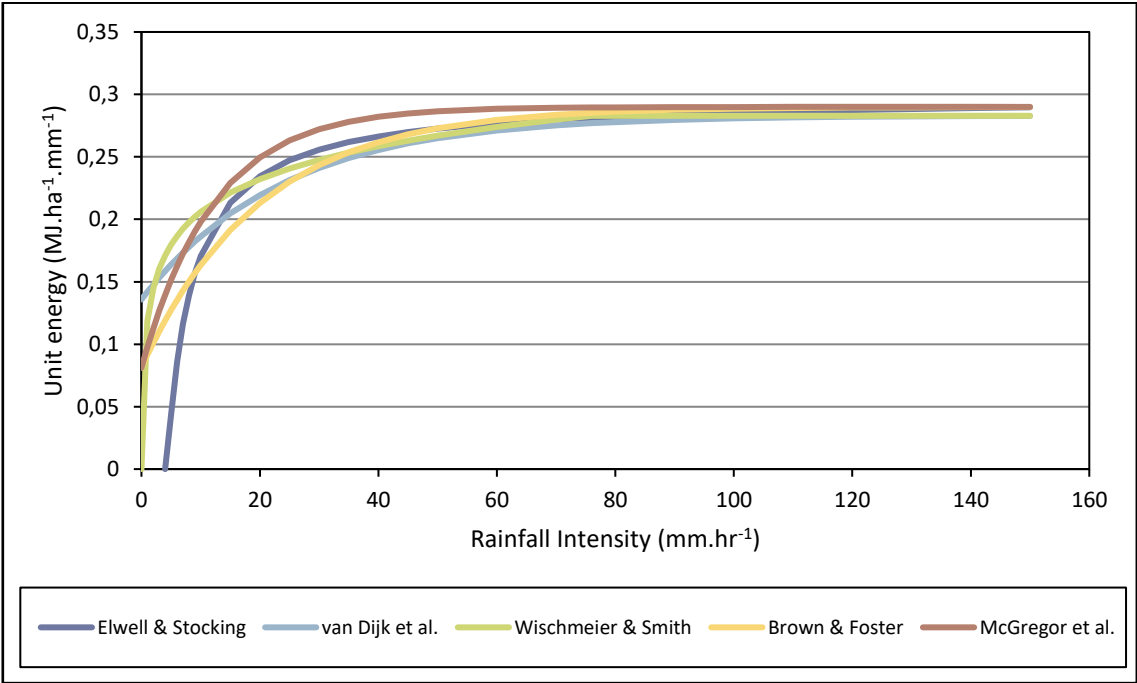


Figure 5.5 Graphical representation of the five selected energy equations for use in RAINX

A further change to the programme was to calculate the maximum 15-minute intensity for each day. This was used in order to determine whether or not a rainfall event with a rainfall depth of less than 12.7 mm was above the threshold intensity (*i.e.* greater than 6.3 mm in 15 minutes).

The RAINX routine was run on data from each short duration station. The output file of interest was the “daily” file. This file provided the kinetic energy, maximum 30- and 15-minute intensity and EI_{30} for each day, calculated from the short duration data. The kinetic energy, and corresponding EI_{30} , was calculated for each of the five energy equations. The output file was then imported into Microsoft Excel.

Any data with a “missing data” flag was removed from the records. The records were then split into individual months. For each month, the EI_{30} values were summed for all qualifying events. Similarly, the rainfall was summed for each month. The EI_{30} totals were then divided by the precipitation totals, to obtain an average erosivity density for each month, as shown in Equation 4.6.

5.1.3 Use of thresholds

EI_{30} values were calculated using all of the data, as well as with thresholds applied, for comparative purposes. Events were filtered out to provide an original data set, a data set with a lower threshold of 12.7 mm/event applied, and a final dataset with both the 12.7 mm/event threshold applied, as well as events which exceeded the 50 year return period, excluded. It was found that the developers of RUSLE2 excluded these ‘extreme’ events on a case-by-case basis and that there was no fixed rainfall duration on which the exclusion was based (Dabney, 2015). For the purpose of this study, the 15-minute, 30-minute, 24-hour and 1-day rainfall durations were analysed.

The 50 year return period events were determined using software developed by Smithers and Schulze (2003) which applies a Regional L-Moment Algorithm, and utilises the scale invariance of growth curves with duration, in order to estimate design rainfall in South Africa. The software allows design rainfall to be estimated for durations between 5 minutes and 7 days, for return periods from 2 to 100 years. The software computes design rainfall depths at the points of intersection of each minute of a degree in South Africa. For this study, the 50 year return period rainfall depths, for the storm durations of interest listed above, were computed. The rainfall events were then filtered and any event with a rainfall depth exceeding the 50 year

return period depth was identified, checked manually and subsequently deleted from the records.

5.1.4 Spatial interpolation of erosivity density data

The purpose of spatial interpolation is to use a limited set of parameter values, measured at a finite number of locations, to estimate the value of the parameter at unmeasured locations (Tomczak, 1998). In order to obtain the erosivity density at any point in the country, the erosivity density had to be interpolated from the values computed at the continuously recording rainfall stations.

There are many interpolation models available and the choice depends on the nature of the data to be interpolated. The Inverse Distance Weighted (IDW) interpolation method was selected for a number of reasons, including being “relatively fast and easy to compute, and straightforward to interpret” (Lu and Wong, 2008). IDW works on the assumption that “things that are close together are more alike than those that are further apart” (Johnston *et al.*, 2001). Based on the sample points’ distance from the prediction point, a distance weighted average of surrounding measured values is calculated. In this way, measured values that are nearest the prediction point have the most influence on the final result.

The only two variables that can be altered in an IDW interpolation are the power value and the neighbourhood search strategy. The power value affects how fast the weighting decreases as the distance from the prediction point increases. The neighbourhood search strategy determines the number of measured values used in the calculation of each prediction point. Either the number of ‘neighbours’ (nearby sample points) can be limited, or a search radius can be implemented. In the former case, the calculation will be performed with the closest number of neighbours specified. In the latter case, all neighbours in the prescribed radius are used for the interpolation. If necessary, a combination of both methods can be used in that a search radius is specified, but a minimum number of neighbours is also prescribed. If the minimum number of neighbours does not occur within the search radius, the nearest stations outside of the radius will be used until the minimum number is reached.

Software developed by the Environmental Systems Research Institute (ESRI) was used to perform the interpolation. The Geostatistical Analyst function in ArcMap 9.3 (ESRI, 2008) was utilised, which allows the user to specify the number of neighbours, power and search radius. The programme also performs cross-validation on the interpolation for a given set of

parameters. Cross-validation is performed by removing each point, in turn, and comparing the predicted value with the measured value for that point. When deciding on the number of neighbours to use, it was found that there was no single number that produced optimal results for each month. For each month, a range of values was tested in order to attempt to minimise the Root Mean Square Prediction Error of the cross-validation. It was found that each month required a different number of neighbours to optimise the interpolation, with no clear trends. In order to produce the USA rainfall erosivity maps for RUSLE2, the developers used 10 neighbours for most of the country, and 5 in areas where the stations were more sparsely distributed (USDA-ARS, 2013). For this reason, it was decided that a maximum of 10 neighbours would be used and a minimum of 5, in order to maintain a standard with the calculation methods of the USA.

The search radius was rather arbitrarily selected as 250 km. A number of radii were tested. It was found that smaller radii rarely included 10 stations, while larger radii did not exclude enough stations in the more sparsely populated areas, resulting in large distances between the prediction point and some of the measured values. The power value was optimised by the Geostatistical Analyst programme. This optimisation occurs by performing a cross-validation on the interpolated data with a number of power values, and selecting the value that produces the lowest Root Mean Square Prediction Error.

The stations were split into “training stations” and “test stations”. The training stations were used to perform the interpolation, while the test stations were used to verify the interpolation, as explained in the following section.

5.1.5 Selection of independent test stations

The verification of any interpolation is crucial in determining how reliable the interpolated data is. In selecting verification stations, it was felt that it was important to select stations that were well distributed spatially (*i.e.* stations should be chosen to represent a number of areas with different rainfall characteristics), as well as having a reasonable record length, to ensure that they were indeed representative of their respective areas.

In order to do this, the stations were categorised according to which of the 15 short duration rainfall clusters, delineated by Smithers and Schulze (2000), they were located in. Short duration rainfall clusters, as explained in detail in the following chapter, are areas which have relatively homogeneous short duration rainfall characteristics. They provide a short duration

rainfall-based means of dividing the country, rather than using provinces or some other arbitrary set of boundaries. The stations in each cluster were ranked in terms of the number of years of record, and the station with the median record length in each cluster was selected as a test station. If the number of stations in a cluster was even, the station with the shorter record of the two median stations was selected. In this way, one station from each cluster was selected as an independent test station, with the exception of Cluster 4, which contained no stations, and Clusters 5 and 14 which contained only 2 stations each. This resulted in a final number of 12 ‘test’ or verification stations across the country, as shown in Figure 5.6.

These stations were removed from the data set before the interpolation of erosivity density. In verifying the interpolation, the prediction of erosivity density at the test stations was compared with the erosivity density calculated from the observed continuously recorded rainfall data.

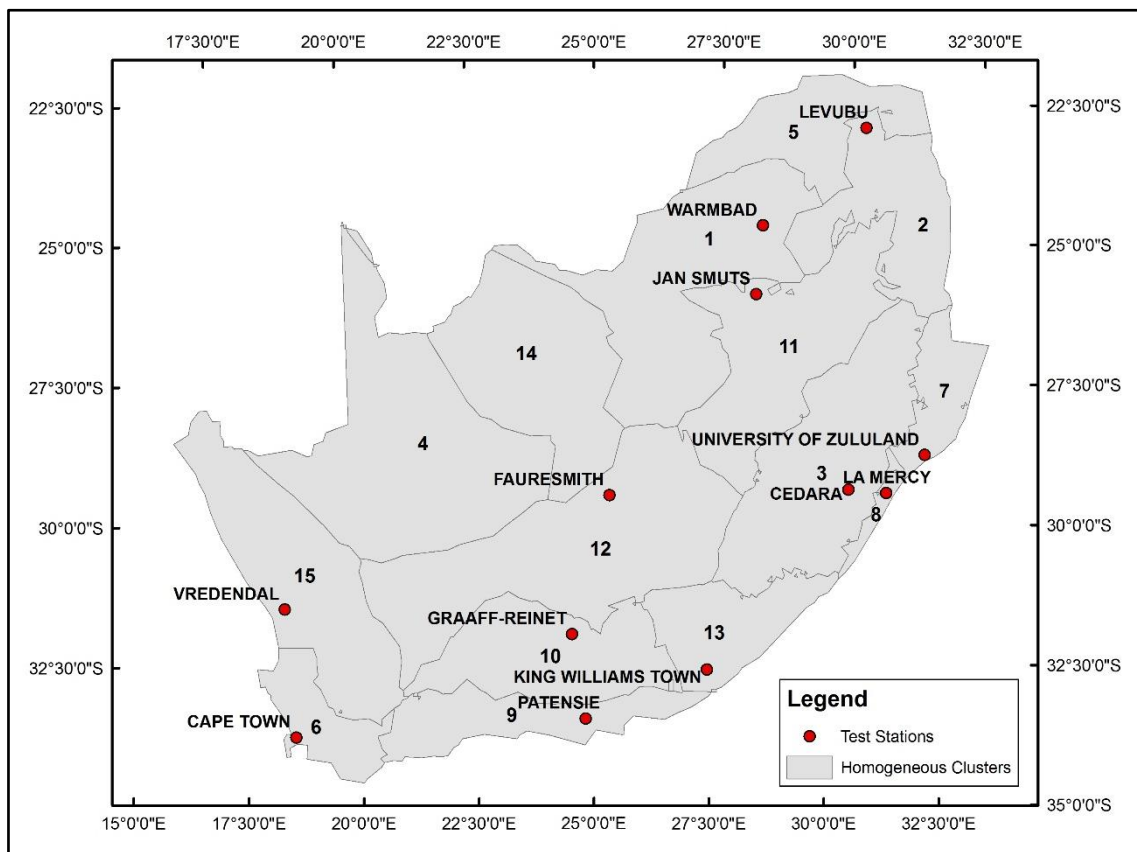


Figure 5.6 Location of verification stations within the homogeneous clusters defined by Smithers and Schulze (2000)

The test stations were used again after the rainfall erosivity had been calculated for the country, as explained in the following sections. The final predicted rainfall erosivity values were extracted at the test stations. These values were then compared with the EI_{30} values calculated

directly from the continuously-recorded data at the stations. This allowed verification of the erosivity density method as a whole.

5.1.6 Use of Quinary Catchment rainfall data

In order to obtain a final rainfall erosivity value at a location, the erosivity density must be multiplied by the monthly rainfall amounts at that location. Although a user could input their own local rainfall values to determine the rainfall erosivity at a point, the aim of this study was to provide countrywide estimates of rainfall erosivity. Countrywide estimates of rainfall were therefore required to obtain a final rainfall erosivity value. The RUSLE2 database has rainfall erosivity data assigned to each county in the USA (USDA-ARS, 2003). Users can simply select their county and obtain rainfall erosivity values applicable to that location. A similar approach is desirable for South Africa, however, a spatial entity equivalent to the USA counties had to be found. One drawback to developing rainfall erosivity values for counties is that the counties are not necessarily hydrologically homogeneous, therefore the values may not be an accurate representation of the area of interest.

For water resource management, South Africa has been disaggregated into 22 Primary Catchments. Within these catchments, subsequent disaggregations have been performed to form secondary, tertiary and quaternary catchments. A study performed by Schulze and Horan (2011) found that large variations in altitude were found to occur in many Quaternary Catchments, and a further disaggregation into relatively homogeneous Quinary Catchments was required. Each Quaternary Catchment was divided into an Upper, Middle and Lower Quinary Catchment based on “natural breaks” in altitude. This resulted in the area comprising South Africa, Lesotho and Swaziland being disaggregated into 5 838 Quinary Catchments, as shown in Figure 5.7.

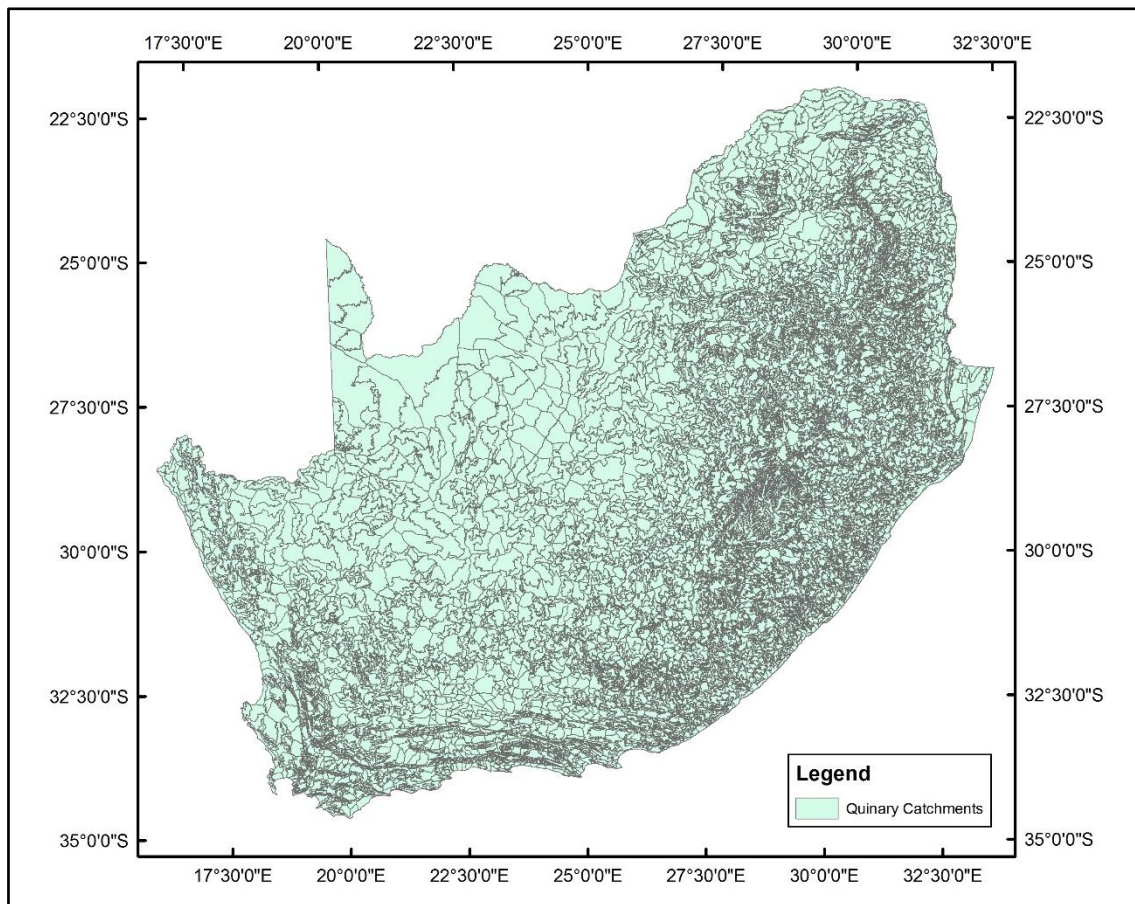


Figure 5.7 Quinary Catchments determined by Schulze and Horan (2011)

In order to allocate rainfall data to the Quinary Catchments, Schulze *et al.* (2011) allocated daily rainfall stations to each Quinary Catchment based on the work done by Schulze *et al.* (2005). Each Quinary Catchment was allocated the same “driver” station as its parent Quaternary Catchment. Each driver station has a quality controlled and, where necessary, infilled daily rainfall record from 1950 to 1999. A unique daily rainfall record was created for each Quinary Catchment by multiplying the data from the driver station by a monthly adjustment factor. These factors were obtained by averaging the one arc minute gridded median rainfall in the Quinary Catchment, developed by Lynch (2004), and forming a ratio with the median monthly rainfall at the driver station. In this way, a median monthly rainfall value was determined for every one of the Quinary Catchments. The annual rainfall, as determined for the individual Quinary Catchments by Schulze *et al.* (2011), is illustrated in Figure 5.8.

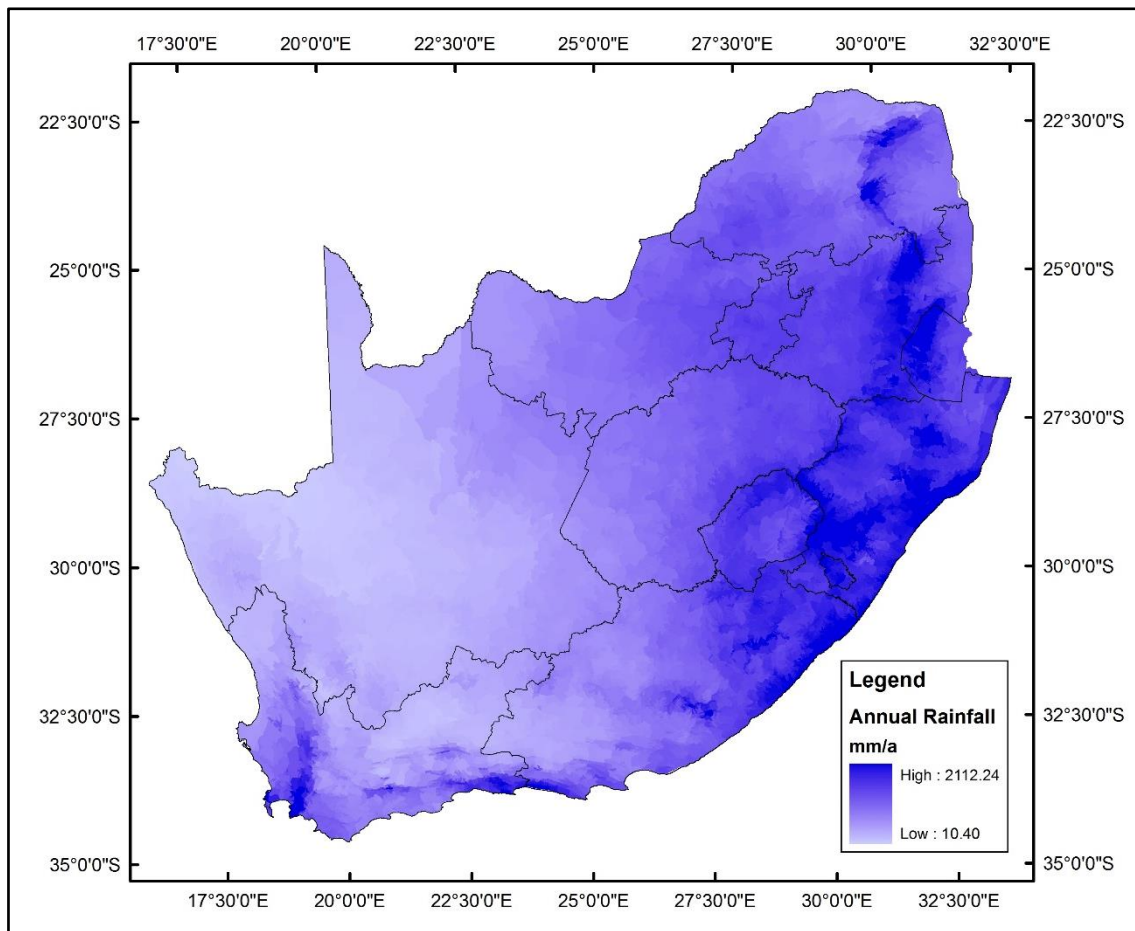


Figure 5.8 Annual rainfall distribution across the Quinary Catchments derived by summing the monthly median rainfall amounts (Schulze *et al.*, 2011)

For this study, the Quinaries Catchments were plotted with their associated median monthly rainfall values, as determined by Schulze *et al.* (2011). The rainfall layer was then multiplied by the relevant monthly erosivity density layer, producing a map of rainfall erosivity for South Africa. The rainfall erosivity was then averaged within the Quinary Catchments to provide a unique monthly set of rainfall erosivity values for each Quinary Catchment.

5.2 Results and Discussion of Erosivity Density Method

This section presents the results obtained using the erosivity density approach to calculate rainfall erosivity across South Africa. The results of the application of different energy equations and thresholds are also presented and discussed in this section.

5.2.1 Effect of different energy equations

Figure 5.9 shows the mean erosivity density for all 83 stations, calculated using the five different energy equations, for each month. The results shown are for the scenario in which both the 12.7 mm threshold and 50 year return period threshold are applied, as used in RUSLE2 (USDA-ARS, 2013). It can be seen that the trends are fairly consistent from month to month. The equation suggested by Wischmeier and Smith (1958) tends to yield the highest values while the values computed using the Elwell and Stocking (1973) equation are the lowest erosivity density values for each month. It is interesting to note that the equation proposed by van Dijk *et al.* (2002), which was derived from data in multiple areas and was deemed to be a “universal” equation, gives the median result in most months. It is therefore effective at finding a “compromise” between various equations.

It can be seen in Figure 5.5 that the Wischmeier and Smith (1958) equation only gives the highest unit energy of the 5 equations between 3 mm.h⁻¹ and 10 mm.h⁻¹. Similarly, the Elwell and Stocking (1973) equation only produces the lowest unit energy value of the 5 equations between 4 mm.h⁻¹ and 9 mm.h⁻¹. This suggests that the long term average of erosivity density is influenced more by the frequent lower intensity rainfall events than the infrequent high intensity rainfall events.

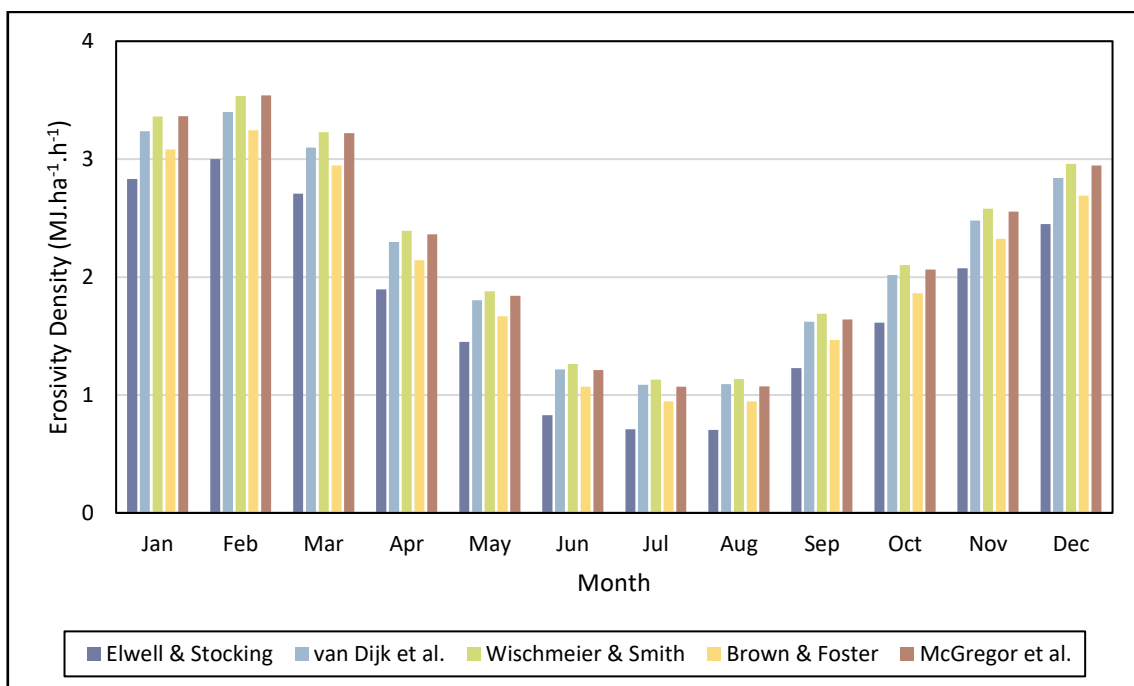


Figure 5.9 The effect of different energy equations on mean monthly erosivity density values for all short duration stations

Figure 5.10 shows the effect of the different energy equations on the mean annual erosivity density of the 83 short duration rainfall stations. The magnitude of the effect of the different energy equations varies depending on the month and the station. However, it is interesting to note that when looking at the average of all 83 stations, for the same rainfall input data, the highest erosivity density value is 26.7 % higher than the lowest value.

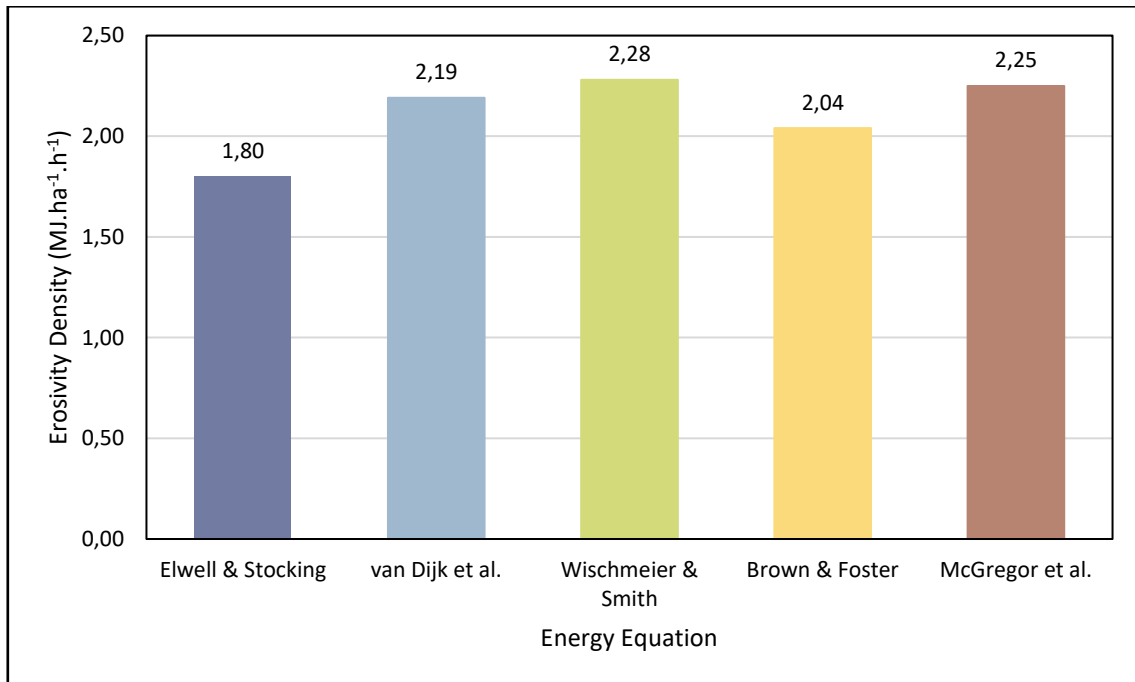


Figure 5.10 The effect of different energy equations on the mean annual rainfall erosivity for all short duration stations

The Cedara station (station number 0239482) is located near Pietermaritzburg in the KwaZulu-Natal midlands, as illustrated in Figure 5.11. This station has a relatively long record of 46 years, and clearly demonstrates the general trends observed in the overall results.

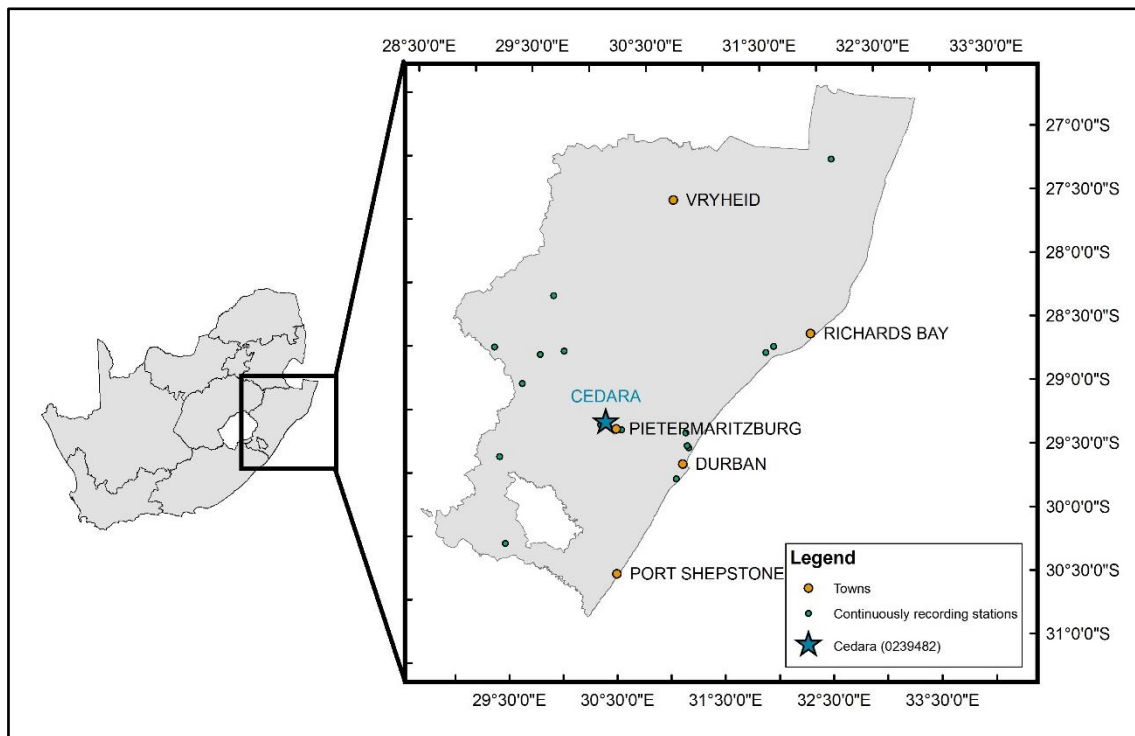


Figure 5.11 Location of the Cedara station (0239482) in KwaZulu-Natal

Figure 5.12 shows the effects of the various energy equations at the Cedara station. Although the same trend is shown by all of the equations, the difference between the highest value and the lowest value for a month can be substantial. For example, in July, the Elwell and Stocking (1973) equation gives an erosivity density value of $0.59 \text{ MJ}\cdot\text{ha}^{-1}\cdot\text{h}^{-1}$, while the Wischmeier and Smith (1958) equation gives a value almost double that, of $1.05 \text{ MJ}\cdot\text{ha}^{-1}\cdot\text{h}^{-1}$. This shows the importance of choosing representative energy equations, as a small difference at this step can mean unnecessary expenditure on soil conservation structures, or conversely, the loss of excessive amounts of soil through erosion.

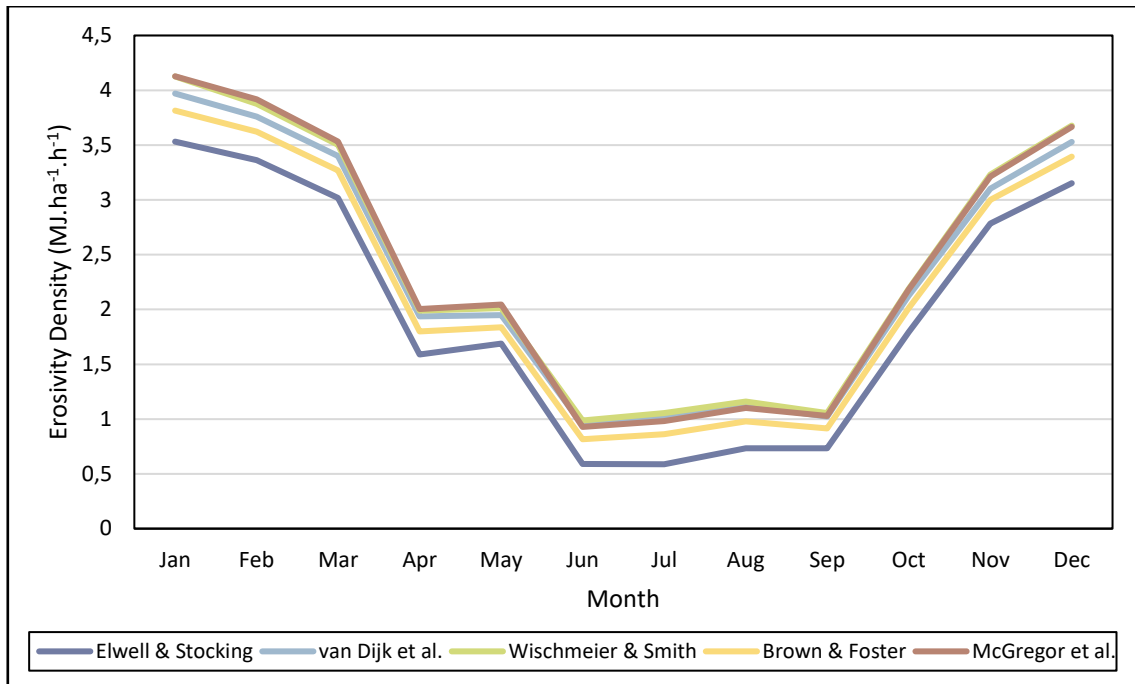


Figure 5.12 The effect of different energy equations on erosivity density values at Cedara, KwaZulu-Natal

The energy equation used in RUSLE2 (USDA-ARS, 2013) is that of McGregor *et al.* (1995). In order to maintain uniformity with the RUSLE2 methodology, the McGregor *et al.* (1995) equation was selected as the energy equation with which to use in the final calculations of rainfall erosivity for this study. In general, this equation gives the second highest erosivity density. This provides a relatively conservative estimate of soil loss and should prevent inadequate design of soil conservation structures.

5.2.2 Effect of thresholds

Figure 5.13 shows the effect of excluding events which exceed various thresholds in the data. The results shown are those produced using the McGregor *et al.* (1995) energy equation (Equation 3.24), as applied in the development of RUSLE2 (USDA-ARS, 2013). The first series shows the erosivity density calculated using all of the data, without thresholds.

The second series shows the erosivity density after removing events less than 12.7 mm. It is evident that applying the 12.7 mm threshold has an effect on the results. The removal of these events decreases the erosivity density for all months. The average decrease in erosivity density over all of the stations was found to be 5 % of the original value. This is a greater effect than the 3.5 % reduction reported in a study conducted by McGregor *et al.* (1995). The main reason

for excluding small events in the earlier studies was to reduce computing time and costs. Wischmeier and Smith (1978) argued that excluding these events would have little effect on rainfall erosivity due to the fact that “the *EI* values for such rains are usually too small for practical significance and that, collectively, they have little effect on monthly percentages of the annual *EP*”. The results in Figure 5.13, however, show that the removal of these events does have an effect on estimates of rainfall erosivity. The magnitude of the effect varies from station to station, depending on the nature of the rainfall that each station. If a large proportion of a station’s rainfall is made up of relatively small events (*i.e.* less than 12.7 mm), the estimate of erosivity density, and hence rainfall erosivity, could be artificially low.

The third series shows the average monthly erosivity density with the 12.7 mm threshold applied, as well as having removed events exceeding the 50 year return period. Owing to the relatively short records of short duration data, it was found that very few events exceeded this return period and only 31 of the 83 stations were affected. Nevertheless, excluding these events did have an effect on the average erosivity density. It was found that the additional threshold reduced the average erosivity density of all of the stations by a further 3 %, resulting in an overall average reduction of 8 % from the original values.

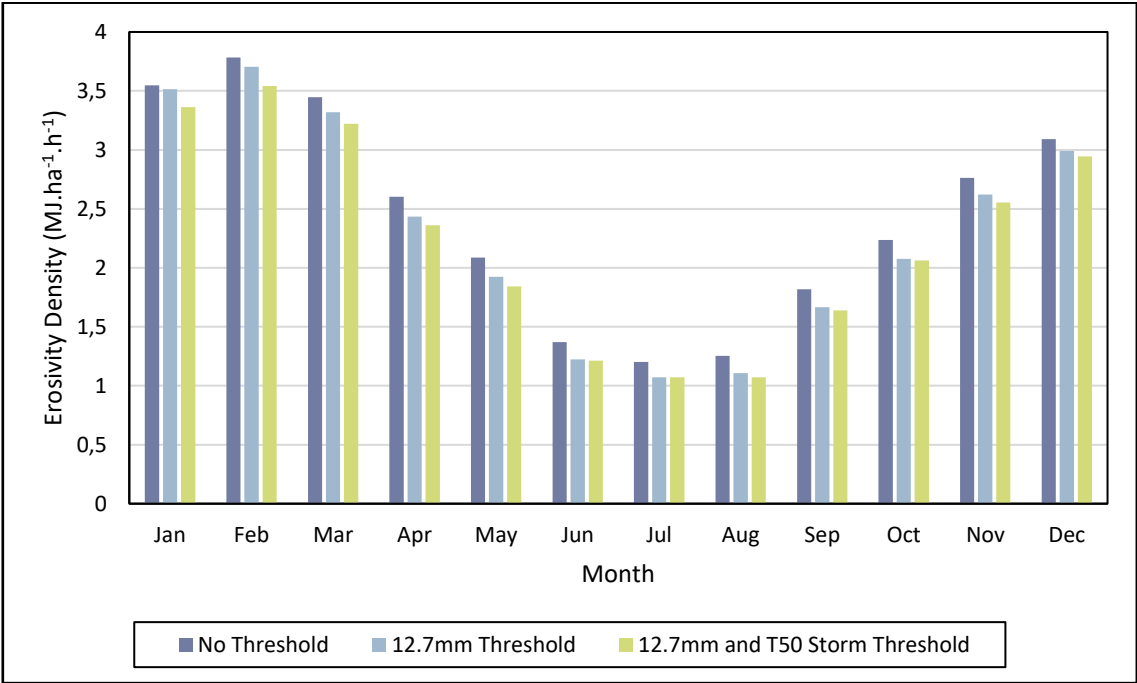


Figure 5.13 The effect of applying thresholds to data on erosivity density values

The impact of excluding events with a return period greater than 50 years shows a relatively small effect on the average of the 83 stations, owing to the fact that storms were only removed

at 31 stations. However, when comparing results at a single station, the effect of large storms can be considerable. Figure 5.14 shows the effect of thresholds on one station, Cedara. It is evident that the exclusion of large events has had a large effect in the month of September. This was found to be a single event, which caused widespread flooding in KwaZulu-Natal in September 1987. The removal of this single event almost halves the erosivity density for September from 1.96 MJ.ha⁻¹.h⁻¹ with just the 12.7 mm threshold applied, to 1.03 MJ.ha⁻¹.h⁻¹ after the removal of the extreme event. Applying the 50 year return period threshold usually results in a ‘smoother’ graph as the peaks caused by large storms are removed.

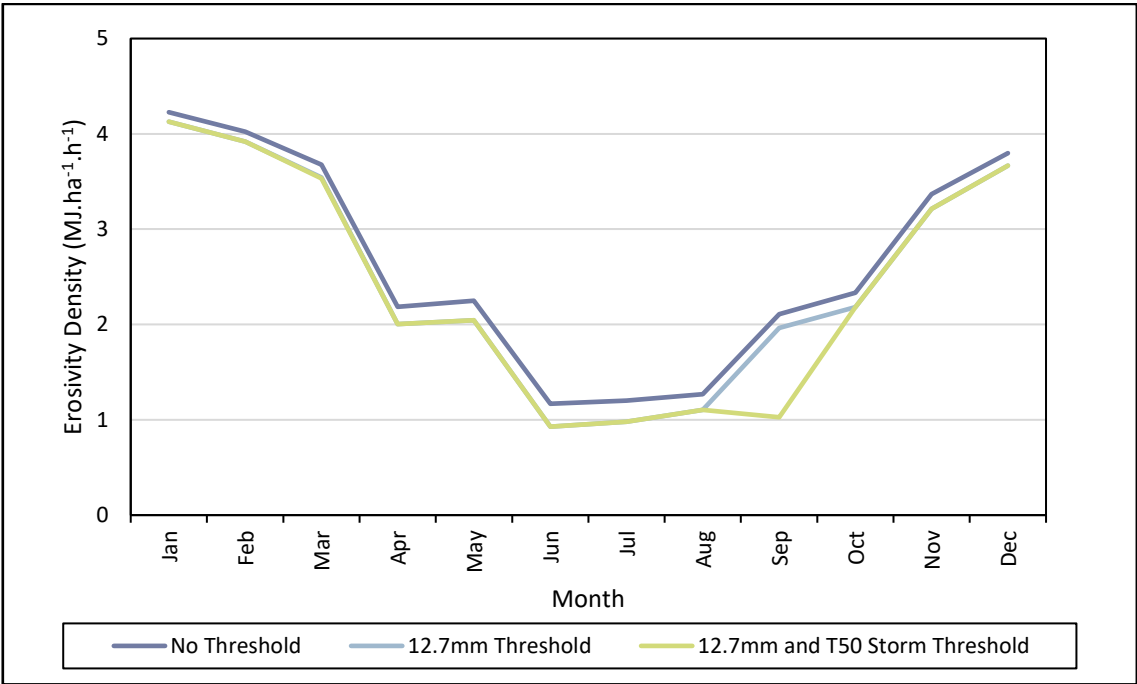


Figure 5.14 The effect of thresholds on erosivity density values at Cedara, KwaZulu-Natal

This study applied both the 12.7 mm threshold and the 50 year return period threshold in order to obtain final estimates of rainfall erosivity. This was to maintain consistency with the practices used in developing rainfall erosivity values for the RUSLE2 software. However, it can be seen that the exclusion of events smaller than 12.7 mm does have an effect on the erosivity density estimates. As computing power improves, and is no longer a major limiting factor in this regard, it is suggested that the 12.7 mm threshold be disregarded in future studies.

Regarding the 50 year return period threshold, it is suggested that this be maintained due to the large effect that these storms have when working with relatively short record lengths. Longer record lengths would allow the high rainfall erosivity of these individual events to be averaged over many years, reducing the impact and arguably providing a more accurate picture of long

term rainfall erosivity. However, when averaged over just 10 years, these large events skew the results substantially and do not provide an accurate representation, of both the magnitude and distribution, of erosivity density.

5.2.3 Cross-validation results

Cross-validation, as explained in Section 5.1.4, involves the exclusion of one training station at a time and the comparison of the predicted interpolated value and the observed value at that point. This provides a first means of assessing the performance of the interpolation. The cross-validation results for the mean annual erosivity density are shown in Figure 5.15. It can be seen that the correlation between the observed and predicted values is fairly low. Although the general trend is correct, the scatter around the line of best fit is relatively large. Owing to the fact that Inverse Distance Weighting uses averaging of nearby values for predictions, it is to be expected that the model under-predicts the higher values and over-predicts the lower values. The predicted value can be no higher or lower than those at the surrounding points, leading to a moderating effect. This is evidenced by the clear trend in the error, moving from a positive value to a negative value as the erosivity density increases. The use of other interpolation models could reduce this effect. Alternatively, an approach such as that of Le Roux *et al.* (2006) could be used, in which IDW interpolation was used, but with the influence of topography taken into account.

The large errors can be attributed to the low spatial density of short duration stations. The errors are caused due to the fact that the surrounding stations have values that differ largely from the station of interest. If the station network was more densely populated, the stations would be closer together and the closest 10 stations would give a much better estimation of the value at the point of prediction. Although the interpolation was performed in order that any stations outside of a 250 km radius were excluded, large geographical and climatic variation can exist within this radius. Having a larger number of continuously recording stations would allow the radius to be reduced, and would be expected to improve the accuracy of the interpolation.

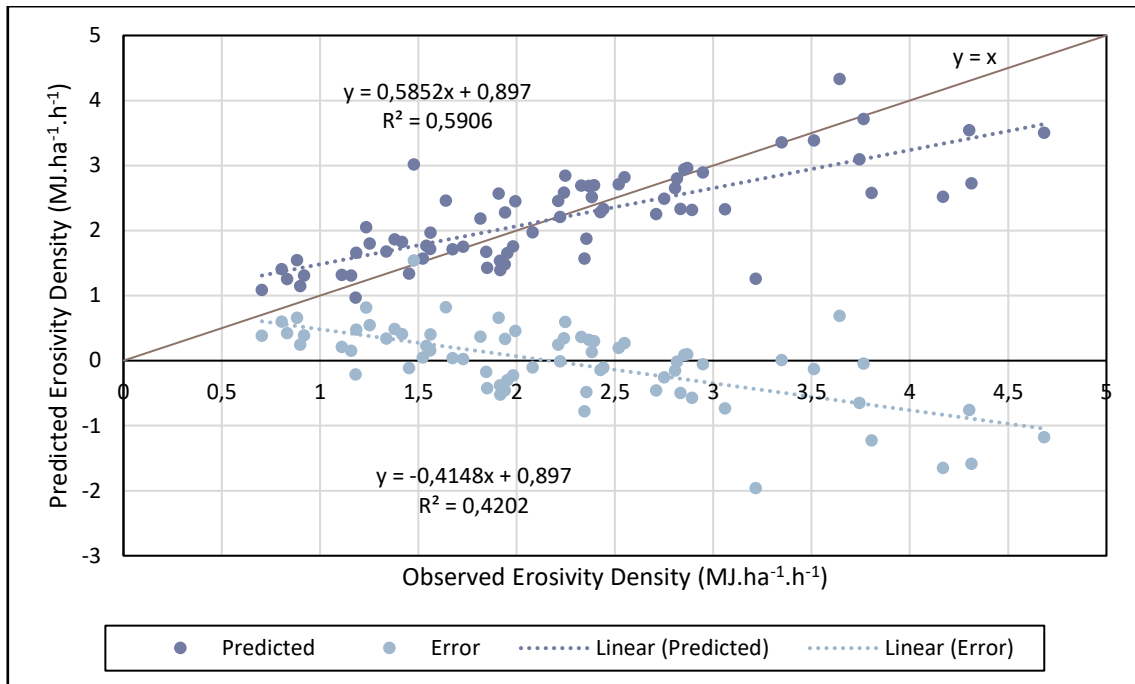


Figure 5.15 Cross validation results for the interpolation of mean annual erosivity density values

5.2.4 Verification results

As discussed in Section 5.1.5, two verification processes were undertaken. The first process involved the removal of the test stations before the interpolation of erosivity density took place. This allowed comparison between the values predicted by the interpolation, and the observed erosivity density values at the stations.

The second process involved the comparison of the final rainfall erosivity value predicted at the test stations, after the multiplication of erosivity density and rainfall amount, and the EI_{30} value calculated directly from the continuously-recorded rainfall data at the station.

5.2.4.1 Verification of the interpolation

The verification in this study involved the exclusion of 12 ‘test’ stations from the dataset used to interpolate erosivity density across South Africa. The erosivity density values calculated at each of these stations were then compared with the erosivity density values obtained through interpolation from the ‘training’ stations. The relative errors between the predicted and observed erosivity density values are presented in Table 5.1. The arithmetic mean of the percentage errors was calculated for each station, as well as for each month. When analysing the monthly erosivity density values, the verification process shows an overall error of 75%.

Although there are exceptions to this, the general trend is that the error increases during the low rainfall months (summer in the Cape and winter for the majority of the remainder of the test stations). This can be attributed to the fact that there are fewer events in these months to generate results. For this reason, the results can be erratic and do not reflect the actual conditions accurately. The largest errors in the table include the month of September at Levubu (station number 0723485), as well as consistently high errors at the stations of Vredendal (station number 0106880) and Graaff-Reinet (station number 0096045).

Table 5.1 Relative errors between predicted and observed erosivity density values at the verification test stations (%)

STATION NO.	LOCATION	JAN	FEB	MAR	APR	MAY	JUN	JUL	AUG	SEP	OCT	NOV	DEC	MEAN
0021178	CAPE TOWN D F MALAN	72	50	104	40	83	24	29	17	93	37	54	446	87
0033556 5	PATENSIE	6	2	28	51	62	10	7	32	287	56	4	48	49
0079712	KING WILLIAMS TOWN	15	8	24	3	30	18	12	70	175	29	8	4	33
0096045	GRAAFF- REINET	14	16	25	258	197	253	97	452	524	18	58	6	160
0106880	VREDENDAL	924	-	458	27	196	52	395	67	182	207	493	646	332
0229556	FAURESMITH	5	33	14	5	51	10	164	29	88	0	16	28	37
0476398	JAN SMUTS	6	2	2	74	70	35	50	4	14	1	2	1	22
0589594	WARMBAD - TOWOOMBA	0	14	6	26	21	15	52	45	22	26	8	22	21
0723485	LEVUBU	47	7	12	91	9	52	-	51	458	16	35	7	71
304473	UNIVERSITY OF ZULULAND	25	29	101	73	29	7	11	47	25	104	91	120	55
c164	CEDARA	26	24	3	28	93	26	54	49	88	24	47	8	39
sal10	LA MERCY	1	2	11	10	19	10	6	60	42	14	19	33	19
MEAN		95	17	66	57	72	43	80	77	167	44	69	114	75

A large verification error is found in the month of September for Levubu. Figure 5.16 shows the locality of this station, as well as the surrounding stations. On investigation, it was found that a nearby station, Skukuza, experienced a number of relatively large, isolated storms in the month of September, with the largest rainfall erosivity being recorded in a storm in 1977. Although Levubu experienced a rainfall event in 1977 around the same time as Skukuza, it was nowhere near as intense. Although none of Skukuza's storms were large enough to be removed by the 50 year return period threshold, they all added up to produce a much higher overall rainfall erosivity than Levubu.

The problem is exacerbated by the low spatial density of short duration stations in the area. Skukuza is approximately 250 km from Levubu, yet it still has a strong effect on the interpolated values as it is one of the closest stations. Coupled with the relatively short records, errors can be expected to be high. Figure 5.16 indicates the erosivity density values for the month of September at the surrounding stations. It can be seen that no definite trend exists and the erosivity density values are erratic.

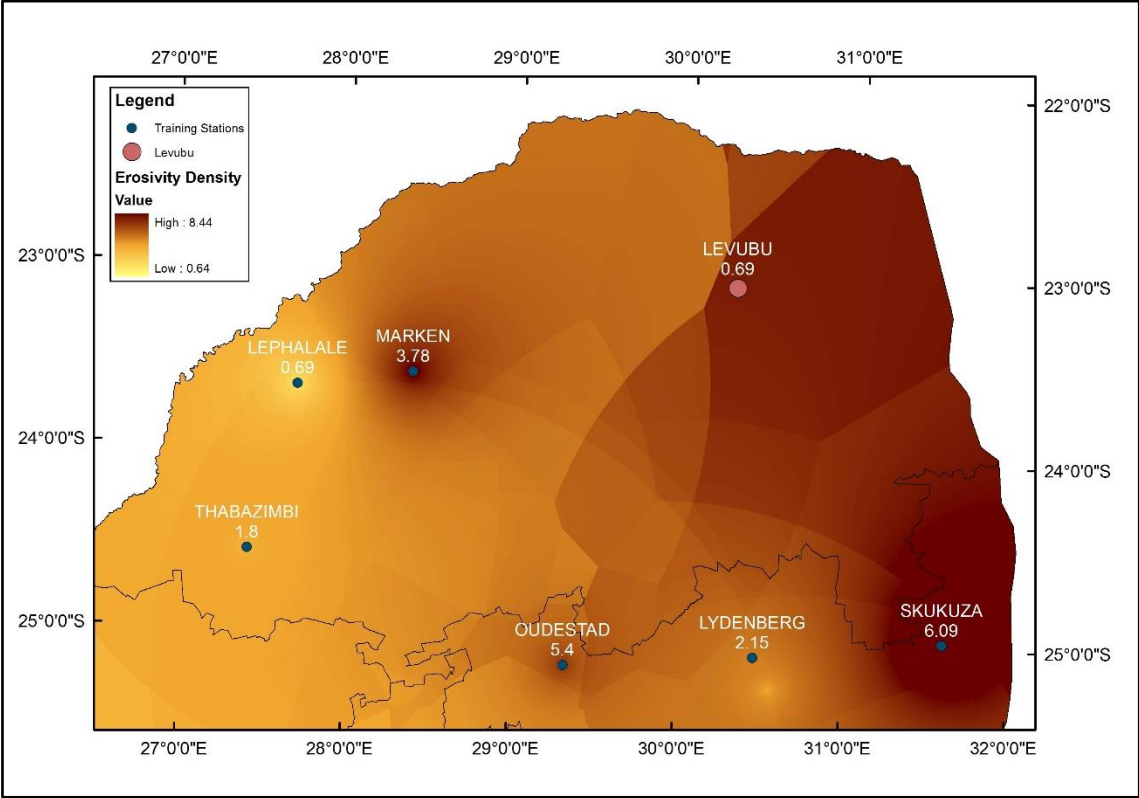


Figure 5.16 Erosivity density for September in the region of the Levubu station

In terms of the errors at Graaff-Reinet, much can be attributed to the low frequency of rainfall events in the winter months. Figure 5.17 shows the percentage error in verification against the number of rainfall records in a month with which erosivity density was calculated. It can be seen that there is a strong correlation between the number of rainfall events and the magnitude of the error.

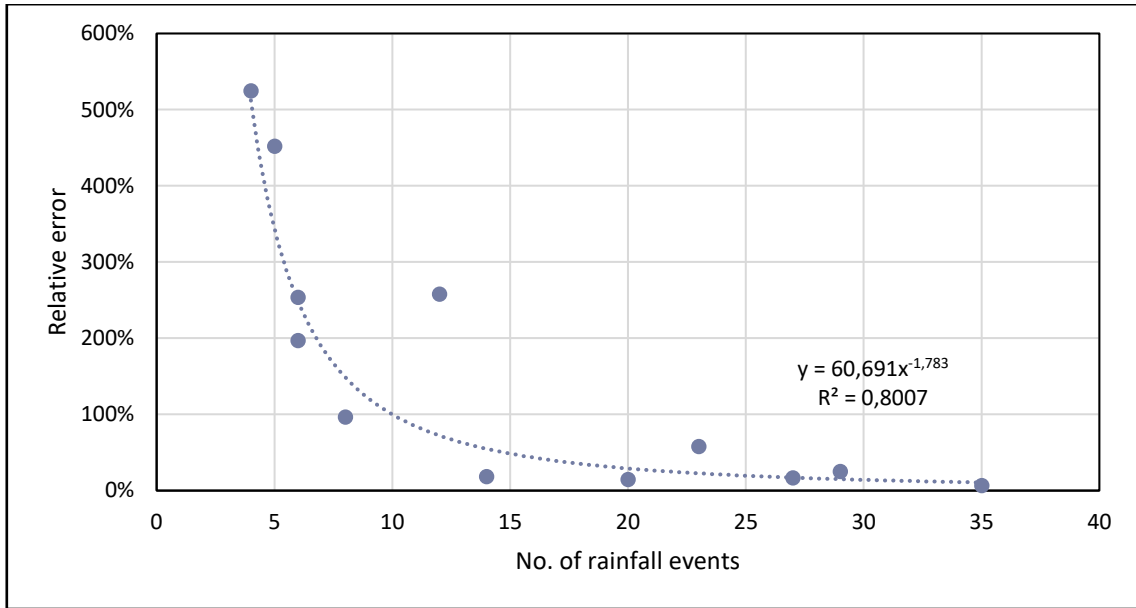


Figure 5.17 The effect of data scarcity on errors in verification at Graaff-Reinet

It was found that a large proportion of the rainfall at Graaff-Reinet falls in smaller events and are excluded by the 12.7 mm threshold. The ratio of results obtained with the thresholds, and the original results, was calculated and this is shown in Figure 5.18. In the worst case, August, applying the 12.7 mm threshold resulted in a monthly erosivity density that was only 36 % of the original value. This reiterates the need to abandon the 12.7 mm threshold, particularly in low rainfall areas.

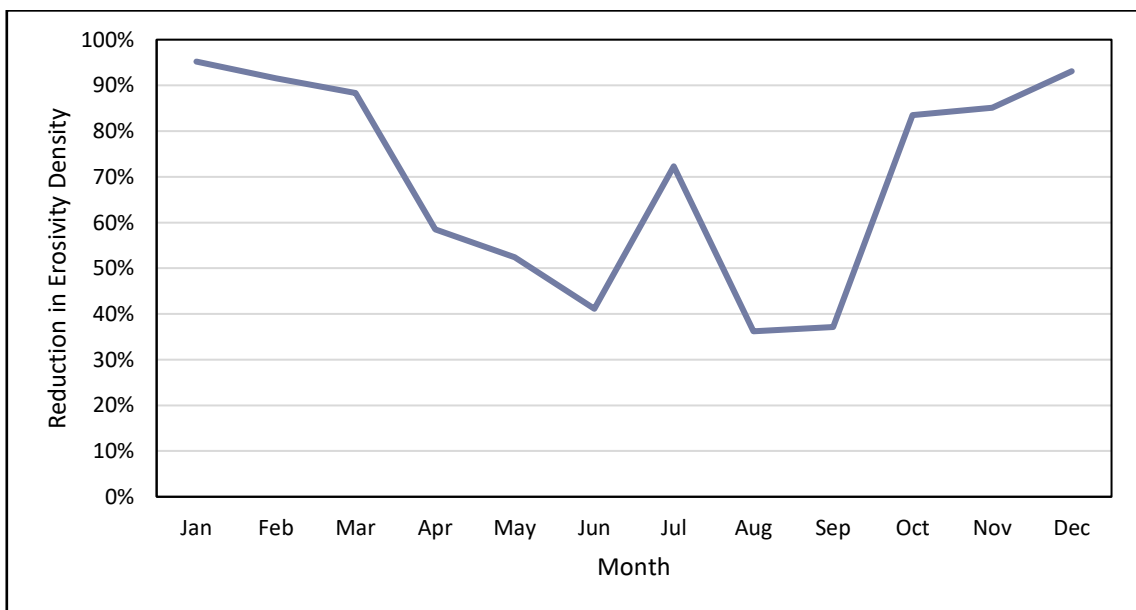


Figure 5.18 Reduction in monthly erosivity density due to application of 12.7 mm threshold at Graaff-Reinet

Another factor contributing to the high relative errors at Graaff-Reinet is the fact that the erosivity density values are very low in the winter months. Therefore, a relatively small absolute error produces a large relative error. Figure 5.19 illustrates this effect at Graaff-Reinet. It can be seen that the absolute error does not fluctuate greatly from month to month and remains below 1.5 MJ.ha⁻¹.h⁻¹ for all months. However, as the erosivity density drops to approximately 0.2 MJ.ha⁻¹.h⁻¹, the absolute error of approximately 1 MJ.ha⁻¹.h⁻¹ relates to a relative error of around 500 %.

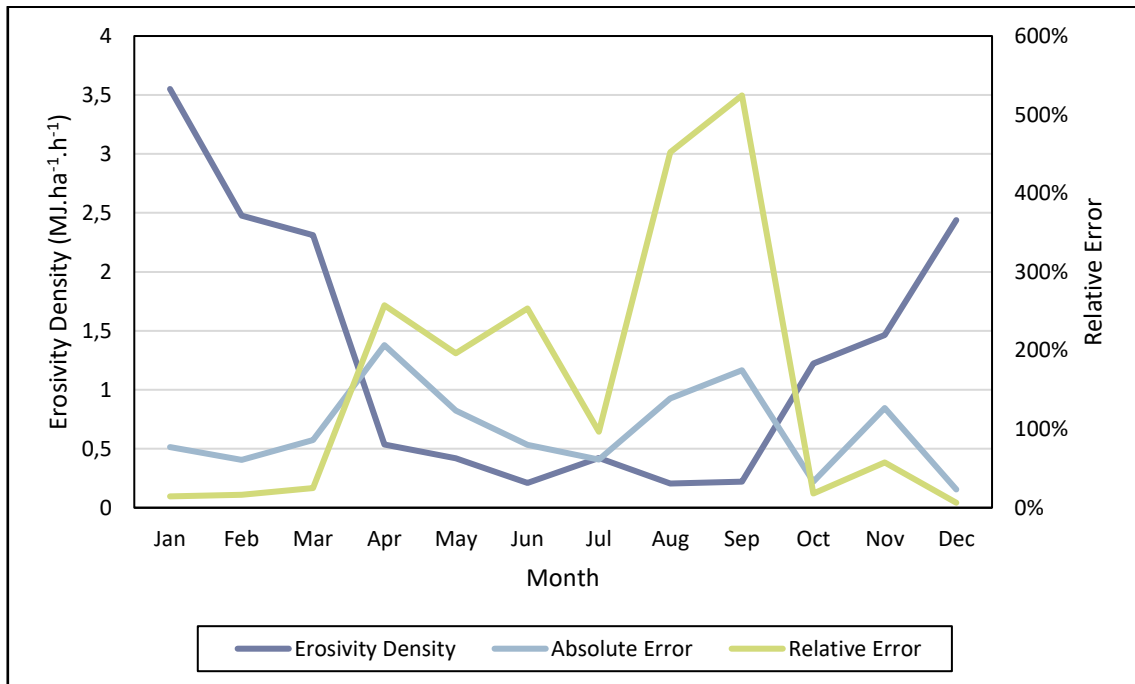


Figure 5.19 Comparison of absolute error and relative error at Graaff-Reinet

The high errors for Vredendal station can also be explained by the reasons stated above. The relative error for Vredendal in the month of January is the highest of all of the relative errors – 924 %. Figure 5.20 illustrates the position of Vredendal relative to the surrounding training stations. It can be seen that the erosivity density value for Vredendal in January is a local minimum. Owing to the nature of IDW interpolation, the interpolated value cannot be lower than any of the surrounding stations. In addition to this, the erosivity density value at Vredendal is particularly low compared to the surrounding stations, meaning that even a small absolute error results in a large relative error.

In addition to the above, South Africa’s west coast generally receives little rainfall, leading to erratic results that are not fully representative of the long term conditions. To highlight this, it can be seen that the station to the north of Vredendal, Koingnaas, does not have an erosivity

density value at all for January. This is due to the fact that no rainfall events occurred in January that met the threshold value of 12.7 mm. This provides additional motivation to disregard the 12.7 mm threshold in future studies, particularly in areas with low rainfall and where rainfall records are relatively short.

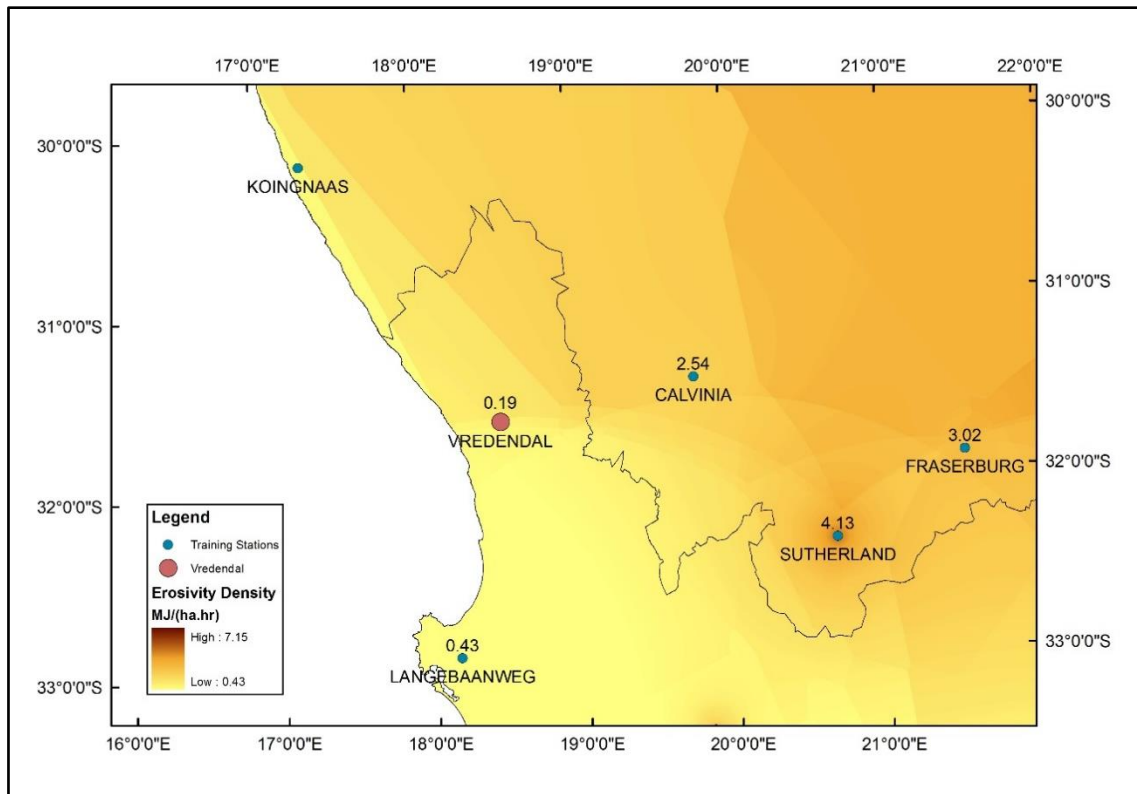


Figure 5.20 Erosivity density for January in the region of the Vredendal station

Although the monthly analysis of the verification process appears to yield relatively poor results, the interpolation of the mean annual erosivity density performs considerably better. The error between the predicted and observed mean annual erosivity density results are presented in Table 5.2. Although the overall relative error is still fairly high at 37 %, the overall absolute error is only $0.37 \text{ MJ}\cdot\text{ha}^{-1}\cdot\text{h}^{-1}$. If the outlier Vredendal is removed, the overall relative error reduces to 19 %. This shows that the relatively high errors in the individual months are evened out and that much more consistent trends are present when analysing annual values.

Table 5.2 Prediction errors of mean annual erosivity density (MJ.ha⁻¹.h⁻¹)

STATION NO.	LOCATION	OBSERVED	PREDICTED	ERROR	RELATIVE ERROR (%)
0021178	CAPE TOWN	1.04	1.62	0.58	56
0033556 5	PATENSIE	1.55	1.57	0.01	1
0079712	KING WILLIAMS TOWN	1.61	1.73	0.12	8
0096045	GRAAFF-REINET	1.29	1.84	0.55	43
0106880	VREDENDAL	0.32	1.09	0.77	239
0229556	FAURESMITH	2.25	2.38	0.13	6
0476398	JAN SMUTS	2.59	2.78	0.19	7
0589594	WARMBAD	3.15	3.27	0.12	4
0723485	LEVUBU	3.09	3.38	0.29	9
304473	UNIVERSITY OF ZULULAND	2.42	3.55	1.13	47
c164	CEDARA	2.05	2.53	0.49	24
sal10	LA MERCY	3.67	3.64	-0.03	1
MEAN		2.09	2.45	0.36	37

In the overall analysis of the interpolation verification results, the interpolation produced correct trends, but the errors are relatively high. Figure 5.21 shows the relationship between the predicted and the observed erosivity density results. The scatter around the line $y = x$ is fairly high, as evidenced by the large errors discussed above.

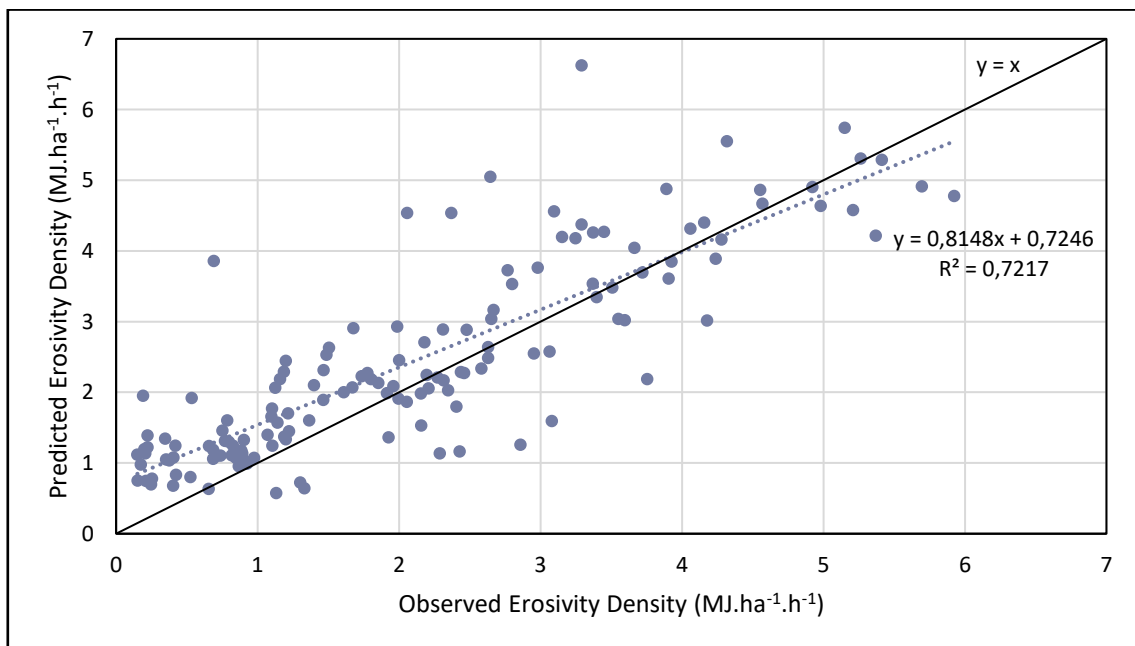


Figure 5.21 Comparison of predicted and observed erosivity density for all months and verification stations

Figure 5.22 shows the cumulative frequency of the absolute errors. As mentioned previously, the large relative (percentage) errors often occur when the absolute values are very low. Figure 5.22 shows that 82 % of the test points have an absolute error of less than 1 MJ.ha⁻¹.h⁻¹ while 96 % of the 142 points have an error less than 2 MJ.ha⁻¹.h⁻¹. In the 22 cases in which the relative error exceeded 100 %, 19 of these cases had an absolute error of less than 2 MJ.ha⁻¹.h⁻¹ and 15 of these had an absolute error of less than 1 MJ.ha⁻¹.h⁻¹.

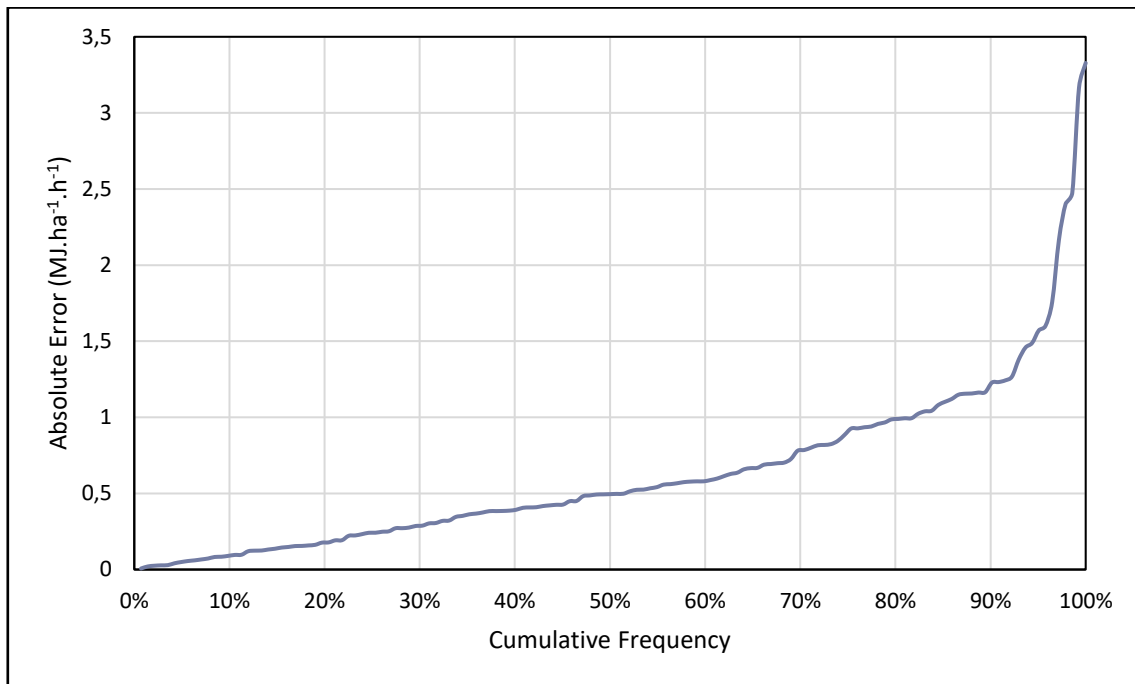


Figure 5.22 Cumulative frequency of relative errors obtained in verification

5.2.4.2 Verification of the method

The final rainfall erosivity results, obtained using the erosivity density method, were compared with the EI_{30} values obtained directly from the continuously-recorded data at the test stations. The relative errors of the predicted values, compared to the actual EI_{30} values are shown in Table 5.3. These are based on the absolute values of the errors, and do not indicate under- or overestimation. The blank cells in the table represent a situation in which either method produced a rainfall erosivity value of zero for the month. The arithmetic mean of the percentage errors was calculated for each station, as well as for each month. The overall arithmetic mean of the monthly relative errors across all of the test stations was found to be 55 %.

Table 5.3 Relative errors between predicted and observed rainfall erosivity values at the verification test stations, for the erosivity density method (%)

STATION NO.	LOCATION	JAN	FEB	MAR	APR	MAY	JUN	JUL	AUG	SEP	OCT	NOV	DEC	MEAN
0021178	CAPE TOWN D F MALAN	65	76	32	14	94	31	71	30	38	31	44	2	44
0033556 5	PATENSIE	63	50	30	29	43	71	57	41	66	75	49	82	55
0079712	KING WILLIAMS TOWN	19	19	79	56	58	72	86	75	60	25	12	34	50
0096045	GRAAFF- REINET	37	11	13	17	37	48	82	54	14	71	11	58	38
0106880	VREDENDAL	-	-	87	68	9	55	10	18	72	79	67	85	55
0229556	FAURESMITH	9	26	10	41	60	97	95	98	75	55	43	51	55
0476398	JAN SMUTS	18	8	1	11	59	99	-	96	76	13	-	11	39
0589594	WARMBAD - TOWOOMBA	8	12	5	33	86	-	-	-	78	11	1	15	28
0723485	LEVUBU	479	124	111	81	76	91	-	91	82	15	145	131	130
304473	UNIVERSITY OF ZULULAND	12	64	182	99	17	30	36	20	33	137	203	187	85
c164	CEDARA	78	38	2	32	17	77	72	52	35	34	57	2	41
sal10	LA MERCY	27	19	12	17	60	78	82	24	72	26	18	34	39
MEAN		74	41	47	42	51	68	66	54	58	48	59	58	55

The difference between the predicted and observed annual rainfall erosivity values is illustrated in Figure 5.23. It is evident that the erosivity density method tends to underestimate rainfall erosivity in areas where the rainfall erosivity is low, and generally overestimates when the rainfall erosivity is higher. The relative errors range from an underestimation of 57 % at Patensie (station number 0033556 5), to an overestimation of 97 % at Levubu (station number 0723485).

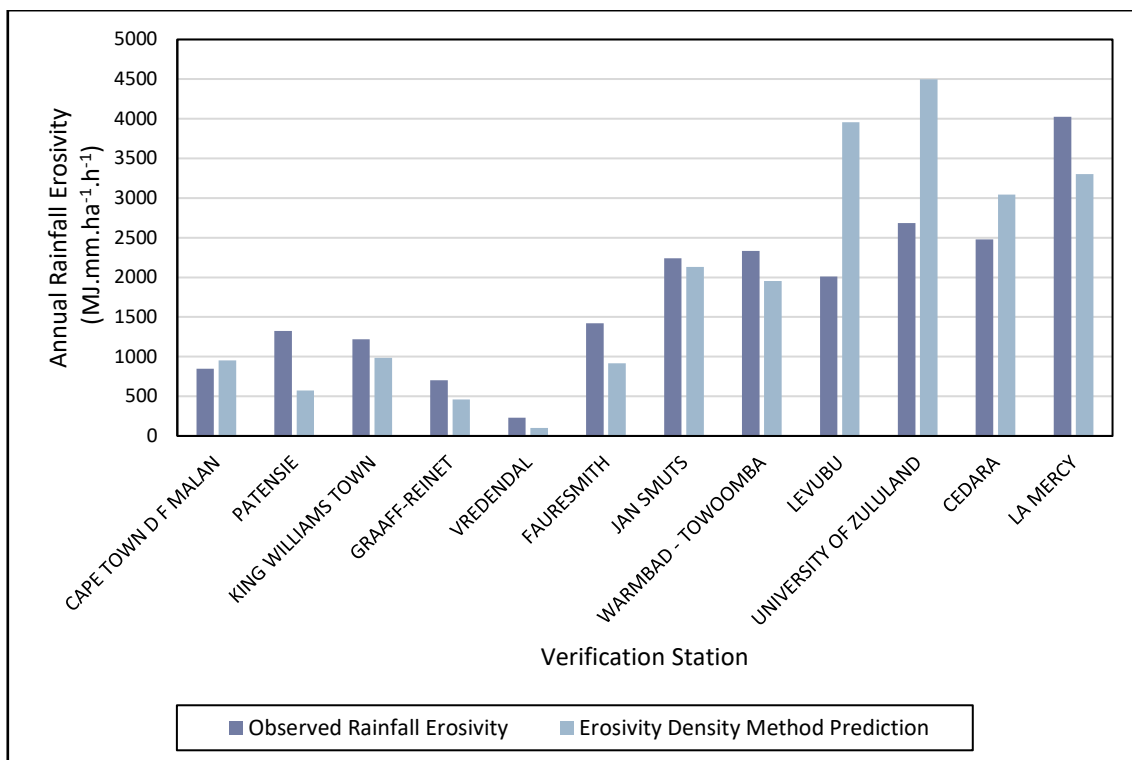


Figure 5.23 Difference between predicted and observed annual rainfall erosivity at the verification test stations, for the erosivity density method

It must be noted that due to the relatively short record lengths at the rainfall stations, even the actual EI_{30} value determined from the continuously-recorded rainfall data is unlikely to be an accurate representation of the long-term rainfall erosivity characteristics at a station. However, in the absence of extensive data records, the EI_{30} values provide a useful comparative tool with which to gauge, to some extent, the success of the method. The errors shown in this verification can be attributed to the same factors as those affecting the interpolation results. These include a low spatial density of short duration stations, short record lengths and a relatively simple method of interpolating the erosivity density values.

5.2.5 Maps

This section contains the erosivity density maps and the final rainfall erosivity maps produced using the erosivity density approach.

5.2.5.1 Erosivity density

The mean annual erosivity density is shown in Figure 5.24. A distinct trend can be seen in which the erosivity density increases from the west to the east of the country. The northern

areas of the east coast, as well as areas in the Limpopo province, experience the highest levels of erosivity density.

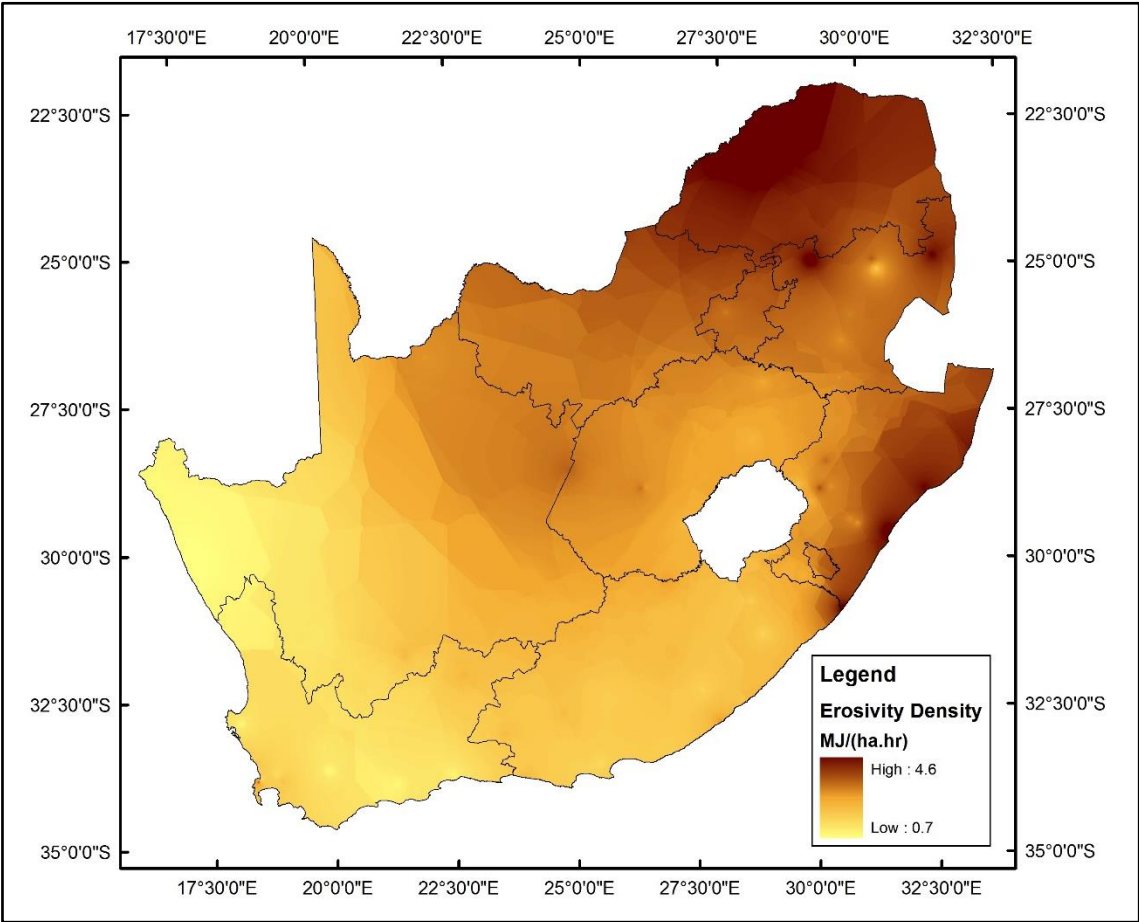


Figure 5.24 Mean annual erosivity density in South Africa

The differences in erosivity density in January and July are shown in Figure 5.25. It can be seen that the two months differ vastly in both the magnitude and distribution of erosivity density. January shows relatively high erosivity density countrywide. A similar trend to the mean annual erosivity density can be observed, with lower densities in the south and west, and higher densities in the north and east of the country. However, the erosivity density in July shows a very different distribution. The erosivity density is much lower overall, and it is also fairly constant across the country. This can be attributed to the nature of rainfall in the different seasons. January is typically characterised by thunderstorms in the summer rainfall areas. These storms are generally intense, with high amounts of rainfall falling over relatively short periods of time. They usually occur in the north, east and interior of South Africa, while the Western Cape does not normally receive rainfall in the summer months. In contrast to this, winter is characterised by cold fronts. Cold fronts typically produce low intensity rainfall, which may

occur over a number of days. The Western Cape tends to experience frequent cold front events in the winter months. This low intensity rainfall results in a much lower erosivity density.

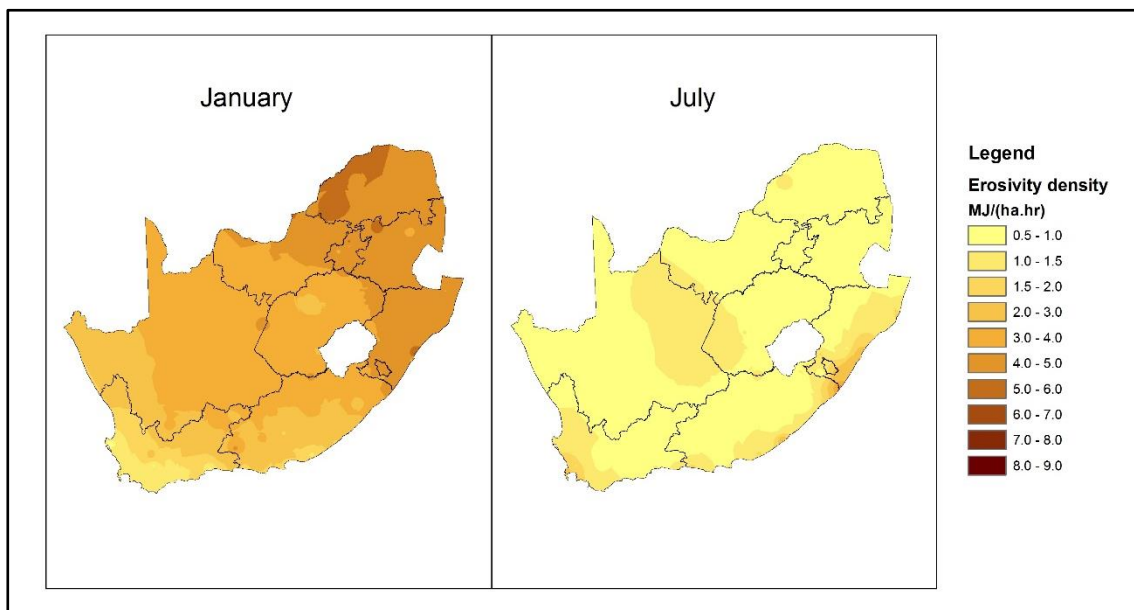


Figure 5.25 Comparison of erosivity density for January and July

The monthly maps of erosivity density, as well as the average annual erosivity density, are included as Figures 10.1 to 10.13 in Appendix A.

5.2.5.2 Rainfall erosivity (R)

The final step in this methodology was to multiply the erosivity density by rainfall depths in order to obtain rainfall erosivity (R) values, for use in the RUSLE model as described in Section 3.2.3. The maps of rainfall erosivity were produced by multiplying the median monthly rainfall amount by the monthly erosivity density. A map of the annual rainfall erosivity across South Africa is shown in Figure 5.26. This map was generated by summing the monthly rainfall erosivity values to produce an annual sum of rainfall erosivity. The map shows that rainfall erosivity generally increases from west to east across the country. In addition to this, isolated areas of higher rainfall erosivity occur along the southern coast of the country.

A 'ridge' of higher rainfall erosivity can be seen extending from the interior of Kwa-Zulu Natal, right through to the province of Limpopo. This 'ridge' generally follows the Drakensberg mountain range. Although the erosivity density remains fairly constant along this mountain range, higher rainfall is experienced in these areas, resulting in higher overall rainfall erosivity values. The USDA-ARS (2013) hypothesised that erosivity density is independent of elevation,

and their results indicated this. Hence these results are consistent with the findings of the USDA-ARS (2013) in that no notable difference in erosivity density can be seen to correlate with the position of the Drakensberg and other mountain ranges.

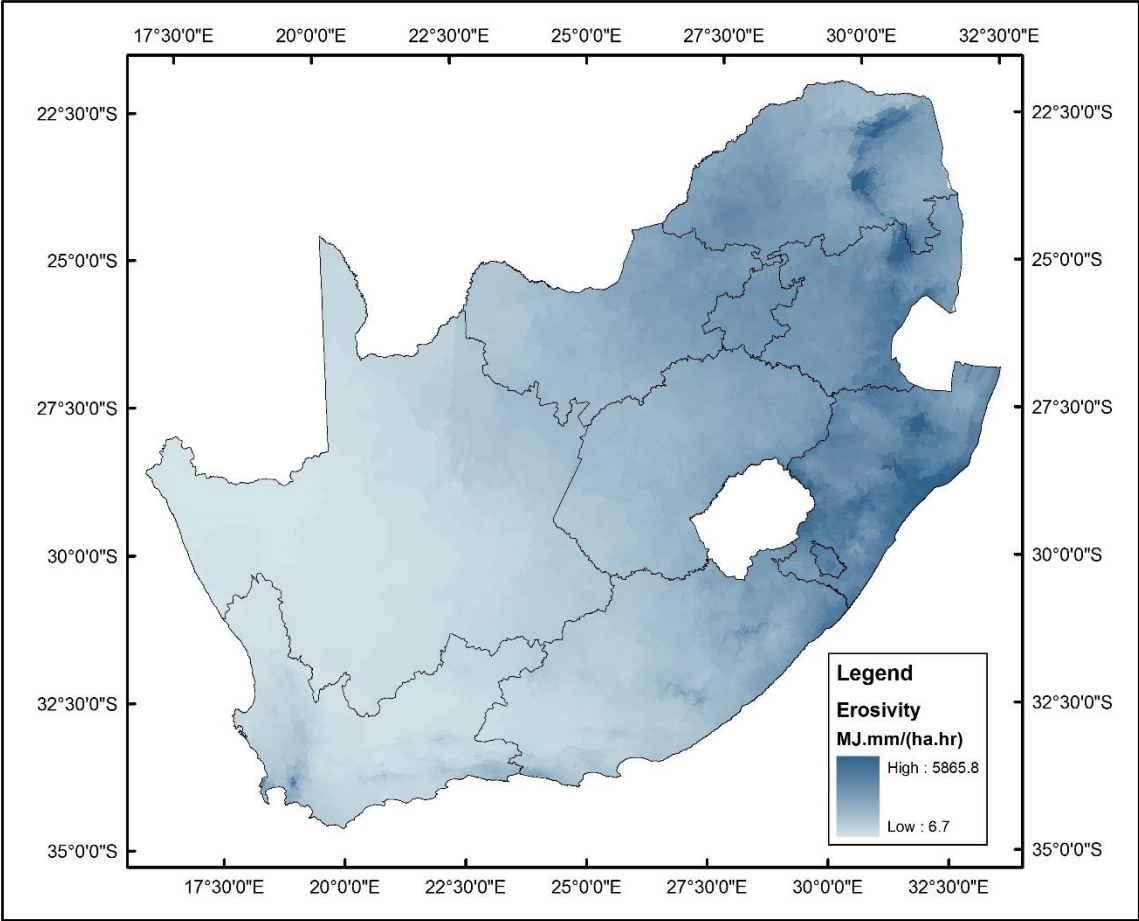


Figure 5.26 Mean annual rainfall erosivity for South Africa calculated using the erosivity density method

Figure 5.27 compares the rainfall erosivity in January and July. The rainfall erosivity distribution in January mimics the erosivity density map, in that the highest values occur in the east and north of the country. It can be seen that rainfall erosivity is generally much higher in the summer months. The map of the July distribution shows that rainfall erosivity is much lower in the winter months. The only exception to this is the Western Cape region, where although the erosivity density is still low, the Western Cape receives most of its rainfall in winter, resulting in higher rainfall erosivity values.

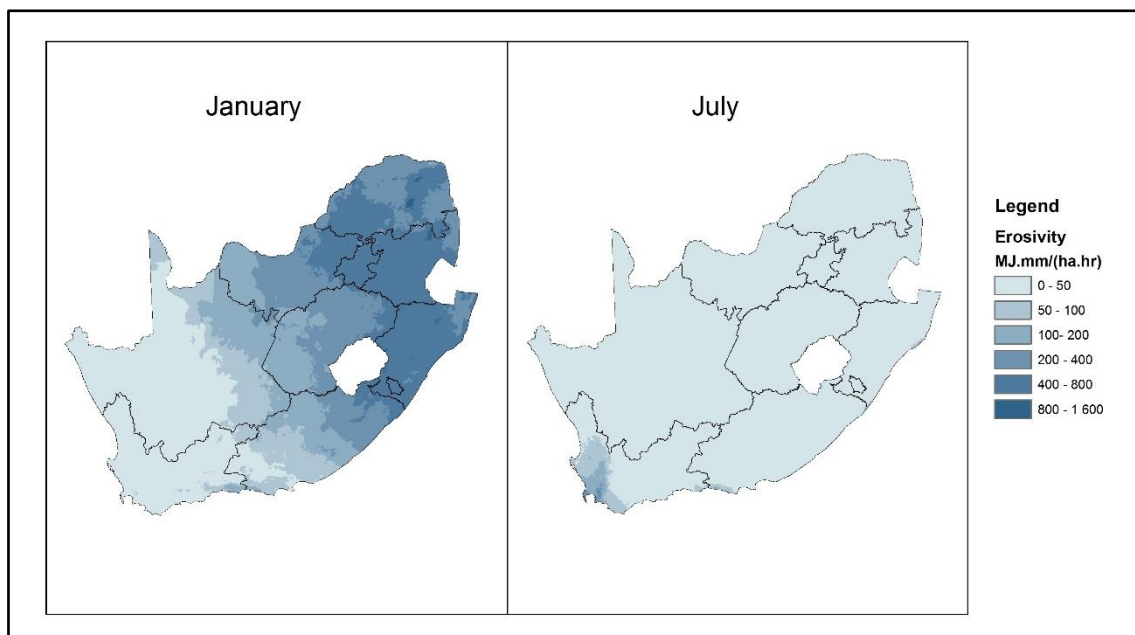


Figure 5.27 Comparison of rainfall erosivity in January and July, calculated using the erosivity density method

The maps of rainfall erosivity calculated using the erosivity density method are included as Figures 11.1 to 11.13 in Appendix B.

5.3 Conclusion on the Erosivity Density Method

The erosivity density method for determining rainfall erosivity was applied using continuously-recording rainfall stations across South Africa. The energy equation used to determine the energy of short duration rainfall had a substantial effect on the results of the rainfall erosivity calculations. Of the five equations tested, the equation proposed by Wischmeier and Smith (1958) yielded the highest erosivity density values, while that proposed by Elwell and Stocking (1973) yielded the lowest erosivity density values, overall. When averaged over all of the months and stations, the Wischmeier and Smith (1958) equation yielded erosivity densities 26.7 % higher than the Elwell and Stocking (1973) equation. Analysis of the energy relationships showed that events with a rainfall intensity of less than 10 mm.h^{-1} had a greater effect on the erosivity density at a station than less frequent, high intensity events. The erosivity density values obtained using the McGregor *et al.* (1995) equation were used in the final calculation of rainfall erosivity, in order to maintain uniformity with the RUSLE2 methodology.

The effect of applying thresholds to the data was also analysed in testing the erosivity density method. The removal of events smaller than 12.7 mm resulted in a decrease in erosivity density

(and, hence, rainfall erosivity) of an average of 5 %. The magnitude of the effect varied from station to station. It was found that the 12.7 mm threshold had a large effect at stations where a large proportion of the rainfall occurs as smaller events. This was a particular problem in low rainfall areas, or where record lengths were short, as some stations had months in which no events occurred that exceeded the threshold. In these cases, an erosivity density value could not be computed for the month. While the original reason to adopt the threshold was to reduce computing requirements, the advance of computing technology is such that this is no longer a major limiting factor. For the reasons above, it is therefore recommended that the 12.7 mm threshold be abandoned.

The effect of removing rainfall events with a return period greater than 50 years was also analysed in this study. It was found that few events exceeded this return period, due to the relatively short records of continuously-recorded rainfall data. When evaluating the overall averages of erosivity density, the removal of these events does not appear to have a large effect, owing to the fact that events were only removed at 31 of the 83 stations. However, when analysing each station separately, the application of this threshold had a substantial influence on a monthly basis, resulting in much smoother erosivity density distributions following the removal of erosivity density 'peaks'. For the purposes of this study, both thresholds were applied in the final calculation of rainfall erosivity, in order to maintain uniformity with the RUSLE2 methodology.

The cross-validation of the erosivity density interpolation revealed that the lower erosivity density values tend to be over-estimated, while the higher values are under-estimated. This is due to the fact that the predicted values obtained through IDW interpolation cannot be higher or lower than the respective maximum and minimum of the surrounding stations. This implies that localised maxima and minima may not be represented accurately. The use of additional variables, such as topography, is recommended in order to refine predictions of erosivity density at unmeasured locations.

Verification was performed by excluding twelve test stations before the interpolation was performed. The erosivity density at these stations was then compared with the predicted values obtained through the interpolation. The verification gave mixed results, with some stations being predicted relatively accurately (*e.g.* the average monthly error for La Mercy was 19 %). However, some stations obtained consistently poor predictions from month to month (*e.g.* the average monthly error for Vredendal was 332 %). The errors are largely attributable to the

sparse distribution of the short duration stations – the closest predictor stations were, in some cases, hundreds of kilometres from the unmeasured point. Particularly in low rainfall areas, the length of data records had a large effect. For low rainfall areas, such as the west coast of South Africa, a 10 year record may have very few events, if any, falling in a particular month – especially if the 12.7 mm threshold is applied. This does not allow an accurate representation of the erosivity density characteristics in these areas.

Although the monthly interpolation verification results showed large relative errors (an overall mean error of 75 %), the high relative errors were often due to small erosivity density values. It was found that 82 % of the verification prediction errors were less than 1 MJ.ha⁻¹.h⁻¹. In addition to this, when the average annual erosivity density values were interpolated, the overall error declined to 37 %. This indicates that the monthly erosivity densities show greater variability, from station to station, than the annual averages, and that the effects of these variations are reduced when analysis is performed on an annual basis. It is expected that as record lengths increase, more prominent trends will emerge within the monthly time steps, resulting in lower interpolation errors.

The final predicted rainfall erosivity values were extracted at the test stations and compared to the actual EI_{30} values calculated directly from the continuously-recorded data. The average monthly error over all of the test stations was found to be 55 %. When analysing the annual rainfall erosivities, the relative errors of the predicted values ranged from -57 % to 97 %.

The final rainfall erosivity maps produced using the erosivity density method show distinct trends regarding rainfall erosivity distributions. The seasonal changes in erosivity density are clearly visible in the erosivity density maps. Summer months show distinctly higher erosivity density values countrywide. This is due to the fact that relatively intense storms are prevalent over the eastern and interior areas of South Africa during the summer months. Conversely, the western coast of South Africa experiences the majority of its rainfall during the winter months. However, this is predominantly rain associated with cold fronts, with a relatively low intensity. The erosivity density maps show reduced erosivity density countrywide during the winter months, however the rainfall erosivity maps show higher rainfall erosivities along the western and southern coast of the country, due to the relatively high amount of rainfall that occurs in these areas during the winter period.

To conclude this chapter, this study applied the erosivity density method for calculating rainfall erosivity in South Africa. Although the results of the verification process show that the application of the method could be improved upon, the final maps show promising trends. It is believed that the inclusion of additional short duration rainfall stations, as well as longer records of short duration rainfall data, would greatly improve the accuracy of the output of the erosivity density method.

Although the network of continuously recording rainfall stations is expected to expand in the future, estimations of soil loss are required now, at the present time. For this reason, a second method was adopted in an attempt to improve rainfall erosivity estimates using the limited amount of continuously recorded rainfall data. The following chapter describes the use of daily rainfall data to supplement the short duration data currently available, in order to estimate rainfall erosivity across South Africa.

6. USING DAILY DATA TO IMPROVE ESTIMATES OF RAINFALL EROSIVITY

Owing to the fact that the continuously recording rainfall stations are sparsely distributed, resulting in poor interpolation results, it was proposed that daily rainfall stations could be used to supplement the short duration data and improve estimates of rainfall erosivity. The objective of this approach was to determine a relationship between the rainfall erosivity (or erosivity density) at a point, calculated using short duration data, and predictor variables, which can be determined using daily rainfall data, as performed by Smithen and Schulze (1982). This relationship could then be applied to data at the more densely distributed daily rainfall stations, and the results interpolated, in order to estimate rainfall erosivity at ungauged sites.

Le Roux *et al.* (2006) made use of the daily rainfall amount to determine rainfall erosivity using the model developed by Yu and Rosewell (1996). However, this model was developed using continuously-recorded rainfall data from Australia, rather than South Africa. The study performed by Le Roux *et al.* (2006) did not make use of regional parameterisation, except for the seasonality factor, obtained from daily rainfall records. While Smithen and Schulze (1982) used continuously-recorded rainfall data from South African stations, they utilised one key (continuously-recorded) station per homogeneous region (fourteen stations), as described in Section 4.1.1. This study aimed to make use of all 83 continuously recording stations available to this study.

6.1 Methodology

This section describes the steps taken to estimate rainfall erosivity across South Africa by supplementing continuously-recorded rainfall data with daily rainfall data.

6.1.1 Identification of homogeneous regions

In order to develop relationships between rainfall erosivity and variables derived from daily rainfall, it is necessary to determine the spatial scope of applicability of the relationships, *i.e.* regionalisation is necessary. Given the large variability in both the amount and timing of rainfall across South Africa, it is highly unlikely that a single relationship would be valid at every station in the country. The short duration rainfall clusters developed by Smithers and Schulze (2000) were chosen as the means of dividing the country. These clusters were large enough to

ensure that relationship development and application were practical. Smithers and Schulze (2000) applied the Regional L-Moment Algorithm (RLMA) suggested by Hosking and Wallis (1997), in order to delineate homogeneous regions. This approach centres on using only site characteristics to identify homogeneous clusters. This allows homogeneity to be tested independently using site statistics (Smithers and Schulze, 2000).

Smithers and Schulze (2000) used cluster analysis to regionalise sites. Each site was represented by a vector of site characteristics. Standard multivariate analysis was performed and, based on the similarity of the vectors, sites were grouped to form clusters. The site characteristics used in the cluster analysis included latitude, longitude, altitude, concentration of precipitation, mean annual precipitation, rainfall seasonality and distance from the sea. The characteristics were transformed to ensure that the range of each characteristic was similar, due to the high sensitivity of cluster analysis to scale (Hosking and Wallis, 1997). After some adjustments of transformations and reassignment of a small number of stations, 15 acceptably homogeneous clusters were created, as shown in Figure 6.1.

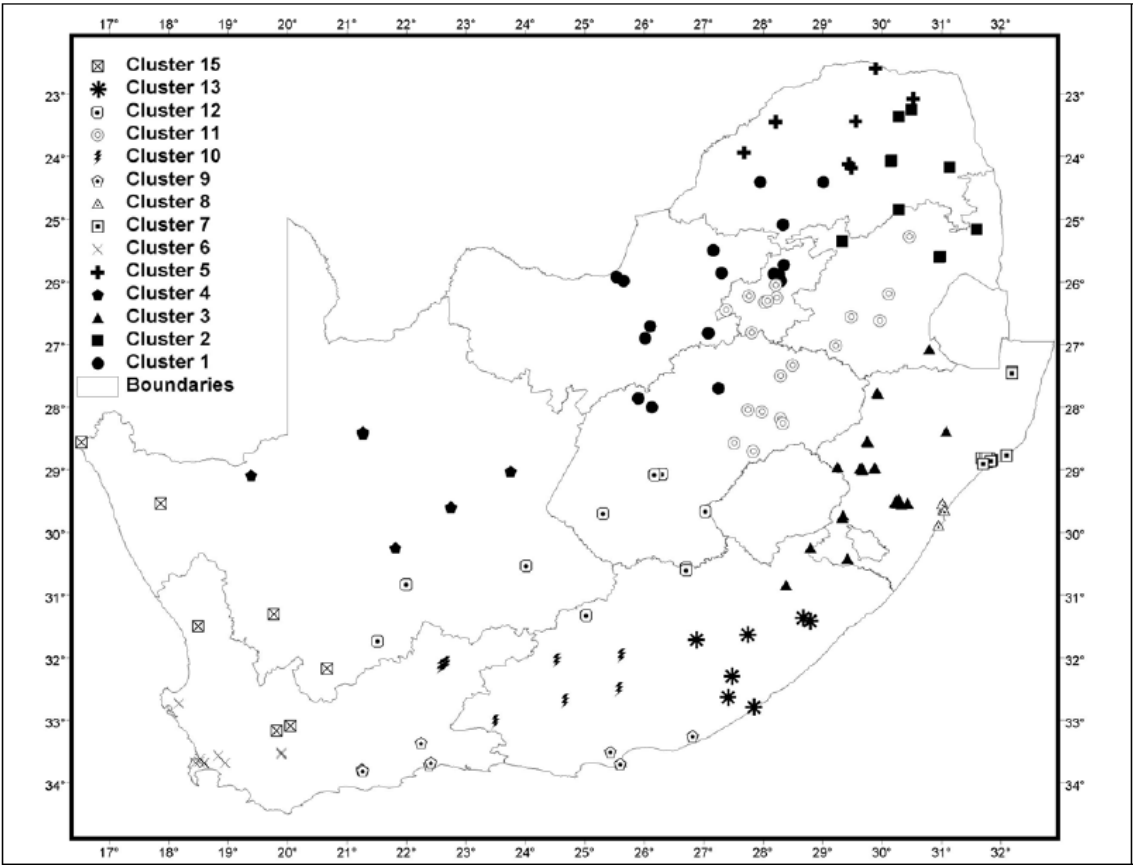


Figure 6.1 Homogeneous clusters identified by Smithers and Schulze (2000)

6.1.2 Development of rainfall erosivity relationships

The same twelve test stations as in the previous approach were excluded when generating the relationships. The remaining 71 short duration rainfall stations were divided according to the 15 clusters. Cluster 4 did not contain any short duration stations and so the approach could not be applied in this cluster. The storm events from all of the stations in a cluster were listed for each month. Various parameters were then calculated. These included rainfall, effective rainfall, Modified Fournier’s Index and the Burst Factor as described in Section 4.1.1, based on the work of Smithen and Schulze (1982). These parameters were calculated on a monthly basis. The parameters were then plotted against the rainfall erosivity, as well as the erosivity density, for each month. Within each cluster, and for each of the parameters, a regression line was fitted to the data and the equation of this regression line, as well as the coefficient of determination (R^2) value, was obtained. A power regression was found to provide the highest coefficient of determination in all cases. Examples of the rainfall erosivity and erosivity density relationships are shown in Figure 6.2 and Figure 6.3 respectively.

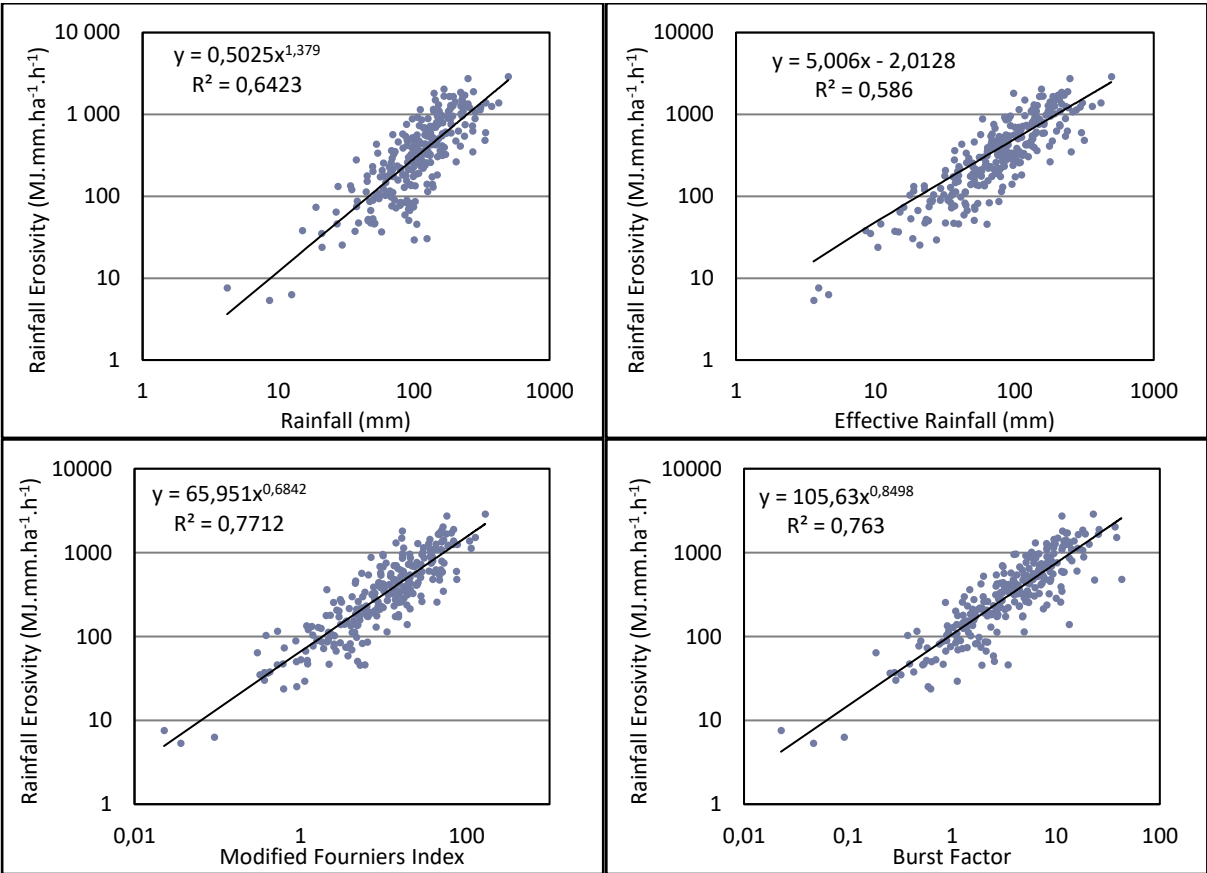


Figure 6.2 Example of monthly regression analysis of rainfall erosivity against various rainfall parameters (January, Short Duration Cluster 3)

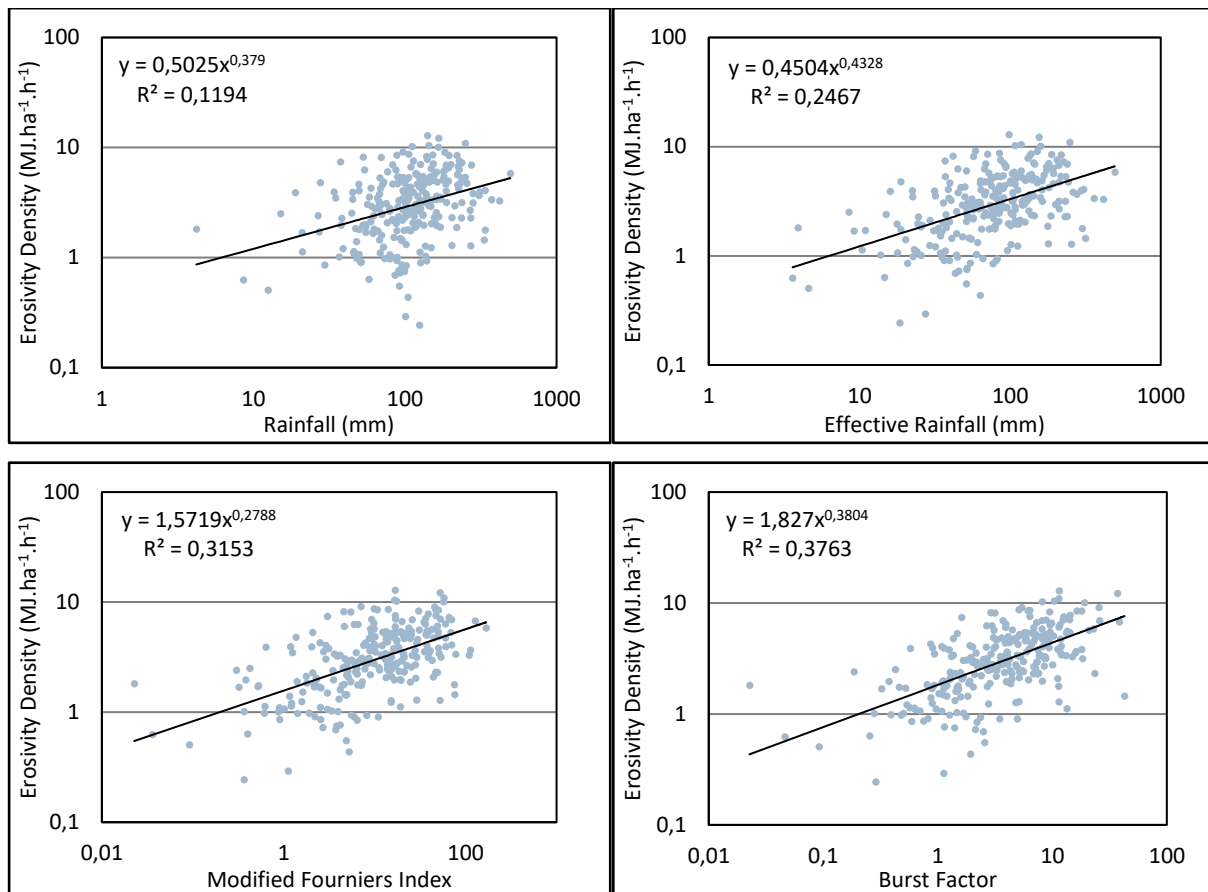


Figure 6.3 Example of monthly regression analysis of erosivity density against various rainfall parameters (January, Short Duration Cluster 3)

From the example shown in Figure 6.3, it is evident that the predictor variables show very low correlation with the erosivity density on a monthly basis. The regression of erosivity density with rainfall shows a particularly poor correlation. A number of outliers are present where high rainfall produces a low erosivity density. This occurred when the majority of the month's rainfall fell in many low rainfall events, usually at low intensities. Therefore, although the total rainfall may have been high, the erosivity density was low, leading to outliers. It is clear that these relationships could not be used to accurately predict erosivity density at daily rainfall stations. Figure 6.2 shows a stronger relationship between the predictor variables and rainfall erosivity, however the correlation is still fairly low. Similar results were obtained for the other months and clusters.

It was decided to try to relate the rainfall erosivity to daily data on a daily basis (rather than monthly), as used in the model developed by Yu and Rosewell (1996), and applied by Le Roux *et al.* (2006). As the Modified Fournier's Index and the Burst Factor are not relevant on a daily

basis, the daily rainfall erosivity was simply plotted against the daily rainfall amount for each month, as shown in the example in Figure 6.4. The highest correlation in the majority of cases was achieved using a power regression relationship. This is consistent with the findings of Richardson *et al.* (1983) and Yu and Rosewell (1996), whereby power relationships were used to relate daily rainfall data and rainfall erosivity. Although linear relationships provided slightly higher correlation coefficients in a limited number of cases, the slight improvement in correlation did not justify the increased complexity in calculations.

It can be seen that the correlation between the daily rainfall amount and daily rainfall erosivity is relatively high. By relating the rainfall amount to the rainfall erosivity on a daily basis, the nature of the rainfall can be taken into account. For example, a station may record a rainfall amount of 100 mm for the month, however, this rainfall could have fallen as one 100 mm event or ten 10 mm events. Using the relationship shown in Figure 6.4, 100 mm falling in one day results in a rainfall erosivity value of 2200.83 MJ.mm.ha⁻¹.h⁻¹. However, a situation in which 10 mm falls on ten days, the resultant rainfall erosivity value is 147.91 MJ.mm.ha⁻¹.h⁻¹. As this detail is missing in the monthly time step, the rainfall erosivity has a greater variability for a given rainfall amount, leading to a lower correlation.

Although the regression of rainfall erosivity against daily rainfall gave relatively high correlations, outliers and inaccuracies were encountered in specific instances. For example, Cluster 2 had only two short duration stations from which the daily relationships were derived. Cluster 2 is located in the north of the country, covering the Mpumalanga and Limpopo provinces. This area has been shown to have highly variable rainfall erosivity. As a result, many of the months show two distinct ‘populations’ of points, due to the two stations recording different conditions over this time period. This indicates that Cluster 2 is not sufficiently homogeneous for an accurate relationship to be derived. Outliers also occurred when uncharacteristic rainfall events were recorded in certain months – for example a large rainfall event in the month of August in Kwa-Zulu Natal. It is expected that as record lengths increase, smoother trends and more accurate depictions of the average climatic conditions will develop. Despite these errors, the daily data method generally produced high correlations with rainfall erosivity.

As this daily time step approach gave a much higher correlation than the monthly time step approach, it was decided to continue with this method and to compare the results with those obtained using the erosivity density method. A different relationship for each month was

determined for every cluster. The figures and relationships can be found in Appendix C (Figures 12.1 to 12.14).

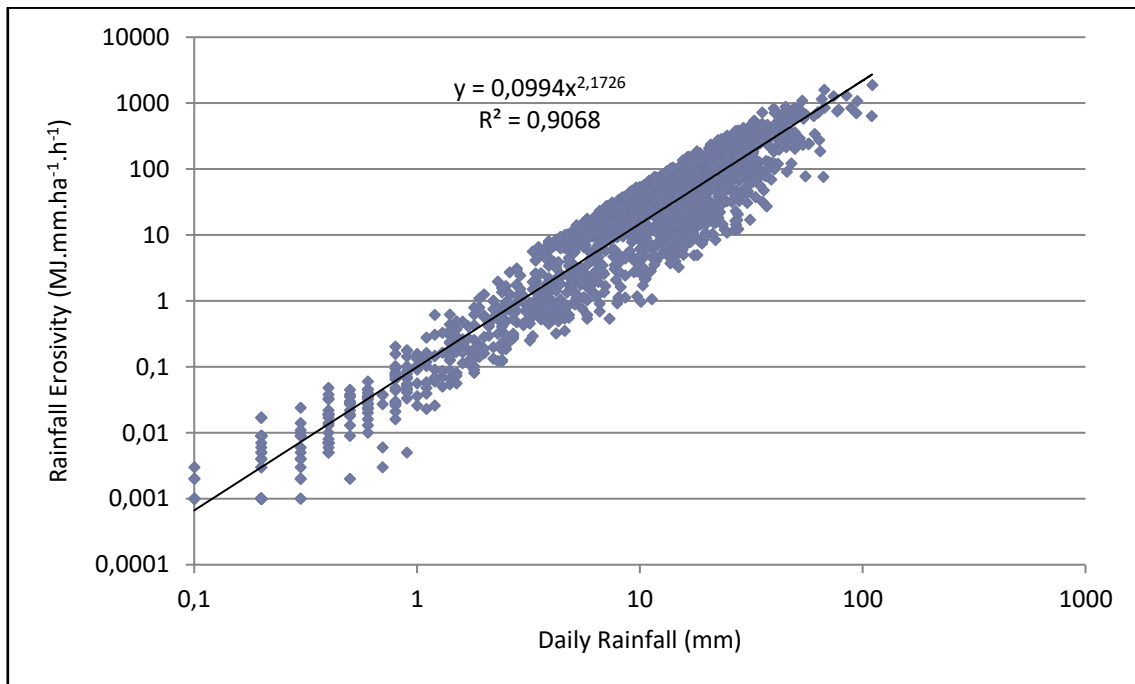


Figure 6.4 Example of power regression analysis of daily rainfall erosivity against daily rainfall (January, Short Duration Cluster 3)

6.1.3 Selection of daily stations

The daily rainfall data were obtained from the database developed by Lynch (2004). The database consists of observed and infilled daily rainfall data for more than 13 000 stations in Southern Africa. A number of infilling techniques were used to estimate missing rainfall records, in order to allow continuous periods of data. These techniques included Inverse Distance Weighting, the Expectation Maximisation Algorithm, the Median Ratio method and a monthly infilling technique, which utilised regression techniques using surrounding stations Lynch (2004).

Owing to the fact that the database contained over 13 000 stations, it would not have been feasible to calculate the rainfall erosivity for every station. A limited number of stations were therefore selected with which to test the approach. It was initially thought that the daily stations would be selected using the longest record length and greatest percentage of reliable data. The stations were sorted by record length and the top 100 stations were plotted. However, it was found that the stations with the longest record length were not evenly distributed around the

country. In a revised approach, all stations with a record length over 50 years and a reliability of at least 50 % were plotted. From these stations, stations within each Short Duration Cluster were selected manually to ensure that an even spatial distribution was maintained. As a relationship could not be obtained for Cluster 4, it was not necessary to select daily stations for this cluster. A total of 204 daily rainfall stations were used. The stations are shown in Figure 6.5. The average record length of the daily stations is 111 years.

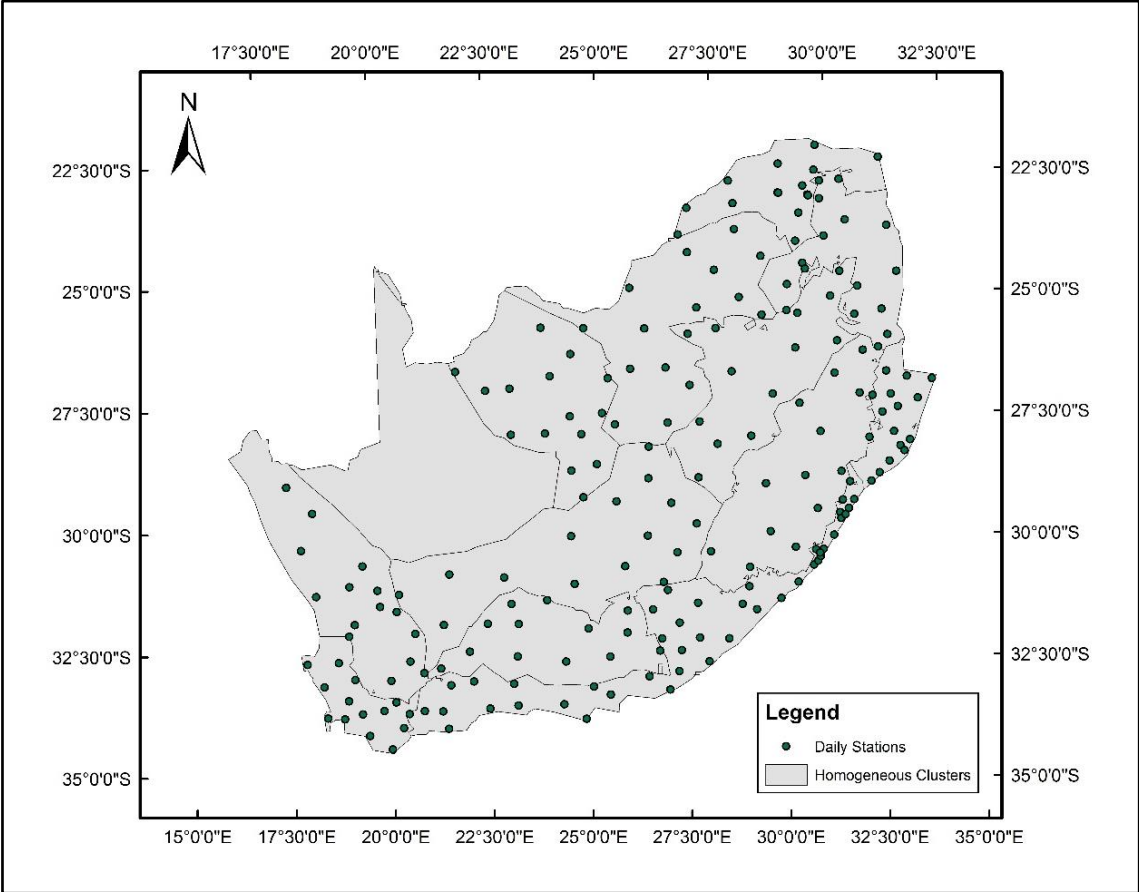


Figure 6.5 Locations of daily rainfall stations used in calculating rainfall erosivity

Having selected the stations, the daily rainfall data was extracted for each station using the Daily Rainfall Data Extraction Utility (Kunz, 2004). The relevant regression equations were applied to the data, depending on which homogeneous short duration cluster each daily rainfall station was located in. This resulted in a rainfall erosivity value being calculated at each daily rainfall station, for each month.

6.1.4 Spatial interpolation of rainfall erosivity data

The rainfall erosivity data at the daily stations was interpolated using IDW interpolation, *i.e.* in the same manner as the erosivity density method, in order to maintain a level of uniformity between the two methods. Once again, a distance of 250 km was used to limit the search radius. The maximum number of neighbours was ten and the minimum was five. Once more, the IDW power variable was optimised automatically, based on an iterative cross-validation method.

6.1.5 Selection of independent test stations

Verification of the interpolation was performed in a manner similar to the erosivity density approach. The daily stations were sorted into the short duration homogeneous clusters and ranked according to record length. The station with the median record length from each cluster was selected as a test station (with the exception of Cluster 4), resulting in 14 test stations. These stations were excluded from the training data set. Verification was performed by comparing the rainfall erosivity calculated at the test stations (observed data) with that obtained from interpolation from the training stations (predicted data). The test stations were distributed as shown in Figure 6.6.

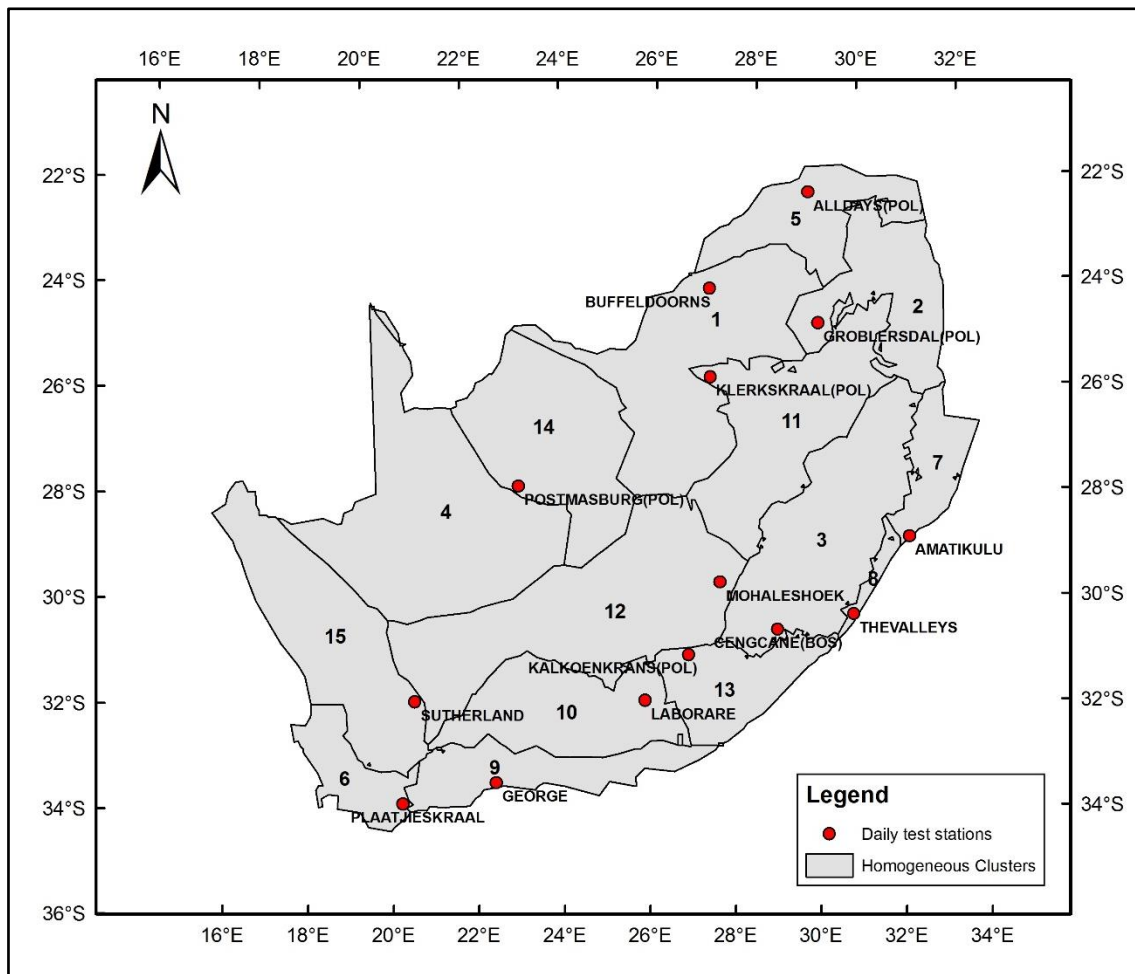


Figure 6.6 Location of daily test stations within the homogeneous clusters

Once more, a second verification process was performed in which the predicted rainfall erosivity was extracted at the test stations used in the erosivity density method. These values were then compared with the EI_{30} values calculated directly from the continuously-recorded rainfall data.

6.2 Results of Daily Data Method

This section presents the results of the approach using daily data stations to calculate rainfall erosivity.

6.2.1 Cross-validation results

As explained in Section 5.1.4, cross-validation is performed by removing each point (station), in turn, and comparing the predicted value with the measured value for that point. Cross-validation provides an initial assessment of the performance of the interpolation. Figure 6.7

shows the results of the cross-validation of the interpolation of rainfall erosivity data at daily rainfall stations. It is clear that the higher rainfall erosivities are severely underestimated. These outliers result in a poor correlation between the predicted and observed values. The underestimation indicates that the locations with the highest rainfall erosivity are isolated, with the surrounding stations having much lower rainfall erosivities. The majority of the outliers in Figure 6.7 originate from Station 0766837W (Sibasa). This station is located in northern Limpopo, in Cluster 2. It has been shown previously that this area is a local maximum in terms of rainfall erosivity. It is therefore not surprising that the predicted values underestimate the rainfall erosivity at this station when it is excluded. These errors should be smaller if the density of stations was increased. A greater number of stations would reflect trends in rainfall erosivity patterns with greater accuracy, thereby reducing the larger errors. It can be seen that the smaller values are generally over-predicted, while the larger values are under-predicted. As with the erosivity density method, this is to be expected with an Inverse Distance Weighting interpolation, and could be solved in future by the inclusion of additional components in the interpolation, such as the topographical features.

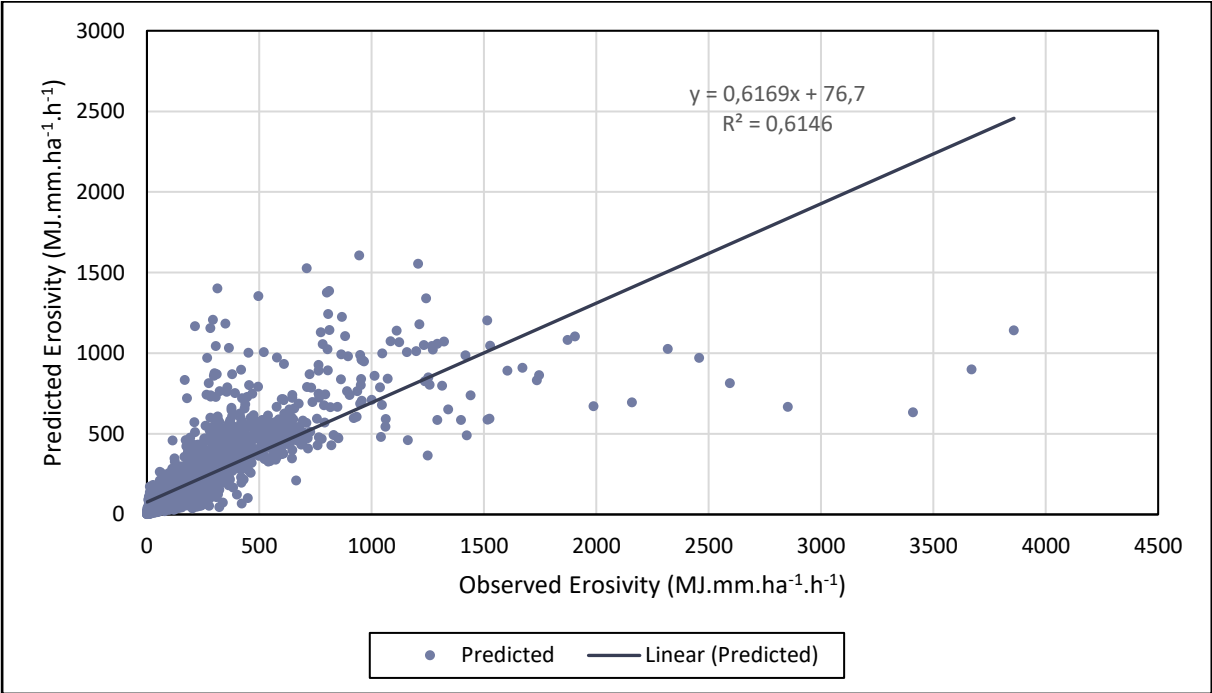


Figure 6.7 Cross-validation results of the interpolation of rainfall erosivity at daily data stations

6.2.2 Verification results

Two different verifications were performed on the results of this method. The first verification tested the reliability of the interpolation between the daily rainfall stations. A major shortfall in the erosivity density method was the low spatial density of continuously-recording rainfall stations. This had a negative impact on the accuracy of the interpolation of erosivity density. The first verification of the daily data method is therefore to ascertain whether the increased spatial density of the rainfall stations improved the results of the interpolation. This verification does not take into account inaccuracies that may have been introduced in the development of the daily rainfall-erosivity relationships.

The second verification compares the results of the daily data method with the rainfall erosivity calculated directly from the short duration rainfall data, thereby testing the accuracy of the method as a whole. For this verification, the same test stations were used as in the verification of the erosivity density method.

6.2.2.1 Verification results of the interpolation

Table 6.1 shows the results of the interpolation verification. The values shown are the relative errors between the rainfall erosivity calculated directly at the 14 independent test stations and that obtained through IDW interpolation of the values from training stations. The average error of all fourteen of the test stations is 43 %, which although is an improvement on the 75 % average error of the erosivity density interpolation, is still fairly high.

Table 6.1 Validation results for the interpolation of rainfall erosivity values (%)

STATION	JAN	FEB	MAR	APR	MAY	JUN	JUL	AUG	SEP	OCT	NOV	DEC	MEAN
BUFFELDOORNS	4	16	4	48	35	38	93	122	2	1	17	5	32
GROBLERSDAL(POL)	18	18	34	13	2	52	47	29	1	9	30	15	22
CENGCANE(BOS)	7	9	34	36	75	171	259	157	87	27	23	3	74
ALLDAYS(POL)	22	88	77	102	39	292	96	-	97	7	46	10	80
PLAATJIESKRAAL	150	211	188	139	152	101	70	88	220	121	200	18	138
AMATIKULU	11	4	18	15	36	11	9	10	3	29	22	65	19
THEVALLEYS	5	13	18	1	0	17	50	20	11	3	7	9	13
GEORGE	49	29	41	25	32	20	37	44	60	33	48	34	38
LABORARE	122	50	19	8	8	50	2	105	44	66	43	14	44
KLERKSKRAAL(POL)	29	38	14	7	28	21	72	20	25	22	5	42	27
MOHALESHOEK	29	34	2	4	20	15	0	19	17	25	8	19	16
KALKOENKRANS(POL)	43	57	45	48	85	93	50	39	176	88	60	7	66
POSTMASBURG(POL)	41	2	25	17	11	32	6	30	10	9	28	82	25
SUTHERLAND	7	1	13	14	22	10	11	31	33	19	8	12	15
MEAN	38	41	38	34	39	66	57	55	56	33	39	24	43

A number of possible reasons exist for the errors shown above. Firstly, the clusters cover large areas with varying topography and climatic characteristics. Although relatively homogeneous, a certain degree of heterogeneity will be present within the clusters. This causes inaccuracies in determining regression equations and the resulting equation is a compromise of all of the available stations, fitting none of them perfectly. Although it could improve accuracy, increasing the number of homogeneous regions would make calculations cumbersome. For example, creating Thiessen polygons around the short duration stations and assigning an equation to each could improve accuracy greatly. However, each time the possibility of adding new stations arose, the polygons would have to be recreated and daily stations reassigned accordingly.

Secondly, the creation of transition areas between clusters was not undertaken in this study. Although two stations may be in close proximity to one another, the different cluster equations could cause the resulting rainfall erosivities to be vastly different. This can have a large effect on interpolation results. It would be advisable to introduce a transition area on each side of the cluster boundaries that would average the results of both clusters and create smooth transitions.

Lastly, the purpose of this study was to gauge the potential of this method in providing rainfall erosivity estimates. As a result, although the number of daily stations used was much greater

than the short duration stations available, it was still somewhat limited. The interpolation would almost certainly have benefited from the use of additional daily rainfall stations. Now that the potential of the method has been shown, the inclusion of greater numbers of daily rainfall stations is recommended for future studies.

6.2.2.2 Verification of the method

Once again, the final rainfall erosivity results, obtained using the ‘daily data’ method, were compared with the EI_{30} values obtained directly from the continuously-recorded data at the test stations. The relative errors of the predicted values, compared to the actual EI_{30} values are shown in Table 6.2. These are based on the absolute values of the errors, and do not indicate under- or overestimation. The overall mean of the monthly relative errors was found to be 91 %. This is a markedly higher relative error than that of the erosivity density method, at 55 %.

Table 6.2 Relative errors between predicted and observed rainfall erosivity values at the verification test stations, for the ‘daily data’ method (%)

STATION NO.	LOCATION	JAN	FEB	MAR	APR	MAY	JUN	JUL	AUG	SEP	OCT	NOV	DEC	MEAN
0021178	CAPE TOWN D F MALAN	10	60	48	26	130	67	128	64	107	5	61	142	71
0033556 5	PATENSIE	36	13	10	77	103	12	42	46	374	53	6	68	70
0079712	KING WILLIAMS TOWN	114	102	241	12	45	2	4	17	351	84	120	52	95
0096045	GRAAFF-REINET	34	76	63	77	168	164	18	19	179	20	136	38	83
0106880	VREDENDAL	13	-	19	20	85	20	171	113	14	22	120	30	57
0229556	FAURESMITH	57	120	90	6	48	72	34	84	18	18	5	3	46
0476398	JAN SMUTS	38	48	27	68	21	76	80	56	66	8	31	61	48
0589594	WARMBAD - TOWOOMBA	41	39	34	10	39	68	94	85	47	70	73	26	52
0723485	LEVUBU	1030	448	500	267	39	81	-	75	78	1	276	361	287
304473	UNIVERSITY OF ZULULAND	88	206	193	407	32	194	55	66	21	150	149	636	183
c164	CEDARA	25	16	4	48	203	205	55	17	58	21	40	23	60
sal10	LA MERCY	15	13	8	52	14	70	42	70	49	11	31	41	35
MEAN		125	104	103	89	77	86	66	59	113	39	87	123	91

The differences between the predicted and observed annual rainfall erosivity values are illustrated in Figure 6.8. It is evident that the ‘daily data’ method generally overestimates rainfall erosivity. The relative errors range from an underestimation of 10 % at Patensie (station number 00335565), to an overestimation of 315 % at Levubu (station number 0723485).

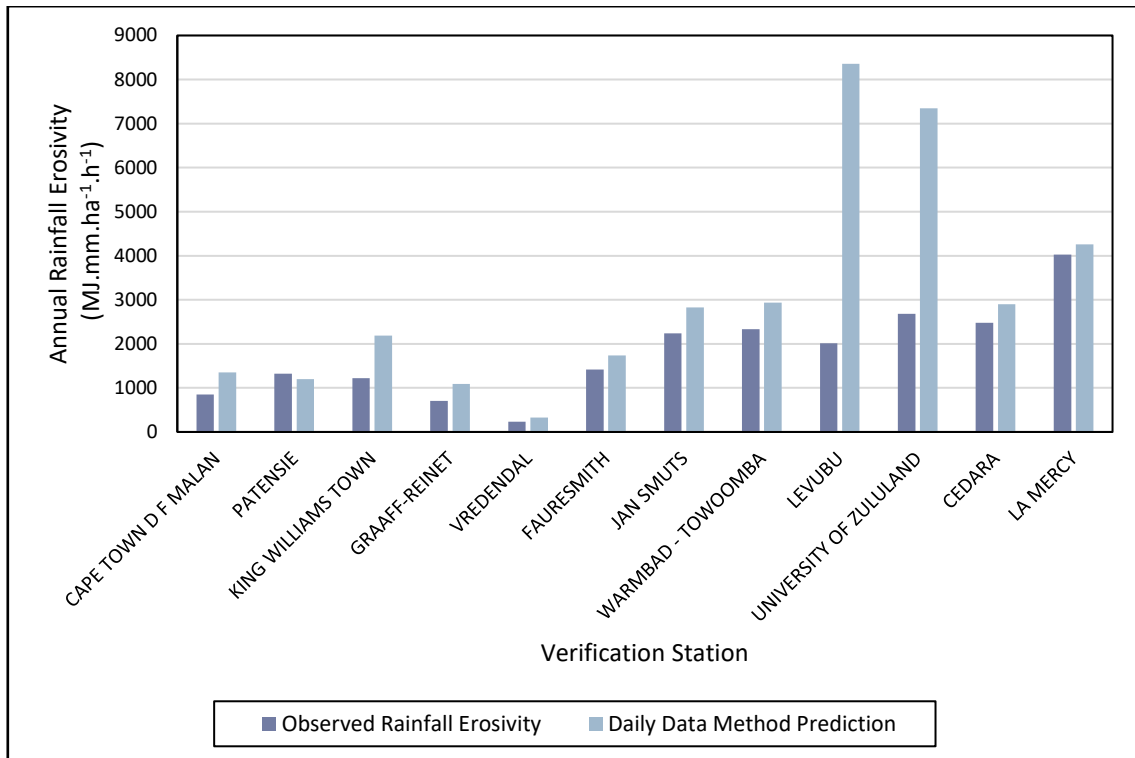


Figure 6.8 Differences between predicted and observed annual rainfall erosivity at the verification test stations, for the ‘daily data’ method

There are a number of likely reasons for the prediction errors using this method. Firstly, the spatial density of short duration stations was low, with an average of 5.5 per cluster. The inter-cluster distribution of stations was uneven, as shown in Figure 6.9. For example, Cluster 14 contained only 2 short duration stations, while Cluster 3 contained 12. One major shortfall was the fact that Cluster 4 contained no short duration stations at all and, as a result, no equation could be derived for it.

Secondly, the intra-cluster distribution of stations was also not uniform. It can be seen that no short duration stations are present in the northern regions of Clusters 2 and 5 – an area already shown to experience particularly high levels of rainfall erosivity. This means that the regression equations were possibly not an accurate representation of the rainfall characteristics of each cluster. This would result in inaccurate estimations of rainfall erosivity.

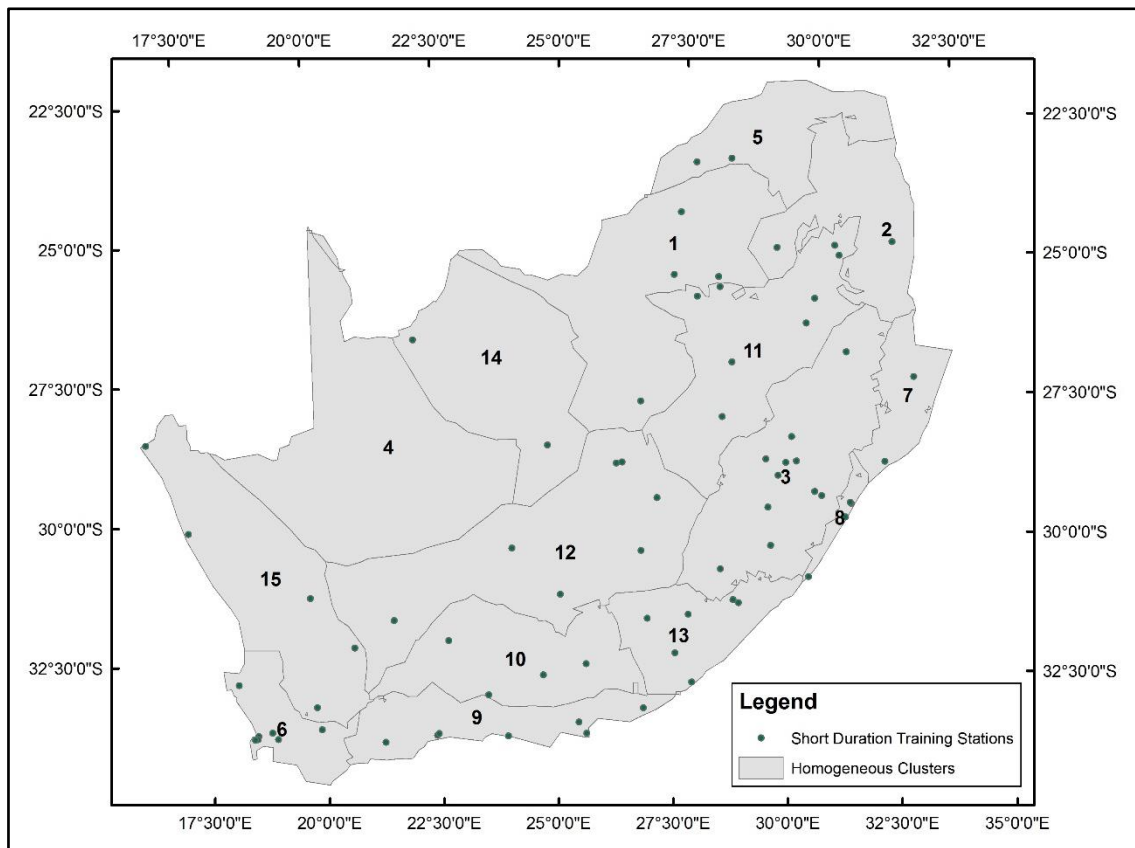


Figure 6.9 Location of short duration stations within short duration clusters

6.2.3 Maps

Figure 6.10 shows the mean annual rainfall erosivity for South Africa derived using the ‘daily data’ approach. It can be seen that there are some problems with this approach. A number of points can be seen where certain stations have a lower rainfall erosivity than the surrounding area. However, the overall trend matches that of the approach utilising the erosivity density method, as well as the trends of previous studies.

As seen in the erosivity density method results, the mean annual rainfall erosivity generally increases from the west of the country to the east of the country. The highest rainfall erosivities are experienced along the east coast of the country, as well as on the eastern sides of the Limpopo and Mpumalanga provinces. The lowest rainfall erosivity values are experienced on the west coast of the country.

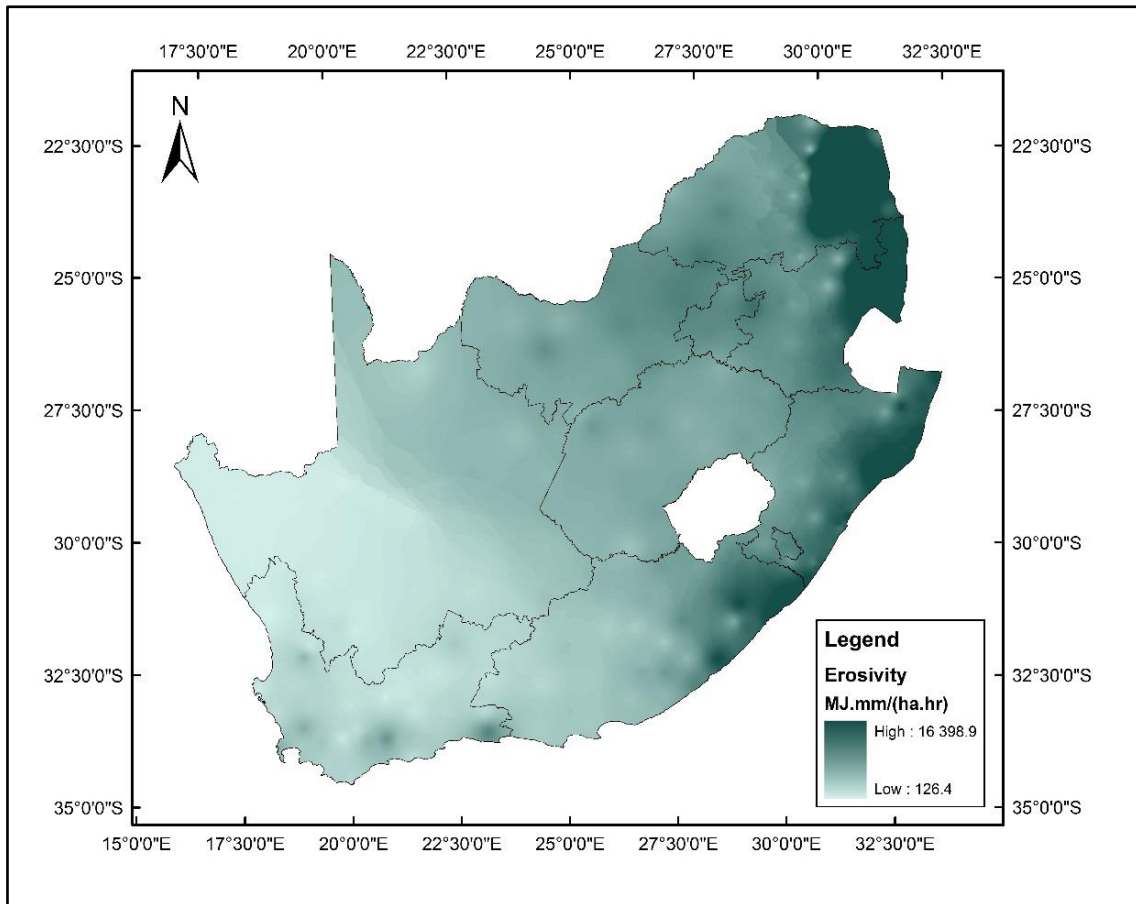


Figure 6.10 Mean annual rainfall erosivity calculated using daily data

Figure 6.11 shows the mean annual rainfall erosivity, overlaid with short duration cluster boundaries for an area in Limpopo. This area displays obvious discrepancies in values, characterised by the lighter coloured ‘bull’s-eyes’. The figure clearly illustrates the effect of different regression equations on stations in close proximity to one another. On the eastern side of the border, the rainfall erosivity values are very high, while on the western side, the values are consistently much lower, despite the stations being in relatively close proximity. The recurring difference highlights the need for a transition area around the cluster borders to prevent such large contrasts due to different equations.

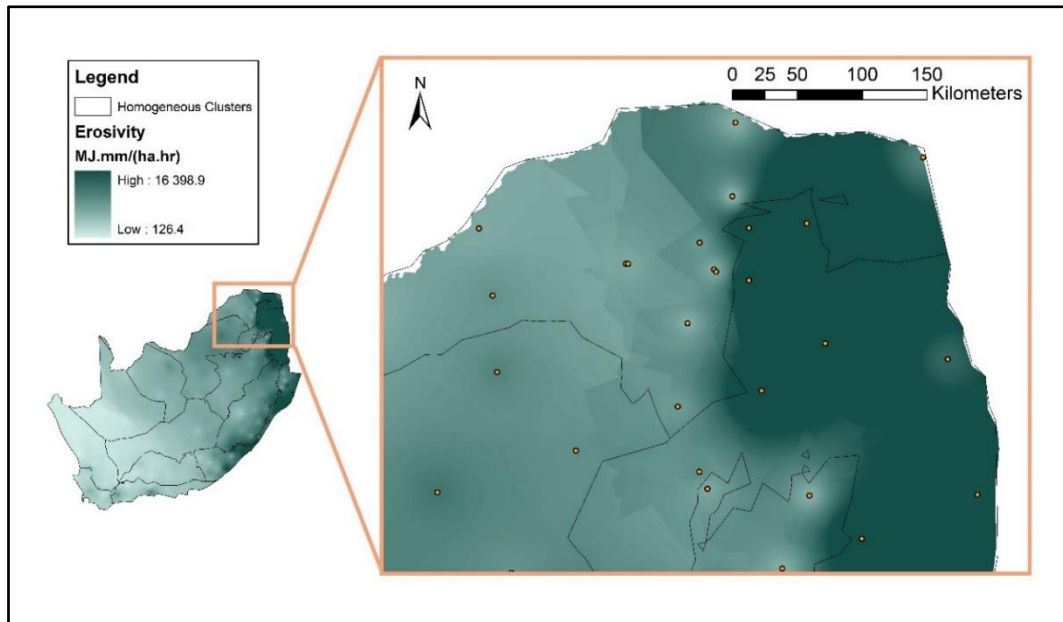


Figure 6.11 Example of 'bull's-eyes' caused by different regression equations on each side of a cluster border

Once again, when comparing January and July, the trends follow a similar pattern to those shown previously. January shows higher rainfall erosivity values overall, particularly towards the north and east of the country. July shows predominantly lower rainfall erosivity values, with the highest values occurring in the Western Cape and along the eastern coast of the country. These differences are shown in Figure 6.12.

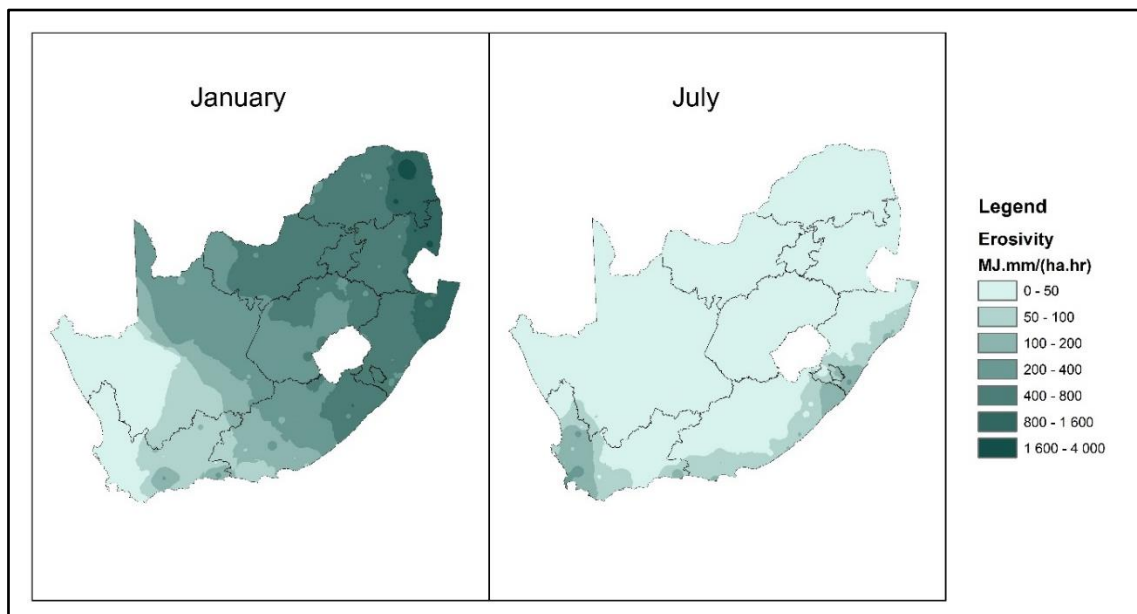


Figure 6.12 Comparison of rainfall erosivity for January and July using the 'daily data' method

The monthly and annual maps of rainfall erosivity generated using the ‘daily data’ approach are included as Figures 13.1 to 13.13 in Appendix D.

6.3 Comparison of Calculation Methods

Figure 6.13 shows a comparison of the annual rainfall erosivity calculated using the two different methods, namely the erosivity density method and the daily data method. Although the trends are similar, the method using daily data results in higher rainfall erosivity values in the north of the country. While the maximum rainfall erosivity determined using the erosivity density method is $5\,865.8 \text{ MJ.mm.ha}^{-1}.\text{h}^{-1}$, that of the daily data method is $16\,398.9 \text{ MJ.mm.ha}^{-1}.\text{h}^{-1}$. Although these numbers may imply that the results are vastly different, this is not the case. Figure 6.13 shows that over the majority of the country, the methods produce comparable results. Although the daily data method generally produces slightly higher rainfall erosivity values, it is only in a few isolated areas that much higher rainfall erosivity values are present for the daily data method than for the erosivity density method.

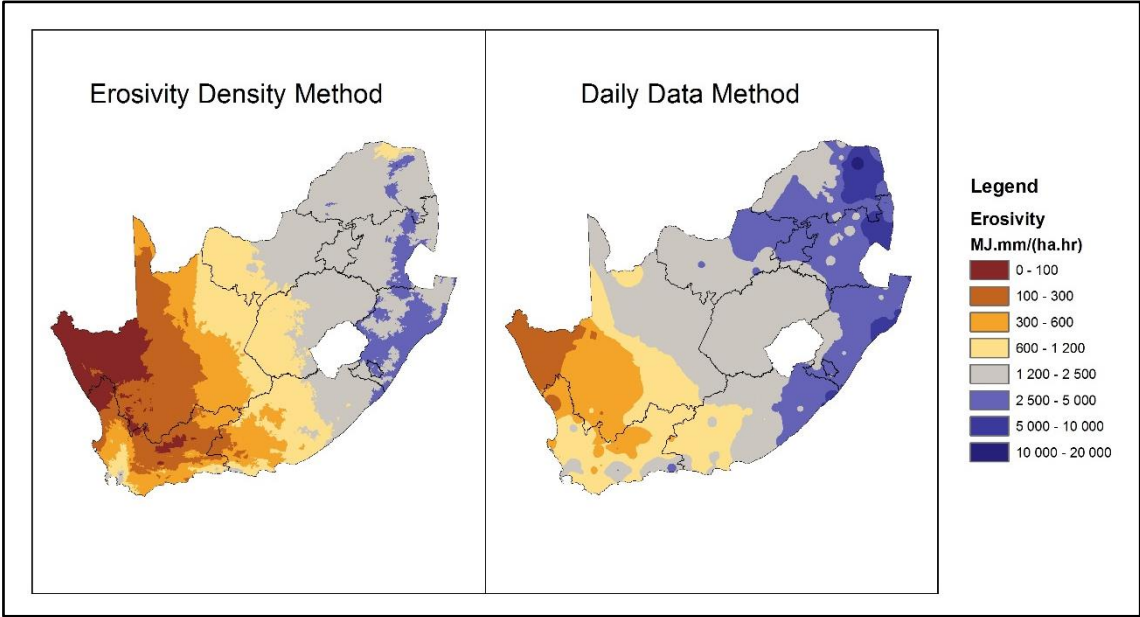


Figure 6.13 Comparison of annual rainfall erosivity using two different calculation methods

Figure 6.14 highlights the areas of considerable difference between the two methods. The map shows the results of the daily data method minus the results of the erosivity density method. It is clear that the methods produce comparable results (less than $2000 \text{ MJ.mm.ha}^{-1}.\text{h}^{-1}$ difference)

across most of the country. However, the daily data method produces much higher rainfall erosivity values for the Limpopo region, while producing lower values for the KwaZulu-Natal Drakensburg region (east of Lesotho).

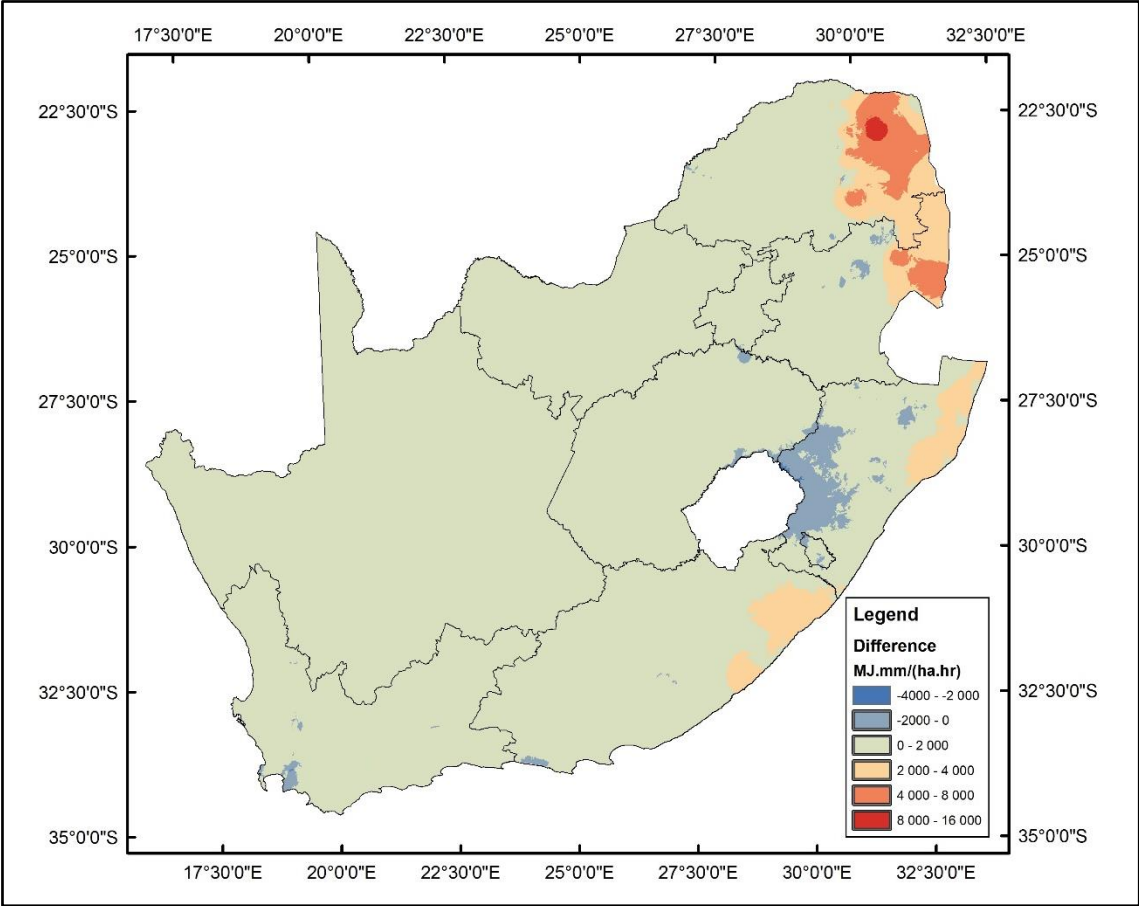


Figure 6.14 Error map to show the difference in magnitude of annual rainfall erosivity using the daily data method compared to the erosivity density method

Figure 6.15 shows the results of calculations of rainfall erosivity for January. It can be seen that the trends between the two sets of results are similar. As with the annual rainfall erosivity results, the daily data method produces higher rainfall erosivity values in the northern parts of the country.

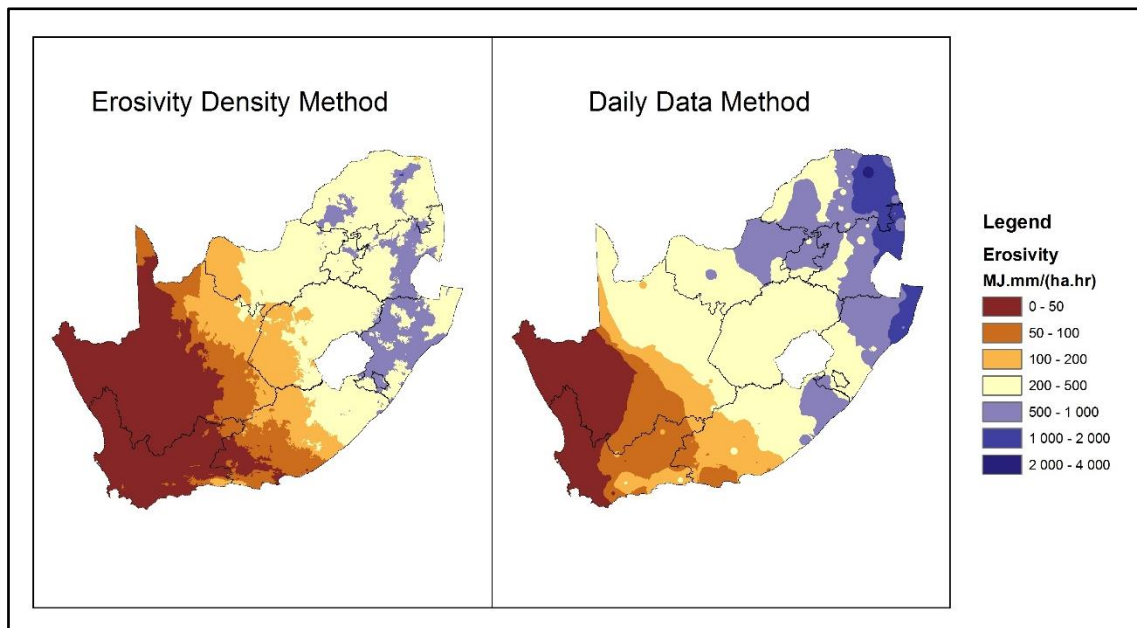


Figure 6.15 Comparison of January rainfall erosivity results using two different calculation methods

Figure 6.16 shows the rainfall erosivity for July calculated using the two different methods. Once again, the trends are similar. However, one outstanding feature is the area of higher rainfall erosivity on the southern coast of KwaZulu-Natal. This is not as obvious in the erosivity density method.

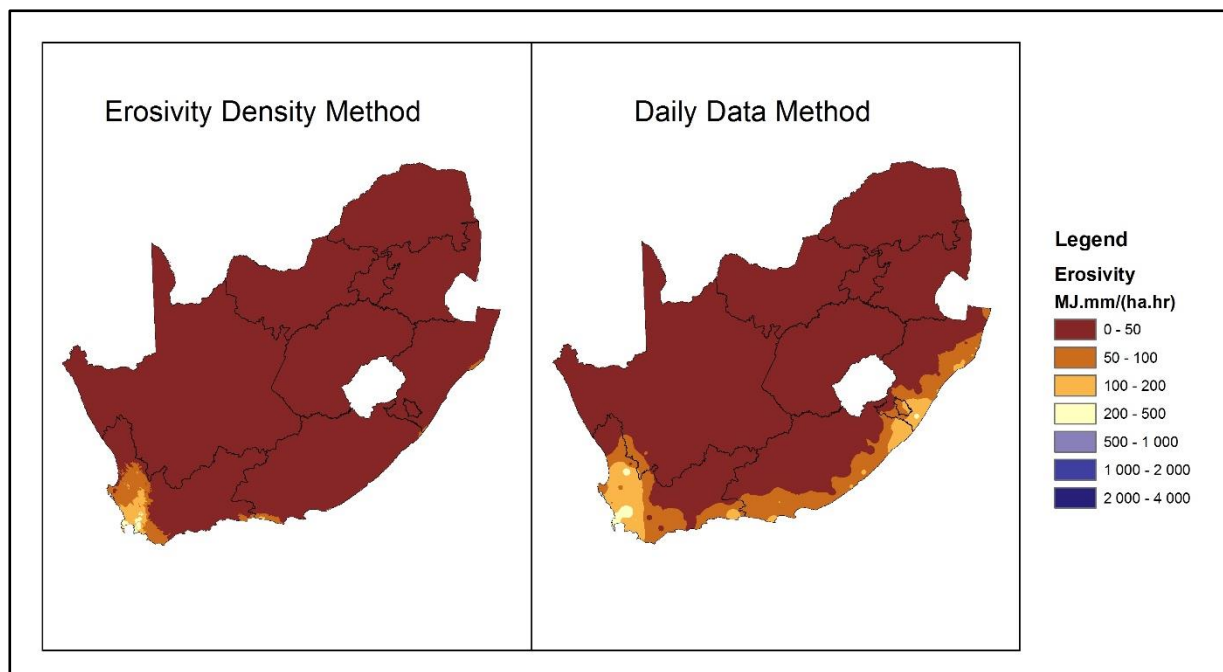


Figure 6.16 Comparison of July rainfall erosivity results using two different calculation methods

One prominent difference in the two methods is the level of detail. Because each Quinary catchment had a median monthly rainfall value assigned to it, the rainfall erosivity map resulting from the erosivity density method shows much finer detail in how the rainfall erosivity varies throughout the country. On the other hand, the daily data method required interpolation between daily rainfall data stations, giving a more generalised picture of the rainfall erosivity.

Figure 6.17 contains a comparison of the rainfall erosivity values obtained at the verification or ‘test’ stations used in the erosivity density method. The first series shows the EI_{30} value calculated directly from the short duration data. The second series shows the rainfall erosivity predicted using the erosivity density method, while the third series shows the rainfall erosivity predicted using the daily data method. The erosivity density method provides annual rainfall erosivities of a similar magnitude to the EI_{30} values calculated directly from the data. This promotes confidence in the method. However, it is evident that the daily data method appears to overestimate the rainfall erosivity greatly in some cases. This is also evidenced by the much higher rainfall erosivity values shown countrywide in the maps. Although the EI_{30} values were calculated using relatively short records, and therefore do not provide a perfect means of verifying the results of the different methods, the trends shown in Figure 6.17 indicate that the erosivity density method provided estimates of rainfall erosivity that were consistently closer to the actual erosivity experienced at the stations, than the daily data method.

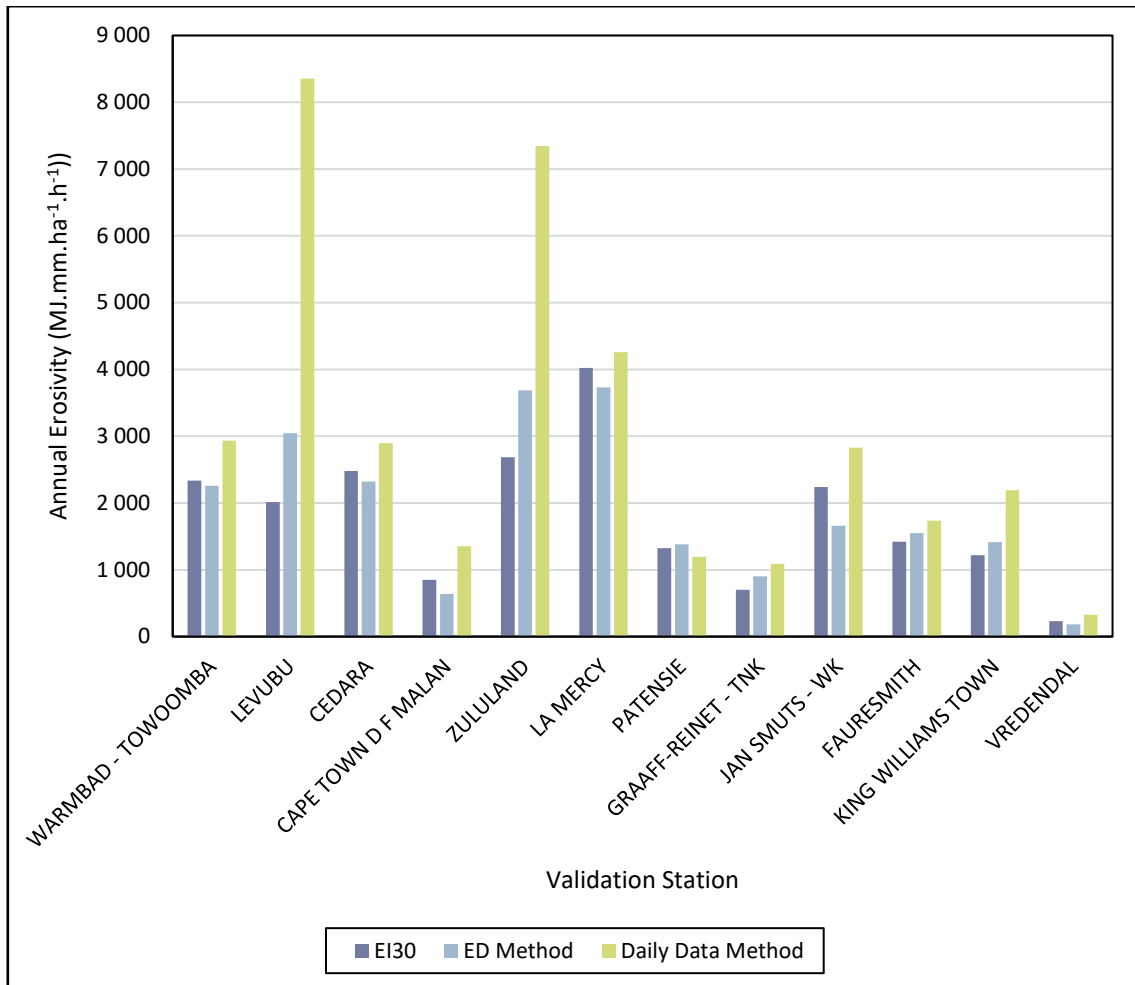


Figure 6.17 Comparison of calculation methods at validation stations

6.4 Comparison with Previous Studies

The two previous studies with which the results of this study were compared are those presented by Smithen and Schulze (1982) and Le Roux *et al.* (2006). Figure 6.18 shows the comparison that Le Roux *et al.* (2006) drew between the results of their study and that of Smithen and Schulze (1982). Figure 6.19 compares the results of the two methods that were adopted in this study, the erosivity density method and the daily data method, with those of the previous studies.

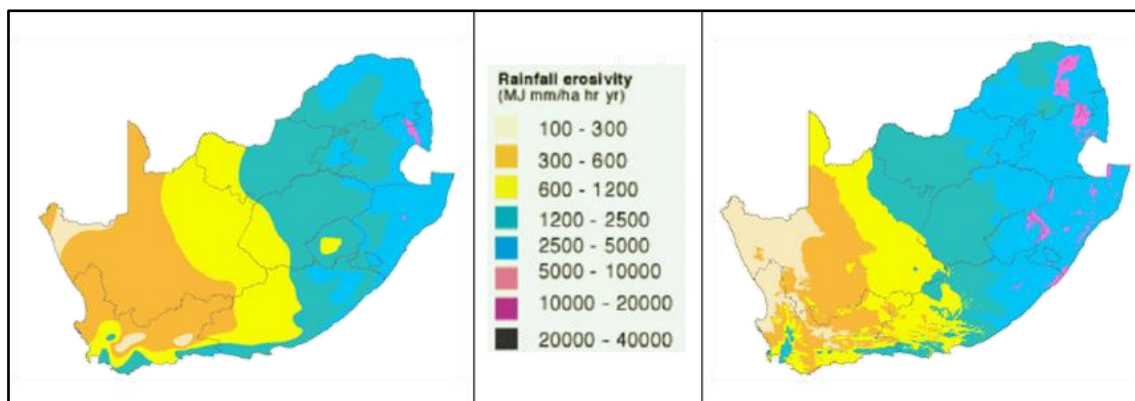


Figure 6.18 Annual rainfall erosivity maps for South Africa as derived by Smithen and Schulze (1981), left, and Le Roux *et al.* (2006), right

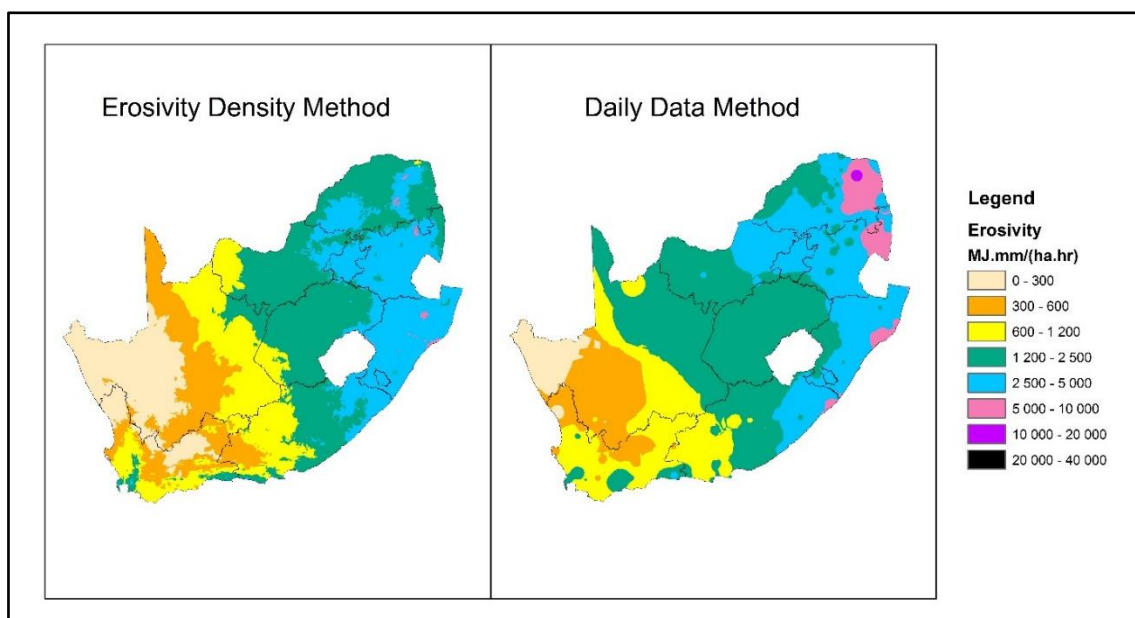


Figure 6.19 Annual rainfall erosivity maps for South Africa as derived using the erosivity density method (left) and the daily data method (right)

The comparisons show distinct similarities in trends. The erosivity density approach produces trends very similar to the results of Le Roux *et al.* (2006). The results of Le Roux *et al.* (2006) show a band of higher rainfall erosivities (exceeding 5000 MJ.mm.ha⁻¹.h⁻¹.a⁻¹) extending along the Drakensberg in KwaZulu-Natal, through to the Limpopo province. While the erosivity density method does not indicate such high erosivities in this region, the daily data method matches the results of Le Roux *et al.* (2006) closely in the eastern half of the country. The results of the daily data method generally shows higher values of rainfall erosivity in the western half of the country, compared with any of the former studies and approaches. Of the

two approaches used in this study, the erosivity density method provides results with a higher spatial resolution. The daily data method gives a more generalised picture of rainfall erosivity patterns, similar to the results obtained by Smithen and Schulze (1982).

Although long records of continuously-recorded rainfall data are required in order to verify the accuracy of rainfall erosivity estimates, the verification processes showed that the daily data method overestimated the erosivity at Levubu by 300 %, compared with an overestimation by 97 % using the erosivity density method. This suggests that the rainfall erosivities in the Limpopo region may not be as high as the results of the Le Roux *et al.* (2006) study, and the daily data method, indicate.

6.5 Conclusion on the Daily Data Method

Daily rainfall data was used to supplement continuously recorded rainfall data, to facilitate the estimation of rainfall erosivity across South Africa. Homogeneous regions identified by Smithers and Schulze (2000) were used in establishing relationships between daily rainfall amounts and rainfall erosivity. While studies have been conducted previously to use daily rainfall data to estimate rainfall erosivity (*e.g.* Smithen and Schulze, 1982; Yu and Rosewell, 1996), this study attempted to improve on these studies.

The daily data method utilised 204 daily rainfall stations in interpolating rainfall erosivity countrywide, compared with the 83 stations used in the erosivity density method. In addition to the larger number of stations, the stations were also selected in such a way that they had a relatively even spatial distribution. The results of the cross-validation showed a higher coefficient of correlation than the erosivity density method. Similarly, a lower error was evident in the verification of the interpolation. This implies that the higher number of stations predicted trends in the interpolation with greater accuracy. However, a similar pattern to the erosivity density method was observed in that the lower rainfall erosivity values were overestimated, while the higher values were underestimated. The inability of the IDW interpolation technique to predict maxima and minima is a limitation of the method and it is recommended that future studies utilise additional features in the interpolation stage, such as topography characteristics.

Although the accuracy of the interpolation was improved by the daily data method, the verification against observed rainfall erosivity data at the test stations showed poor results, compared with the erosivity density method. The average of the monthly relative errors at the test stations was found to be 91 % for the daily data method, compared with 55 % for the

erosivity density method. The daily data method appears to consistently overestimate rainfall erosivity. This is particularly evident in areas with relatively high rainfall erosivities. The poor performance in verification is attributed to a number of factors, including inaccurate relationships between rainfall amount and rainfall erosivity, due to low spatial density and uneven distribution of continuously-recording stations. The results of both methods highlight the need for a larger network of continuously-recording stations.

7. DEVELOPMENT OF A TOOL TO ESTIMATE CONTOUR INTERVALS

While RUSLE2 provides a very detailed analysis of soil loss, problems occur when insufficient data are available to run the model. In many cases, variables can be difficult or expensive to measure. This study attempted to provide a tool with which soil loss could be estimated to a reasonable degree of accuracy, while still limiting the amount of input data required. The spreadsheet developed provides a compromise between accuracy and simplicity, being more detailed than the original USLE equation, which calculated average annual values, while being simpler to use than RUSLE2 which requires extensive detail. This tool incorporates the updated rainfall erosivity values produced using the erosivity density method in this study.

The spreadsheet was developed for use with sugarcane cultivation and generates a recommended contour interval based on sustainable soil loss. The spreadsheet focussed on sugarcane due to the fact that it is a crop grown extensively in KwaZulu-Natal. In addition to this, much research has gone into soil erosion during sugarcane cultivation (Platford, 1987; McFarlane and Maher, 1993; McCulloch and Stranack, 1995; Meyer *et al.*, 1996).

The nomograph produced by Platford (1987), as shown in Figure 3.2, provides a benchmark against which the spreadsheet can be compared. While the spreadsheet focuses only on sugarcane, there is no reason why additional sheets could not be added to include other crops and land uses.

7.1 Structure of the Contour Interval Calculation Tool

The tool works by rearranging the RUSLE equation (Equation 3.2) to solve for the slope factor, and thereafter the slope length, given the tolerable soil loss, as well as climatic, soil and cropping conditions. Soil parameters are assumed to remain constant throughout the crop cycle, as are management practices (*e.g.* trashing vs. burning) and slope. Rainfall erosivity is based on a monthly time step (as calculated in this study). Crop information is calculated on a bi-monthly time step. Each month is split into two periods – the first period being 15 days long and the second period making up the remainder of the month (*i.e.* 16 days in January, 13 days in February). Leap years are not accounted for, in order to simplify calculations. The product of rainfall erosivity and the cover factor is calculated for every half-month period of the entire crop cycle. The crop cycle in this instance includes the land preparation before planting,

planting of the crop and the successive ratoons (harvesting and regrowth), until the land is prepared once more for replanting. Each aspect of the calculation tool is explained in turn below.

7.1.1 Tolerable soil loss

The first step in the soil loss calculator tool is to determine a tolerable soil loss. As explained in Chapter 2, the tolerable soil loss is the loss of soil that would allow agriculture to be sustained indefinitely. The soil loss tolerance depends on a number of variables, including soil parent material, climate and soil depth. The suggested values contained in Table 2.1, or values derived from other sources, can be used as input data.

7.1.2 Rainfall data

The rainfall data were taken from the results of the erosivity density approach used in this study. The final monthly rainfall erosivity was averaged for each quinary catchment. The spreadsheet does not disaggregate the rainfall in the same way that RUSLE2 does. In RUSLE2, equations are used to vary the rainfall continuously from month to month (USDA-ARS, 2013). Figure 7.1 shows how RUSLE2 disaggregates discrete monthly values into continuous daily values.

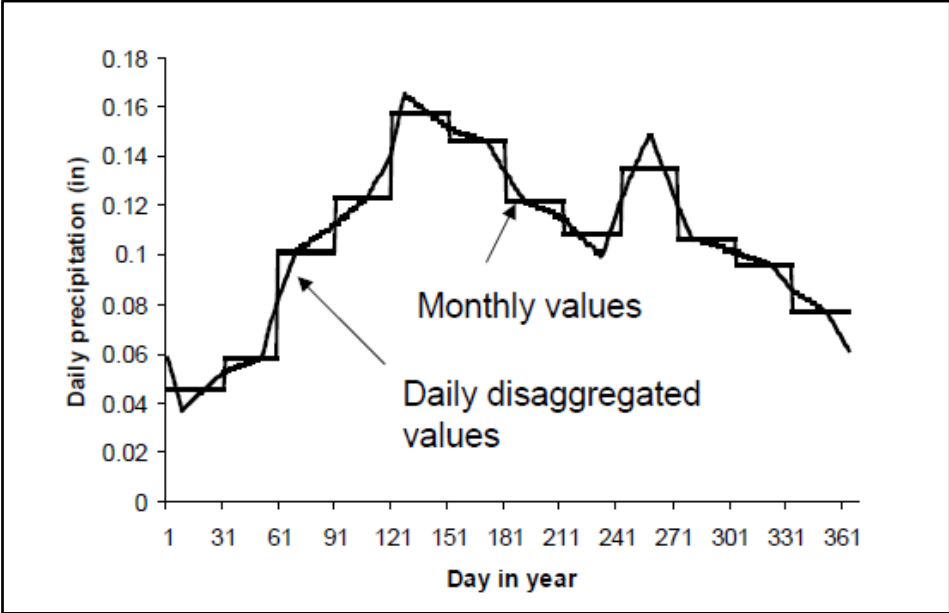


Figure 7.1 An example of how RUSLE2 disaggregates monthly precipitation values to obtain daily values (USDA-ARS, 2013)

In the interests of simplifying the calculations, a discrete value for the mean daily rainfall erosivity was used for each month. An average daily rainfall erosivity for each Quinary Catchment was calculated by dividing the monthly rainfall erosivity by the number of days in each month. These results are stored in the spreadsheet. When the user selects a Quinary Catchment, the daily rainfall erosivity for each month is extracted from the database.

7.1.3 Soil erodibility

The equation for the modified nomograph (Equation 3.7) was used to calculate the *K* factor in the spreadsheet, as explained in Section 3.2.3.2. The user is required to input the clay, silt and sand fractions, as well as the organic matter, permeability class and soil structure class.

7.1.4 Slope

The slope is entered by the user, in the form of a percentage. This is used to calculate the slope factor, using Equations 3.12 and 3.13 as shown in Section 3.2.3.3.

7.1.5 Support practice factor

The support practice factor is applied using the factors shown in Table 3.3 in Section 3.2.3.5. Factors taking harvesting method into account are also used. These were taken from the nomograph derived by Platford (1987). According to Platford (1987), if the trashing method is used during harvesting, the harvesting sub-factor is 0.8. If the cane is burnt (scattered tops present), the factor is 0.9, while if the cane is burnt and the tops reburnt, a factor of 1.0 applies.

7.1.6 Cover factor

The cover factor provided the greatest challenge in the calculations. RUSLE2 uses Equation 3.18 in order to calculate the cover factor. However, as mentioned previously, this is comprised of a number of sub-factors – each requiring extensive data to calculate.

The aim of creating the spreadsheet tool was to simplify calculations. However, little literature is available regarding sugarcane cover factors. Platford (1987) suggests average values ranging between 0.05 and 0.15 depending on the location and time of planting. This was for the KwaZulu-Natal region. Franks and Swartz (1971) suggest a value of 0.268 without the use of a cover crop, and 0.175 with a cover crop. This study was performed in the Queensland state of Australia. Morgan (2005) provides a cover factor estimate ranging between 0.13 and 0.40.

Generic cover factors could not be copied across from RUSLE2 as they are dependent on variables such as temperature and rainfall, and are therefore site specific.

Owing to the fact that tillage only occurs after approximately 10 ratoons (Platford, 1987), for a minimum period of approximately 10 years, factors such as ridge height and soil roughness are expected to remain relatively constant over the production cycle of sugarcane. The sugarcane was assumed to be kept weed-free, reducing the effect of the ground surface cover sub-factor. Although these factors would vary, with the aim of simplifying the calculations, they were assumed to have a negligible long term effect on the variability of the cover factor. The sub-factor that is expected to vary the most, is the canopy sub-factor. As cane grows and is cut, the canopy cover varies substantially from 0 % to about 95 %, according to the RUSLE2 database. The variables required to calculate the canopy cover sub-factor are shown in Equations 7.1 and 7.2, and can be abstracted from the RUSLE2 database (USDA-ARS, 2013).

$$c_c = 1 - f_{ec} \exp(-0.1h_f) \quad (7.1)$$

where

c_c = daily canopy sub-factor,

f_{ec} = daily effective canopy cover, and

h_f = daily effective fall height.

$$f_{ec} = f_c(1 - f_g) \quad (7.2)$$

where

f_c = daily canopy cover, and

f_g = daily net ground cover.

It was decided that an average cover factor would be determined from literature. However, the daily values would vary relative to the canopy cover sub-factor. In this way, the long term average will be consistent with that of previous studies, while still accounting for temporal changes in cover. This relationship is illustrated in Figure 7.2. The annual cover factor chosen was that of Franks and Swartz (1971), without a cover crop. The factor is 0.268 and this was chosen as it falls in the middle of the cover factor ‘spectrum’ for sugarcane. It was assumed in

this case that the farmer does not use a cover crop, although the value can be easily changed if this practice is adopted, or if updated values emerge from future studies.

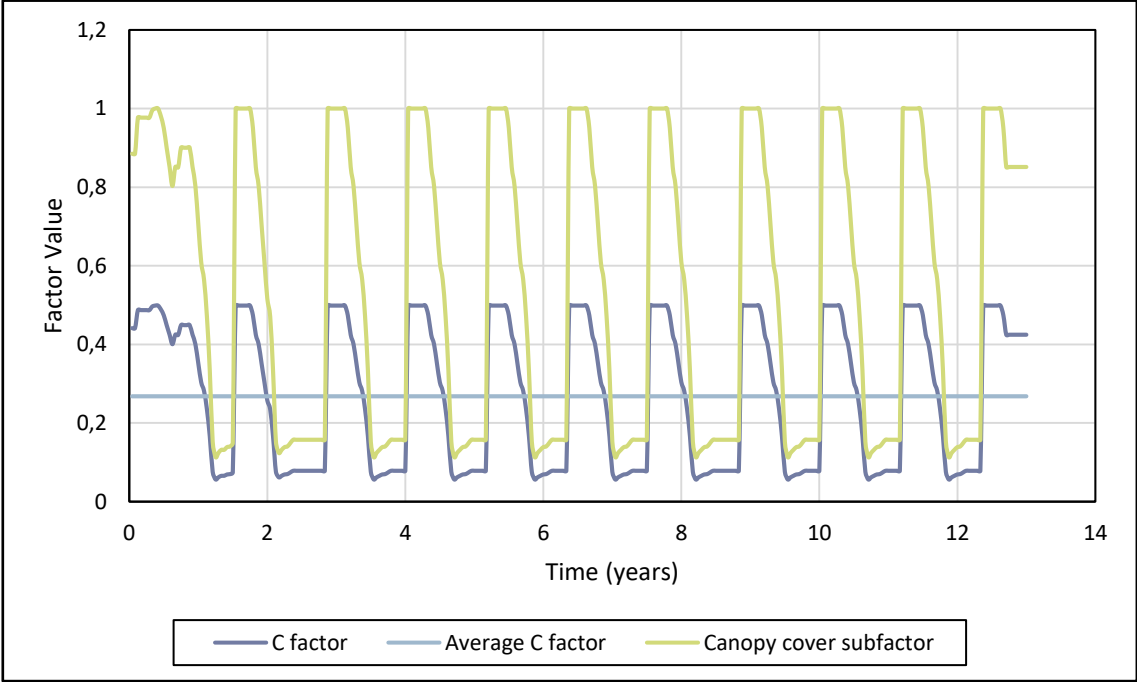


Figure 7.2 Relationship between the canopy cover sub-factor and the C factor for sugarcane adopted in this study

The daily cover and rainfall erosivity values are multiplied together, and the products for each half-month are summed to provide a combined CR factor for the entire crop cycle. The CR factor can then be multiplied by the remaining factors (which are assumed to remain constant over the crop cycle), in order to provide the total estimated soil loss over the crop cycle. This value can then be divided by the crop length in order to calculate the average annual soil loss.

The user is able to input the harvesting cycle length, with options for 12, 14, 16, 18 and 24 months. Based on the crop cycle length, the crop was modelled based on a number of assumptions. A field will not necessarily always be planted in the same month, however it is almost impossible to model every potential planting and harvesting permutation. A ‘worst case scenario’ was assumed for each harvesting cycle length. For the 12 and 24 month cycle, it was assumed that the worst case would be for the crop to be cut in the rainy season every harvest (*i.e.* minimal cover occurs with maximum erosivity). The planting month was selected as October, with harvesting occurring on the 1st December each year). For the 14 and 16 month cycles, the harvesting dates shift each ratoon and so no ‘worst case scenario’ applies. The planting month for these cycle lengths was retained as October. For the 18 month cycle, similar

assumptions were made for the worst case scenario. The planting month was selected as September and the harvesting months as December and June. The earlier planting date in this case is due to the slower growth rate.

The planting programme entailed the following:

- Assumed fallow period preceding tillage, in which previous sugarcane crop has had a herbicide applied, in order to kill it. In each case the cane was presumed to have been killed at a stage when the canopy cover was 15%.
- Land is prepared with a subsoiler/ripper on the 1st June. This breaks up the soil.
- Land is disked on the 1st July to chop up crop residue.
- Land is disked again on the 15th of the month preceding planting (*e.g.* the 15th of September if planting on the 1st October).
- The land is ridged the day before planting.
- The sugarcane is planted on the 1st day of the month.
- For the 12 month cycle, the 1st cut occurs 15 months after planting. The cane is then cut on the same day, every year thereafter.
- For the longer cycles, the cover factors are ‘spread out’ over a longer time period.
- After the last (tenth) cut, the cane is allowed to grow to a canopy cover of 15% before herbicide is applied.

The timing of each operation was determined manually and gives a general guideline, rather than an exact representation of the farming operations. For example, depending on the conditions, the farmer may decide to carry cane over to the next season, without harvesting it, thereby changing the pattern of the cycle. One major shortfall in this approach is the estimation of the growth pattern. The growth parameters were extracted from the RUSLE2 database and are a generic value based on the crop being a certain number of days after planting/harvest, as shown in Figure 7.3. The values do not take into account local climatic conditions (*e.g.* heat units). For this reason, the cane may be modelled to be growing vigorously in the cold winter months, when this would not be the case in reality. Although this compromises accuracy, no simple better alternative is available and this is an aspect that future studies could address.

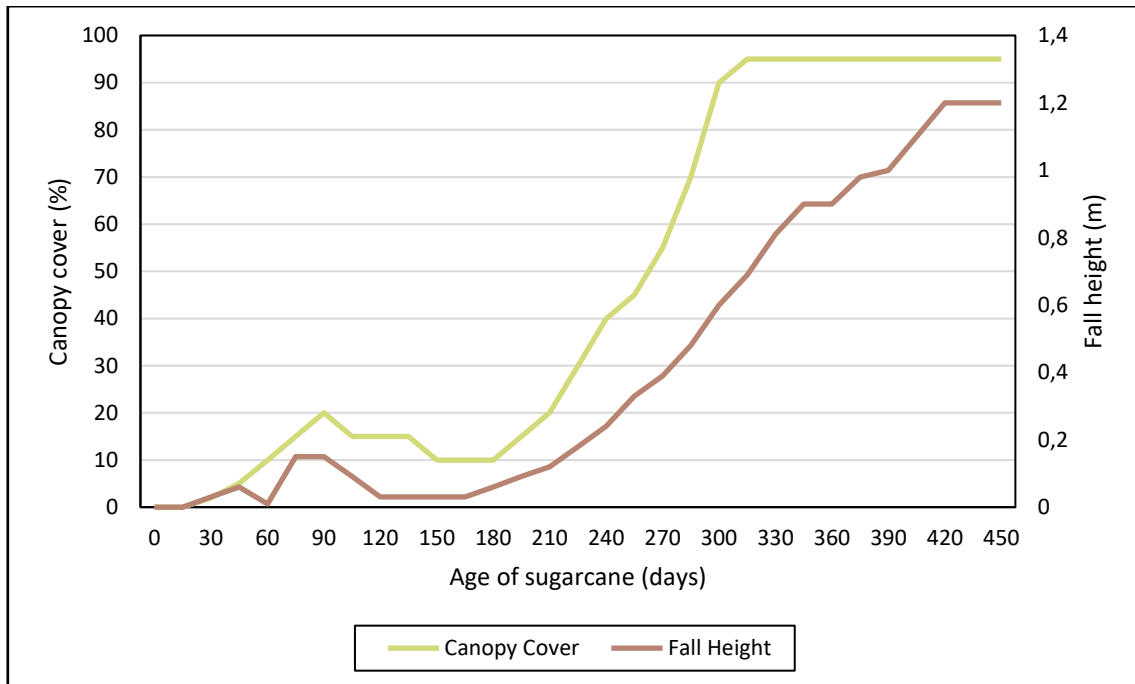


Figure 7.3 Canopy cover characteristics for sugarcane, from planting until 1st harvest

Another factor influencing the timing of operations was the operating season of the sugarcane mills. It was assumed that the mills would be closed between the 2nd December and 31st March, inclusive. This implies that no cane is cut during this period. When the calculated cutting date fell during this period (for the 14 and 16 month harvest cycles), the actual day of cutting was shifted to the 1st December or 1st April, depending on which date was closest.

In terms of the effects of tillage, soil disturbance factors were ignored (such as soil roughness and ridge height), while the effects on canopy cover were taken into account. Prior to any tillage, the crop parameters are assumed to be that of sugarcane with a 15 % canopy cover. Pre-set operations in RUSLE2 were used to mimic the effects of tillage on the vegetation parameters. These operation templates provided values for the burial ratio and the flattening ratio. The burial ratio is defined as the “portion of existing (flat) cover mass that is buried by a soil disturbing operation” (USDA-ARS, 2013). The flattening ratio is defined as “how much standing residue that an operation flattens”. The ‘subsoiler’ and ‘disk, offset, heavy’ operations were used for the land preparation operations described above. The values for these ratios are shown in Table 7.1.

Table 7.1 Ratios used to apply effects of tillage on sugarcane canopy cover and fall height

Operation	Burial Ratio	Flattening Ratio
Subsoiler	0.23	0.45
Disk	0.80	0.80

The relevant burial ratio was applied to the canopy cover value after each tillage operation, to represent the canopy material that had been buried. The flattening ratio was applied to the fall height, as the average fall height of the remaining residue would be reduced to this amount.

7.1.7 Calculation of slope length

The recommended slope length is calculated by rearranging the RUSLE equation in the form of Equation 7.3.

$$L = A/RKSCP \quad (7.3)$$

Once the allowable L factor is determined, the slope length can be calculated by rearranging Equation 3.8 to calculate λ_1 , the slope length.

A limit was placed on the slope length according to the maximum slope length limits described in Section 3.2.3.5. The effect of contour tillage is not considered effective on slope lengths exceeding these limits (Wischmeier and Smith, 1978). In addition to this, particularly on the flatter slopes, field lengths exceeding the limits would not be practical to manage or harvest.

7.2 Comparison of Spreadsheet and Nomograph Results

In order to assess the performance of the spreadsheet, recommended contour intervals were computed for a number of scenarios using the spreadsheet. The results were then compared with the values obtained by modelling the same scenarios using the nomograph developed by Platford (1987), hereafter referred to as “the nomograph”. In order to make comparisons between the results, a number of assumptions had to be made in modelling the scenarios using the spreadsheet. Firstly, the nomograph does not make provision for varied rainfall erosivity values and was developed based on a rainfall erosivity of 3 500 MJ.mm.ha⁻¹.h⁻¹.a⁻¹ (based on a KwaZulu-Natal coastal region). Secondly, the nomograph simplifies the erodibility of soils into “resistant”, “moderate” and “erodible”, rather than providing actual K values (Platford, 1987).

Based on the planting area and rainfall erosivity used for the nomograph, a Quinary Catchment with a similar rainfall erosivity and location was selected for the comparison. The Quinary Catchment selected was W11B3, with an annual rainfall erosivity of 3 497 MJ.mm.ha⁻¹.h⁻¹. This quinary is located approximately 35 km north-east of Stanger, on the north coast of KwaZulu-Natal, as illustrated in Figure 7.4.

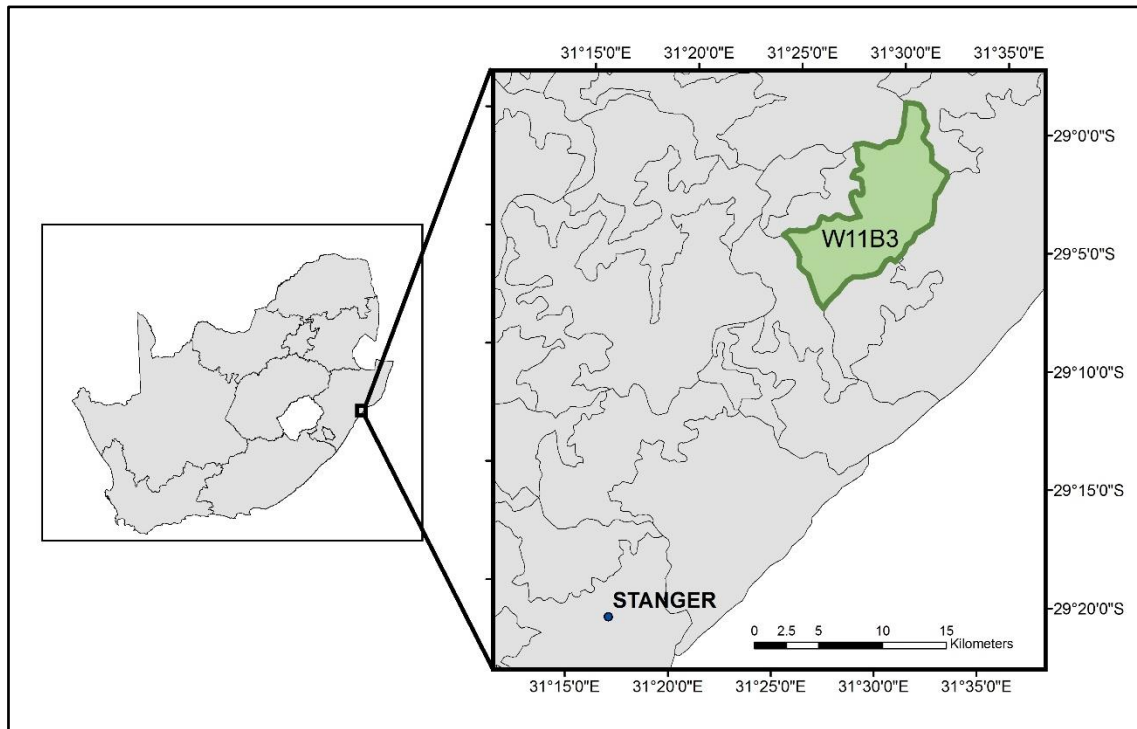


Figure 7.4 Location of test Quinary W11B3

Platford (1987) describes a highly erosive soil as having high proportions of silt and fine sand, as well as low organic matter contents. On the other hand, resistant soils are described as having high clay and high organic matter contents. The *K* values used in the development of the nomograph are listed in Table 7.2.

Table 7.2 Soil erodibility factors used in the development of the nomograph (after Platford, 1987)

Erodibility	<i>K</i> (t.h.MJ⁻¹.mm⁻¹)
Very high	0.065
High	0.042
Moderate	0.028
Low	0.022
Very low	0.015

In computing the spreadsheet results, soil types were selected in order to match these descriptions in an effort to model comparable scenarios. The soil types, properties and resultant *K* factor values used in the spreadsheet are summarised in Table 7.3.

Table 7.3 Soil properties used in the testing of the spreadsheet

Erodibility class	Soil type	% sand	% silt	% clay	Soil organic matter (%)	Soil structure class	Soil permeability class	<i>K</i>
Resistant	Clay	20	20	60	3	1	5	0.020
Erodible	Silt	8	87	5	1	2	2	0.075
Moderate	Silty Clay Loam	10	56	34	2	2	4	0.040

The acceptable soil loss on which the nomograph is based is 20 t.ha⁻¹.a⁻¹, and this figure was carried through to the spreadsheet for the calculations. Although Platford (1987) does not specify a crop cycle length, a 14 month cycle was adopted in the spreadsheet for computing the recommended contour intervals.

As evidenced in Figure 7.5, the spreadsheet is highly sensitive to changes in slope. For a scenario entailing a moderate soil erodibility and the burning method of harvesting, a change of slope from 5 % to 10 % leads to a reduction in recommended contour interval from 91.50 m to 16.86 m. The steps in the graph are due to the slope length limits suggested by Wischmeier and Smith (1978). It can be seen that all three of the soil erodibility classes are affected by the

slope length limits for flatter slopes. As the slope steepens, the calculated recommended contour interval drops below the limiting value and a smoother graph results.

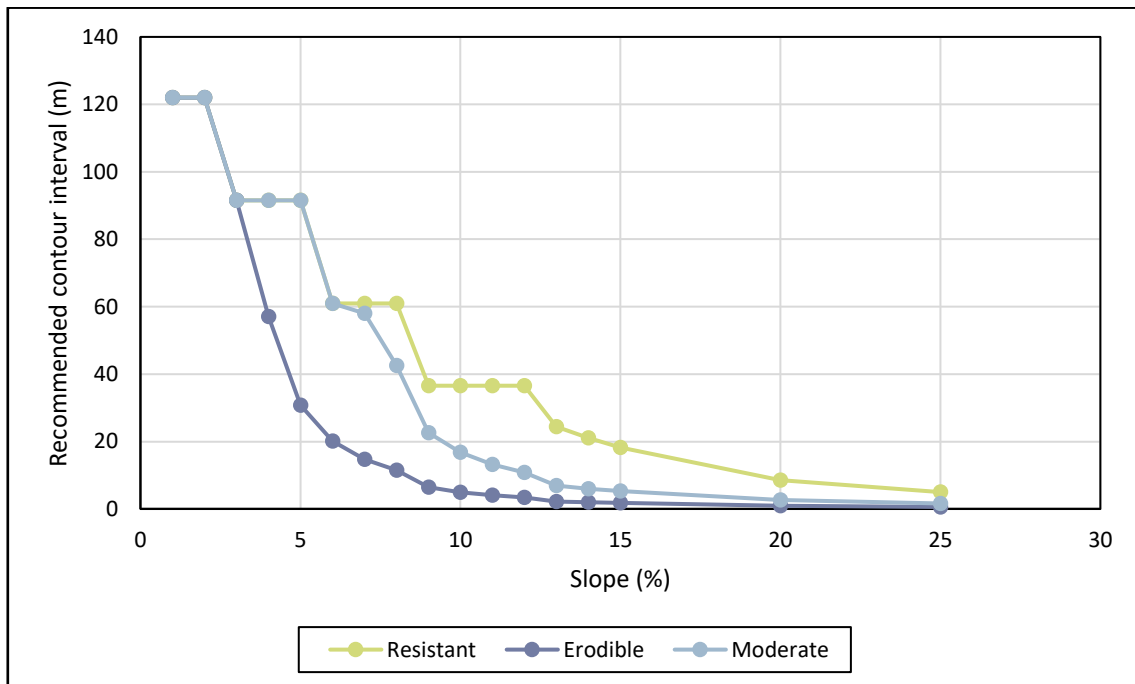


Figure 7.5 The effect of slope on the spreadsheet calculations of recommended contour interval for various levels of soil erodibility

In comparison with the spreadsheet, the nomograph is much less sensitive to changes in slope. Figure 7.6 compares the nomograph and the spreadsheet for a moderately resistant soil and the burning method of harvesting. While the nomograph provides practical contour intervals throughout the range from 5 % to 25 %, it can be seen that the spreadsheet provides significantly smaller contour intervals, and that any slope greater than 10 % cannot practically achieve sustainable soil loss, according to the spreadsheet. While it is not possible to verify the results without physical measurements of soil loss, the results of the spreadsheet suggest that a soil loss of 20 t.ha⁻¹.a⁻¹ is difficult to achieve, and that fields may be losing significantly greater amounts of soil than previously thought.

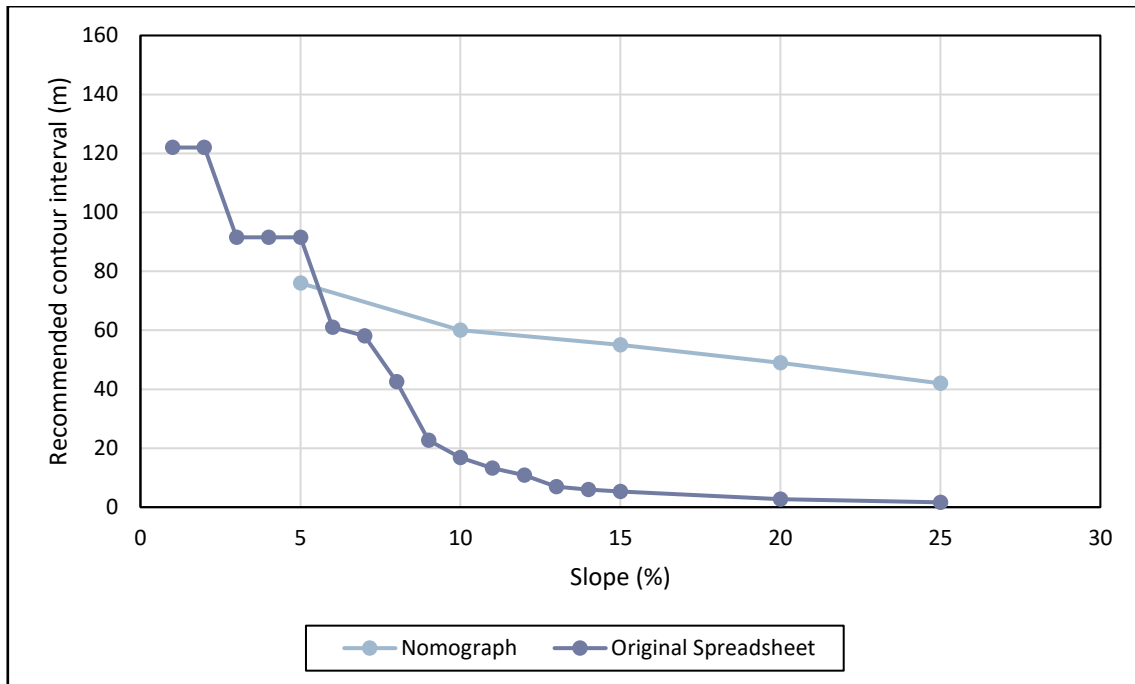


Figure 7.6 Comparison of the nomograph and spreadsheet results for a moderately erodible soil and burnt cane harvesting

The distinct differences regarding the effect of slope necessitated investigation into the dissimilarities between the two methods regarding the calculation of the slope factor. The nomograph calculates the slope factor using the equation presented by Wischmeier and Smith (1978), as shown in Equation 3.18. The slope factor used in the spreadsheet is calculated using Equations 3.19 and 3.20, developed by McCool *et al.* (1987), as described in Section 3.2.3.3.

Figure 7.7 illustrates the relationship between slope and the *S* factor for the two methods. It can be seen that for steeper slopes, the *S* factor used in the spreadsheet is actually lower than the equivalent *S* factor determined in the nomograph. The spreadsheet would therefore be expected to calculate even smaller recommended contour intervals for steep slopes, if the equations used to determine the slope factor in the nomograph were used.

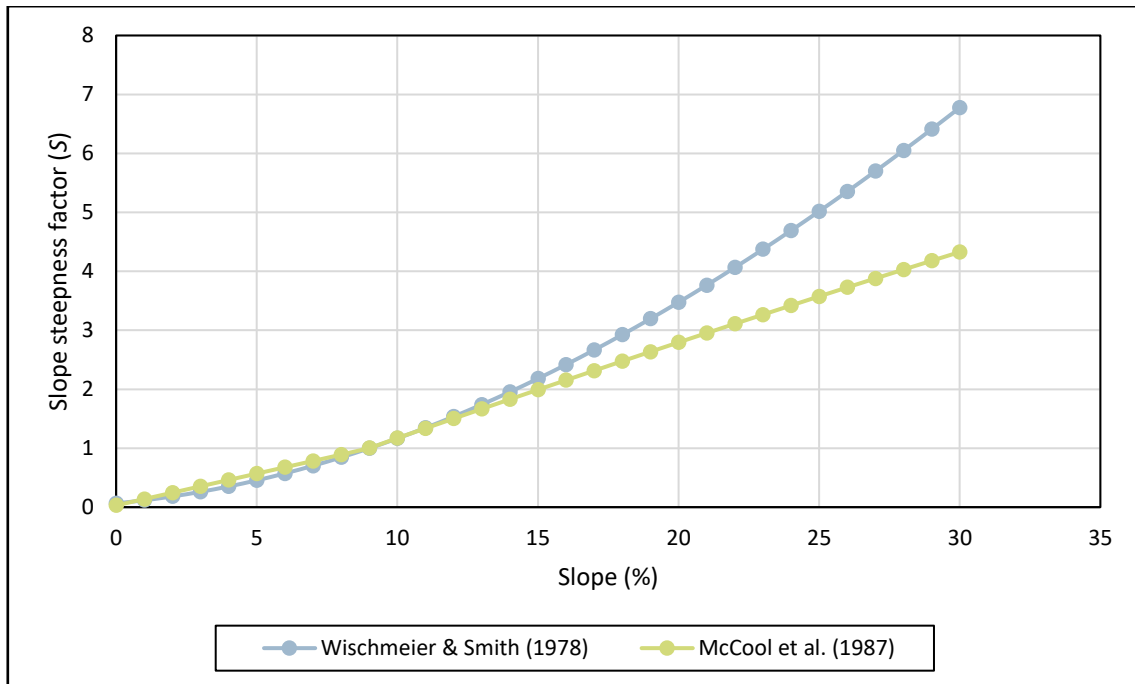


Figure 7.7 Comparison of the effect of slope on *S* factor values for the spreadsheet (McCool *et al.*, 1987) and the nomograph (Wischmeier and Smith, 1978)

The discrepancies in the results can also be attributed to the different magnitudes of the *C* factors. The average cover factor used in the spreadsheet (0.268) is more than double that of the cover factor used in the nomograph (0.11). When comparing the two methods, the product of the average *C* and *R* factors, *CR*, for the nomograph is 385 MJ.mm.ha⁻¹.h⁻¹.a⁻¹, while that used in the testing of the spreadsheet is 937 MJ.mm.ha⁻¹.h⁻¹.a⁻¹. Figure 7.8 illustrates the difference in results if the average *C* factor of the nomograph (0.11) is adopted in the spreadsheet. Although the lower cover factor does make a substantial difference in the results of the spreadsheet, the recommended contour intervals are still impractical on steeper slopes.

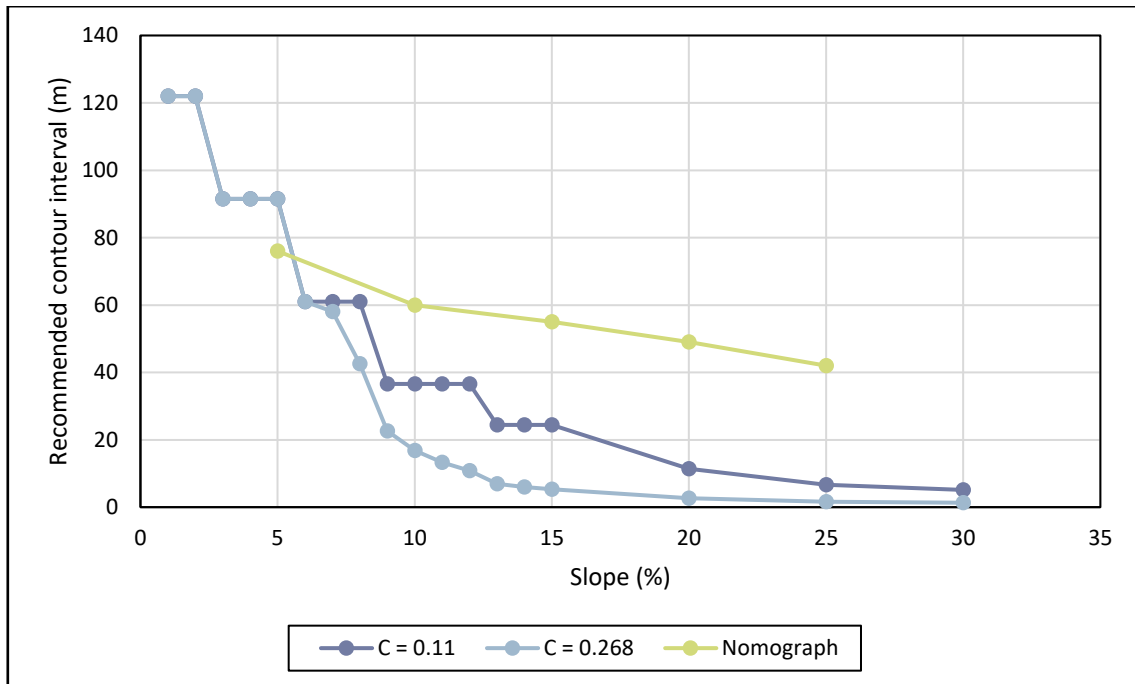


Figure 7.8 The effect of the C factor on the results of the spreadsheet

In addition to the different magnitudes of the C factors, the timing and inter-relationship of the C and R factors play a significant role in the discrepancies between the two methods. If the average C factors are made equal in the spreadsheet and the nomograph, the timing of the crop growth and rainfall still leads to large discrepancies. For example, if the cover factor and rainfall erosivity of the nomograph were made to match the spreadsheet (*i.e.* the C factor was increased to 0.268 and the rainfall erosivity was made to equal $3\,497\text{ MJ}\cdot\text{mm}\cdot\text{ha}^{-1}\cdot\text{h}^{-1}\cdot\text{a}^{-1}$), and, the product CR would equal $937\text{ MJ}\cdot\text{mm}\cdot\text{ha}^{-1}\cdot\text{h}^{-1}\cdot\text{a}^{-1}$. However, the results of the spreadsheet show that under these conditions, the CR product ranges from $888.50\text{ MJ}\cdot\text{mm}\cdot\text{ha}^{-1}\cdot\text{h}^{-1}\cdot\text{a}^{-1}$ to $1\,214.27\text{ MJ}\cdot\text{mm}\cdot\text{ha}^{-1}\cdot\text{h}^{-1}\cdot\text{a}^{-1}$, depending on the crop cycle length (a variation of between - 5.18 % and 29.59 % from the product of the average values).

Figure 7.9 compares the average annual CR product with the actual CR product over time, for a 14 month harvesting cycle. The peaks in the graph occur when the cane is cut (*i.e.* the C factor increases). Owing to the fact that the harvesting cycle is 14 months in this case, the low crop cover coincides with high rainfall erosivity in some cycles and low rainfall erosivity in others. This is evidenced by the different magnitude of the peaks. It is evident that the timing of erosive rainfall and crop growth have a large influence on the soil loss and, hence required contour intervals.

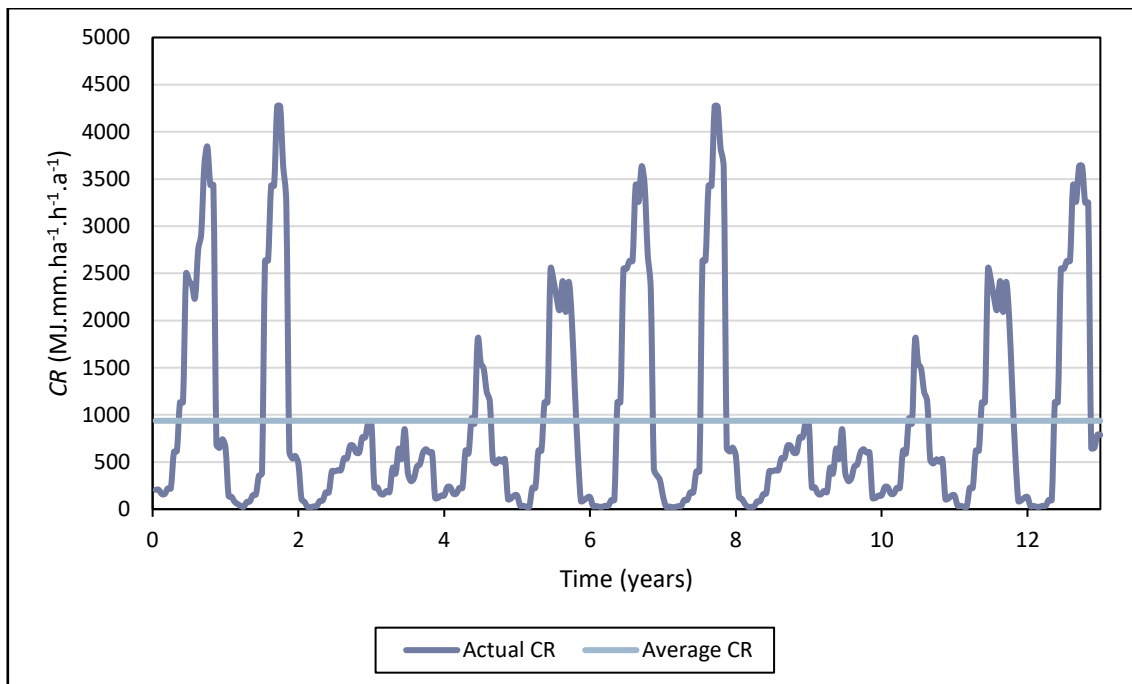


Figure 7.9 Comparison of the average annual *CR* product and the actual *CR* product throughout the crop cycle

Another aspect which results in the large discrepancies between the spreadsheet and the nomograph is the ‘minimum tillage’ factor used in the nomograph. The nomograph forces minimum tillage over conventional tillage beyond a certain slope (depending on the erodibility of the soil). The support practice factor assigned to chemical minimum tillage in the nomograph is 0.15. The application of this factor has a drastic result as it essentially reduces estimated soil loss to 15 % of the value with conventional tillage, which relates to a much longer recommended slope length. At present, the spreadsheet does not cater for different tillage methods, other than the use of contour tillage. The tillage practices currently modelled in the spreadsheet combine both conventional and minimum tillage techniques – whereby the old crop is killed using herbicides, but limited subsoiling and disking still occurs. This is considered to be a realistic land preparation scenario for many farms.

Figure 7.10 shows the effect of the addition of a ‘minimum tillage’ support practice factor to the spreadsheet. It would be preferable to model the conditions accurately during the land preparation stage of the crop cycle, rather than apply a single factor without regard for the timing or specific methods of tillage. However, this method allows a simple comparison of the results. The support practice factor used in the previous calculations was simply multiplied by 0.15 in order to obtain the new support practice factor.

It can be seen in Figure 7.10 that the addition of the minimum tillage factor increases the recommended contour interval substantially. In fact, the limiting factor was the maximum slope length described in Section 3.2.3.5. Removing the slope length limits revealed that the spreadsheet recommended longer contour intervals than the nomograph suggested for all slopes less than 22%. Although this is not strictly a direct comparison, due to the fact that the spreadsheet did not represent typical conventional tillage practices beforehand, it explains, to some extent, the large discrepancies between the results of the spreadsheet and nomograph.

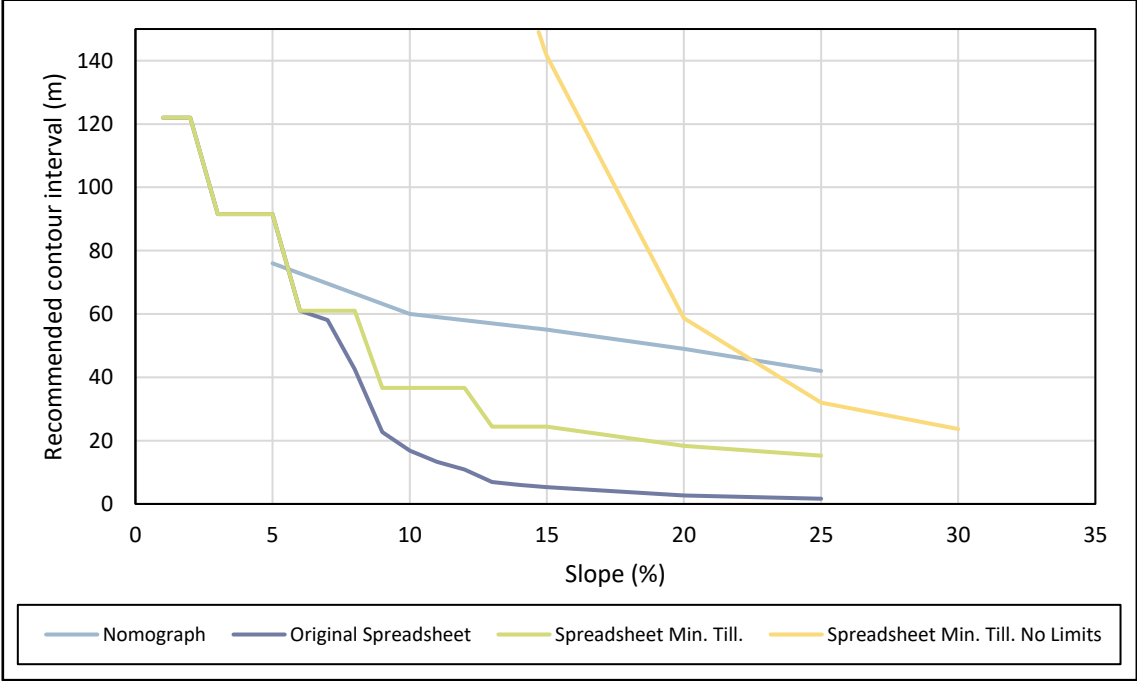


Figure 7.10 The effect of the application of a 'minimum tillage' support practice factor to the spreadsheet

7.3 A Synthesis of the Comparison and Suggestions for the Way Forward

While the spreadsheet developed in this study is a first attempt, it provides insight into the shortfalls of existing contour interval determination tools. The importance of the timing of erosive rainfall, coupled with varying crop cover has been highlighted. The spreadsheet also highlights the potential for adapting the RUSLE equation for specific crops. This results in much more user-friendly tools for each sector of agriculture, where scenarios can be pre-programmed by experts – leaving less decision-making for users of the tool and ensuring accurate results. The shortfalls of the tool developed in this study include limited insight into different tillage mechanisms, as well as cover factors that may not be synchronised with climatic conditions (for example, vigorous growth during winter months). It is recommended

that further research be undertaken into determining the cover factor for various crops simply and effectively. While strict minimum tillage practices were not modelled by the spreadsheet the tillage practices are considered realistic for many farms. Without utilising the minimum tillage support practice factor used in the nomograph, the spreadsheet provided substantially lower recommended contour intervals than the nomograph. Although refinement of the spreadsheet is required, the first assessment suggests that sustainable soil loss from sugarcane fields is difficult to achieve practically, particularly on steep slopes. The results also imply that existing fields may be losing greater amounts of soil than previously thought.

The development of this tool enabled the application of the rainfall erosivity values determined in this study. The spreadsheet also met the desired objectives to produce a tool which has limited input data requirements, while utilising advancements made in the development of the RUSLE, such as a greater focus on temporal aspects of erosivity and crop characteristics. The tool was successful in determining recommended contour intervals, although further refinement is suggested and validation against measured soil loss values would be necessary before application of the tool in industry.

8. DISCUSSION AND CONCLUSIONS

This document contains a review of the mechanical measures used to reduce soil loss in South Africa, as well as design methods used in determining recommended contour bank intervals. A review of the literature indicates that site-specific evaluation, using a soil loss prediction tool, is the preferred approach to the determination of contour bank spacing, rather than the use of simple empirical equations. The empirical equations used in South Africa are subjective and can be inaccurate, particularly on steep slopes. In addition to this, South Africa lacks detailed, experiment-based information on which factors to use under various conditions. As a consequence, contour intervals are found using a generalised empirical equation, or a simple graph which takes very few site-specific factors into account.

On the other hand, a review of empirical soil loss models used in site-specific evaluation showed that the RUSLE model is able to provide accurate results under a large range of conditions. It was found that the SLEMSA model did not provide accurate results when applied in areas other than that in which it was developed. It was able to provide comparative answers, but was not accurate in determining absolute values of soil loss. Although efforts have been made to generate South African-specific factors, the USLE model also has its limitations and was considered to be outdated. The RUSLE was found to be the most suitable empirical model for determining contour bank intervals in South Africa. The RUSLE is widely used internationally and has significant improvements over the USLE model, including more detailed input data requirements and increased flexibility. All but one of the RUSLE factors are transferable from other areas and studies (*e.g.* soil types and effects of tillage), however the rainfall erosivity factor must be determined using local climatic data. While South African rainfall erosivity values have been updated in recent years (Le Roux *et al.*, 2006), the rainfall erosivity factor was still calculated based on daily rainfall values, rather than continuously recorded data from which rainfall intensity can be derived. The erosivity density method, used in the development of RUSLE2 (USDA-ARS, 2013), had not yet been tested in South Africa. The application of this method, therefore, formed the major aim of this study. A second method was also adopted, whereby daily data were used to supplement the continuously recorded data.

This study was successful in updating rainfall erosivity values for South Africa. Short duration data were utilised and rainfall erosivity was calculated using two methods, namely the erosivity density method and the daily data method. The low spatial density of the continuously recording

rainfall stations was found to be a major limiting factor in the application of the erosivity density method. The verification of the interpolation of values produced an error of 75 % for the erosivity density method. In comparison, the use of a larger number of stations for the daily data method resulted in an interpolation error of 43 %. However, when comparing the predicted results at the test stations with the actual EI_{30} values, the erosivity density method was found to perform much better than the daily data method, with an average error of 55 %, compared with 91 % for the daily data method. The erosivity density method also provided output with much finer detail when compared to the broad, generalised results of the daily data method.

Both methods showed similar trends in terms of the magnitudes and distribution of rainfall erosivity across South Africa. However, the daily data method produced consistently higher rainfall erosivity values across the country. Across the majority of the country this difference was less than 2 000 MJ.mm.ha⁻¹.h⁻¹. However, the daily data method produced much higher ‘peaks’ of rainfall erosivity, producing a maximum annual rainfall erosivity value of 16 398.9 MJ.mm.ha⁻¹.h⁻¹, compared to the erosivity density method maximum of 5 865.8 MJ.mm.ha⁻¹.h⁻¹. The daily data method only estimated lower rainfall erosivities than the erosivity density method in small localised areas in the Western Cape, as well as in the Drakensberg region of KwaZulu-Natal. The monthly, rather than annual, rainfall erosivity output for both methods is valuable in agricultural applications to assess erosion in respect of cropping timing and practices.

The comparison of a number of energy equations showed that the energy equation used can have a large effect on erosivity density, and hence overall rainfall erosivity, values. It was found that the equation proposed by Wischmeier and Smith (1958) generally produced the highest energy values, while that of Elwell and Stocking (1973) tended to produce the lowest energy values. It was noted that these two equations only produce the highest and lowest unit energy values respectively, of the five equations, below 10 mm.h⁻¹. This suggests that frequent low intensity rainfall events have a greater effect on erosivity density values than infrequent high intensity storms. The “universal equation” proposed by van Dijk *et al.* (2002) gave the median energy value in most cases. The equation used in RUSLE2, that of McGregor *et al.* (1995), produced the second highest energy values in general, and these were used in the final calculations of rainfall erosivity. Although the magnitude of the energy values differed substantially according to the energy equation used, the general pattern and distribution of energy was consistent between equations.

The study also tested the effects of applying thresholds to the rainfall data. Contrary to previous studies, it was found that the removal of rainfall events less than 12.7 mm had a substantial effect on the rainfall erosivity values. The application of the 12.7 mm threshold was found to reduce estimates of erosivity density, and hence rainfall erosivity, by 5 %. Similarly, the effect of excluding storms larger than the 50 year return period storm was explored. Owing to the relatively short record lengths at the short duration stations, it was found that few storms were removed. Looking at the averages of all of the values, the exclusion of these storms resulted in an average reduction in rainfall erosivity of 3 %. While the average effect does not seem considerable, when analysing individual months at the effected stations, the removal of these storms had a substantial effect on the rainfall erosivity values.

One major drawback of the study was the paucity of suitable data. The erosivity density method would have benefitted greatly from a denser network of short duration stations. In addition to this, the majority of the short duration stations had relatively short records, compared to record length of daily data stations. This led to inaccurate representation of the rainfall characteristics at a number of stations. It is recommended that this study be repeated after a suitable period of time in order to make use of the expanding short duration station network and longer records. While the daily data method performed better in the interpolation of the results, the daily data relationships were still based on the same limited continuously-recorded data. Although additional daily stations could be included to improve the interpolation further, this would not remove the errors associated with the regression equations, and this error will simply be carried through to the final results.

Both approaches produced results consistent with previous studies. Although there were some discrepancies, the general trend of the results agreed with those of Smithen and Schulze (1982) and Le Roux *et al.* (2006). The erosivity density approach generally produced erosivities lower than both the previous studies and the daily data approach, however the verification results showed that the rainfall erosivity calculated using the erosivity density method closely matched the EI_{30} values calculated directly from short duration data, promoting confidence in this approach.

A tool was developed in order to utilise the updated rainfall erosivity values in determining contour bank intervals on sugarcane farms. The rainfall erosivity values obtained using the erosivity density method were used. The RUSLE model was used to determine the maximum allowable slope length for a specified soil loss tolerance, given the relevant field and cropping

parameters. A compromise between simplicity and accuracy allowed the tool to remain user friendly, while still utilising a relatively short time step to model the temporal changes of rainfall erosivity and crop growth. For a number of scenarios, the recommended contour bank interval obtained using the tool was compared with that obtained using the nomograph developed by Platford (1987). The tool was found to be highly sensitive to slope and did not produce practical contour bank intervals on steep slopes. Discrepancies between the results of the tool and the nomograph were attributed to a number of factors, including the timing of erosive rain compared to crop cover, as well as the different modelling techniques of tillage operations.

While further refinement of the tool is recommended, the first assessment suggests that sustainable soil loss is not achievable on steep slopes. The developed tool is considered to be an improvement on the nomograph in that a unique rainfall erosivity value can be selected for each quinary, compared to the one rainfall erosivity value used in the nomograph. In addition to this, the combined effect of the crop cover and rainfall erosivity is modelled twice in a month, rather than using average annual values. It is recommended that further refinements to the tool link the cover factor to climatic conditions (*e.g.* canopy cover and fall height are unlikely to increase substantially in the winter months, as the sugarcane does not grow significantly during this period).

In conclusion, the objectives of the study have been met. Following the review of literature regarding soil loss modelling and soil conservation structures, the erosivity density method to determine rainfall erosivity in South Africa was successfully tested. An additional method, using daily rainfall data, was applied in a further attempt to use short duration rainfall data to determine rainfall erosivity. However this method proved less promising and was more cumbersome in determining relationships. The erosivity density approach was found to be relatively simple and compared favourably with both observed data and previous studies. Although the continuously-recorded data was insufficient to provide suitably accurate results, the method has been shown to be applicable in South Africa and can be repeated when additional short duration rainfall records become available.

9. REFERENCES

- Aksoy, H and Kavvas, ML. 2005. A review of hillslope and watershed scale erosion and sediment transport models. *Catena* 64(2005):247-271.
- American Society of Agricultural and Biological Engineers (ASABE) Standard*. 2012. ASAE S268.5 JAN2012. Design, layout, construction, and maintenance of terrace systems. ASABE, St. Joseph, Michigan, USA.
- Brown, LC and Foster, GR. 1987. Storm erosivity using idealised intensity distributions. *Transactions of the American Society of Agricultural Engineers (ASAE)* 30:379-386.
- Carter, CE, Greer, JD, Braud, HJ and Floyd, JM. 1974. Raindrop characteristics in South Central United States. *Transactions of the ASAE* 17(6):1033-1037.
- Conservation of Agricultural Resources Act. 1983. RSA Government Gazette No. 43 of 1983, No. 8673. Cape Town, RSA.
- Dabney, S. 2015. Personal communication, USDA-ARS, Washington D.C., USA, 10 March 2015.
- Department of Agricultural Technical Services. 1976. Soil loss estimator for southern Africa. No. 7. Natal Agricultural Research Bulletin, Pietermaritzburg, RSA.
- El-Swaify, SA, Dangler, EW and Armstrong, CL. 1982. *Soil erosion by water in the tropics*. University of Hawaii, Honolulu, Hawaii.
- Elwell, HA and Stocking, MA. 1973. Rainfall parameters for soil loss estimation in a subtropical climate. *Journal of Agricultural Engineering Research* 18:169-177.
- ESRI. 2008. ArcGIS Desktop: Release 9.3. Environmental Systems Research Institute, Redlands, California, USA.
- Franks, HD and Swartz, GL. 1971. Predicting rainfall erosion losses in sugar cane lands. *Proceedings of the 38th Queensland Society of Sugar Cane Technologists*, 41-46. Watson Ferguson, Queensland, Australia.
- Garland, G, Hoffman, M and Todd, S. 2000. Soil degradation. In: eds. Hoffman, M, Todd, S, Ntshona, Z and Turner, S, *A National Review of Land Degradation in South Africa*, Unpublished report, Ch. 6, 69-107. South African National Biodiversity Institute, Pretoria, RSA.
- Hosking, JRM and Wallis, JR. 1997. *Regional Frequency Analysis: An Approach Based on L-Moments*. Cambridge University Press, Cambridge, UK.

- Hudson, B. 1994. Soil organic matter and available water capacity. *Journal of Soil and Water Conservation* 49(2):189-194.
- Hudson, NW. 1965. The influence of rainfall on the mechanics of soil erosion with particular reference to Southern Rhodesia. Unpublished M.Sc. Thesis, University of Cape Town, Cape Town, RSA.
- Huffman, RL, Fangmeier, DD, Elliot, WJ, Workman, SR and Schwab, GO. 2011. *Soil and Water Conservation Engineering*. ASABE, St. Joseph, USA.
- Johnston, K, Ver Hoef, JM, Krivoruchko, K and Lucas, N. 2001. *Using ArcGIS Geostatistical Analyst*. ESRI Press, Redlands, California, USA.
- Kinnell, PIA. 2010. Event soil loss, runoff and the Universal Soil Loss Equation family of models: A review. *Journal of Hydrology* 385(2010):384-397.
- Kunz, RP. 2004. *Daily Rainfall Data Extraction Utility User Manual: Version 1.4*. Institute for Commercial Forestry Research, Pietermaritzburg, RSA.
- Le Roux, JJ, Morgenthal, TL, Malherbe, J, Pretorius, DJ and Sumner, PD. 2008. Water erosion prediction at a national scale for South Africa. *Water SA* 34(3):305-314.
- Le Roux, JJ, Morgenthal, TL, Malherbe, J, Smith, HJ, Weepener, HL, Newby, TS, Pretorius, DJ. 2006. *Improving Spatial Soil Erosion Indicators in South Africa*. Report No. GW/A/2006/51. Agricultural Research Council – Institute for Soil, Climate and Water, Pretoria, RSA.
- Liu, BY, Nearing, MA, Risse, LM. 1994. Slope gradient effects on soil loss for steep slopes. *Transactions of the ASAE* 37(6):1835-1840.
- Lorentz, S and Schulze, R. 1995. Sediment Yield. In: ed. Schulze, R, *Hydrology and Agrohydrology: A Text to Accompany the ACRU 3.00 Agrohydrological Modelling System*. Report No. TT69/95. Water Research Commission, Pretoria, RSA.
- Lu, GY and Wong, DW. 2008. An adaptive inverse-distance weighting spatial interpolation technique. *Computers and Geosciences* 34(2008):1044-1055.
- Lynch, SD. 2004. *Development of a Raster Database of Annual, Monthly and Daily Rainfall for Southern Africa*. Report No. 1156/1/04. Water Research Commission, Pretoria, RSA.
- MacVicar, CN, De Villiers, JM, Loxton, RF, Verster, E, Lambrechts, JIN, Merryweather, FR, Le Roux, J, Van Rooyen, TH and Harmse, HJvM. 1977. Soil classification – A binomial system for South Africa. Science Bulletin 390. Department of Agricultural Technical Services, Pretoria, South Africa.

- Matthee, JF la G. 1984. A Primer on Soil Conservation. Bulletin No. 399. National Department of Agriculture, Pretoria, RSA.
- Matthee, JF la G. 1989. Beskerming van Bewerkte Land. In: ed. Matthee, JF la G, *National Soil Conservation Manual*, Ch. 8, i-vii. Department of Agriculture and Water Supply, Silverton, RSA.
- McCool, DK, Brown, LC, Foster, GR, Mutchler, CK and Meyer, LD. 1987. Revised slope steepness factor for the Universal Soil Loss Equation. *Transactions of the ASAE* 30(5):1387-1396.
- McCulloch, DJ and Stranack, RA. 1995. Some benefits and costs of implementing soil conservation practices on farms on the north coast of KwaZulu-Natal. *Proceedings of The South African Sugar Technologists' Association* 69:94-97.
- McFarlane, K and Maher, GW. 1993. Assessment of sugarcane farms in terms of the Conservation of Agricultural Resources Act 1983. *Proceedings of The South African Sugar Technologists' Association* 67:110-113.
- McGregor, KC, Bingner, RL, Bowie, AJ and Foster, GR. 1995. Erosivity index values for northern Mississippi. *Transactions of the ASAE* 38(4):1039-1047.
- McGregor, KC and Mutchler, CK. 1976. Status of the R factor in northern Mississippi. In: *Soil Erosion: Prediction and Control – Proceedings of the 1976 National Conference on Soil Erosion*, 135-142. Soil Conservation Society of America, Ankeny, Iowa, USA.
- Merritt, WS, Letcher, RA and Jakeman, AJ. 2003. A review of erosion and sediment transport models. *Environmental Modelling and Software* 18(2003):761-799.
- Meyer, JH, van Antwerpen, R and Meyer, E. 1996. A review of soil degradation and management research under intensive sugarcane cropping. *Proceedings of The South African Sugar Technologists' Association* 70:22-28.
- Morgan, RPC. 2005. *Soil Erosion and Conservation*. Blackwell Publishing, Oxford, UK.
- Nearing, MA, Foster GR, Lane LJ and Finkler, SC. 1989. A process-based soil erosion model for USDA – Water Erosion Prediction Project technology. *Transactions of the ASAE* 32(5):1587-1593.
- Øverland, H. 1990. *Einfluss der Landnutzung auf Hochwasserabfluss und Schwebstofftransport*. Report No. 35/1990. Institut für Wasserwesen, Universität der Bundeswehr München, Munich, Germany.
- Pimentel, D, Harvey, C, Resosudarmo, P, Sinclair, K, Kurz, D, McNair, M, Crist, S, Shpritz, L, Fitton, L, Saffouri, R and Blair, R. 1995. Environmental and economic costs of soil erosion and conservation benefits. *Science* 267(5201):1117-1123.

- Platford, GG. 1987. A new approach to designing the widths of panels in sugarcane fields. *Proceedings of The South African Sugar Technologists' Association* 61:150-155.
- Renard, KG, Foster, GR, Weesies, GA, McCool, DK and Yoder, DC. 1997. *Predicting soil erosion by water: A guide to conservation planning with the Revised Universal Soil Loss Equation (RUSLE)*. Agriculture Handbook No. 703, USDA, Washington D.C., USA.
- Renard, KG, Foster, GR, Weesies, GA and Porter, JP. 1991. RUSLE: Revised Universal Soil Loss Equation. *Journal of Soil and Water Conservation* 46(1):30-33.
- Richardson, CW, Foster, GR and Wright, DA. 1983. Estimation of erosion index from daily rainfall amount. *Transactions of the ASAE* 26:153-156, 160.
- Russell, WB. 1998a. The cost of farmland degradation. In: ed. Russell, WB, *Conservation of Farmland in KwaZulu-Natal*, Ch. 1.5, 30-34. National Department of Agriculture, Pietermaritzburg, RSA.
- Russell, WB. 1998b. Runoff control planning on cultivated land. In: ed. Russell, WB, *Conservation of Farmland in KwaZulu-Natal*, Ch. 2.2, 41-45. National Department of Agriculture, Pietermaritzburg, RSA.
- Russell, WB. 1998c. A farmer's guide to surveying contour banks. In: ed. Russell, WB, *Conservation of Farmland in KwaZulu-Natal*, Ch. 2.3, 46-53. National Department of Agriculture, Pietermaritzburg, RSA.
- Schulze, RE. 1995. *Hydrology and Agrohydrology: A Text to Accompany the ACRU 3.00 Agrohydrological Modelling System*. Report No. TT69/95. Water Research Commission, Pretoria, RSA.
- Schulze, RE and Arnold, H. 1980. *Digitizing and Routine Analyses of Hydrological Data*. Water Research Commission, Pretoria, RSA.
- Schulze, RE and Horan, MJC. 2007. Soils: Hydrological attributes. In: ed. Schulze, RE, *South African Atlas of Climatology and Agrohydrology*. Report No 1489/1/06. Water Research Commission, Pretoria, RSA.
- Schulze, RE and Horan, MJC. 2011. Methods 1: Delineation of South Africa, Lesotho and Swaziland into quinary catchments. In: eds. Schulze, RE, Hewitson, BC, Barichievy, KR, Tadross, MA, Kunz, RP, Horan, MJC and Lumsden, TG, *Methodological Approaches to Assessing Eco-Hydrological Responses to Climate Change in South Africa*. Report No. 1562/1/10, Ch. 6, 55-62. Water Research Commission, Pretoria, RSA.
- Schulze, RE, Horan, MJC, Kunz, RP, Lumsden, TG and Knoesen, DM. 2011. Methods 2: Development of the southern African quinary catchments database. In: eds. Schulze,

- RE, Hewitson, BC, Barichiev, KR, Tadross, MA, Kunz, RP, Horan, MJC and Lumsden, TG, *Methodological Approaches to Assessing Eco-Hydrological Responses to Climate Change in South Africa*. Report No. 1562/1/10, Ch. 7, 63-74. Water Research Commission, Pretoria, RSA.
- Schulze, RE, Warburton, M, Lumsden, TG and Horan, MJC. 2005. The southern African quaternary catchments database: Refinements to, and links with, the ACRU system as a framework for modelling impacts of climate change on water resources. In: ed. Schulze, RE, *Climate Change and Water Resources in Southern Africa: Studies on Scenarios, Impacts, Vulnerabilities and Adaptation*. Report No. 1430/1/05, Ch. 8, 111-139. Water Research Commission, Pretoria, RSA.
- Scotney, DM and McPhee, PJ. 1990. The dilemma of our soil resources. *Proceedings of the National Veld Trust Conference: The Conservation Status of South Africa's Agricultural Resources*. National Veld Trust, Pretoria, RSA.
- Smith, HJ. 1999. Application of empirical soil loss models in southern Africa: a review. *South African Journal of Plant and Soil* 16(3):158-163.
- Smithen, AA. 1981. Characteristics of rainfall erosivity in South Africa. Unpublished M.Sc. Eng. Thesis, Department of Agricultural Engineering, University of Natal, Pietermaritzburg, RSA.
- Smithen, AA. 1989. Beskerming van Bewerkte Land. In: ed. Matthee, JF la G, *National Soil Conservation Manual*, Ch. 8.3, 1-44. Department of Agriculture and Water Supply, Silverton, RSA.
- Smithen, AA and Schulze, RE. 1979. The Universal Soil Loss Equation and the Soil Loss Estimation Model for Southern Africa: Concepts, variables and areal application. In: ed. Schulze, RE, *Field Studies, Data Processing, Techniques and Models for Applied Hydrological Research*. ACRU Report No. 7(1). Department of Agricultural Engineering, University of Natal, Pietermaritzburg, RSA.
- Smithen, AA and Schulze, RE. 1982. The spatial distribution in southern Africa of rainfall erosivity for use in the Universal Soil Loss Equation. *Water SA* 8(2):74-78.
- Smithers, JC and Schulze, RE. 2000. *Development and Evaluation of Techniques for Estimating Short Duration Design Rainfall in South Africa*. Report No. 681/1/00. Water Research Commission, Pretoria, RSA.
- Smithers, JC and Schulze, RE. 2003. *Design Rainfall and Flood Estimation in South Africa*. Report No. 1060/1/03. Water Research Commission, Pretoria, RSA.

- Soil Classification Working Group. 1991. Soil classification – A taxonomic system for South Africa. Memoirs on the Agricultural Natural Resources of South Africa No. 15. Department of Agricultural Development, Pretoria, RSA.
- Sorooshian, S. 1991. Parameter estimation, model identification, and model validation: Conceptual-type models. In: eds. Bowles, DS and O’Connell, PE, *Recent Advances in the Modeling of Hydrologic Systems*, Ch. 20, 443-467. Kluwer Academic Publishers.
- Tomczak, M. 1998. Spatial interpolation and its uncertainty using automated anisotropic Inverse Distance Weighting (IDW)-Cross-validation/Jackknife approach. *Journal of Geographic Information and Decision Analysis* 2(2):18-30.
- USDA-ARS. 2013. Science Documentation, Revised Universal Soil Loss Equation, Version 2. [Internet]. USDA-ARS, Washington D.C., USA. Available from: http://www.ars.usda.gov/sp2UserFiles/Place/60600505/RUSLE/RUSLE2_Science_Doc.pdf. [Accessed: 7 July 2014].
- USDA-NRCS. 1986. *Urban Hydrology for Small Watersheds*. Technical Release No. 55. USDA, Washington D.C., USA.
- USDA-NRCS. 2007a. Grassed waterways. In: *Engineering Field Handbook*. Part 650. USDA, Washington D.C., USA.
- USDA-NRCS. 2007b. Hydrologic soil groups. In: *National Engineering Handbook*. Part 630 Hydrology, USDA, Washington D.C., USA.
- USDA-NRCS. 2011. Terraces. In: *Engineering Field Handbook*. Part 650. USDA, Washington D.C., USA.
- USDA-NRCS. 2012. Code 412. Conservation Practice Standard: Grassed Waterway (Ac.). NRCS, Minnesota, USA.
- van Dijk, AIJM, Bruijnzeel, LA and Rosewell, CJ. 2002. Rainfall intensity-kinetic energy relationships: a critical literature appraisal. *Journal of Hydrology* 261(2002):1-23.
- van Rooy, MP. 1972. District rainfall for South Africa and the annual march of rainfall over southern Africa. In: *Climate of South Africa*. South African Weather Bureau WB 35 – Part 10, Department of Transport, Pretoria, RSA.
- Williams, JR. 1975. Sediment-yield prediction with universal equation using runoff energy factor. In: *Present and Prospective Technology for Predicting Sediment Yield and Sources*. ARS-S-40, USDA, Washington D.C., USA.
- Wischmeier, WH, Johnson, CB and Cross, BV. 1971. A soil erodibility nomograph for farmland and construction sites. *Journal of Soil and Water Conservation* 26:189-193.

- Wischmeier, WH and Smith, DD. 1958. Rainfall energy and its relationship to soil loss. *Transactions of the American Geophysical Union* 39(1):285-291.
- Wischmeier, WH and Smith, DD. 1965. *Predicting rainfall-erosion losses from cropland east of the Rocky Mountains: Guide for selection of practices for soil and water conservation*. Agriculture Handbook No. 282, USDA, Washington D.C., USA.
- Wischmeier, WH and Smith, DD. 1978. *Predicting rainfall erosion losses: A guide to conservation planning*. Agriculture Handbook No. 537, USDA, Washington D.C., USA.
- Yu, B and Rosewell, C. 1996. An assessment of a daily rainfall erosivity model for New South Wales. *Australian Journal of Soil Research* 34:139-152.

10. APPENDIX A: EROSIIVITY DENSITY MAPS

Appendix A contains Figures 10.1 to 10.13, which illustrate the erosivity density across South Africa for each month of the year, as well as the average annual erosivity density.

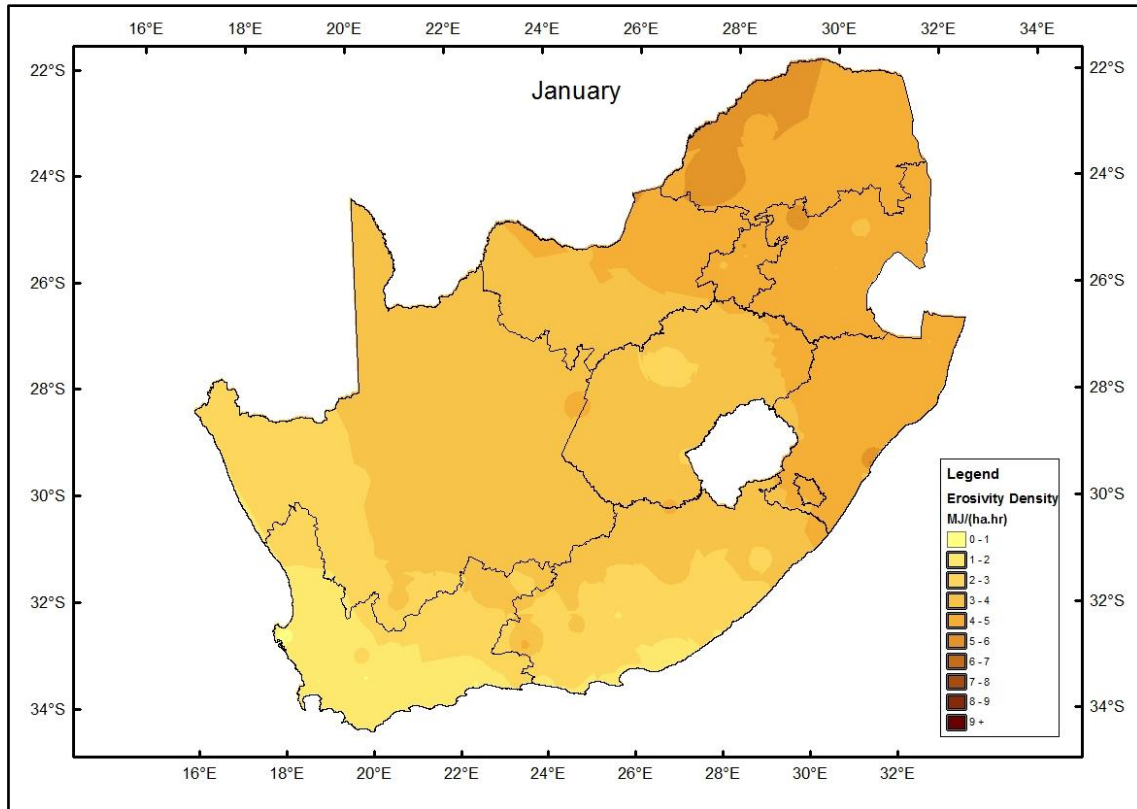


Figure 10.1 Erosivity density map of South Africa for January

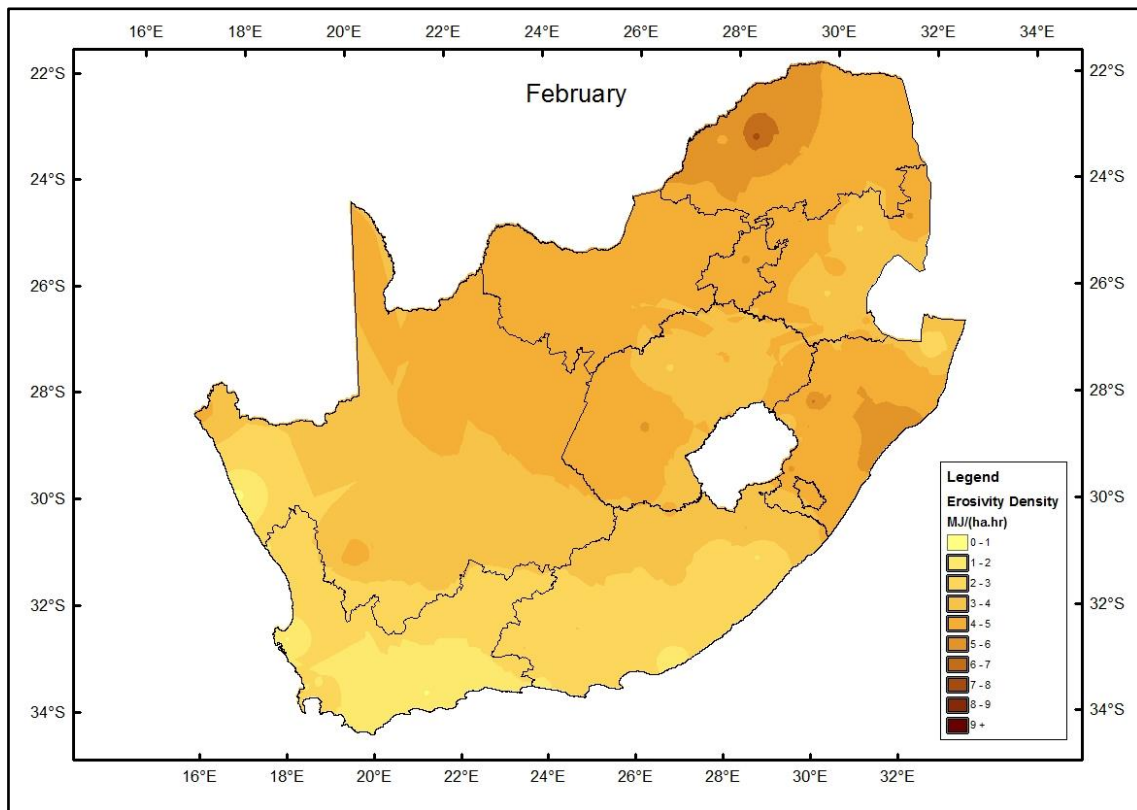


Figure 10.2 Erosivity density map of South Africa for February

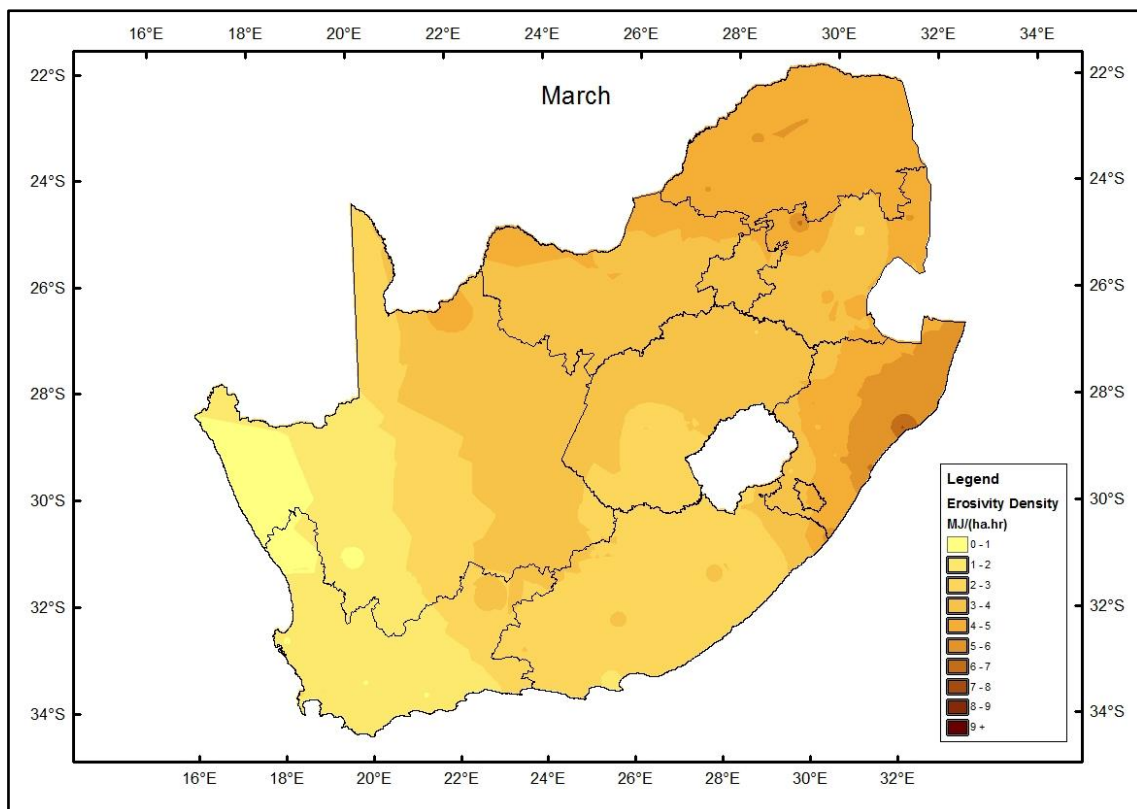


Figure 10.3 Erosivity density map of South Africa for March

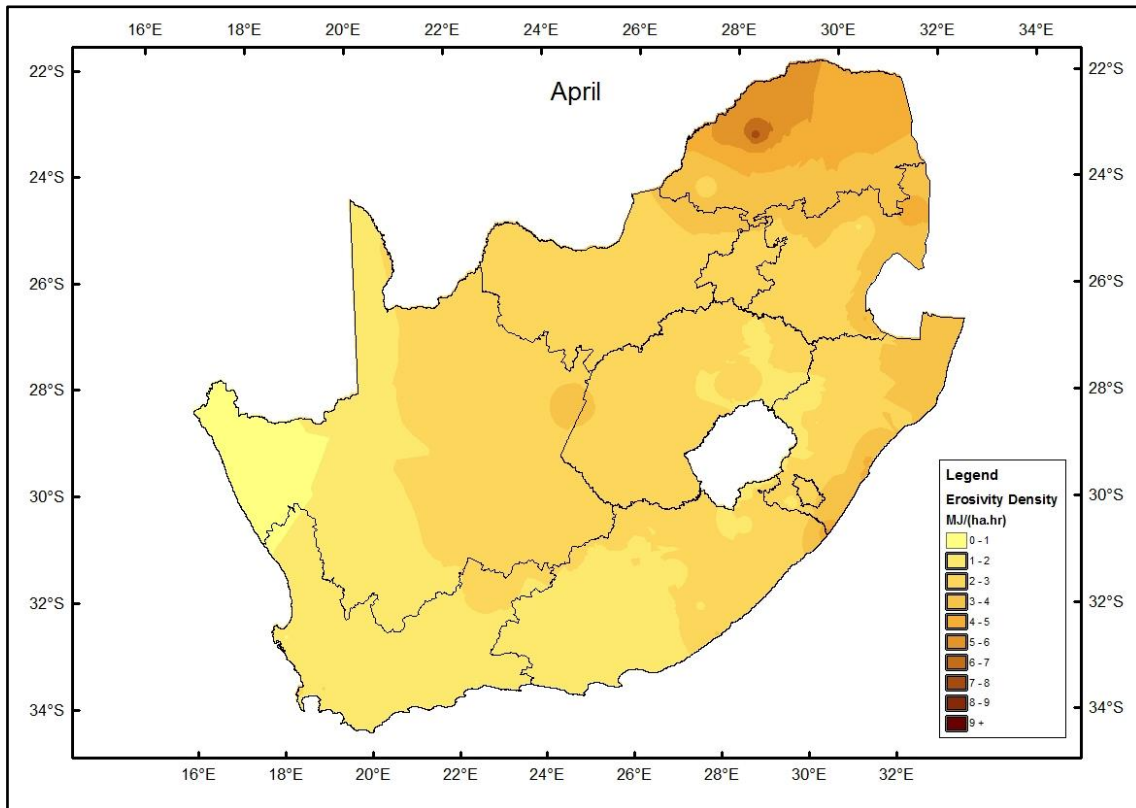


Figure 10.4 Erosivity density map of South Africa for April

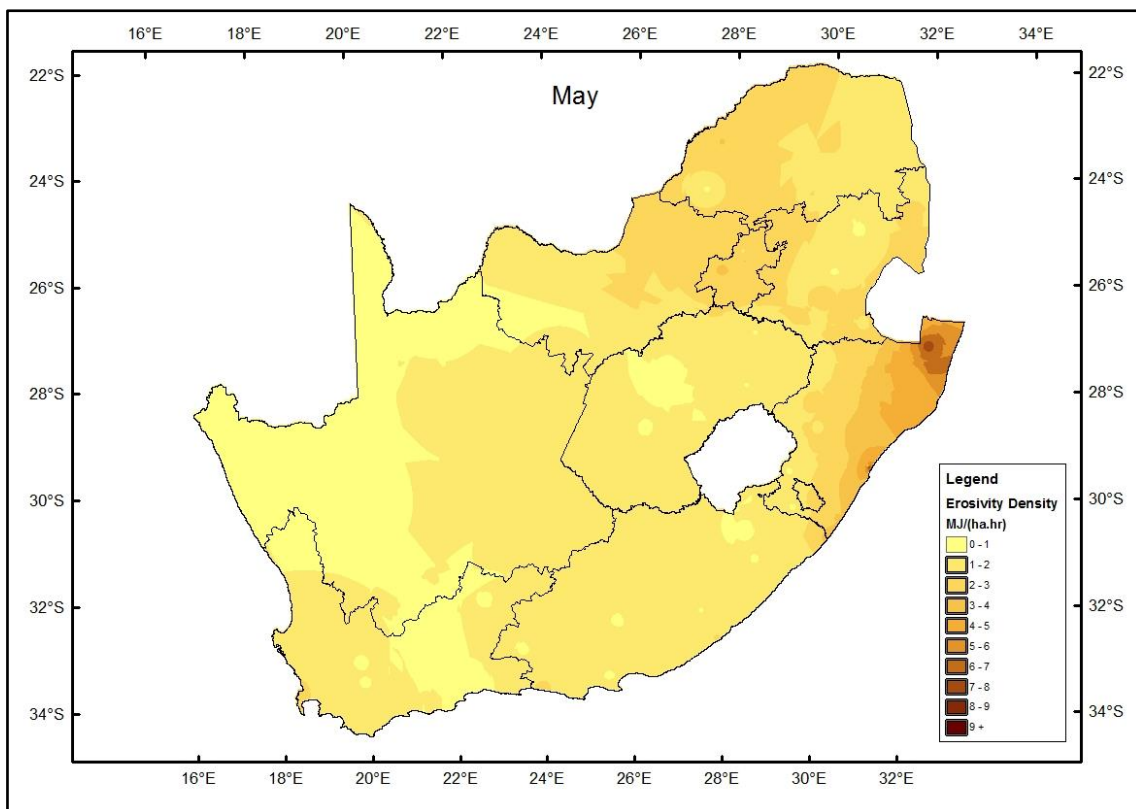


Figure 10.5 Erosivity density map of South Africa for May

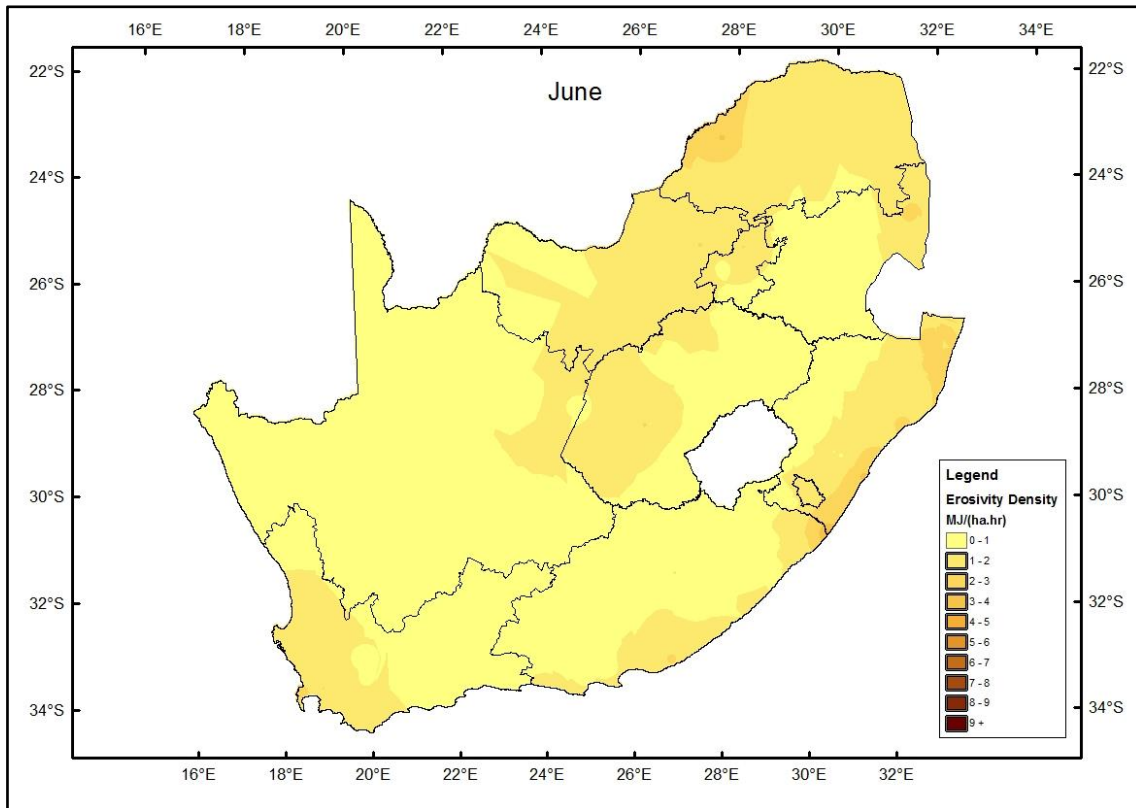


Figure 10.6 Erosivity density map of South Africa for June

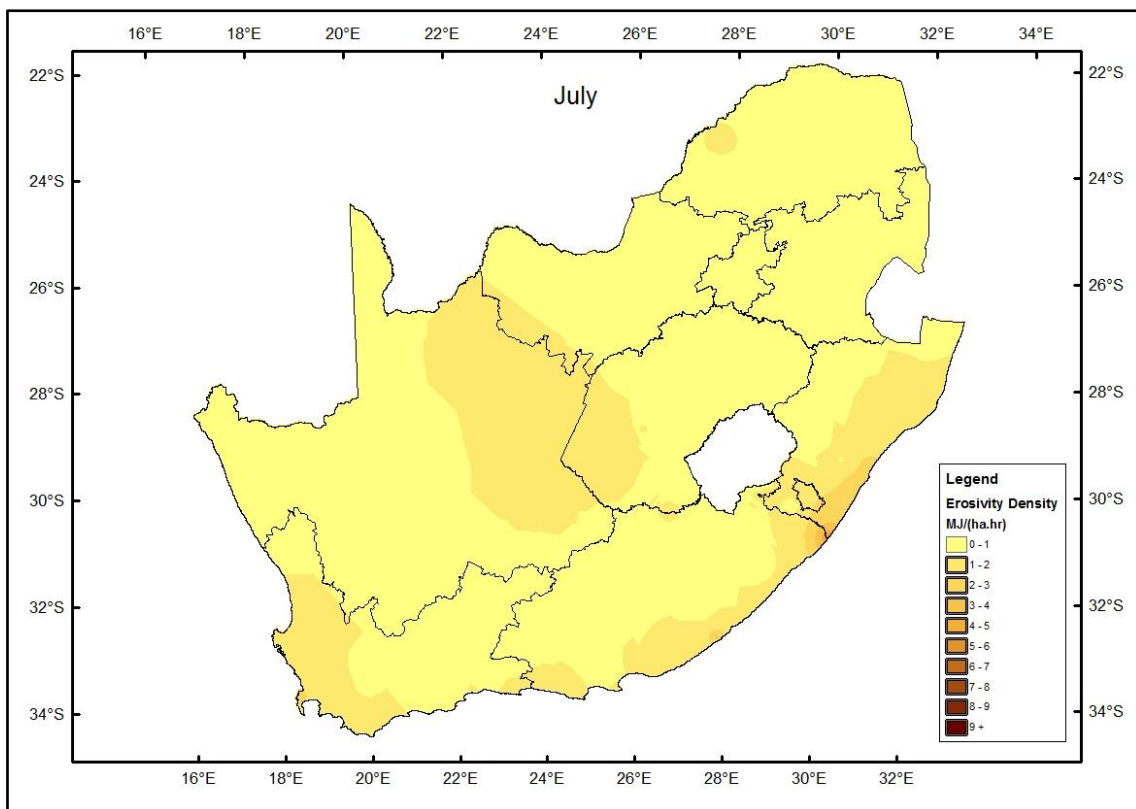


Figure 10.7 Erosivity density map of South Africa for July

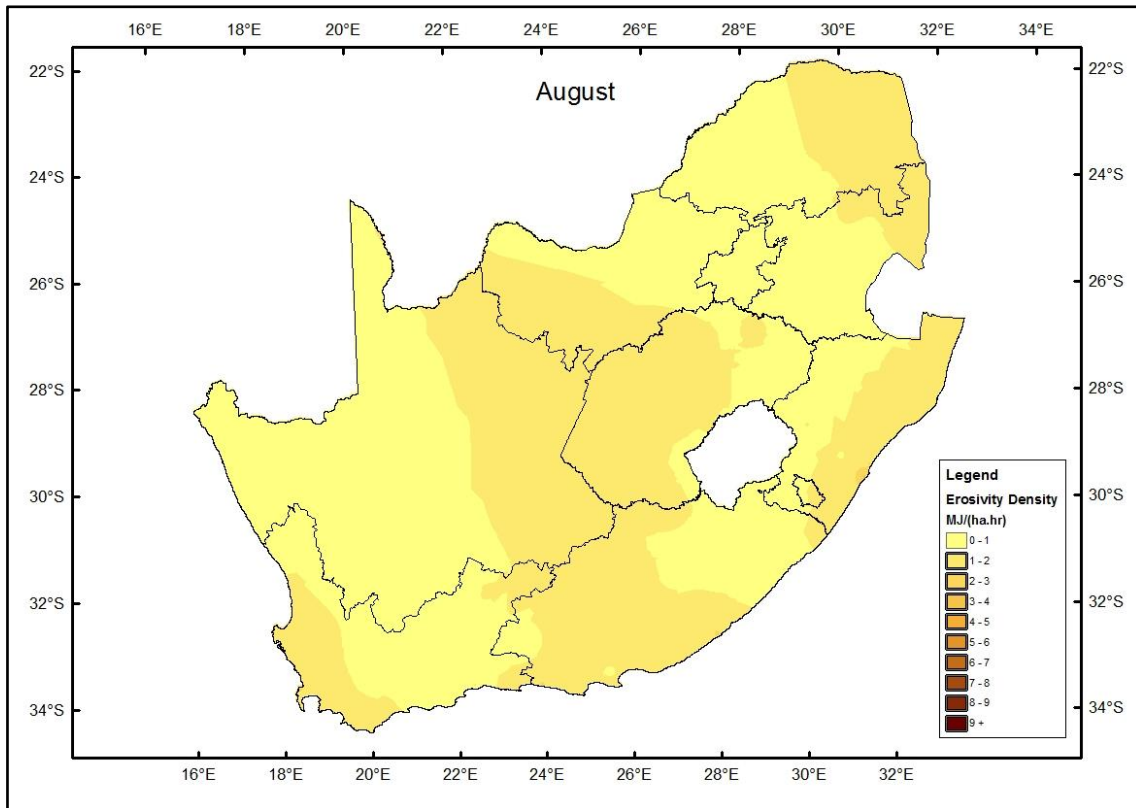


Figure 10.8 Erosivity density map of South Africa for August

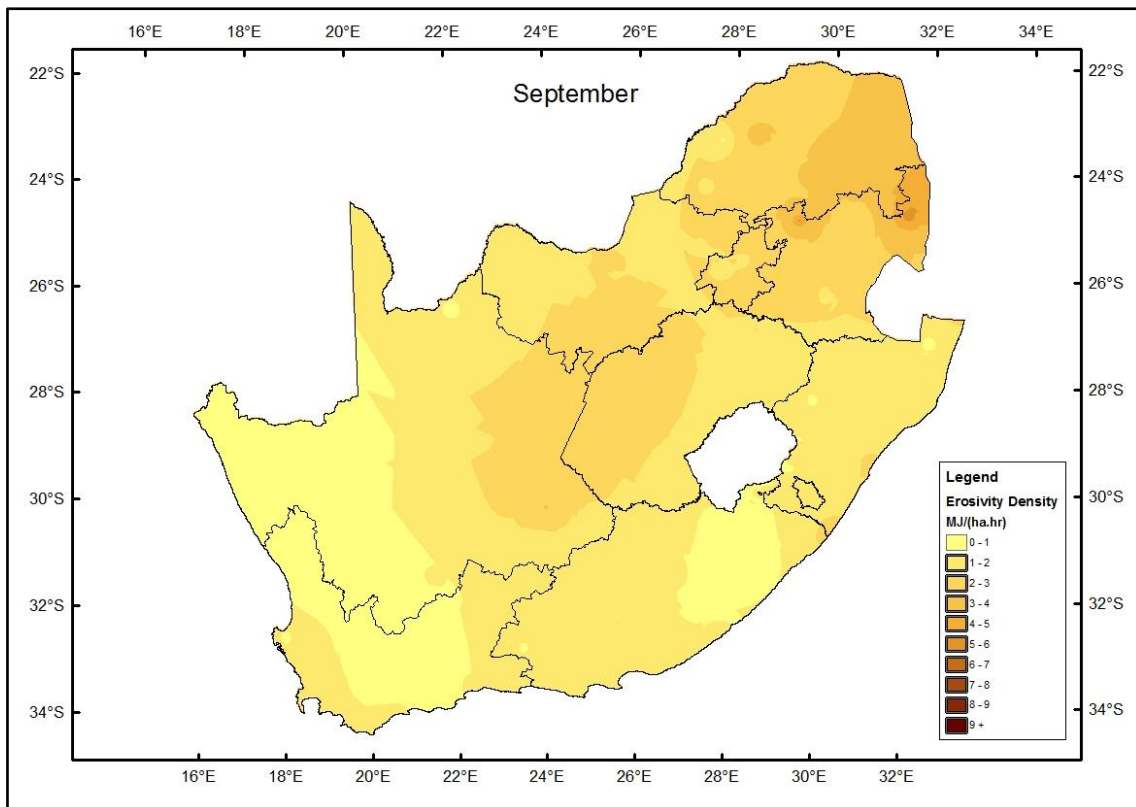


Figure 10.9 Erosivity density map of South Africa for September

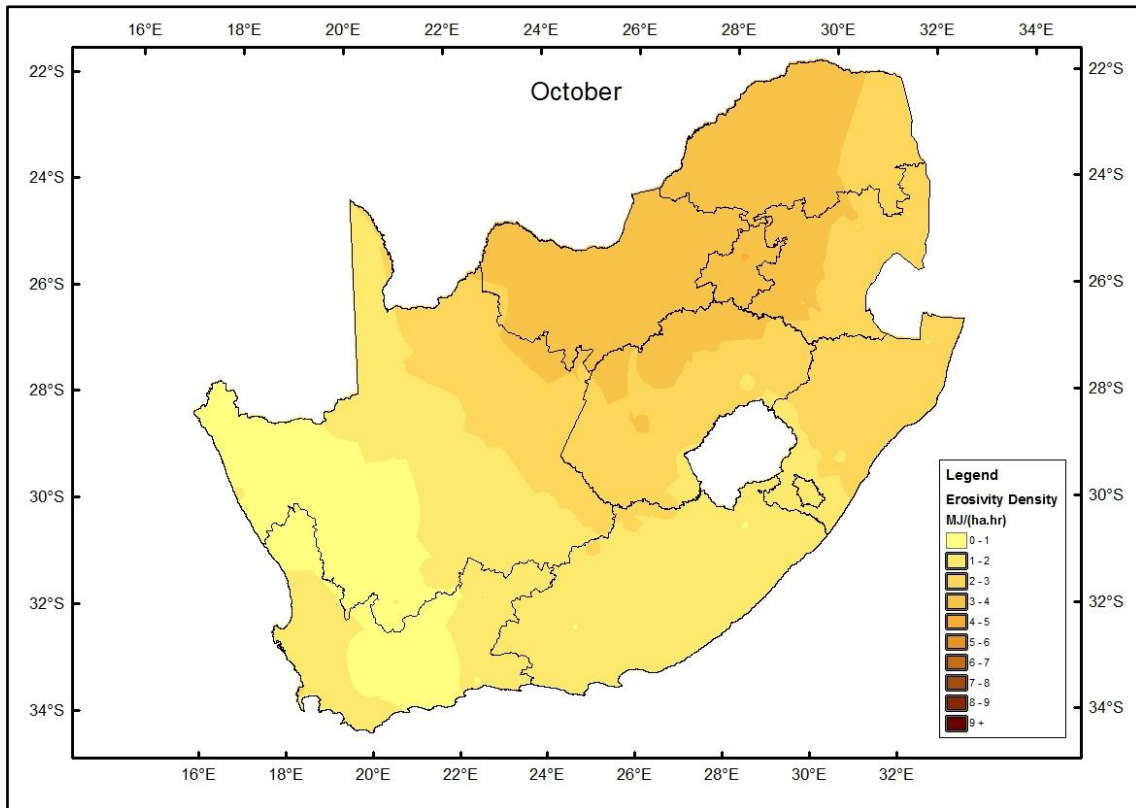


Figure 10.10 Erosivity density map of South Africa for October

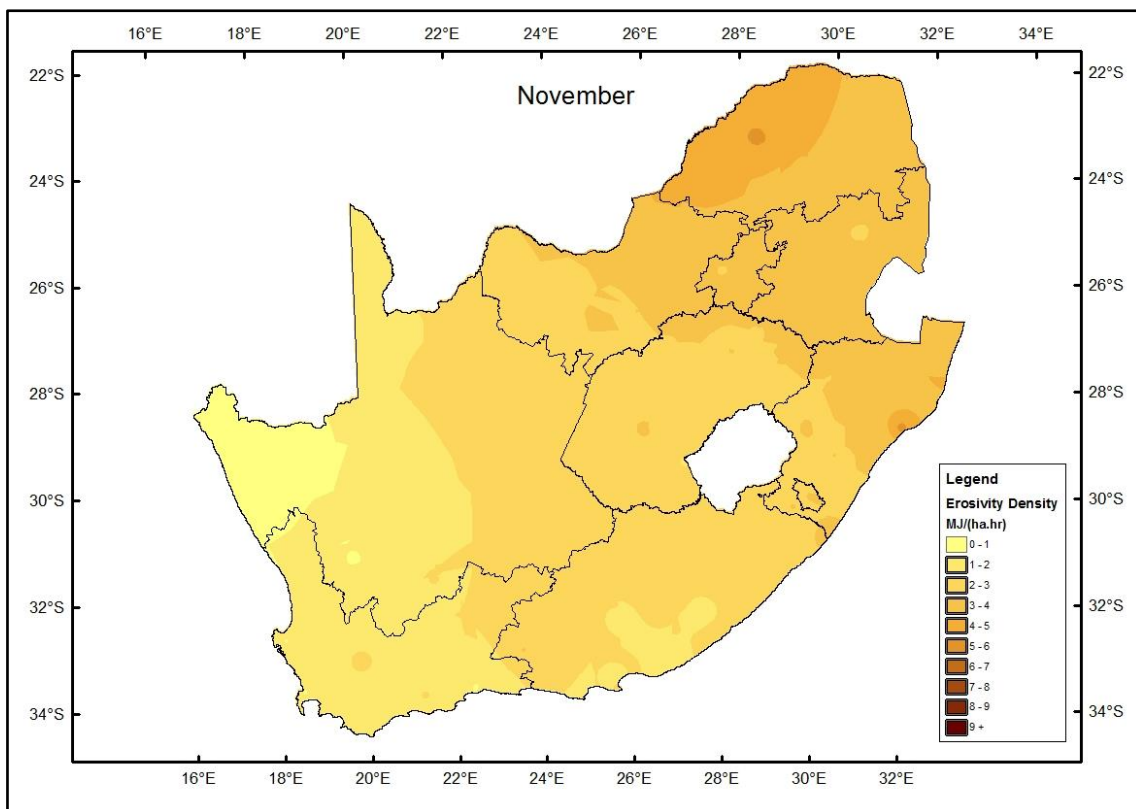


Figure 10.11 Erosivity density map of South Africa for November

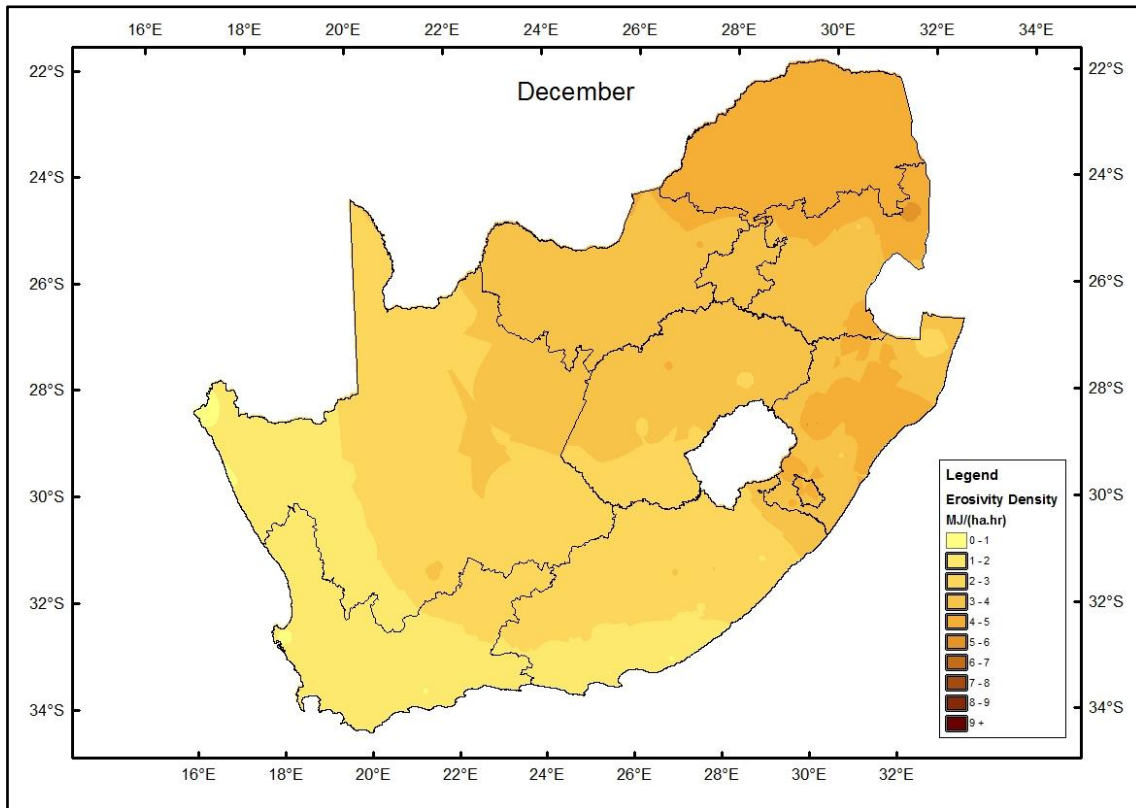


Figure 10.12 Erosivity density map of South Africa for December

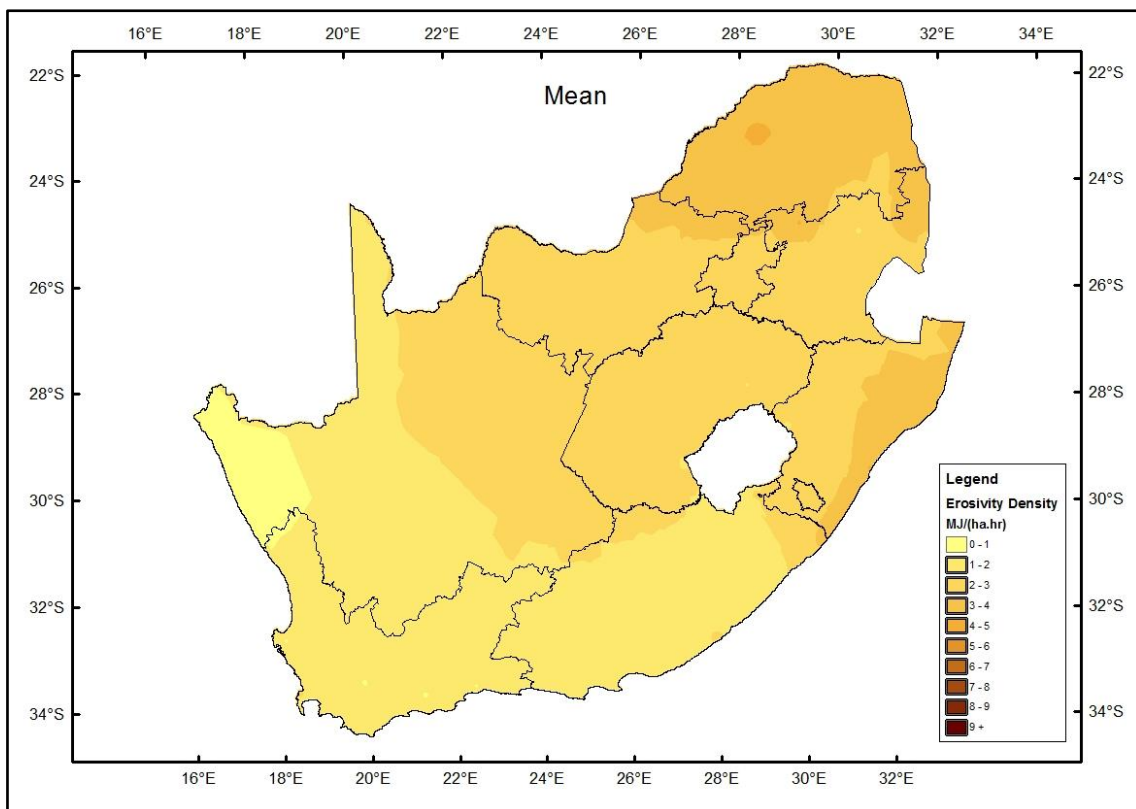


Figure 10.13 Mean annual erosivity density map of South Africa

11. APPENDIX B: RAINFALL EROSIIVITY MAPS OBTAINED USING THE EROSIIVITY DENSITY METHOD

Appendix B contains Figures 11.1 to 11.13, which illustrate the rainfall erosivity across South Africa for each month, as well as the annual sum of rainfall erosivity, calculated using the erosivity density method.

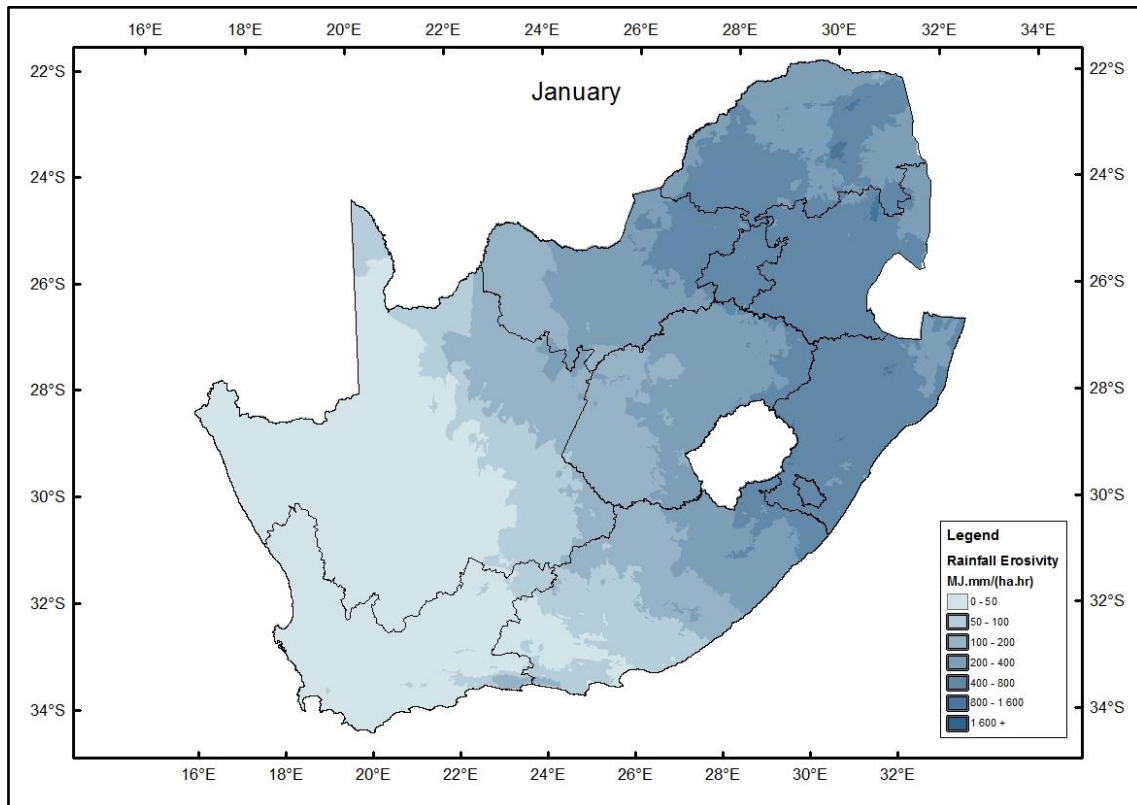


Figure 11.1 Rainfall erosivity map of South Africa for January, calculated using the erosivity density method

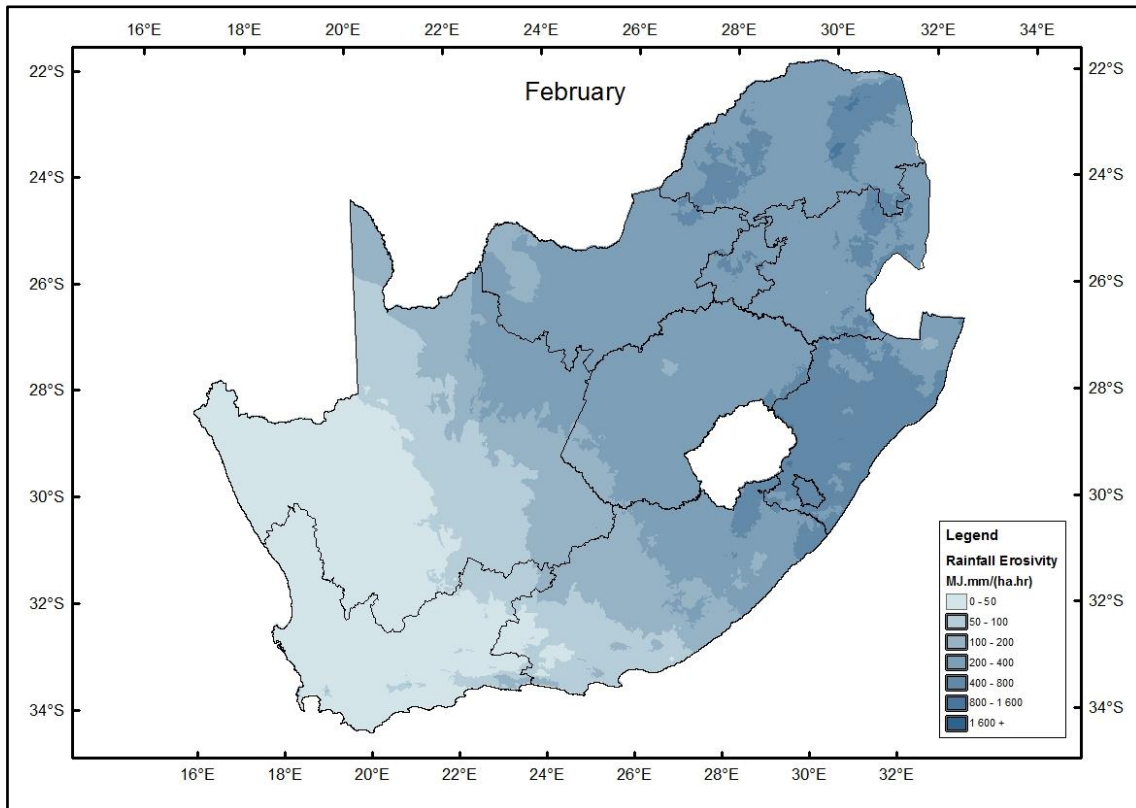


Figure 11.2 Rainfall erosivity map of South Africa for February, calculated using the erosivity density method

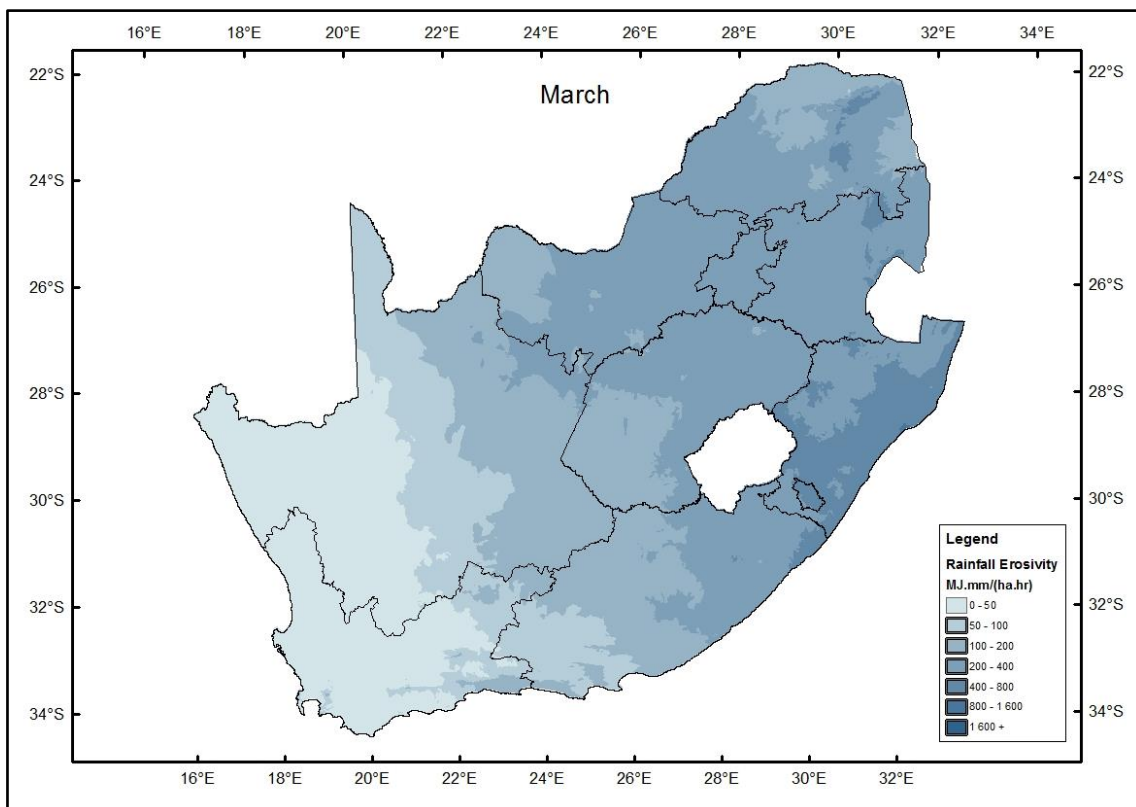


Figure 11.3 Rainfall erosivity map of South Africa for March, calculated using the erosivity density method

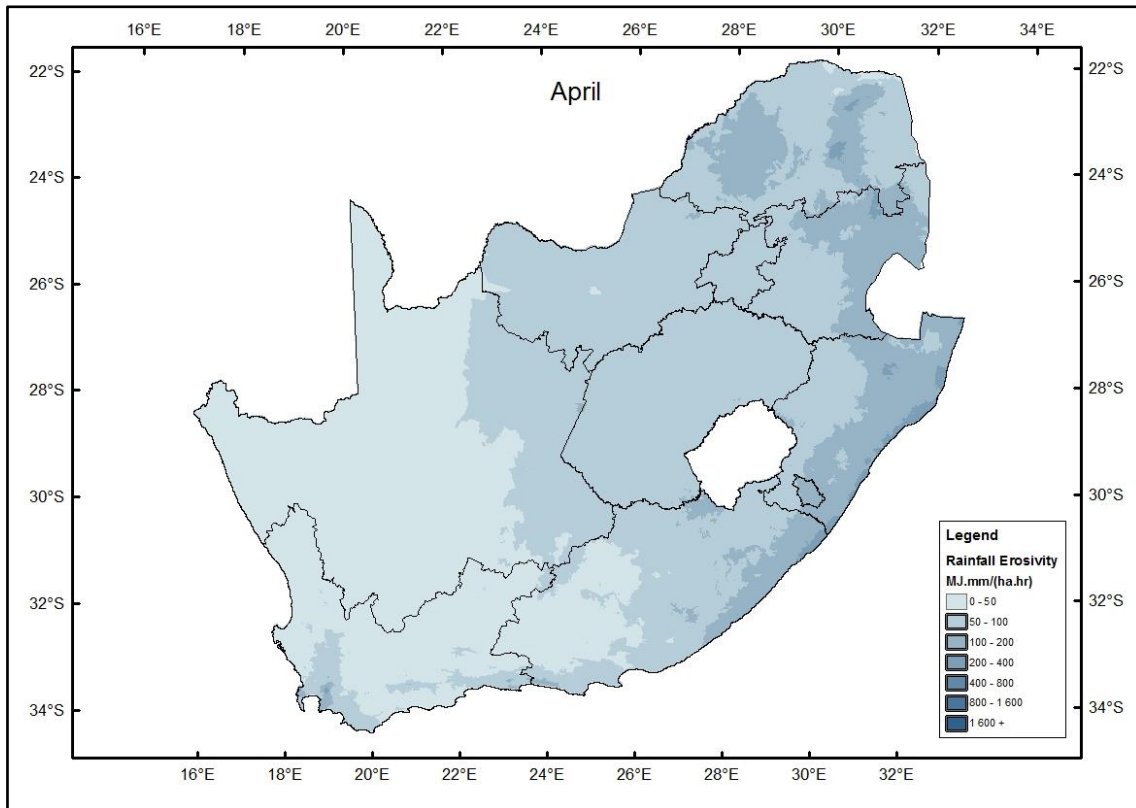


Figure 11.4 Rainfall erosivity map of South Africa for April, calculated using the erosivity density method

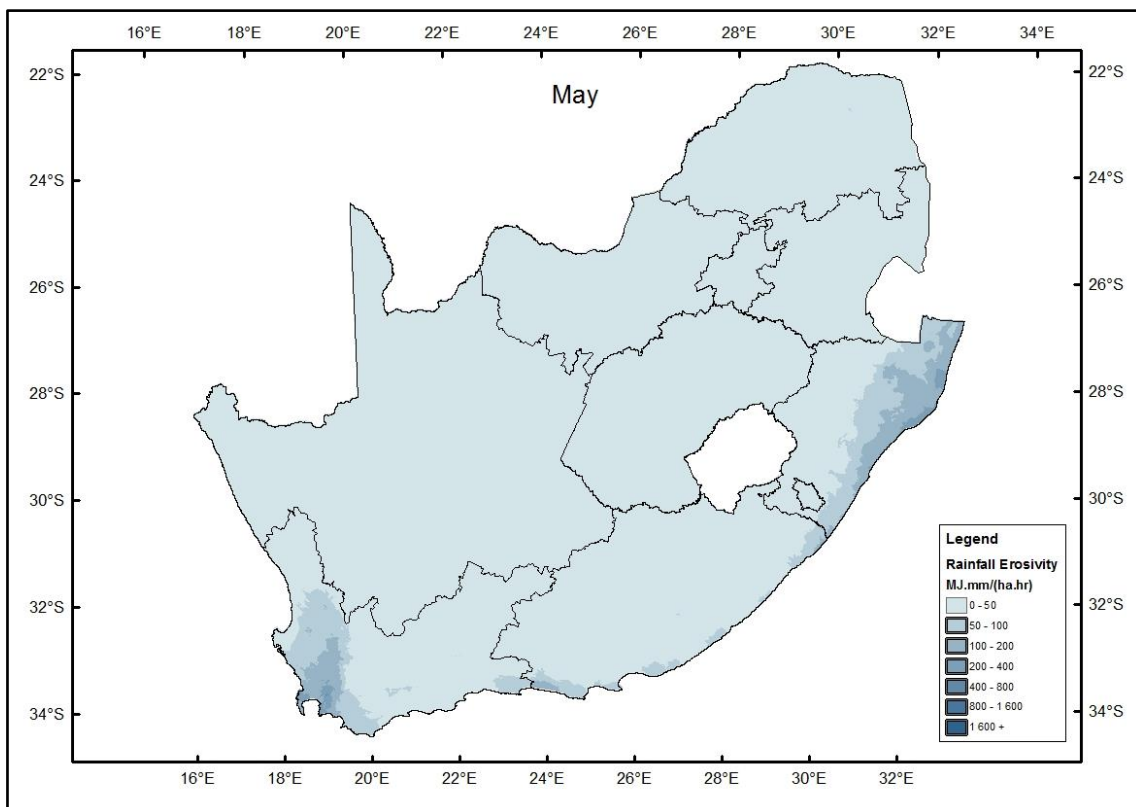


Figure 11.5 Rainfall erosivity map of South Africa for May, calculated using the erosivity density method

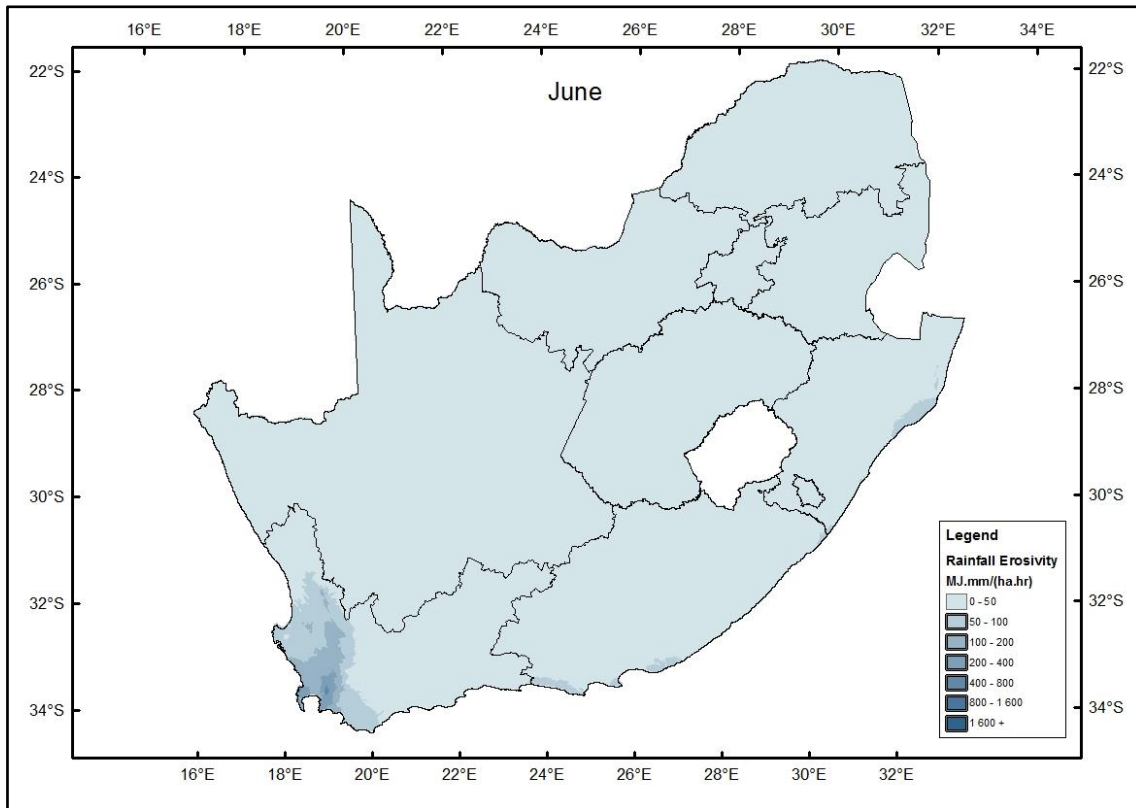


Figure 11.6 Rainfall erosivity map of South Africa for June, calculated using the erosivity density method

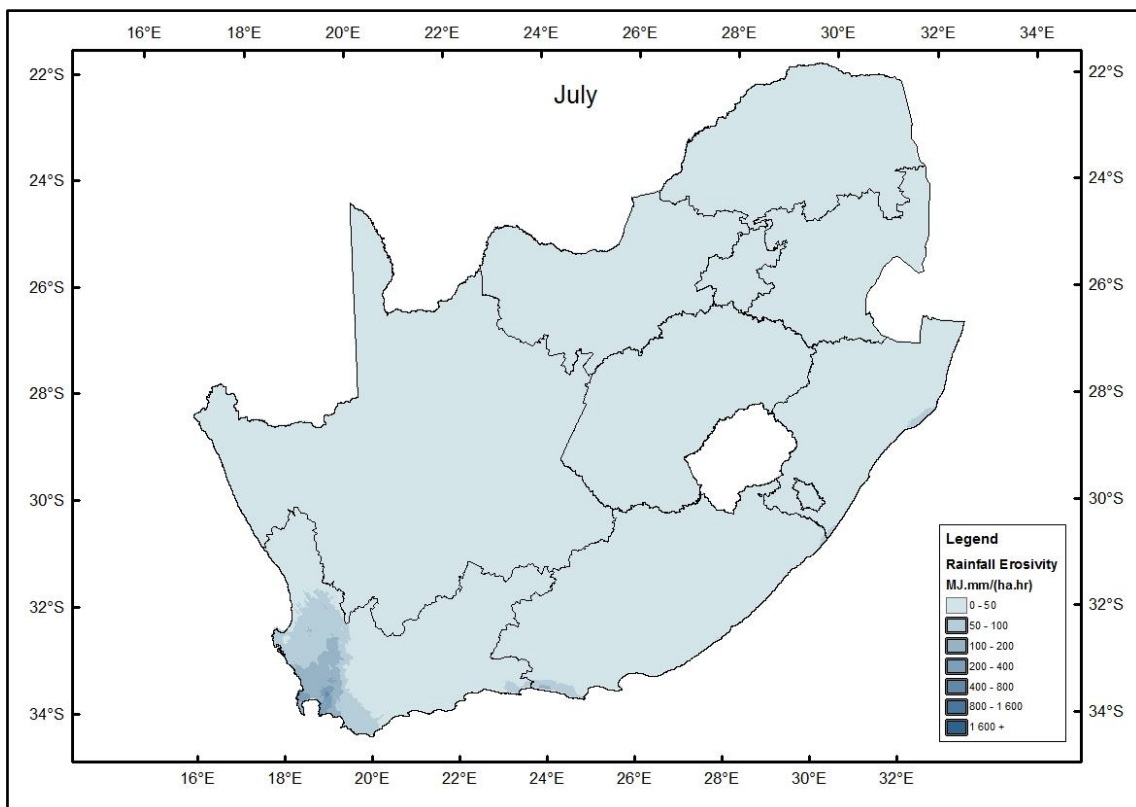


Figure 11.7 Rainfall erosivity map of South Africa for July, calculated using the erosivity density method

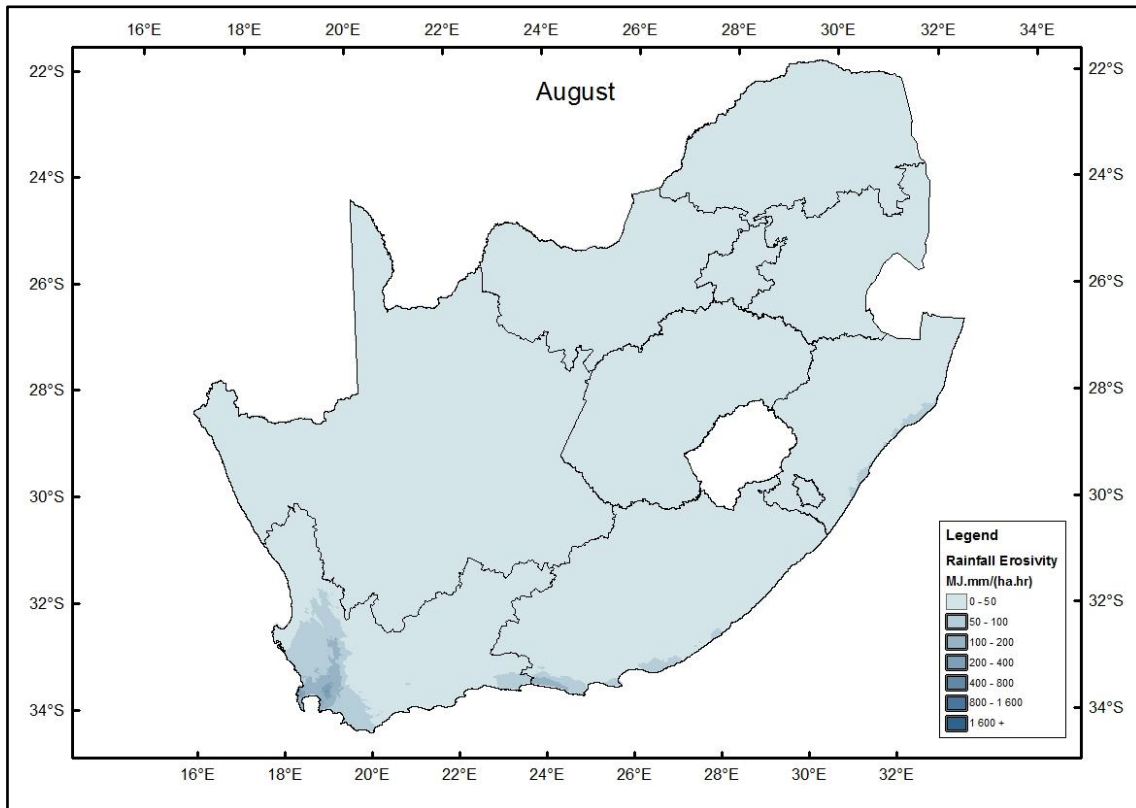


Figure 11.8 Rainfall erosivity map of South Africa for August, calculated using the erosivity density method

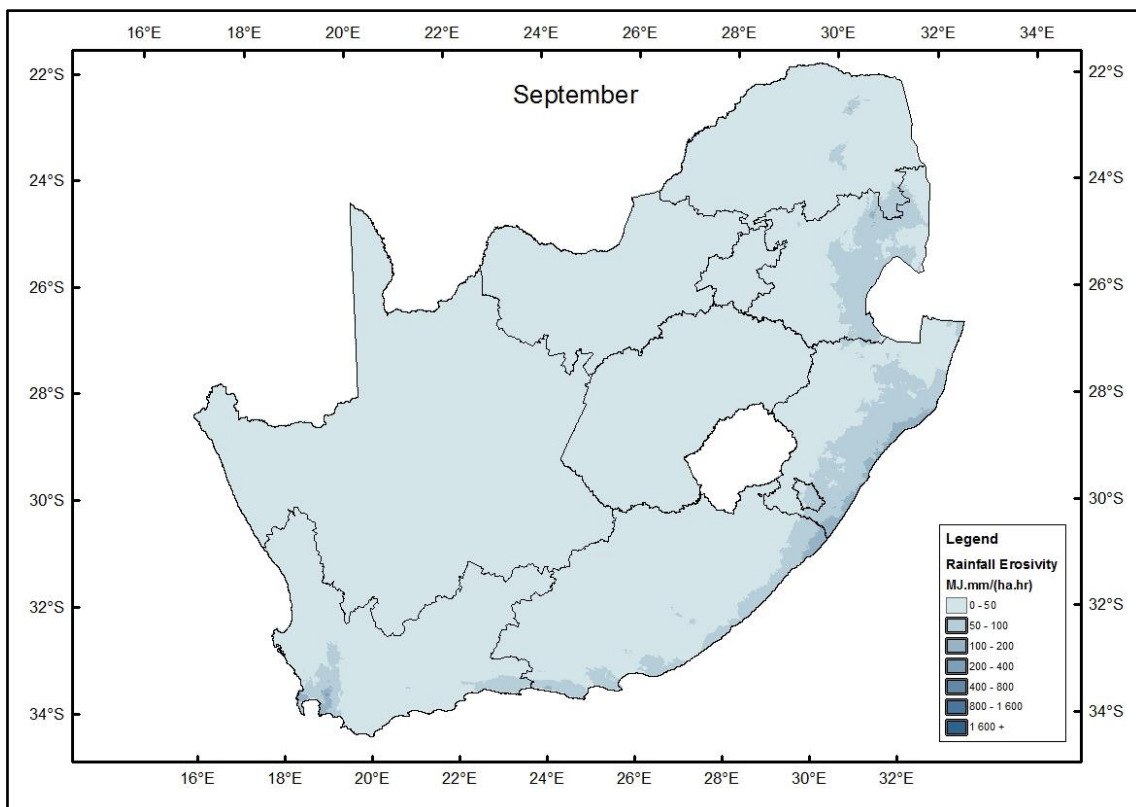


Figure 11.9 Rainfall erosivity map of South Africa for September, calculated using the erosivity density method

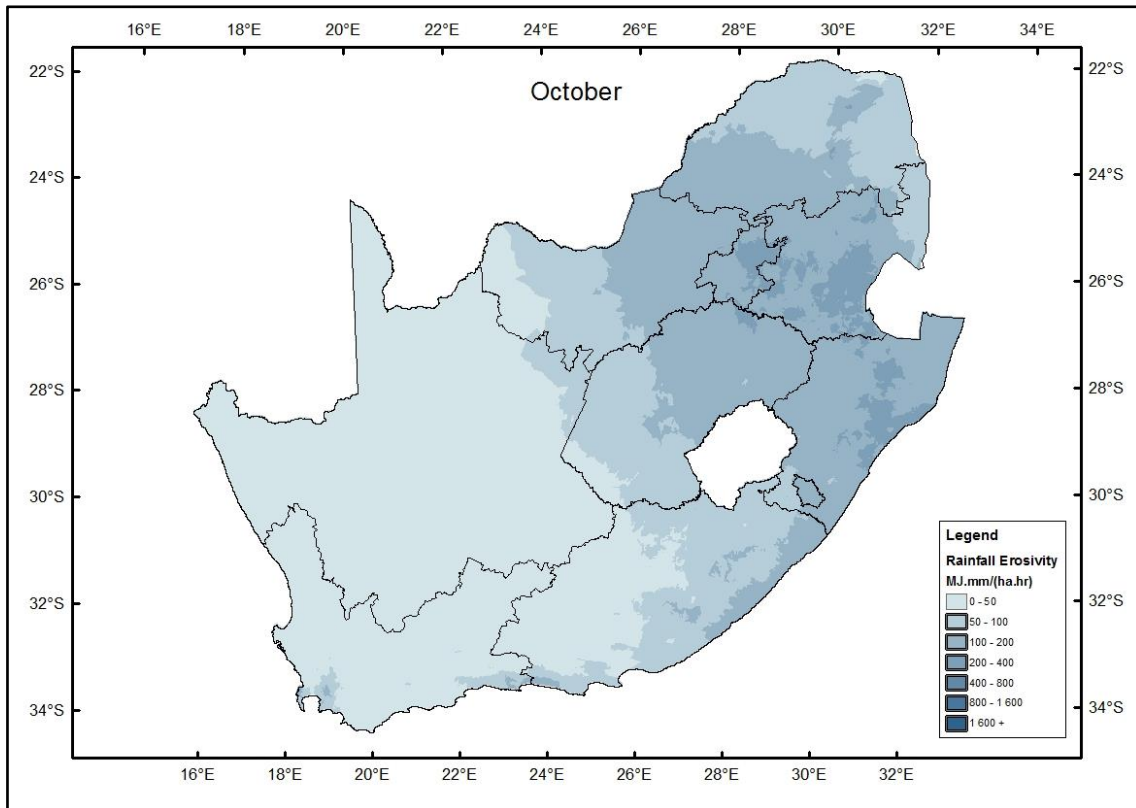


Figure 11.10 Rainfall erosivity map of South Africa for October, calculated using the erosivity density method

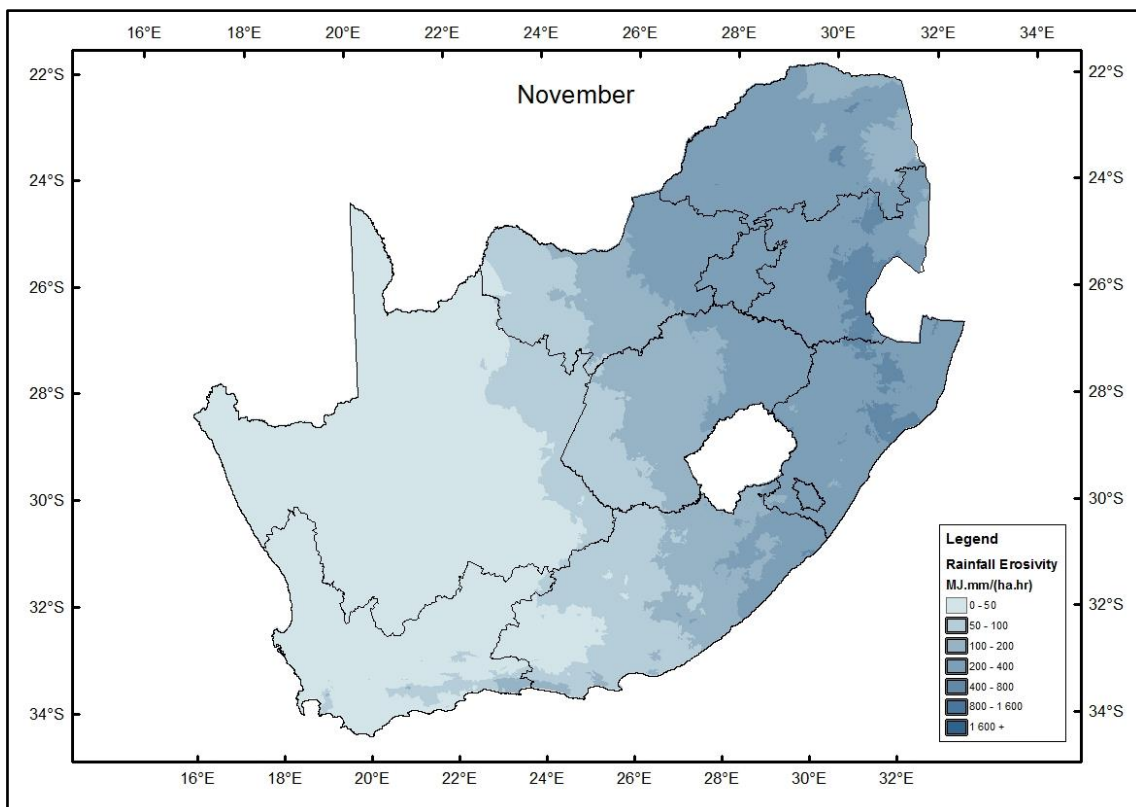


Figure 11.11 Rainfall erosivity map of South Africa for November, calculated using the erosivity density method

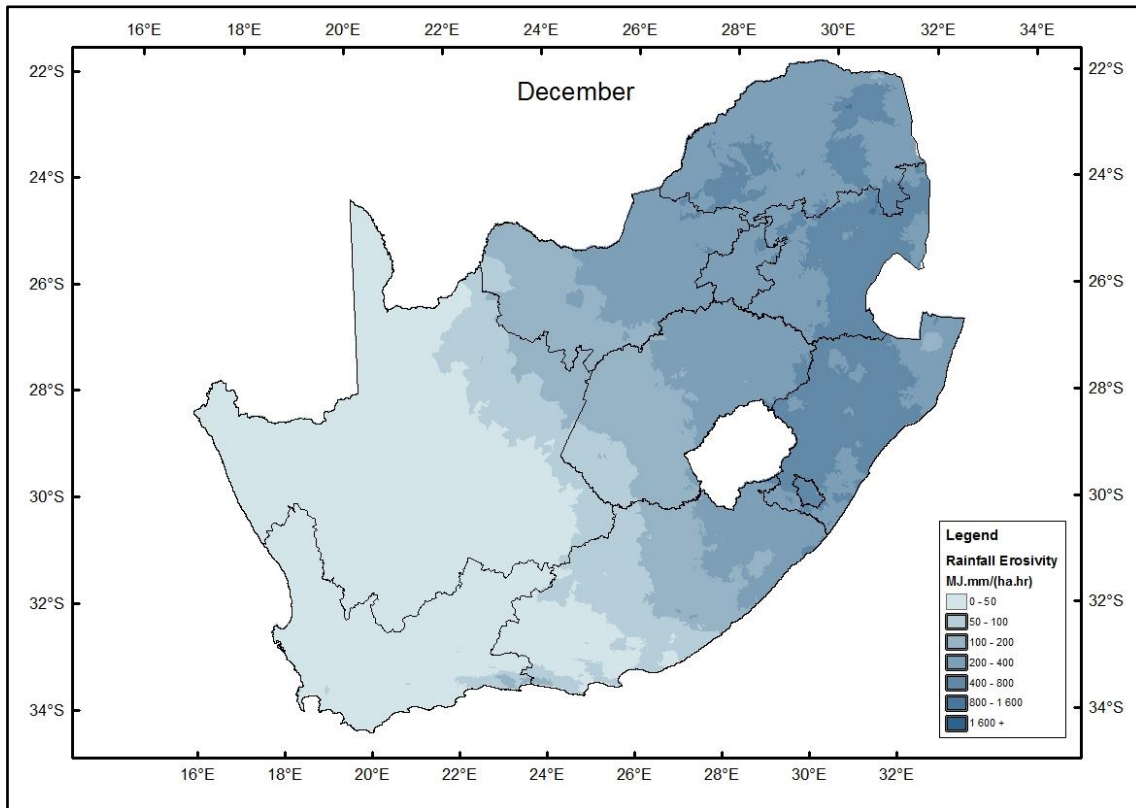


Figure 11.12 Rainfall erosivity map of South Africa for December, calculated using the erosivity density method

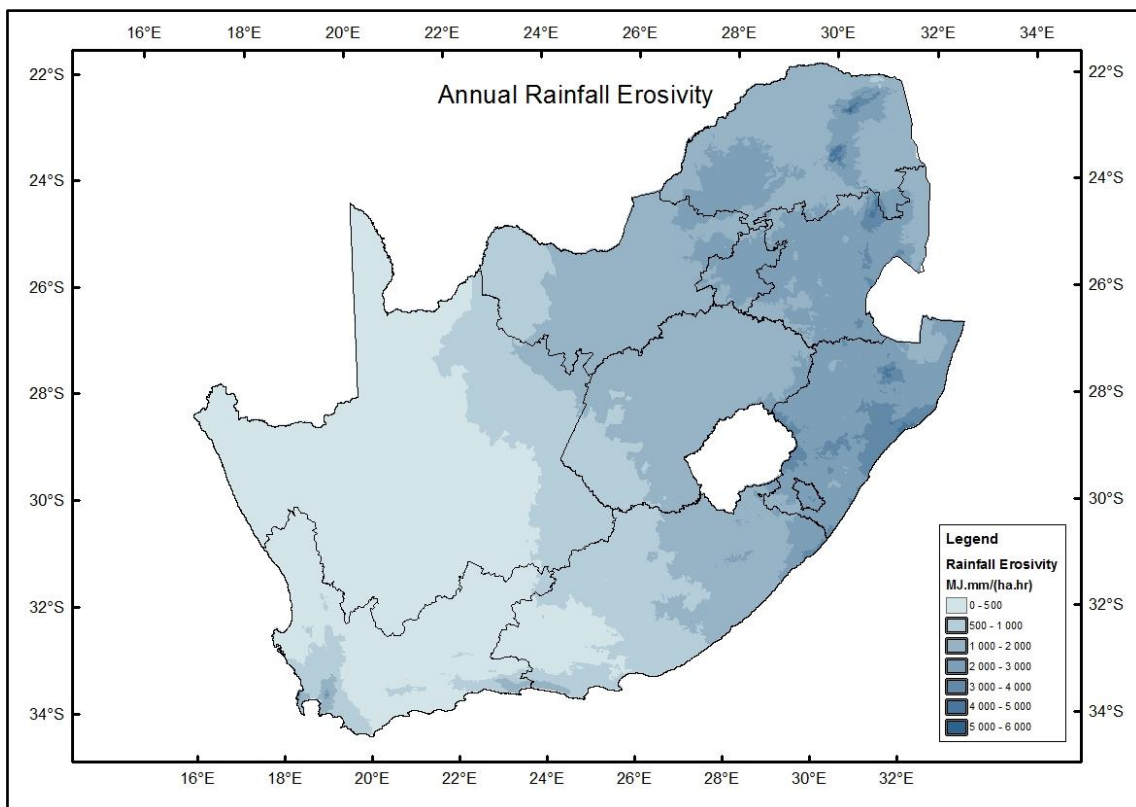


Figure 11.13 Annual rainfall erosivity map of South Africa, calculated using the erosivity density method

12. APPENDIX C: RELATIONSHIPS BETWEEN DAILY RAINFALL AMOUNTS AND RAINFALL EROSIVITY

Appendix C contains Figures 12.1 to 12.14, which illustrate the relationships between daily rainfall amount and rainfall erosivity (the EI_{30} index) for each month, in each homogeneous short-duration rainfall cluster.

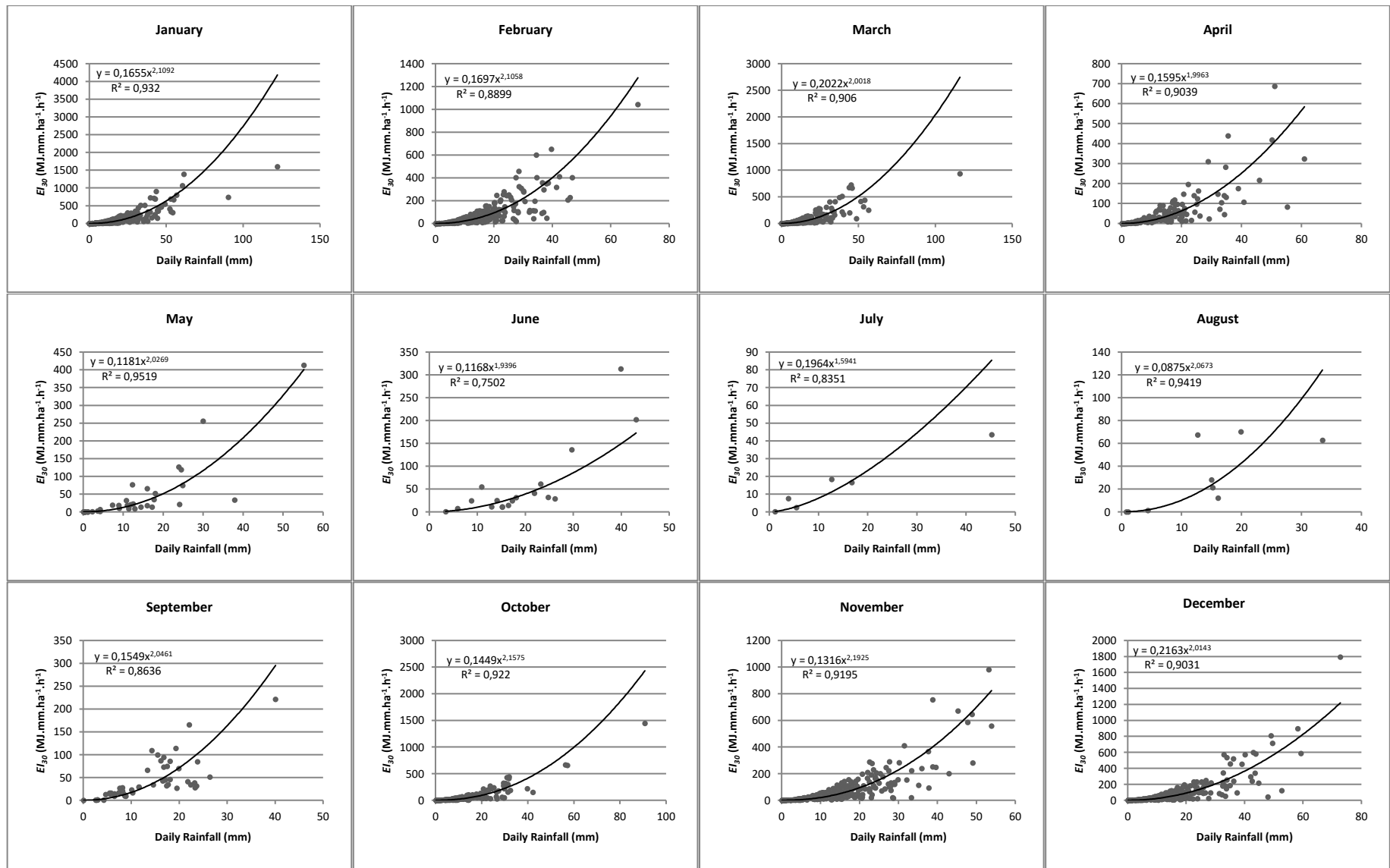


Figure 12.1 Regression analysis of daily rainfall amount and rainfall erosivity for Cluster 1

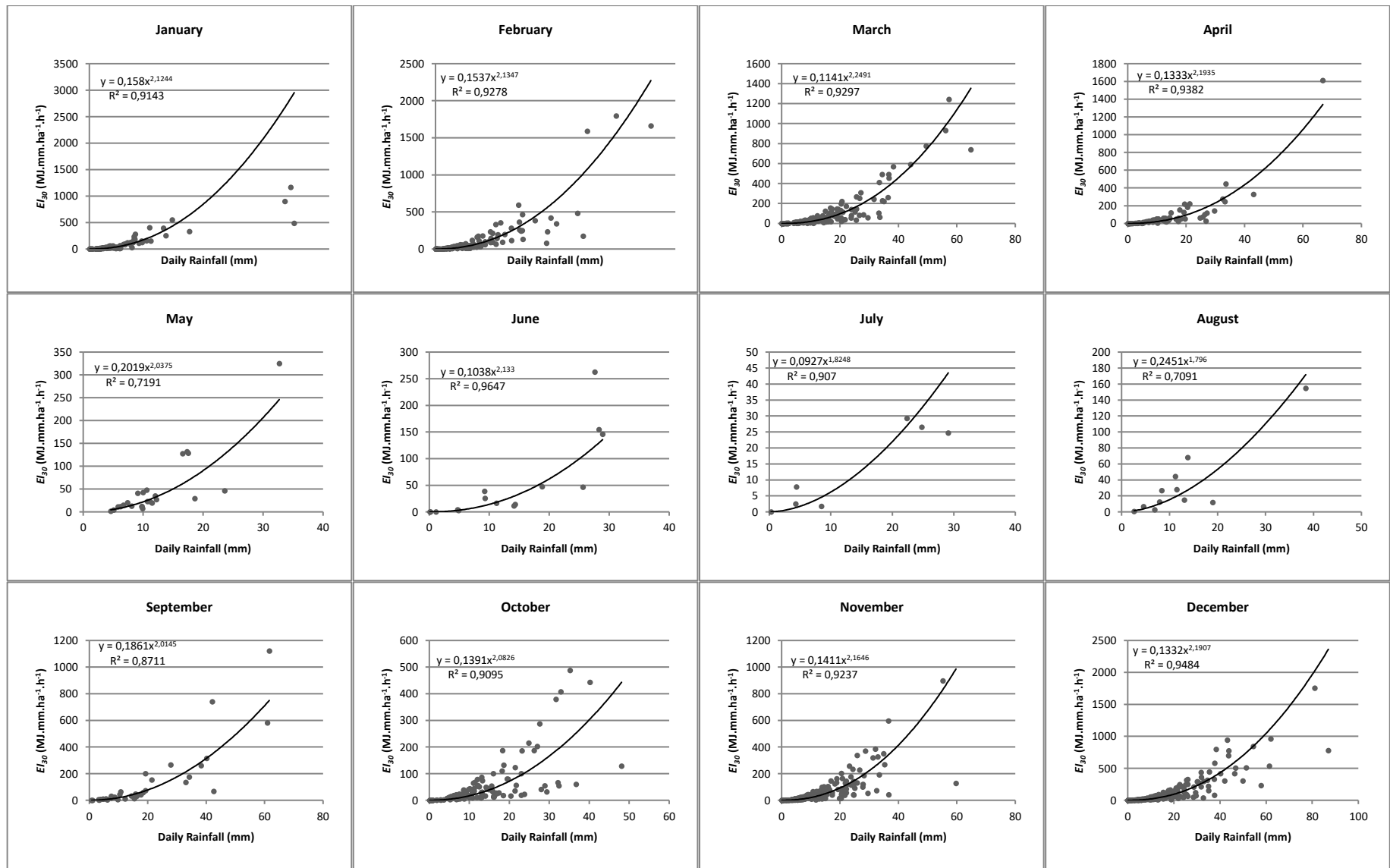


Figure 12.2 Regression analysis of daily rainfall amount and rainfall erosivity for Cluster 2

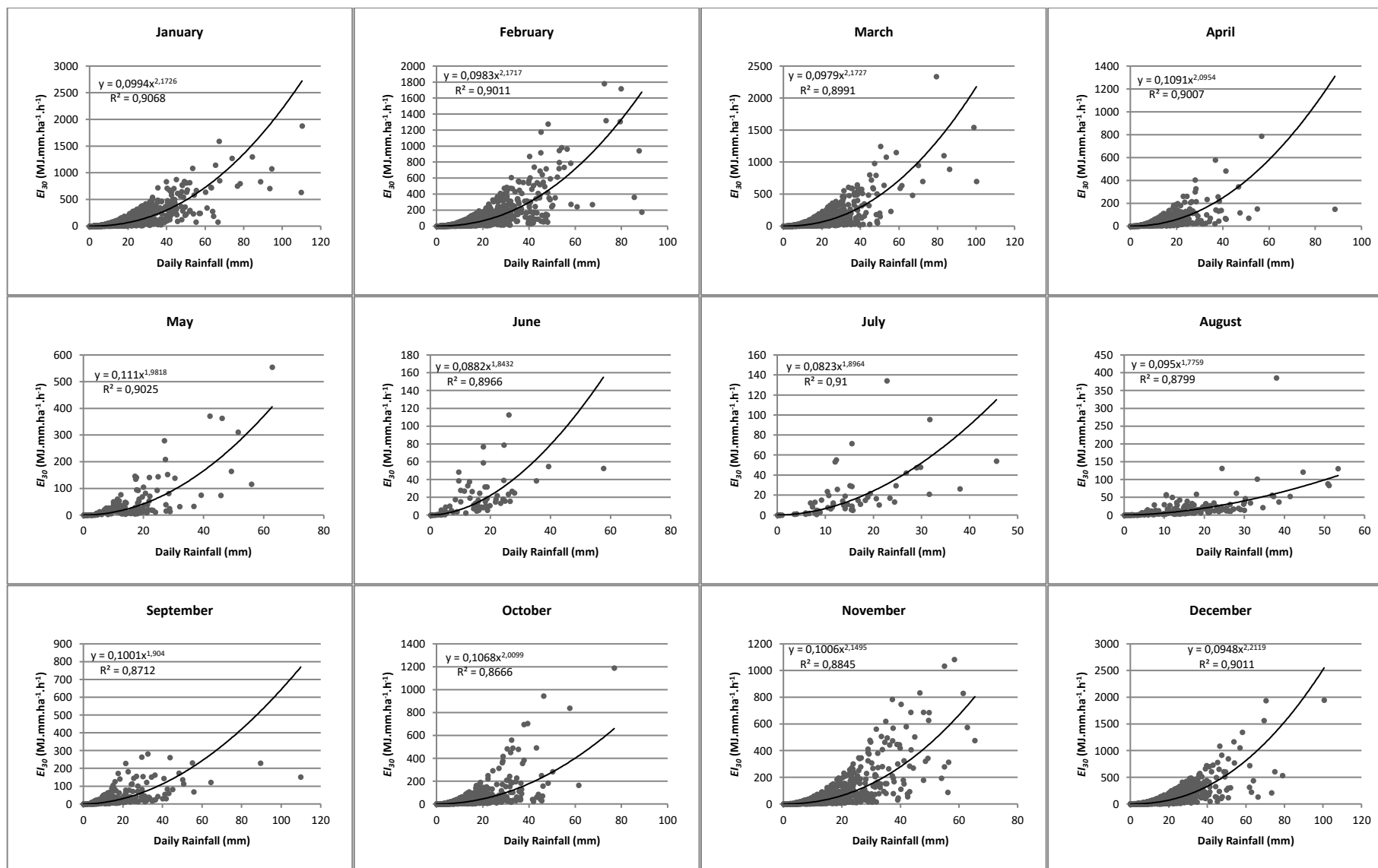


Figure 12.3 Regression analysis of daily rainfall amount and rainfall erosivity for Cluster 3

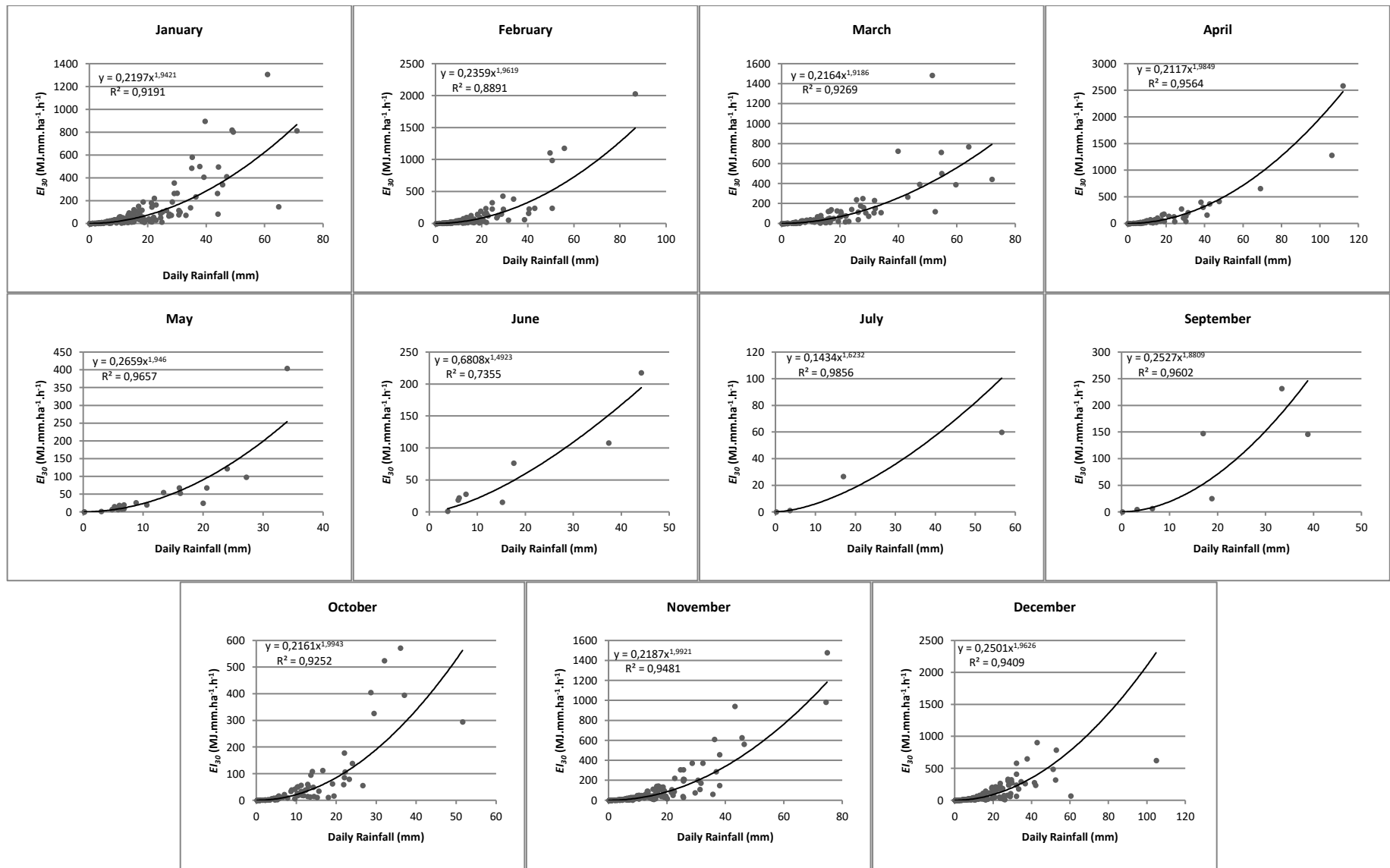


Figure 12.4 Regression analysis of daily rainfall amount and rainfall erosivity for Cluster 5

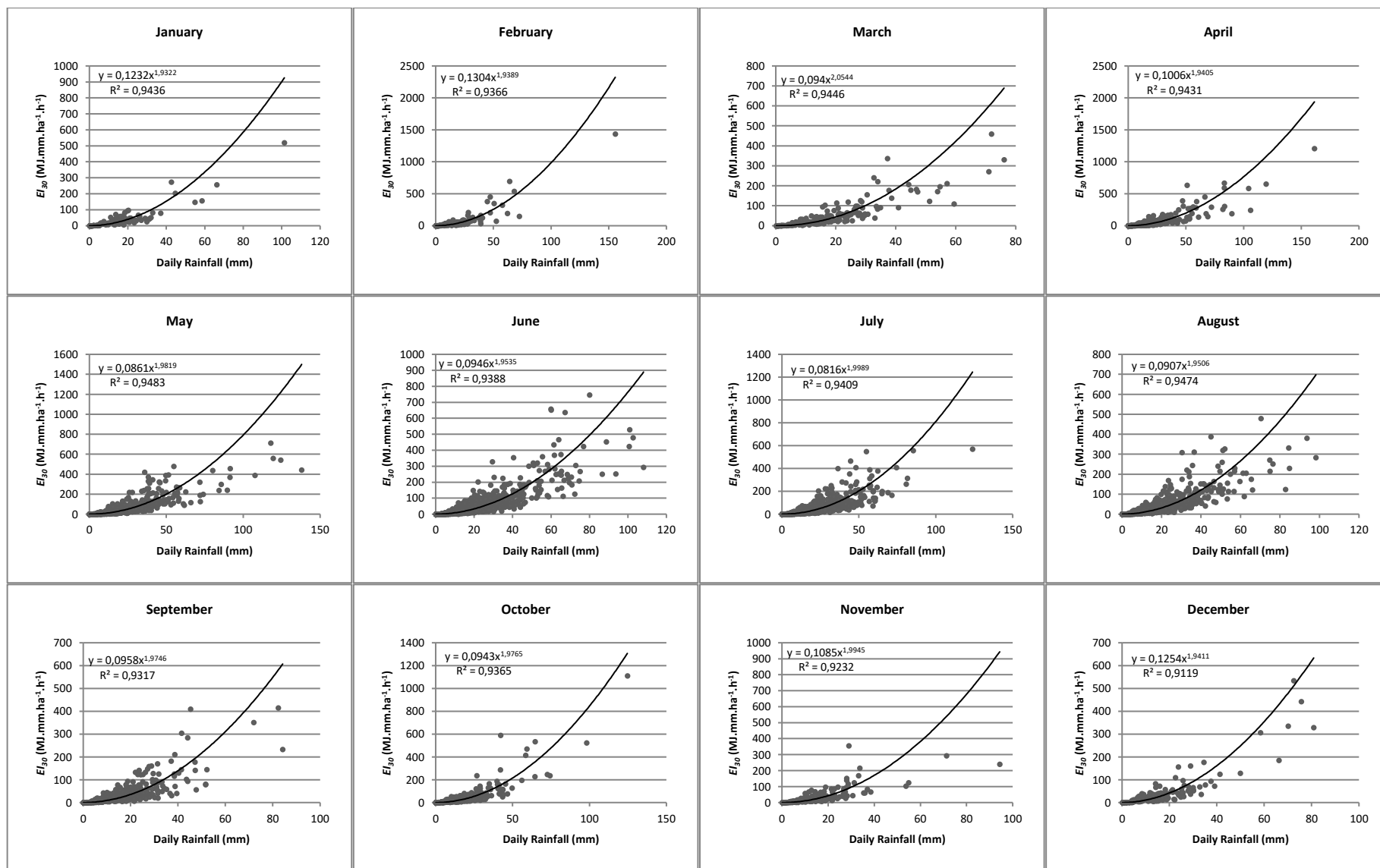


Figure 12.5 Regression analysis of daily rainfall amount and rainfall erosivity for Cluster 6

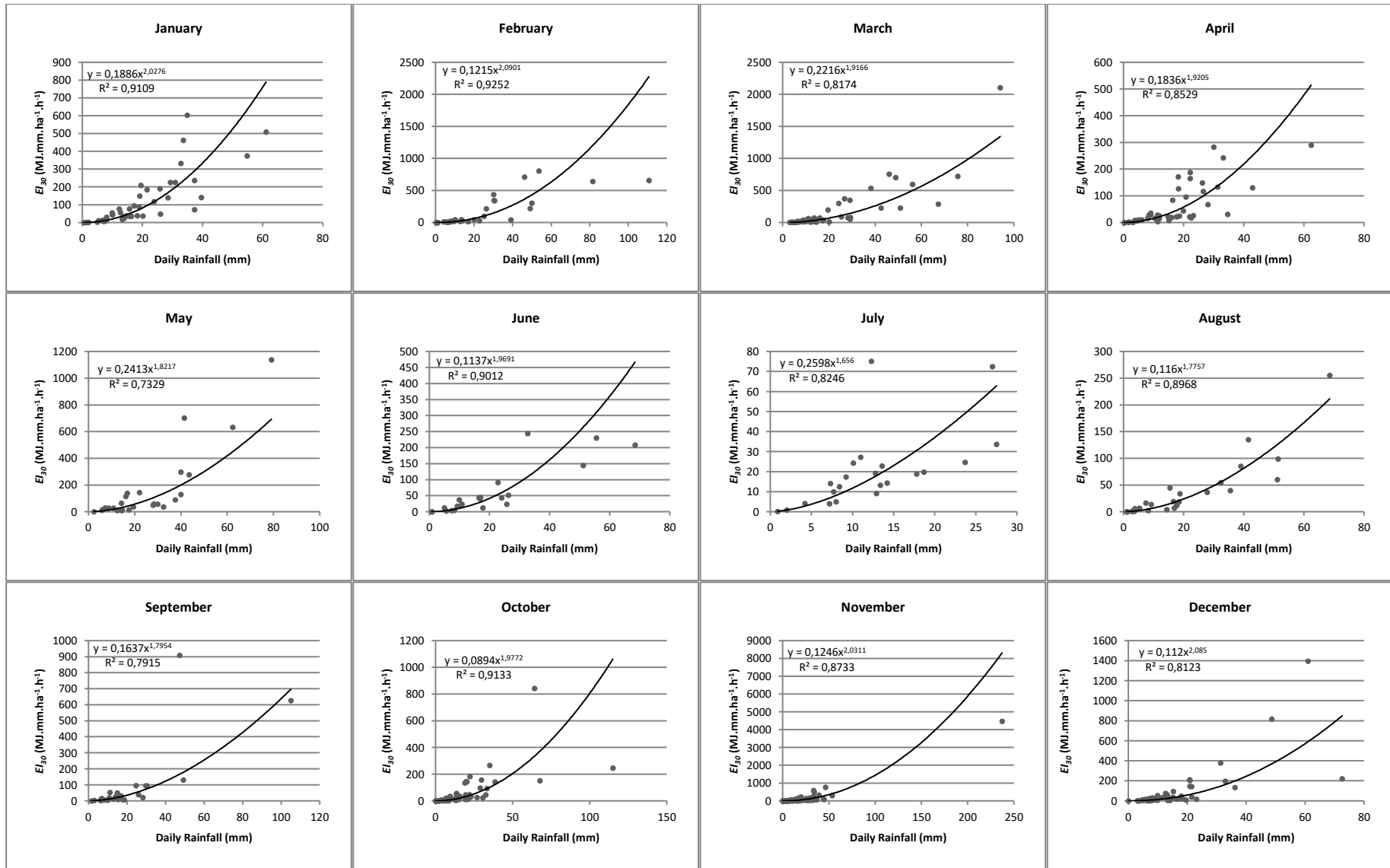


Figure 12.6 Regression analysis of daily rainfall amount and rainfall erosivity for Cluster 7

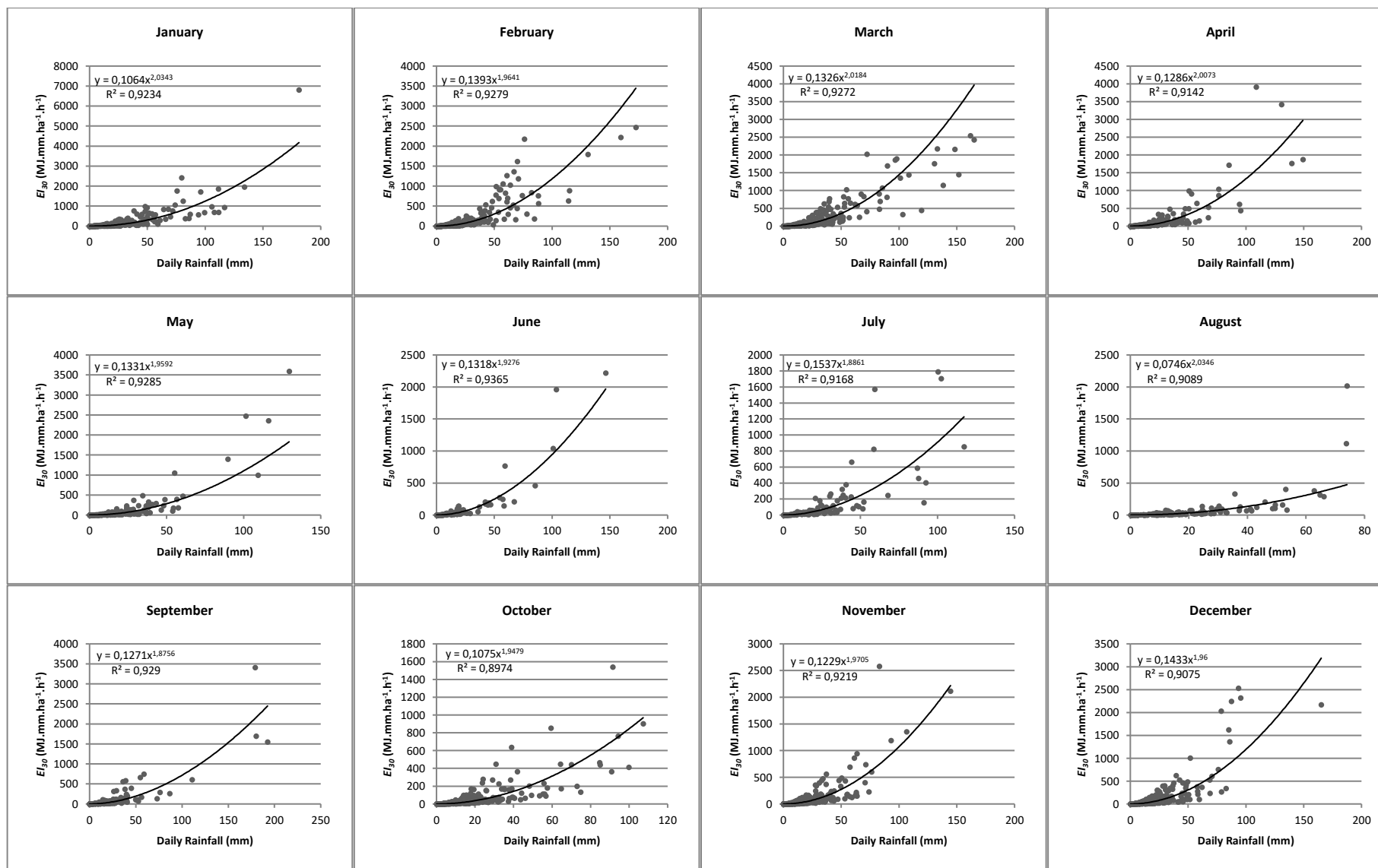


Figure 12.7 Regression analysis of daily rainfall amount and rainfall erosivity for Cluster 8

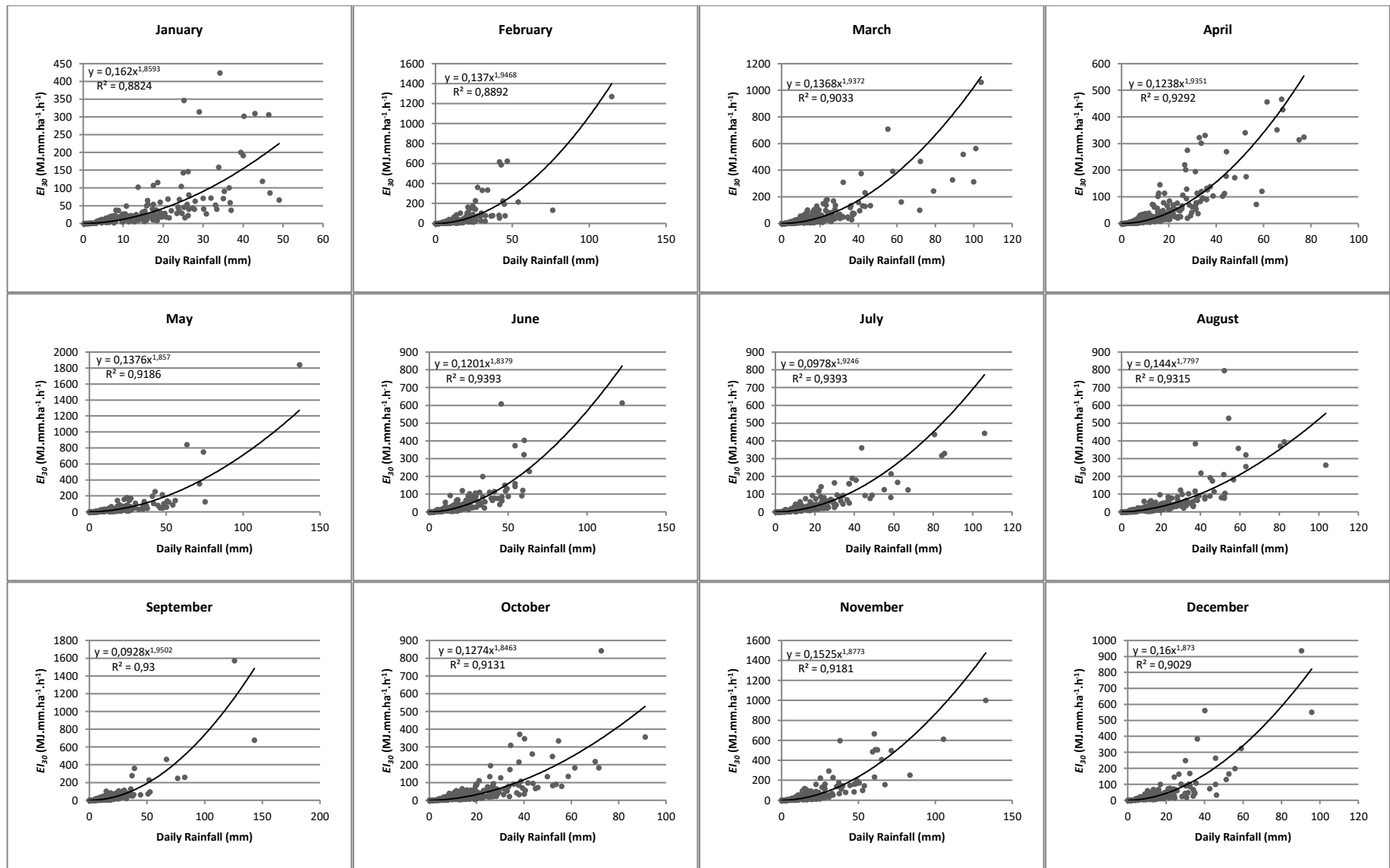


Figure 12.8 Regression analysis of daily rainfall amount and rainfall erosivity for Cluster 9

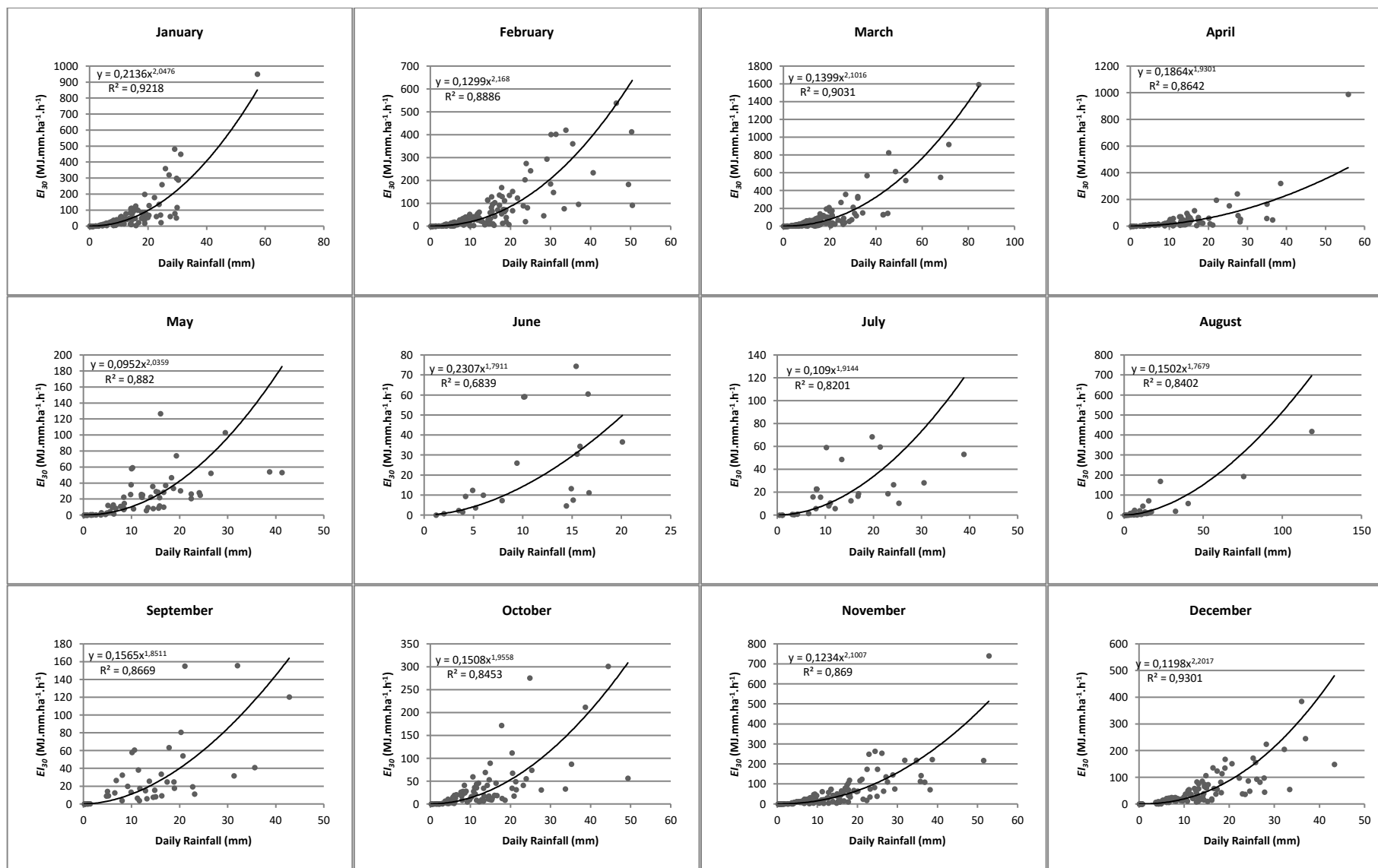


Figure 12.9 Regression analysis of daily rainfall amount and rainfall erosivity for Cluster 10

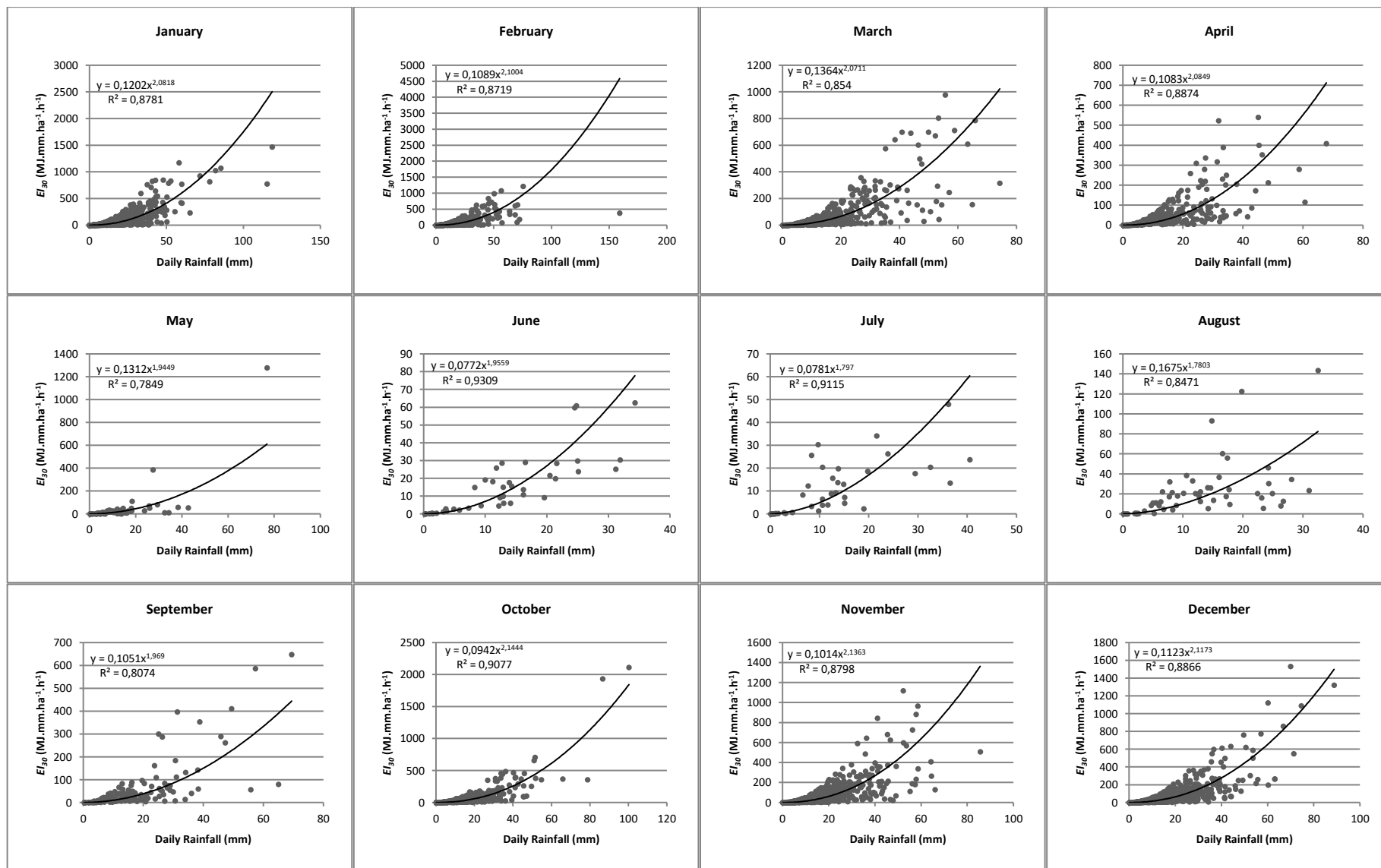


Figure 12.10 Regression analysis of daily rainfall amount and rainfall erosivity for Cluster 11

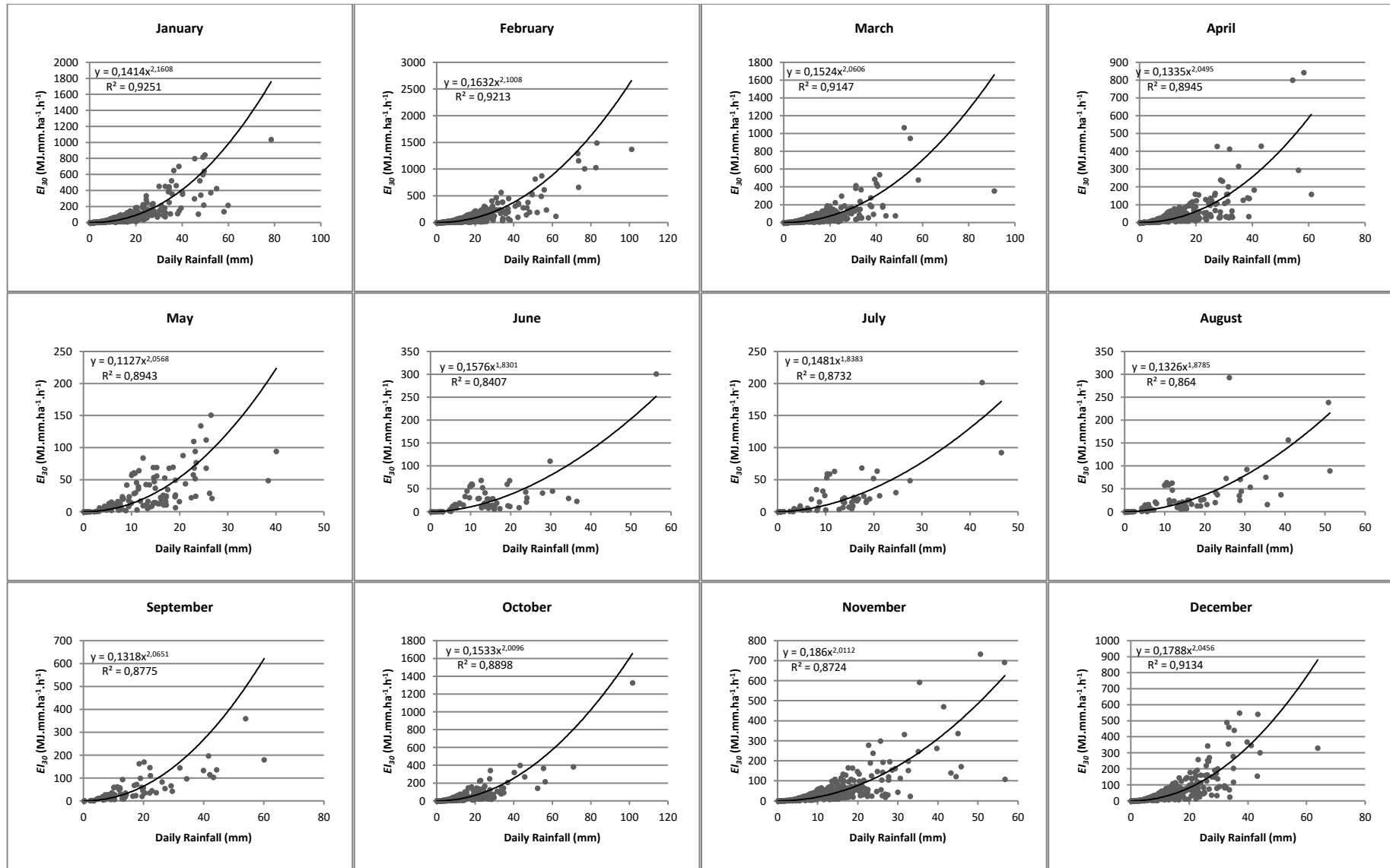


Figure 12.11 Regression analysis of daily rainfall amount and rainfall erosivity for Cluster 12

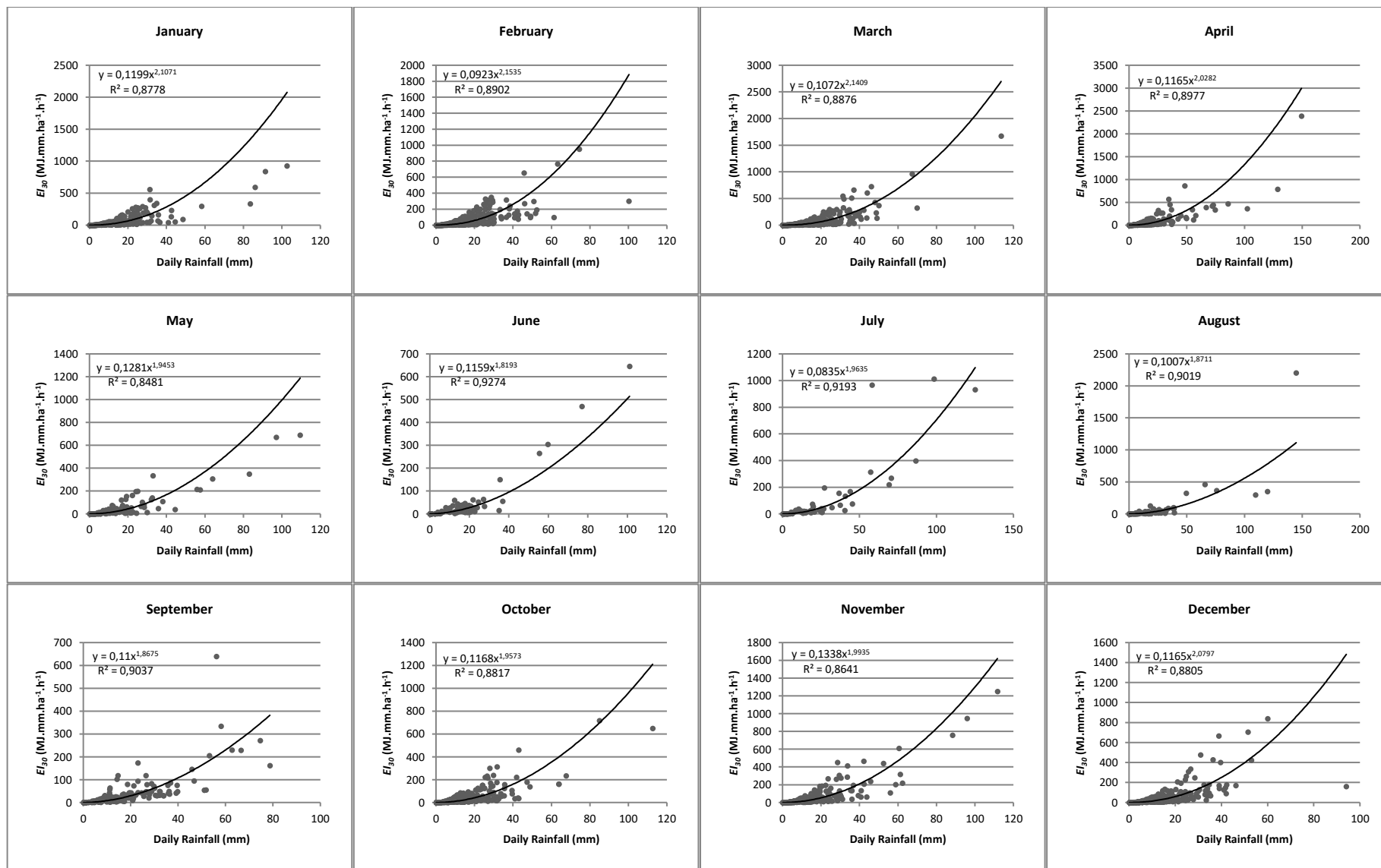


Figure 12.12 Regression analysis of daily rainfall amount and rainfall erosivity for Cluster 13

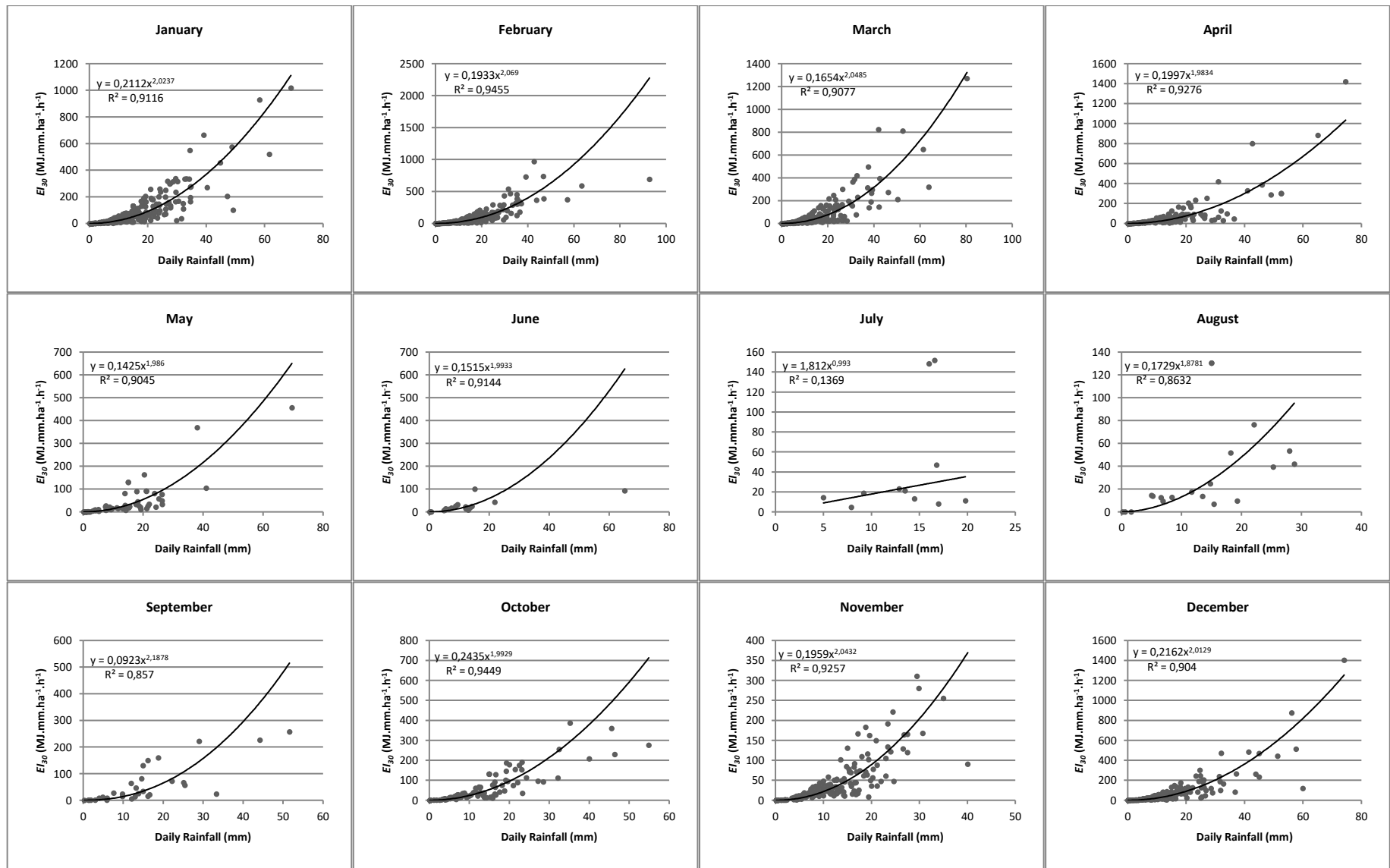


Figure 12.13 Regression analysis of daily rainfall amount and rainfall erosivity for Cluster 14

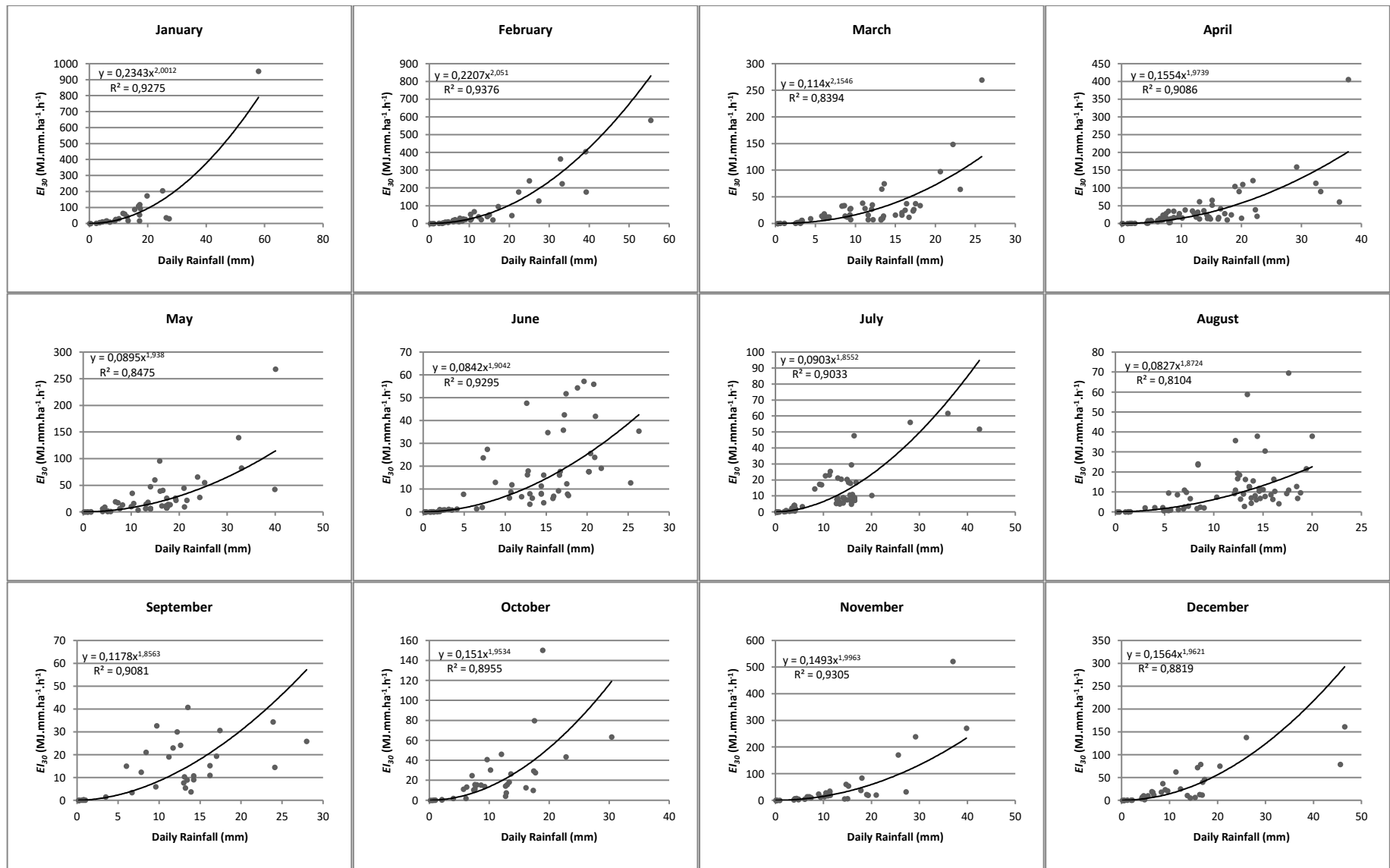


Figure 12.14 Regression analysis of daily rainfall amount and rainfall erosivity for Cluster 15

13. APPENDIX D: RAINFALL EROSIIVITY MAPS OBTAINED USING THE DAILY DATA METHOD

Appendix D contains Figures 13.1 to 13.13, which illustrate the rainfall erosivity across South Africa for each month, as well as the annual sum of rainfall erosivity, calculated using the daily data method.

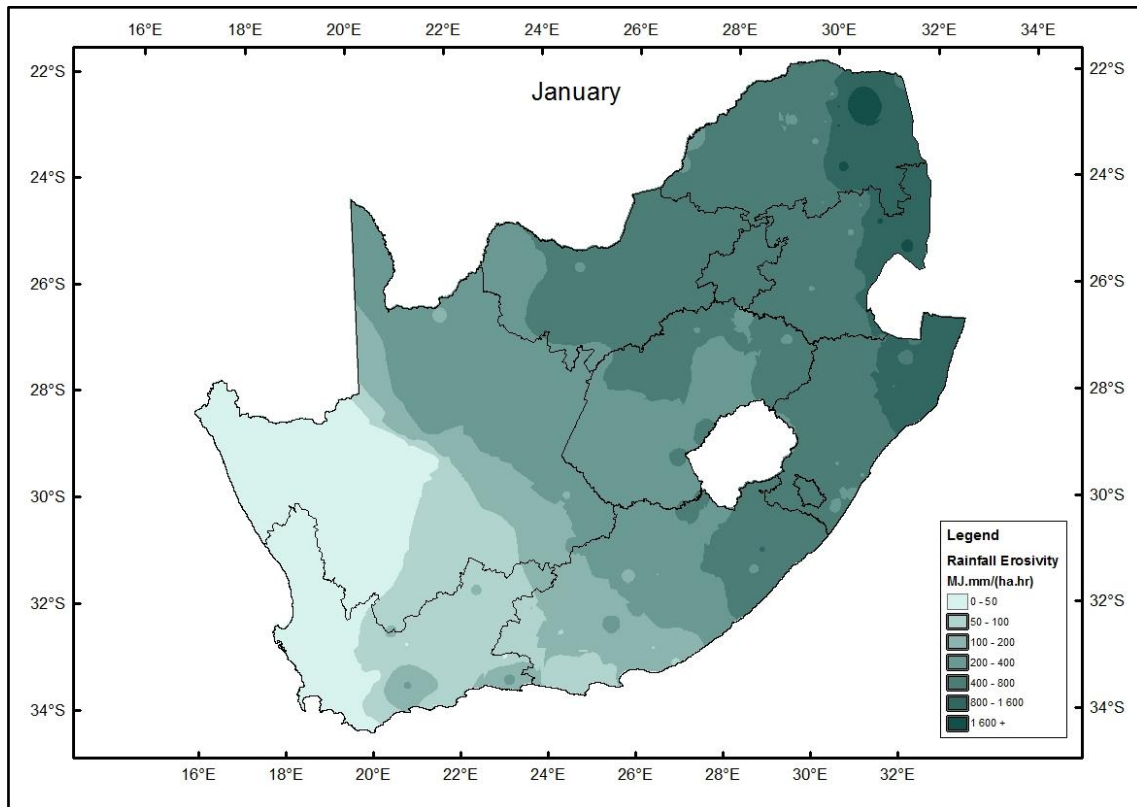


Figure 13.1 Rainfall erosivity map of South Africa for January, calculated using the daily data method

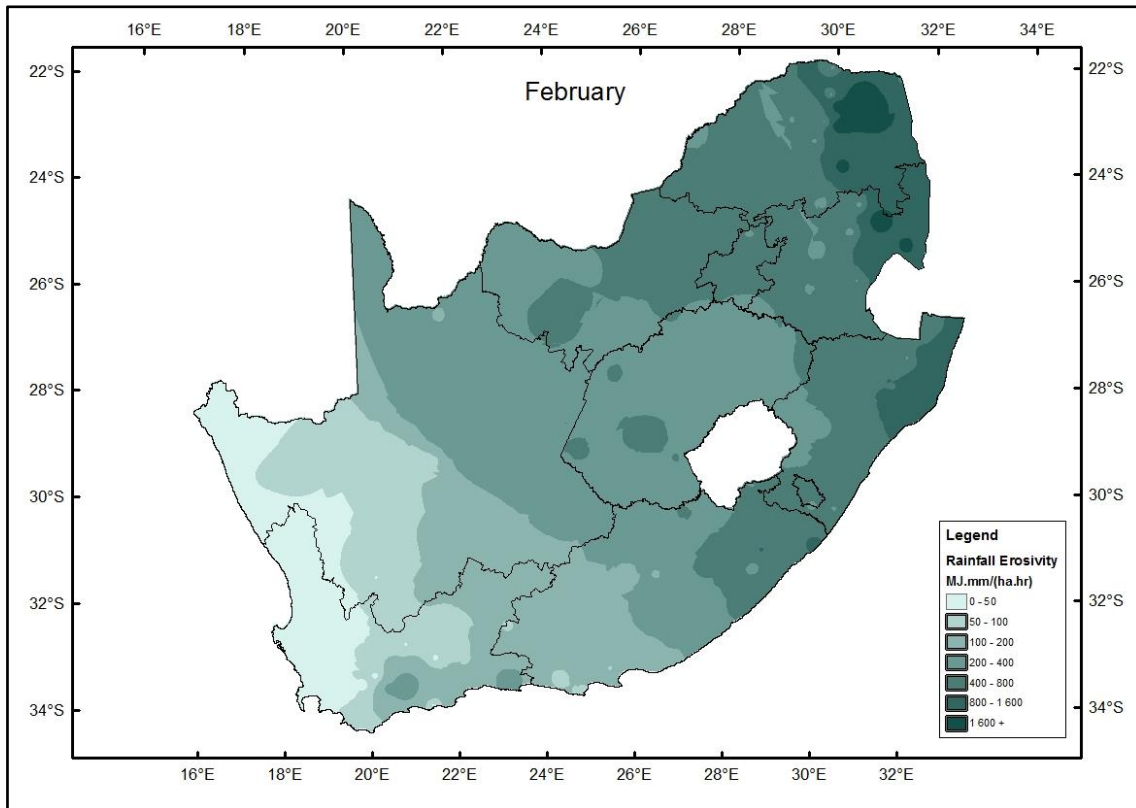


Figure 13.2 Rainfall erosivity map of South Africa for February, calculated using the daily data method

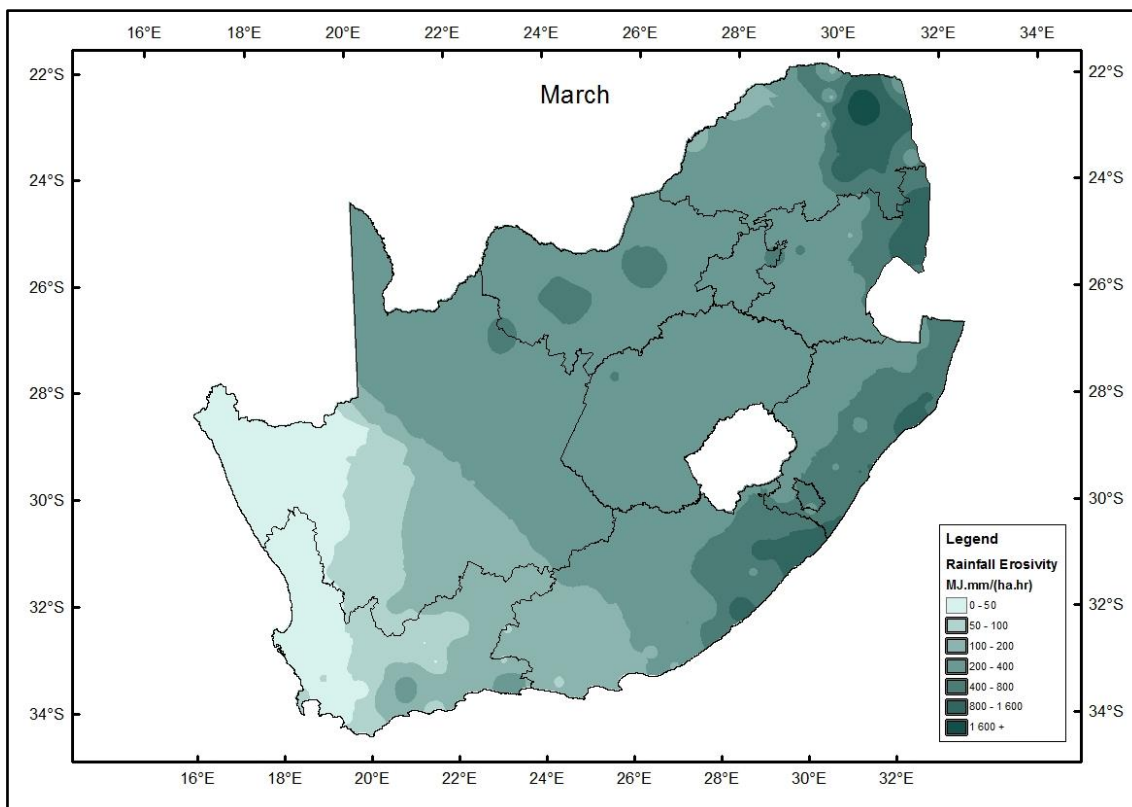


Figure 13.3 Rainfall erosivity map of South Africa for March, calculated using the daily data method

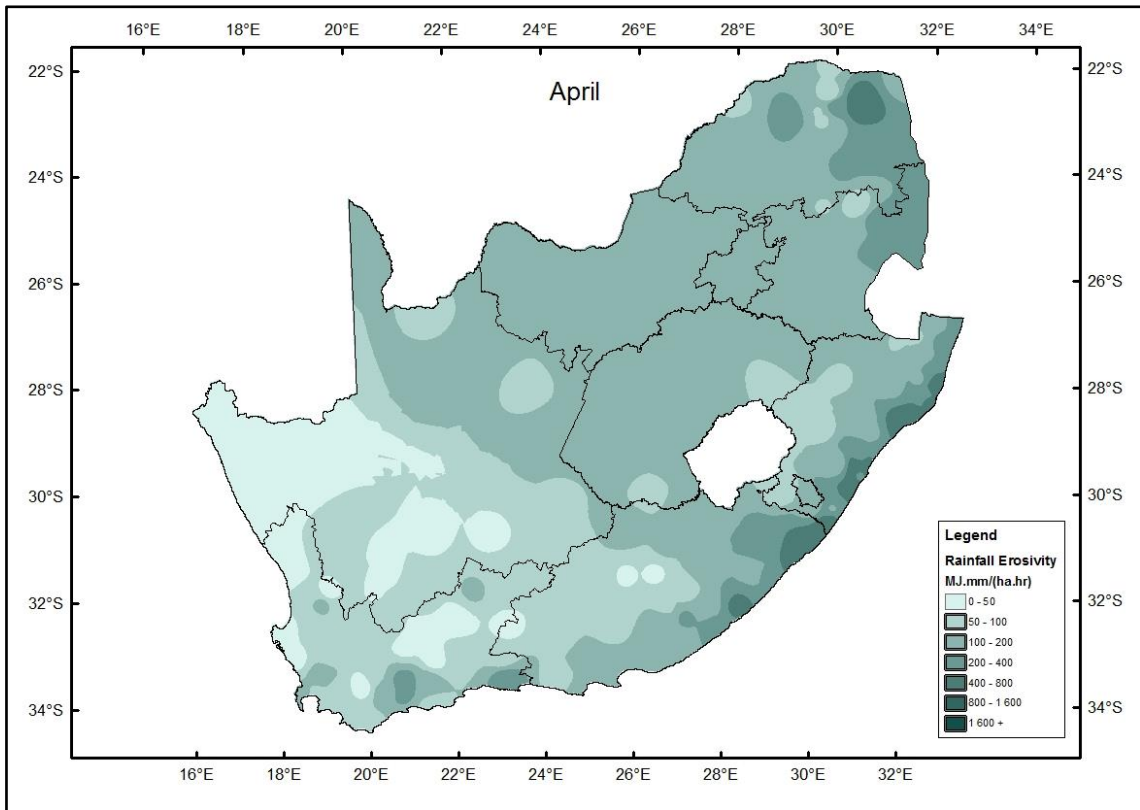


Figure 13.4 Rainfall erosivity map of South Africa for April, calculated using the daily data method

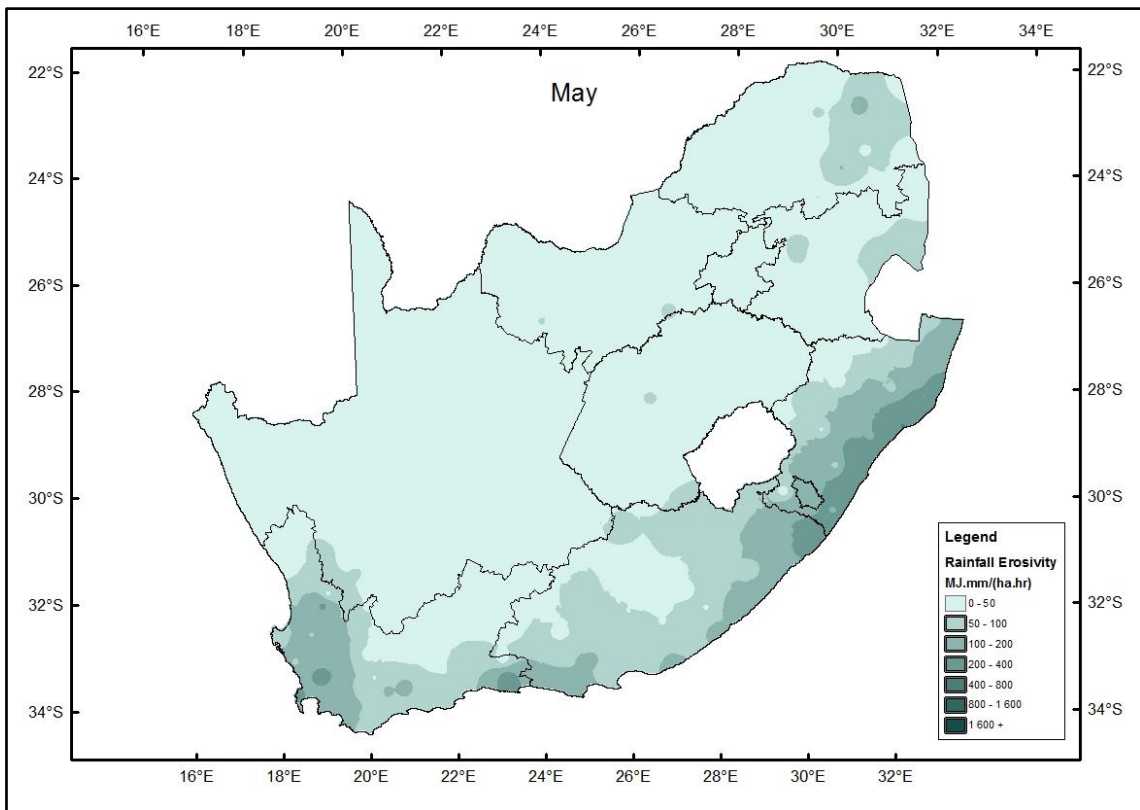


Figure 13.5 Rainfall erosivity map of South Africa for May, calculated using the daily data method

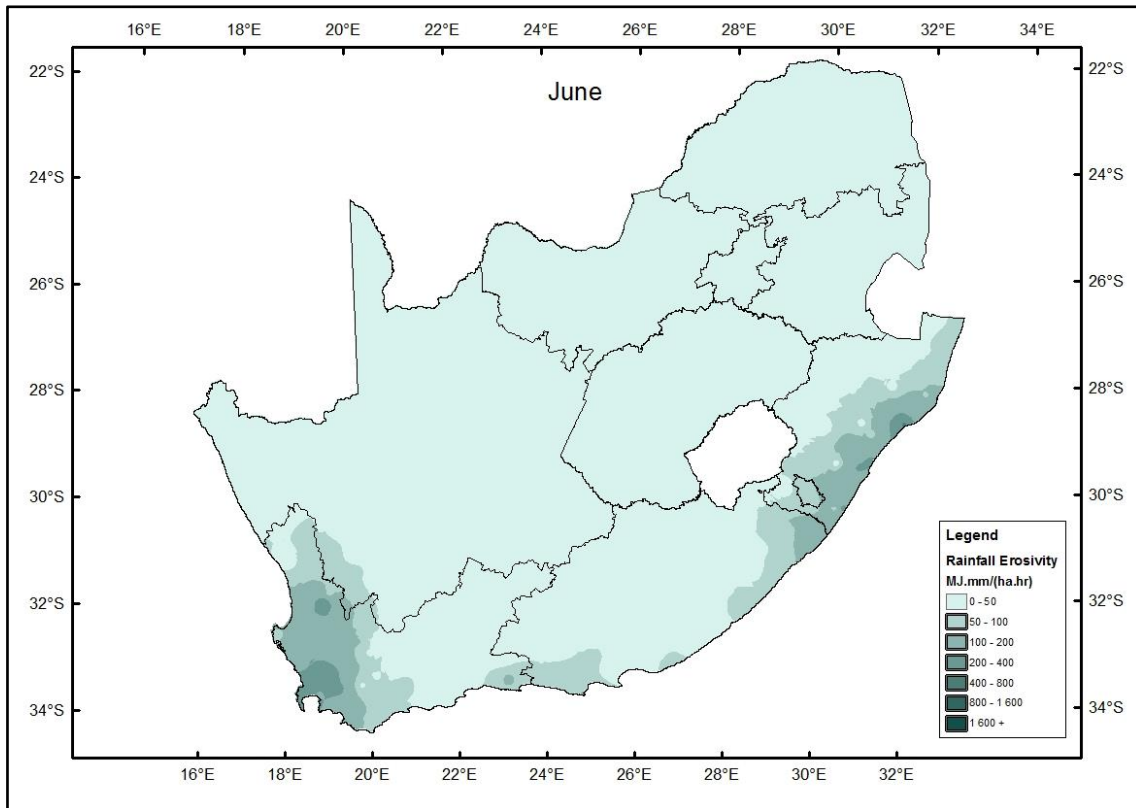


Figure 13.6 Rainfall erosivity map of South Africa for June, calculated using the daily data method

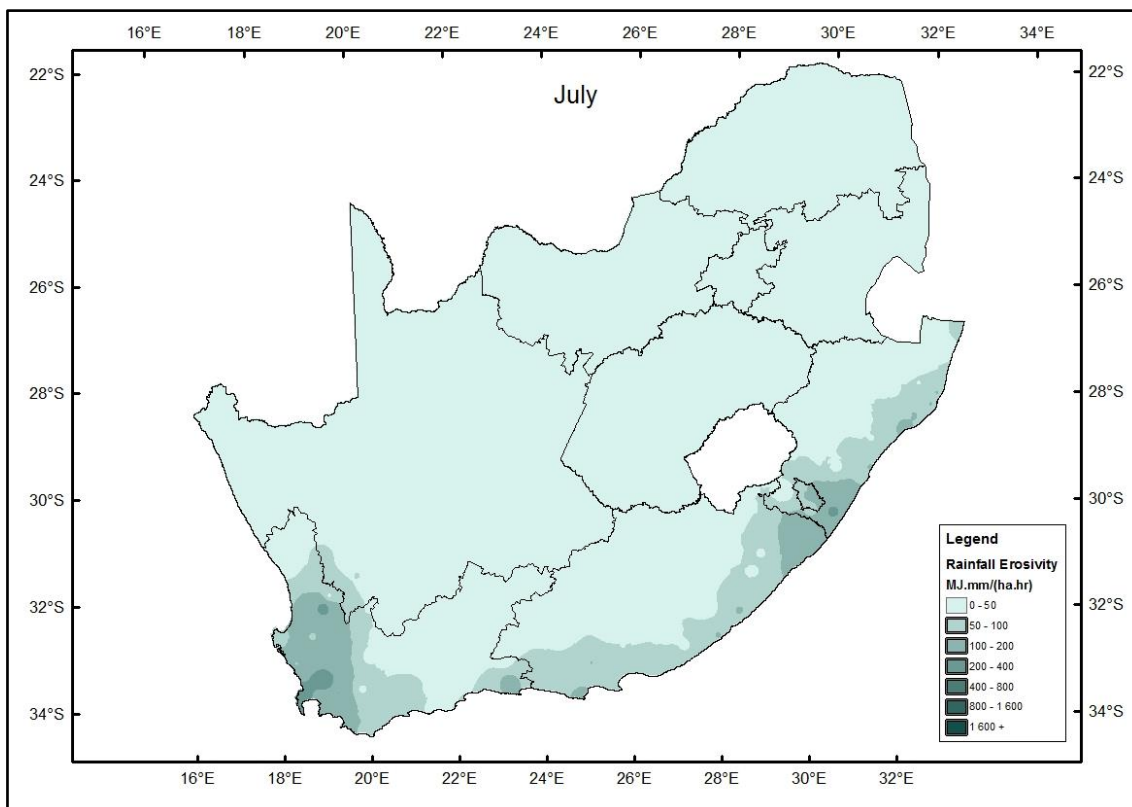


Figure 13.7 Rainfall erosivity map of South Africa for July, calculated using the daily data method

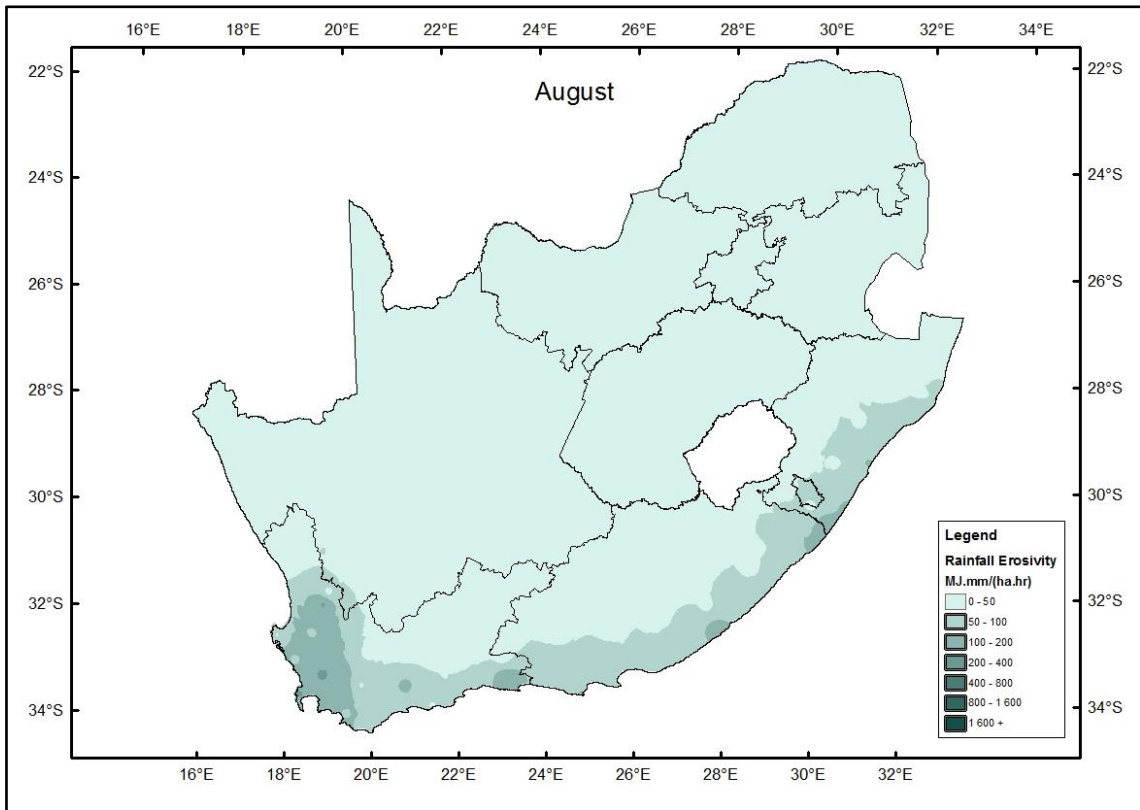


Figure 13.8 Rainfall erosivity map of South Africa for August, calculated using the daily data method

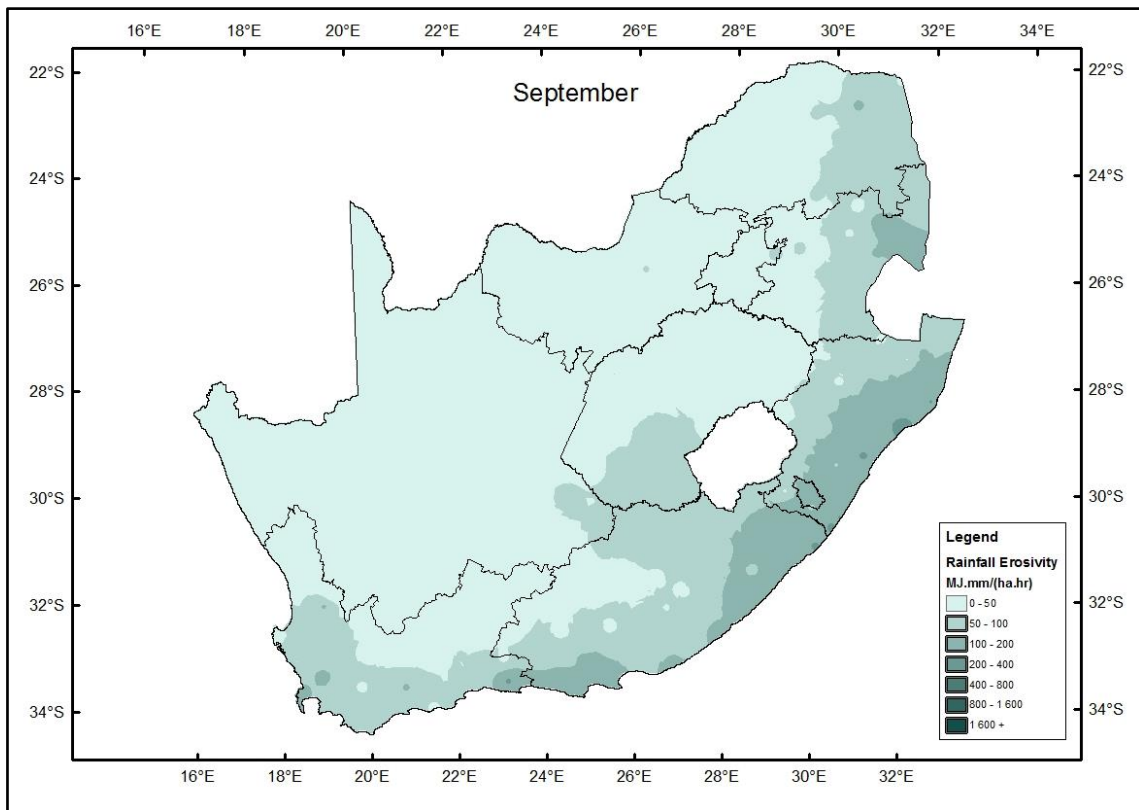


Figure 13.9 Rainfall erosivity map of South Africa for September, calculated using the daily data method

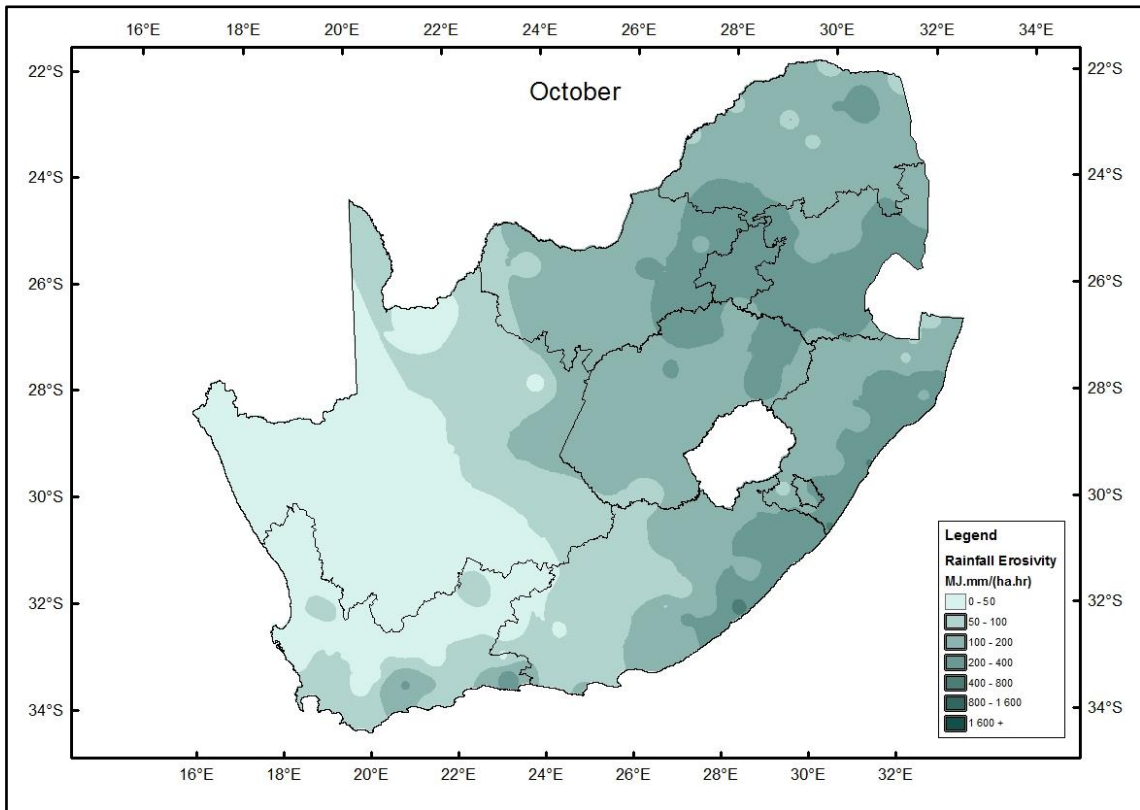


Figure 13.10 Rainfall erosivity map of South Africa for October, calculated using the daily data method

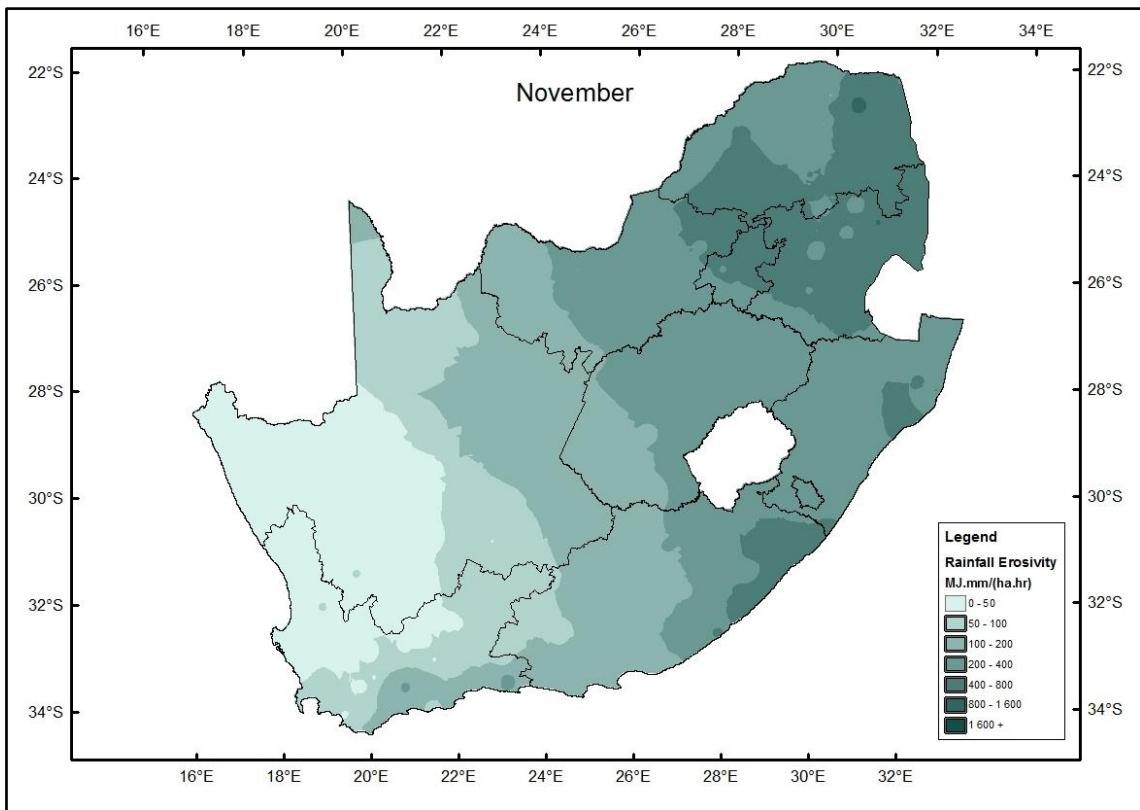


Figure 13.11 Rainfall erosivity map of South Africa for November, calculated using the daily data method

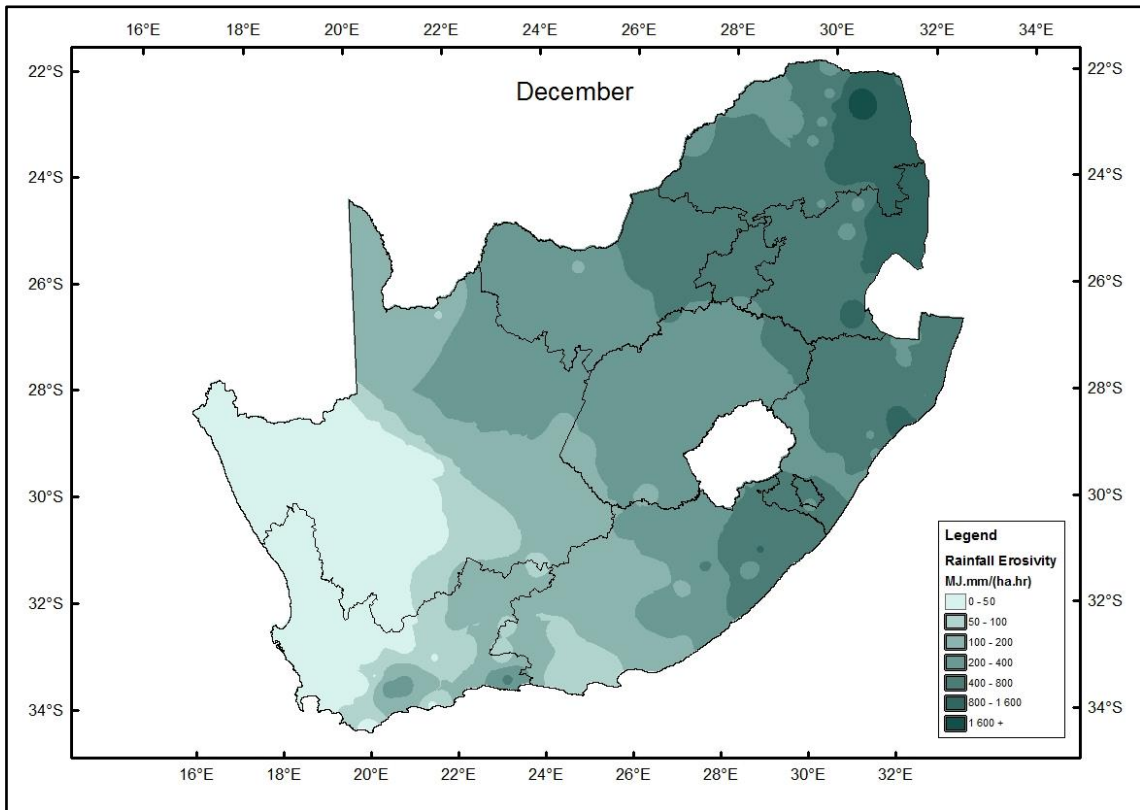


Figure 13.12 Rainfall erosivity map of South Africa for December, calculated using the daily data method

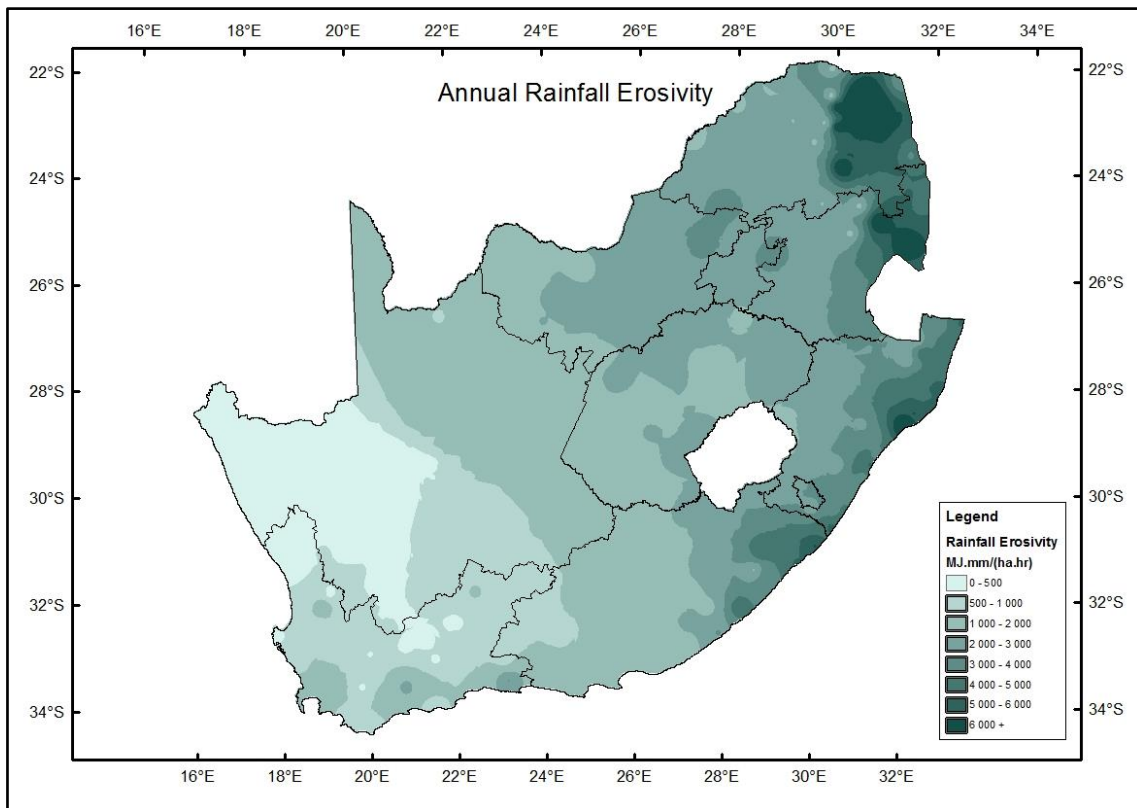


Figure 13.13 Annual rainfall erosivity map of South Africa, calculated using the daily data method